Genetic and environmental influences on the brain functional networks in older adults

Author:
Foo, Heidi

Publication Date:
2021

DOI:
https://doi.org/10.26190/unsworks/1604

Genetic and environmental influences on the brain functional networks in older adults

Foo Jing Ling Heidi

Scientia PhD Scholar

A thesis in the fulfilment of the requirements for the degree of

Doctor of Philosophy

School of Psychiatry

Faculty of Medicine and Health

September 2021

THE UNIVERSITY OF NEW SOUTH WALES
Thesis/Dissertation Sheet

Surname/Family Name: Foo

Name: Heidi, Jing Ling

Abbreviation for degree as give in the University calendar: PhD

Faculty: Medicine and Health

School: Psychiatry

Thesis Title: Genetic and environmental influences on the brain functional networks in older adults

Abstract

As humans age, the functional organisation of their brain networks undergoes complex changes that are associated with observed changes in cognition. Both genetics and the environment play a crucial role in influencing changes in the network topology of the ageing brain. In addition, the network topology is influenced by age-related brain diseases. To date, there is a paucity of population-based studies investigating the contributions of age, genetic and environmental factors, and brain disease to the architecture of the functional brain networks. The broad aim of this thesis, therefore, was to examine the influence of genetics, environmental factors, and disease-states on functional brain networks in older individuals using the United Kingdom (UK) Biobank data (N~18,455; ages 44-80 years). To study functional brain networks, I modelled large-scale brain networks from resting-state functional magnetic resonance imaging (fMRI) scans using graph theory, defined by a collection of nodes (brain regions) and edges (magnitude of temporal correlation in activity on fMRI between two brain regions).

Four studies are reported in the thesis. In the first study, I investigated the genetic determinants of functional brain networks. I first estimated single nucleotide polymorphism (SNP) heritability (h^2). Subsequently, genome-wide association studies (GWAS) were performed to identify genetic variants associated with each graph theory measure. Gene-based association analysis was carried out to uncover gene-level associations, and the functional consequences of the significant genetic variants were explored. As brain reorganisation of the functional networks has been differentially observed with ageing in the two sexes, I examined in the second study how age and sex are associated with the topology of functional brain networks in association with cognitive performance. In the third study, I examined the association of sleep and other lifestyle factors such as exercise, alcohol, and smoking, with functional network properties. In the final study, I studied how disease phenotypes, in particular depressive symptoms, influence functional network properties.

This thesis provides several novel contributions to the literature by identifying important genetic, environmental, and disease-related factors that are associated with measures of functional networks in the ageing brain. The findings highlight biological pathways relevant to the ageing human brain functional network integrity and diseases that affect it.

ORIGINALITY STATEMENT

‘I hereby declare that this submission is my own work and to the best of my knowledge it contains no materials previously published or written by another person, or substantial proportions of material which have been accepted for the award of any other degree or diploma at UNSW or any other educational institution, except where due acknowledgement is made in the thesis. Any contributions made to the research by others, with whom I have worked at UNSW or elsewhere, is explicitly acknowledged in the thesis. I also declare that the intellectual content of this thesis is the product of my own work, except to the extent that assistance from others in the project’s design and conception or in style, presentation and linguistic expression is acknowledged.’

Signed _____

Date _____

COPYRIGHT STATEMENT

Signed _____

Date _____

AUTHENTICITY STATEMENT

‘I certify that the Library deposit digital copy is a direct equivalent of the final officially approved version of my thesis. No emendation of content has occurred and if there are major variations in formatting, they are the result of the conversion to digital format.’

Signed _____

Date _____

ABSTRACT

As humans age, the functional organisation of their brain networks undergoes complex changes that are associated with observed changes in cognition. Both genetics and the environment play a crucial role in influencing changes in the network topology of the ageing brain. In addition, the network topology is influenced by age-related brain diseases. To date, there is a paucity of population-based studies investigating the contributions of age, genetic and environmental factors, and brain disease to the architecture of the functional brain networks. The broad aim of this thesis, therefore, was to examine the influence of genetics, environmental factors, and disease-states on functional brain networks in older individuals using the United Kingdom (UK) Biobank data (N~18,455; ages 44-80 years). To study functional brain networks, I modelled large-scale brain networks from resting-state functional magnetic resonance imaging (fMRI) scans using graph theory, defined by a collection of nodes (brain regions) and edges (magnitude of temporal correlation in activity on fMRI between two brain regions).

Four studies are reported in the thesis. In the first study, I investigated the genetic determinants of functional brain networks. I first estimated single nucleotide polymorphism (SNP) heritability (h^2). Subsequently, genome-wide association studies (GWAS) were performed to identify genetic variants associated with each graph theory measure. Gene-based association analysis was carried out to uncover gene-level associations, and the functional consequences of the significant genetic variants were explored. As brain reorganisation of the functional networks has been differentially observed with ageing in the two sexes, I examined in the second study how age and sex are associated with the topology of functional brain networks in association with

cognitive performance. In the third study, I examined the association of sleep and other lifestyle factors such as exercise, alcohol, and smoking, with functional network properties. In the final study, I studied how disease phenotypes, in particular depressive symptoms, influence functional network properties.

This thesis provides several novel contributions to the literature by identifying important genetic, environmental, and disease-related factors that are associated with measures of functional networks in the ageing brain. The findings highlight biological pathways relevant to the ageing human brain functional network integrity and diseases that affect it.

ACKNOWLEDGMENTS

I am truly privileged to be able to pursue my doctoral study at the University of New South Wales (UNSW), Sydney, with full scholarship from UNSW Scientia PhD Scholarship and the support of many amazing people, both directly and indirectly.

I am especially thankful to my supervisory team, Perminder Sachdev, Anbupalam Thalamuthu**,** Wei Wen, Jiyang Jiang, and Karen Mather, for their support throughout the process. Their insightful feedback and guidance have sharpened my thinking, brought my work to a higher level, and allowed me to grow both academically and personally. I am also grateful to my other mentors, Kim Delbaere, Nagaendran Kandiah, Edward Robins, and Joanes Grandjean for all the amazing opportunities and encouragements showered upon me. I would also like to express my sincere gratitude to experts of the field, including Stephen Smith, Alexander Fornito, Andrew Zalesky, Samuel Jones, and Naomi Wray, who took the time to answer my queries. Special mention to Forrest Koch who spent hours helping me with the Matlab scripts and for brainstorming the graph theory measures with me. I am also grateful to Jing Du who is ever ready to lend her helping hand. To Josie and Min Yee, thank you for your friendships. I am also glad to have all the random drink nights with my Centre for Healthy Brain Ageing (CHeBA) colleagues where they frequently listened to me lament about the progress of my PhD and assured me that I was doing alright. To my New College Village (NCV) friends, despite my short stay, thank you for bringing colour into college experience.

I am forever indebted to my one and only grandfather, Heng Yee Ho, for always believing in me and instilling in me the value of “persons for others.” I would have

never become the person I am today without his love and care. To my family, thank you for believing in me. I am also immensely appreciative of my friends who have walked with me during all the difficult times in my life. I am particularly thankful towards my former partner, Marius, who showed me what it meant to love someone and to have supported me selflessly; Keane, my best friend, for always pushing me to pursue my dreams and for being my constant; Auntie Eng, for all the words of wisdom; Pearlynne, Paula, Zachariah, Levinia, Tricia, Kang Yong, and many more, for providing me with the emotional support and for the sympathetic ear I needed prior to and during my PhD.

I am also thankful to *BTS* for the inspiring music, which got me through the difficult periods and motivated me to do better. Lastly, in all things, thanks be to God.

Thank you all for being a part of this milestone in my life.

TABLE OF CONTENTS

LIST OF TABLES

LIST OF FIGURES

LIST OF ABBREVIATIONS AND SYMBOLS

A1	Coded allele
A2	Non-coded allele
AFNI	Analysis of Functional Neuroimages
AN	Affective network
ANOVA	One-way analysis of variance
ARN	Affect and reward network
BCT	Brain connectivity toolbox
BOLD	Blood oxygen level-dependent
CCN	Cognitive control network
Charpath	Characteristic path length
Chr	Chromosome
CIDI-SF	Composite International Diagnostic Interview (CIDI) short form
DEG	Differentially expressed gene
DAN	Dorsal attention network
DMN	Default mode network
EAF	Effect allele frequency
Eglob	Global efficiency
Eloc	Local efficiency
EPI	Echo-planar imaging
eQTL	Expression quantitative trait loci
FPCN	Frontoparietal control network
FUMA	Functional Mapping and Annotation
GWAS	Genome-wide association studies
h^2	Trait heritability

h^2_{SNP}	SNP heritability
HRC	Haplotype Reference Consortium
ICA	Independent component analysis
ICD	International Classification of Diseases
IDP	Image-derived phenotypes
LD	Linkage disequilibrium
LDSC	Linkage disequilibrium (LD) score regression
LIMB	Limbic network
MAO	Monoamine oxidase
MDD	Major depressive disorder
MRI	Magnetic resonance imaging
ncRNA	Non-coding RNA
PRS	Polygenic risk score
QC	Quality control
REM	Rapid eye-movements
RSFC	Resting-state functional connectivity
Rs-fMRI	Resting-state functional magnetic resonance imaging
RSN	Resting-state networks
SE	Standard error
SM	Somatomotor network
SNPs	Single nucleotide polymorphisms
SPT	Sleep period time
SVAN	Salience/ ventral attention network
VIS	Visual network

LIST OF GENE SYMBOLS

AMER3	APC Membrane Recruitment Protein 3
EPHA3	EPH Receptor A3
INPP5A	Inositol Polyphosphate-5-Phosphatase A
LANCL1-AS1	LANCL1 Antisense RNA 1
LINC01101	Long Intergenic Non-Protein Coding RNA 1101
LINC01826	Long Intergenic Non-Protein Coding RNA 1826
LOC101928386	Uncharacterised LOC101928386
MIR3679	MicroRNA 3679
NR2F1-AS1	NR2F1 Antisense RNA 1
PAX8	Paired box gene 8
PICALM	Phosphatidylinositol-binding clathrin assembly protein
PLCE1	1-Phosphatidylinositol-4,5-bisphosphate phosphodiesterase epsilon-1
SH2B3	SH2B Adaptor Protein 3
SLC25A33	Solute Carrier Family 25 Member 33
SORL1	Sortilin-related receptor
TMEM201	Transmembrane Protein 201
ZEB1	Zinc Finger E-Box Binding Homeobox 1
ZIC4	Zic Family Member 4

PUBLICATIONS, PRESENTATIONS, AND AWARDS

Parts of this thesis have been included in the following publications and presentations:

Publications

Foo H, Thalamuthu A, Jiang JY, Koch FC, Mather KA, Wen W, Sachdev PS. Age- and sex-related topological organisation of human brain functional networks and their relationship to cognition. *Frontiers of Aging Neuroscience 2021*. In press.

Foo H, Thalamuthu A, Jiang JY, Koch FC, Mather KA, Wen W, Sachdev PS. Novel genetic variants associated with brain functional networks in 18,445 adults from the UK Biobank. *Scientific Reports 2021;* 11: 14633. doi: 10.1038/s41598-021-94182-9.

Foo H, Thalamuthu A, Jiang JY, Koch FC, Mather KA, Wen W, Sachdev PS. Associations between Alzheimer's disease polygenic risk scores and hippocampal subfield volumes in 17,161 UK Biobank participants. *Neurobiology of Aging 2021;* 98: 108-115. doi: 10.1016/j.neurobiolaging.2020.11.002

Foo H, Mather KA, Jiang JY, Thalamuthu A, Wen W, Sachdev PS. Genetic influence on ageing-related changes in resting-state brain functional networks in healthy adults: a systematic review. *Neuroscience and Biobehavioural Reviews 2020*; 113: 98-110. doi: 10.1016/j.neubiorev.2020.03.011

Foo H, Mather KA, Thalamuthu A, Sachdev PS. The many ages of man: Diverse approaches to assessing ageing-related biological and psychological measures and their relationship to chronological age. Current Opinions of Psychiatry 2019; 32(2):130-137. doi: 10.1097/YCO.0000000000000473

Poster Presentations

Foo H, Thalamuthu A, Jiang JY, Koch FC, Mather KA, Wen W, Sachdev PS. Associations between Alzheimer's disease polygenic risk scores and hippocampal subfield volumes in 17,161 UK Biobank participants. Organization for Human Brain Mapping (OHBM) Conference, Rome, Italy, June 2019.

Other Presentations

Foo, H. Brain ageing and degeneration: difference between normal and pathological ageing using T1-weighted MRI data. University of Melbourne, A/Prof Andrew Zalesky's lab. December 2020.

Scholarships and Travel Awards

University of New South Wales (UNSW) Scientia PhD Scholarship, Australia (2018 – 2021)

Tan Kah Kee Postgraduate Scholarship, Tan Kah Kee Foundation, Singapore (2018)

CHAPTER 1: INTRODUCTION

1.1 Context

Globally, the population is rapidly ageing. In 2019, there were 703 million persons aged 65 years and over and this number is projected to increase to 1.5 billion by 2050, representing 16% of the world's population (United Nations Department of Economic and Social Affairs, 2019). Similarly, in Australia, people aged 65 years and above increased from 12.3% to 15.9% between 1999 and 2019, and is projected to further increase to 28.4% by 2053 (McDonald, 2016). This transition towards an ageing population has also changed the leading cause of disease and death to noncommunicable diseases, such as cardiovascular disease, cancer, neurodegenerative disorders, and diabetes. It is estimated that by 2030, noncommunicable diseases will account for more than one-half of the diseases in low-income countries and three-fourths in middle-income countries (United Nations Department of Economic and Social Affairs, 2019). In Australia alone, a typical 78-year old individual costs the government approximately $24,000 per annum (McDonald, 2016). The ageing of the population therefore poses a financial challenge for governments. In turn, this has important implications for the socioeconomic and healthcare systems in both developing and developed countries.

Biologically, ageing is associated with declines at the molecular, cellular, and physiological levels (López-Otín, Blasco, Partridge, Serrano, & Kroemer, 2013). However, the relationship between aging and functional impairments, chronic disease, and mortality is heterogeneous in the health outcomes of older individuals as the impact of ageing differs markedly across individuals, which may be dependent on one's genetics, environment, and disease states (Lowsky, Olshansky, Bhattacharya, & Goldman, 2014). As increased life expectancy is not always accompanied by improved health and quality of life, considerable discussions about healthy ageing have been

raised. According to the World Health Organisation, healthy ageing is defined as "the process of developing and maintaining the functional ability that enables wellbeing in older age." This definition encapsulates intrinsic capacity, such as the mental and physical abilities, as well as the environment, which includes the home, community, and society, of an individual (World Health, 2015). In order to understand the multifactorial process in ageing, it is imperative to study the underlying biological mechanisms and environmental factors that seemingly separate healthy ageing from disability; as well as how disease states may result in dysfunction in ageing.

There is evidence to show that ageing is associated with decline in cognitive function (i.e. mental capacity) that may, in part, be accounted for by changes in neural plasticity and function of the brain (Chan, Park, Savalia, Petersen, & Wig, 2014; Shen et al., 2017). While the brain is structurally organised grossly into different regions specialised for processing and relaying neural signals, it is functionally subspecialised for perceptual and cognitive processing (Lv et al., 2018). Given the constraints of the underlying structural network, understanding the functional brain networks in healthy brain and using it to identify the abnormalities in brain disorders has become a common practice in ageing neuroscience (Meier et al., 2016). Changes in the dynamics of functional brain architecture may be influenced by an individual's genetics, environment, and disease states. In turn, the disruption of the brain's functional connectivity may result in overt cognitive decline.

1.2 Rationale

Complete understanding of genetics, environment, and disease-states influencing the differential topology of the functional networks remains to be elucidated. Investigating

how these factors affect functional connectivity in the human brain may potentially allow for better understanding of changes in functional network topology with ageing and the development of disease.

1.3 Aims of this thesis

The primary aim of this thesis is to explore the multifactorial processes that influence the functional brain networks using graph theory measures in older adults.

Specific aims are as follow:

1. To review existing evidence for genetic variants and environmental influences associated with functional brain networks;
2. To study the heritability and genetic variants associated with the graph theory measures;
3. To examine the relationships of age and sex with the graph theory properties, and how these relationships modify cognitive performance;
4. To study the relationship of sleep and other lifestyle factors including exercise, alcohol, and smoking, with graph theory measures; and
5. To investigate how major depressive disorder (MDD) phenotype and genotype are related to the graph theory measures.

1.4 Thesis outline

Chapter 2 provides a comprehensive review of the factors, including genetics, environmental factors, and disease states that have been suggested to influence resting-state functional connectivity (RSFC).

Chapter 3 investigates the genetic contributions to the functional brain networks. It examines the single nucleotide polymorphism (SNP) and gene level associations with functional network measures using graph theory analysis in a large population of older adults.

Chapter 4 focuses on the relationship of age and sex with the functional network measures and how this relationship modifies cognitive performance in older adults. Cognitive measures include processing speed, memory, and executive function.

Chapter 5 examines the association of sleep and other lifestyle factors with functional network measures. Sleep measures include both accelerometer derived data as well as self-reported sleep duration. Lifestyle factors include exercise, alcohol consumption, and smoking.

Chapter 6 focuses on disease contributions to functional network measures in a large population sample of older adults. It examines the relationship the genetics (as measured by polygenic risk score) and phenotype of depression with the functional network measures, respectively.

A summary of the main findings is presented in Chapter 7, followed by a discussion of their significance and clinical implications in light of the current literature. Limitations are also considered. Finally, future research directions are suggested.

CHAPTER 2: BACKGROUND

2.1 Background

The ageing human brain undergoes complex functional changes, which are associated with changes in cognition (Chan et al., 2014; Shen et al., 2017). These include significant age effects on the functional organisation of brain networks (Huang et al., 2015). Functional connectivity reflects the magnitude of temporal correlations in neural activity and may occur between pairs of anatomically unconnected brain regions (Rubinov & Sporns, 2010). Resting-state functional connectivity (RSFC) measures are commonly derived from resting-state functional magnetic resonance imaging (rs-fMRI) data, which examine the synchronisation of neural activity between regions by measuring the blood oxygen level-dependent (BOLD) signal fluctuations that occur at low frequencies (<0.1 Hz), where participants are scanned in the absence of a stimulus or task (Lv et al., 2018; Rosazza & Minati, 2011). Characterising resting-state functional changes in the ageing brain may increase our understanding of age-associated cognitive changes, even in the absence of disease (Burke & Barnes, 2006; Otte et al., 2015).

Many studies have explored the associations between age and RSFC either by using region of interest-based correlations (i.e. seed-based) or data-driven reduction techniques (i.e. independent component analysis - ICA), or whole brain approaches (i.e. graph theoretical analysis) (Grayson & Fair, 2017; Lee, Smyser, & Shimony, 2013). Within graph theory, quantitative measures of topological properties of networks, such as small-worldness, highly-connected hubs, and modularity (Otte et al., 2015; Perry et al., 2015; Rubinov & Sporns, 2010), can be calculated. Although these analytical approaches vary in their underlying assumptions and interpretation, it is assumed that functional connectivity measures the same neurophysiological processes (Thompson,

Ge, Glahn, Jahanshad, & Nichols, 2013). Using these techniques – including seed-based, ICA, and graph theory – several resting-state networks (RSNs), which are strong functionally linked sub-networks during rest (van den Heuvel & Hulshoff Pol, 2010), have been identified. These networks include but are not exclusive to the default mode (DMN), dorsal attention (DAN), frontoparietal control (FPCN), limbic (LIMB), salience/ ventral attention (SVAN), somatomotor (SM), and visual (VIS) networks (Lee et al., 2013; Yeo et al., 2011) (Table 2.1). Patterns of functional connectivity within and between major RSNs are regarded as intrinsic properties of brain function as they strongly predict patterns of co-activation during common processing tasks (Chan et al., 2014; Grayson & Fair, 2017). More specifically, DMN has been involved in cognitive control and higher cognitive demands for working memory. FPCN and DAN are implicated in attention, memory, and executive functions (Jiang et al., 2018; Vatansever et al., 2017).

Table 2.1 Composition and functions of commonly assessed functional networks

Networks	Composition	Functions
DMN	Precuneus, posterior cingulate cortex, bilateral inferior parietal cortices and medial prefrontal cortices (Fallon, Chiu, Nurmikko, & Stancak, 2016)	Emotional processing, self-referential mental activity, and recollection of prior experiences (Raichle, 2015)
DAN	Visual motion area, frontal eye fields, superior parietal lobule, intraparietal sulcus, and ventral premotor cortex (Spreng, Shoemaker, & Turner, 2017)	Engaged during externally directed attentional tasks (Spreng et al., 2017)
FPCN	Dorsolateral and dorsal medial prefrontal cortex and dorsal anterior cingulate cortex (Spreng et al., 2017)	Cognitive control processes to maintain goals, inhibit distractions, and shift behaviour in the service of goal attainment (Spreng et al., 2017)
LIMB	Anterior cingulate cortex, the amygdala, and hippocampus (de Carvalho et al., 2010)	Emotional regulation, executive control, and reward processing (Tang et al., 2019)
SVAN	Dorsal anterior cingulate cortex and bilateral anterior insula (Seeley et al., 2007)	Assesses the relevance of internal and external stimuli to guide behaviour (Seeley et al., 2007)
SM	Supplementary motor area, central sulcus, secondary somatomotor region, putamen, thalamus, contralateral cerebellum (Carter et al., 2012)	Planning, preparation, and execution of voluntary movements (Sánchez-Castañeda et al., 2017)
VIS	Primary, dorsal, and ventral visual networks (Shen et al., 2019)	Object recognition (Yang, Deng, Xing, Xia, & Li, 2015)

Abbreviations: DMN, default mode network; DAN, dorsal attention network; FPCN, frontoparietal control network; LIMB, limbic network; SVAN, salience/ventral attention network; SM, somatomotor network; VIS, visual network

Graph-based network theory models the brain as a complex network that is represented by a collection of nodes (e.g. brain regions) and edges (e.g. connectivity) (Wang, Zuo, & He, 2010b). Graph theoretical metrics may be used to capture the topological organisation of the human brain connectome through the computation of both global and local features, including global efficiency, characteristic path length, transitivity, modularity, and strength of the brain networks (Lv et al., 2018) (Table 2.2). This technique of studying rs-fMRI has proven to be useful in identifying normal development, ageing, and various brain disorders (Wang et al., 2010b).

There is evidence from neurodevelopmental studies of RSFC to show that strong functional connectivity between nearby brain regions and that selected local correlations tend to weaken while correlations with more distant brain regions tend to strengthen across childhood and adolescence (Power, Fair, Schlaggar, & Petersen, 2010). The observed changes in functional connectivity may be due to synaptic pruning (Huttenlocher, 1979) and myelination that occur throughout early life (Brody, Kinney, Kloman, & Gilles, 1987). Due to the constant state of alterations in the brain that accompany neurodevelopment, this review will only consider ageing-related changes in adults above 20 years old. In addition, this review will summarise published research on the influence of genetics, environmental factors, and disease-states on functional connectivity and graph theory measures using rs-fMRI in healthy adults.

Table 2.2 Graph theory measures and their association with age and ageing-related diseases

Graph theory measures	Definition	Associations with age and ageing-related diseases
Global efficiency	How effectively the information is transmitted at a global level and is the average inverse shortest path length. Higher values imply greater efficiency.	Older age was associated with reduced global efficiency compared to younger participants (Achard & Bullmore, 2007)
Characteristic path length	Integrity of the network and how fast and easily information can flow within the network. It is the average of all the distances between every pair of nodes in the network. Shorter characteristic path length reflects more efficient transmission of information.	Older age was associated with longer characteristic path lengths compared to younger participants (Sala-Llonch et al., 2014)
Louvain Modularity	Community detection method, which iteratively transforms the network into a set of communities, each consisting of a group of nodes. Higher modularity values indicate denser within-modular connections but sparser connections between nodes that are in different modules.	Brain networks in the elderly showed decreased modularity (less distinct functional networks) but findings were mixed (Chan et al., 2014)
Transitivity	Total of all the clustering coefficients around each node in the network and is normalized collectively. Higher values represent greater specialisation of the brain.	Patients with Alzheimer's disease (AD) showed lower normalized clustering coefficient (i.e. transitivity) (Supekar, Menon, Rubin, Musen, & Greicius, 2008)
Strength	Sum of all neighbouring edge weights. High connectivity strength indicates stronger connectivity between the regions.	Age-related differences were observed in network-level functional connectivity. However, findings were mixed (Betzel et al., 2014; Geerligs, Renken, Saliasi, Maurits, & Lorist, 2015; Song et al., 2014).

2.2 The influence of genetics on functional brain networks

Genetics may play a crucial role in influencing changes in the resting-brain functional organisational properties observed in ageing. Brain functional connectivity can be studied as endophenotypes for characterising disorders that are not yet observable (Dennis, Thompson, & Jahanshad, 2019). There is evidence to show that brain measures, including RSFC, are heritable (Buckner, 2004; Glahn et al., 2010). Therefore, studying genetics and RSFC may increase our understanding of the underlying biological mechanisms that influence functional specialisation across various brain regions in the ageing brain.

2.2.1 Heritability of functional brain networks

Heritability analysis estimates the relative influence of genes and the environment on a particular phenotype. It is defined as the proportion of the observed variation in a particular trait that can be attributed to genetic versus environmental factors. Classical heritability studies include twin, family, and adoption studies. Alternatively, SNP heritability (h^2_{SNP}), uses SNP data, commonly provided by genome-wide genotyping to assess genetic similarity between individuals (Mayhew & Meyre, 2017; Speed et al., 2017). Trait heritability (h^2) of less than 0.30 is considered as low, 0.30 to 0.60 as moderate, and above 0.60 as high (Visscher, Hill, & Wray, 2008). A significant h^2 estimate implies that a trait is significantly influenced by genetic factors, making it an appropriate target for genetic analyses (Thompson et al., 2013). Given the complex relationship between BOLD fMRI measures – including blood flow, blood volume, and oxygen metabolism – and the molecular mechanisms that control neuronal firing patterns, the exact biological mechanisms contributing to signal variation of rs-fMRI remain unclear. Establishing heritability of RSFC is therefore important in order to

justify further genetic studies and to improve our understanding of the biological pathways involved (Fornito et al., 2011; Glahn et al., 2010; Korgaonkar, Ram, Williams, Gatt, & Grieve, 2014)

As shown in Table 2.3 and Figure 2.1, heritability of functional connectivity measures has been assessed by a number of studies, although many of them have examined different RSN properties. The majority of studies observed significant heritability. Using a twin study design, one study found that within-network connectivity in DMN, sensory-somatomotor, dorsal attention, and visual networks were more heritable than averaged between-network connectivity as a whole (Reineberg, Hatoum, Hewitt, Banich, & Friedman, 2020). Functional connectivity within DMN as a whole was moderately heritable (h^2: 30% - 42%) in both family and twin studies in middle-aged adults (Glahn et al., 2010). Other networks, including precuneus-dorsal posterior cingulate network, visual network, frontoparietal, dorsal attention network, auditory, executive control, and salience, showed low-to-strong heritability (h^2: 20% - 80%) in both young and middle-aged twins (Ge, Holmes, Buckner, Smoller, & Sabuncu, 2017; Miranda-Dominguez et al., 2018; Yang et al., 2016). Using both twins and family cohorts of young and middle-aged adults, h^2 estimates were low-to-moderate across various regions within networks such as auditory, frontoparietal, visual, executive control, salience, and attention (Adhikari et al., 2018). Middle-aged adults had weakly-to-moderately heritable (h^2: 10% – 42%) connectivity of subcomponents of DMN in a family study (Glahn et al., 2010). Moderate heritability was observed for connectivity between the posterior cingulate cortex and inferior parietal cortex (h^2 = 41%) (Korgaonkar et al., 2014), and connectivity between DMN and sensory/somatomotor networks was also moderately heritable (h^2 = 36%) (Reineberg et al., 2020). Graph

theoretical measures in twin studies showed low heritability for connection strength (h^2: 15% - 18%) (Colclough et al., 2017), moderate heritability (h^2 = 60%) for cost-efficiency (Fornito et al., 2011), and moderate heritability (h^2: 38% – 64%) for mean clustering coefficient, modularity, global efficiency, and small worldness (Sinclair et al., 2015). Interestingly, one twin study observed higher estimated within-network heritability when leveraging shared features across both rs-fMRI and task-based fMRI than rs-fMRI alone (Elliott et al., 2019). Using genome-wide genotyping to estimate h^2_{SNP}, one study found that 235 of 1,771 rs-fMRI image-derived phenotypes (IDPs) showed low to moderate h^2_{SNP} (Elliott et al., 2018). Importantly, h^2_{SNP} typically provides smaller heritability estimates relative to those provided by the classic design.

In general, low to moderate heritability estimates were reported for RSFC measures in healthy adults from a range of ages, implying significant genetic underpinnings for variability in RSFC measures across brain regions in cognitively unimpaired populations. Interestingly, Reineberg et al. (2018) demonstrated higher heritability of within network than between network properties, suggesting that genetic influence on the connectivity of regions involved in the same process may be driving functional brain organisation (Reineberg et al., 2018). As demonstrated by Elliott et al. (2019), heritability estimates increase when combining both rs-fMRI and task-based fMRI data, thus future studies should investigate the genetic influence on functional connections both at rest and when in active states. There may be potential age effects on the heritability of resting-state networks. The heritability findings summarised here are from a range of ages.

Table 2.3 Studies examining the heritability of functional connectivity using rs-fMRI in healthy adults

Measure	Method	Total sample size	Sex	Age (years); M (SD)/ age range (years)	Ethnicity	Heritability (h^2) results	Reference (year)
5 nodes within DMN	Seed based correlation	277 from 2 cohorts: (1) twin cohort (250 twins: 79 MZ & 46 DZ); (2) 27 unrelated/nontwins	(1) 96M & 154F; (2) 15M & 12 F	39.7 (12.8)	European ancestry	Posterior cingulate cortex - R inferior parietal cortex (PCC-RIPC) connectivity - 41% Other measures n.s.	Korganokar et al. (2014)
AN, DMN, FPN, VN, ECN, SN, AttN, SMN	Seed-based & dual-regression	2 cohorts: (1) GOBS (334 individuals - 29 extended pedigrees); (2) HCP (518 - MZ, DZ, non-twin siblings)	GOBS: 124M & 210F; HCP: 240M & 278F	GOBS: 47.9 (13.2); HCP: 28.7 (3.7)	GOBS: Mexican-Americans; HCP: Mainly Caucasians	20% - 40% across the 8 networks	Adhikari et al. (2018)
1 cm spherical ROIs drawn from each of the 264 functional areas	Power parcellation, ROI	2 cohorts: (1) LTS (251 - 102 MZ pairs, 91 DZ pairs, 34 MZ twin singletons, 45 DZ twin singleton); (2) HCP (442 -	LTS: 97M & 154F; HCP: 171M & 271F	LTS: 28.7 (0.63); HCP: 29.2 (3.46)	LTS & HCP: Mainly Caucasians	36% for DMN to sensory/SMN connection as a whole	Reineberg et al. (2020)

		136 MZ pairs, 75 DZ pairs)					
DMN (8 anatomical regions)	Dual-regression, ICA	GOBS: 333 individuals - 29 pedigrees	123M & 210F	48.38 (12.9)	Mexican-American	42.4% as a whole	Glahn et al. (2010)
PCN, VN, DMN, FPN, SN, SMN, DAN	ICA	QTIM: 105 - 80 DZ, 25 singletons	51M & 54F	19-29	Caucasians	5/7 networks heritable (i.e. PCN, VN, DMN, FPN, DAN) h^2 = 23.3% - 65.2%	Yang et al. (2016)
Network edges. SNP heritability estimated.	ICA	UK Biobank: 8428 (unrelated individuals)	4045M & 4383F	40-69	English	235/1771 functional connectivity edges heritable	Elliot et al. (2018)
39 cortical regions (network nodes)	Parcellation from resting-state 100-dimensional group ICA decomposition	HCP: 820 - MZ & DZ twin pairs	Information not available	22 – 35	Mainly Caucasians	15.0% - 18.0% for connection strength between components of nodes (eg. DMN, motor network, VN, DAN)	Colclough et al. (2017)
7 network parcellations (i.e. VN, SMN, DAN, salience ventral attention, limbic, control, DMN) split	Yeo seven-network parcellation	2 cohorts: (1) HCP (528 - 92 MZ, 46 DZ twin pairs, 250 full siblings, 56 singletons); (2) GSP (809 unrelated younger subjects)	HCP: 203M & 325F; GSP: 362M & 447F	HCP: 29.21 (3.47); GSP: 20.84 (2.77)	Mainly Caucasians	~ 45.0% - 80.0% for all network parcellations	Ge et al. (2017)

into 51 spatially contiguous regions across 2 hemispheres							
12 functional networks (i.e. auditory, cingulo-opercular, cingulo-parietal, DMN, DAN, FPN, retrosplenial temporal, SN, SMN hand, SMN mouth, VAN, & VN) into 333 ROIs	Gordon parcellation	2 cohorts: (1) longitudinal study in Oregon (159); (2) HCP (198 – MZ, DZ, non-twin siblings)	HCP: 89M & 109F	HCP: 28.4 (3.50)	Mainly Caucasians	~ 20% across the whole brain; driven by high-order systems including the FPN, DAN, VAN, cingulo-opercular, & DMN	Miranda-Dominguez et al. (2018)
Network edges	Power and Yeo parcellation	2 cohorts: HCP (298 - MZ, DZ, full siblings); (2) Dunedin Study (591)	Information not available	HCP: 25-35; Dunedin Study: 45	Mainly Caucasians	Within-network heritability ↑ from 22% in rs-fMRI to 28% when combining task-based fMRI & rs-fMRI at 40 minutes scan time	Elliot et al. (2019)

Network cost-efficiency (global & regional communication efficiency, connection distance, connection density)	1041 cortical regions parcellated, graph theory	58 - 16 MZ & 13 DZ twin pairs	28M & 30F	40.48 (11.77)	Caucasians	60% in network-cost efficiency	Fornito et al. (2011)
Mean clustering coefficient, global efficiency, modularity, & rich club coefficient	AAL template, 116 regions, graph theory	QTIM: 591 - 84 MZ & 89 DZ twin pairs, 246 single twins	MZ: 23M & 61F; DZ: 34M & 55F; single twins information not provided	23.0 (2.5)	Caucasians	47% – 61% for mean clustering coefficient; 38% – 59% for modularity; 52% - 64% for global efficiency; 51 – 59% for small worldness	Sinclair et al. (2015)

L, left; R, right; fMRI, functional magnetic resonance imaging; Rs-fMRI, resting-state functional magnetic resonance imaging; ROI, region of interest; LAN, auditory network; AttN, attention network; DAN, dorsal attention network; DMN, default mode network; ECN, executive control network; FPN, fronto-parietal network; PCN, posterior cingulate network; SMN, sensorimotor network; SN, salience network; VAN, ventral attention network; VN, visual network; ICA, independent component analysis; MZ, monozygotic; DZ, dizygotic; GOBS, Genetics of brain structure and function study; HCP, Human connectome project; GSP, Genomics superstruct project; LTS, Colorado longitudinal twin study; QTIM, Queenland Twin Imaging study; USA, United States of America; UK, United Kingdom; n.s., no significant results

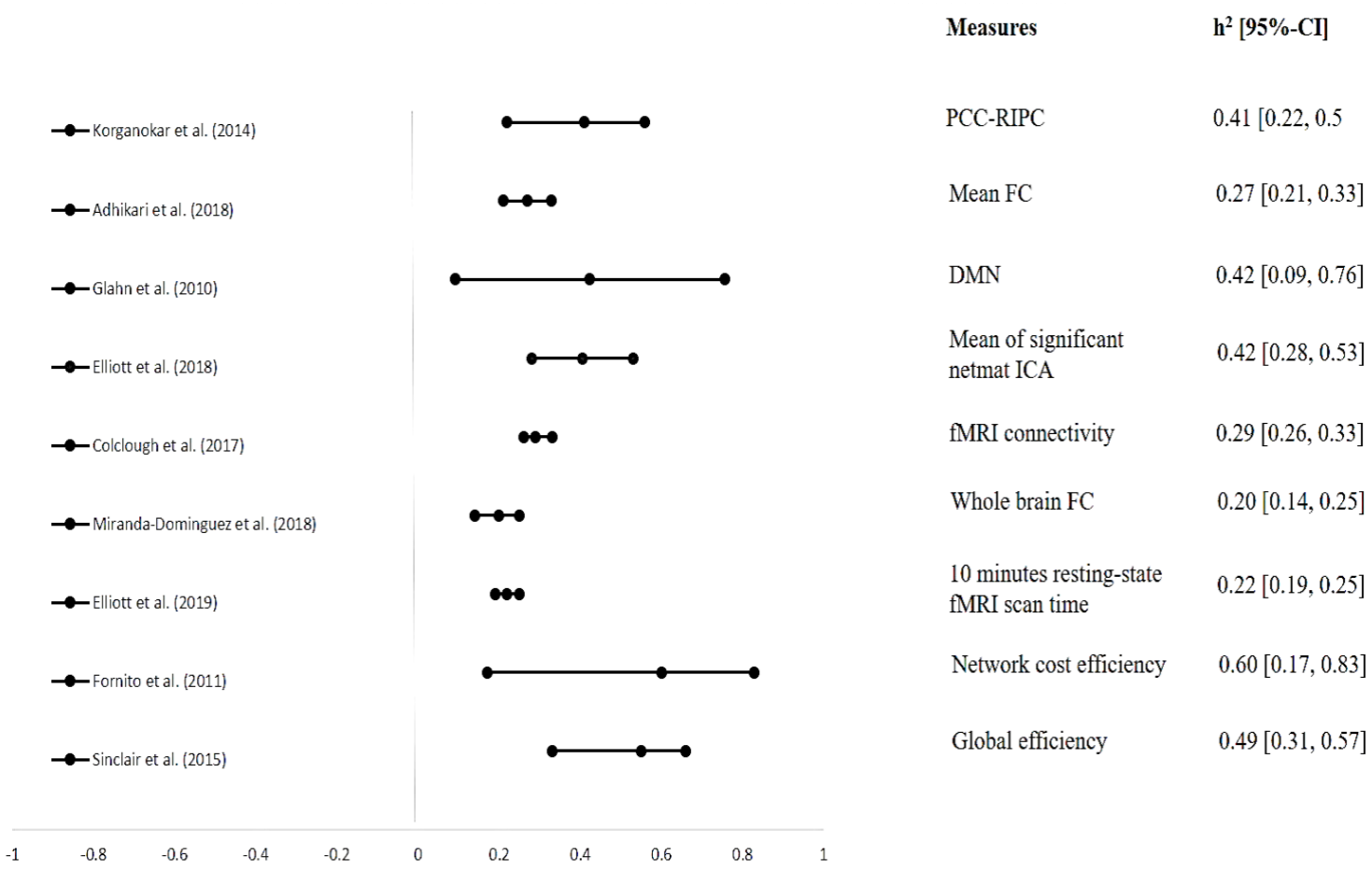

Figure 2.1 Forest plot showing the heritability estimates of various resting-state network measures from 9 studies.

Three of the 12 studies did not report confidence intervals and/or standard errors, which precluded them from being added into the forest plot. Note that non-significant heritability results are not included. Abbreviations: PCC-RIPC, posterior cingulate cortex-right inferior parietal/temporal cortex; FC, functional connectivity, DMN, default mode network, ICA, independent component analysis.

2.2.2 GWAS of functional brain networks

GWAS use a hypothesis-free approach to systematically test multiple genetic variants across the genome. It has been used to identify many genetic variants, commonly SNPs, associated with a wide range of traits (Choi, Mak, & Reilly, 2018).

However, thus far, there has only been one GWAS investigating the genetics of rs-fMRI. This was performed in 8428 adults aged between 40 and 69 years old using the United Kingdom (UK) Biobank data (Elliott et al., 2018). They used group-ICA to identify the major RSNs and estimated network matrices for all participants. Their findings demonstrated several SNPs, including rs60873293, rs35124509, rs2279829, rs7442779, rs2274224, and rs11596664 were associated with RSN measures. This study highlights the potential contributions of genetic variation in influencing resting-state functional connectivity in mid-late life. Findings from a GWAS investigating imaging phenotypes found several SNPs to be associated with RSFC measures (Elliott et al., 2018). A reported variant for middle temporal sulcus nodes and edges, rs35124509, is a non-synonymous SNP located in the EPH Receptor A3 (*EPHA3*) gene and is also an eQTL for *EPHA3*. Notably, the product of this gene has been associated with the regulation of cell migration, axon guidance, and trans-axonal signalling (Gallarda et al., 2008; Shi et al., 2010). Another SNP identified from the RSFC GWAS, namely rs2279829 (Elliott et al, 2018), which is located in the 3' untranslated region of the gene *ZIC4,* has been linked to brain development and is associated with parietal lobe volume and a rare brain disease, Dandy-Walker Malformation (van der Lee et al., 2019). SNPs close to or located in other genes were also identified, including *PLCE1*, *NR2F1*-AS1 and *INPP5A*. Many of these polymorphisms had not been previously identified in regard to RSFC measures or other neuroimaging/brain phenotypes. Identification of

these variants may have implications in the maintenance and/or disruption of RSFC observed across adulthood. However, due to the paucity of literature, more GWAS are required to identify further loci. Independent replication of the aforementioned results is required to confirm the relationships between previously identified genetic variants and resting-state functional connectivity measures in adults over the lifespan.

2.3 Ageing-related changes in functional brain networks

Ageing-related changes in resting-state functional connectivity have been observed. Previous studies found increased inter-network (between RSNs) connections and decreased intra-network (within RSNs) connections in healthy older adults compared to younger adults (Betzel et al., 2014; Geerligs et al., 2015; Grady, Sarraf, Saverino, & Campbell, 2016; Huang et al., 2015). The increased connectivity may be explained by possible compensatory mechanisms (Seidler et al., 2010) or even early stages of neurodegenerative pathologies (Vemuri, Jones, & Jack, 2012).

Most consistently, studies showed that ageing is associated with lower within-network connectivity and decreased functional connectivity in the DMN compared to younger adults (Damoiseaux, 2017; Dennis & Thompson, 2014). This is particularly apparent in the anterior and posterior components of the DMN (Andrews-Hanna et al., 2007; Ng, Lo, Lim, Chee, & Zhou, 2016), such as the hippocampus (Damoiseaux, Viviano, Yuan, & Raz, 2016) and frontoinsular cortex (He et al., 2013). Besides the DMN, other studies also showed that aging disrupts the connectivity in the salience and visual networks (Onoda, Ishihara, & Yamaguchi, 2012), and putamen-occipital, and frontal-occipital connectivity (Fjell, Sneve, Grydeland, Storsve, & Walhovd, 2017; Fjell et al., 2016). However, another study showed preservation of visual networks (Geerligs et al., 2015).

Generally, decrease in connectivity is mainly found in the high-function networks, including DMN, cingulo-opercular, and frontoparietal control networks, while the primary function networks, such as somatomotor network, are mainly preserved (Geerligs et al., 2015).

In addition, findings from the graph theoretical approach demonstrate that normal ageing is associated with reduced global and local efficiency, increased local network clustering, and reduced centrality of hub regions (Achard & Bullmore, 2007; Dennis et al., 2013; Geerligs et al., 2015; Gong et al., 2009; Hagmann et al., 2008; Meunier, Achard, Morcom, & Bullmore, 2009; Montembeault et al., 2012; Otte et al., 2015; Spreng & Schacter, 2012; Wu et al., 2012; Zhu et al., 2012).

2.4 Sex differences in functional brain networks

Sex differences have been observed in the human brain – men have larger crania, higher percentage of white matter (Gur et al., 1999) whereas women have higher percentage of gray matter (Goldstein et al., 2001). Several regions in the brain, including the hippocampus, amygdala (Giedd, Castellanos, Rajapakse, Vaituzis, & Rapoport, 1997), and corpus callosum (Allen, Richey, Chai, & Gorski, 1991), have also been shown to differ in sex. These anatomical brain differences may underlie the behavioural differences such as better motor and spatial skills for men and enhanced memory and social cognition for women (Gur et al., 2012; Halpern et al., 2007).

Previous studies have revealed sex-by-hemispheric interaction where men showed greater rightward lateralisation and women showed greater leftward lateralisation (Tomasi & Volkow, 2012b), with higher local functional connectivity in women than

men (Tomasi & Volkow, 2012a). In addition, sex has been shown to differ in connectivity where men showed network segregation (i.e. specialised processing of the brain at a local level) whereas women showed more network integration (i.e. how rapidly the brain can integrate specialised information at a global network level) (Zhang et al., 2016). Another study observed that men had higher clustering coefficient in the right hemisphere than the left hemisphere (Tian, Wang, Yan, & He, 2011). Despite this, the influence of sex on functional connectivity remains to be elucidated.

2.5 Lifestyle factors

Lifestyle factors, such as sleep, exercise, alcohol, and smoking, may interact with each other to influence the organisational properties of the brain functional networks. Importantly, it is noteworthy that most of these previous works look at associations between these factors, which imply that causality cannot be inferred.

2.5.1 The influence of sleep behaviour on functional brain networks

Sleep is a complex and dynamic process for maintaining homeostasis, where sleep deprivation can disrupt whole-body functioning with the most pronounced impact on the central nervous system (Farahani et al., 2019a). Adults increasingly experience sleep problems with age (Foley et al., 1995), which have been associated with the development of stroke (Wu, Chen, Yu, Wang, & Guo, 2018) and dementia (Shi et al., 2018). Therefore, identifying the underlying brain functional changes associated with sleep patterns may help to contribute to the understanding between sleep and disease states.

Rs-fMRI data has frequently been used to measure the hemodynamic fluctuations as a proxy for neural activity to investigate the neurophysiological mechanisms underlying sleep-related abnormalities (Farahani et al., 2019a). Using ICA, Lysen et al. (2020) observed that in the middle-aged and elderly population, total sleep time affected prefrontal activity but did not find any associations of objective and subjective sleep measures with between or within resting-state networks. This is contrary to a study by Nilsonne et al. (2017) who showed that sleep deprivation had a consistent impact on the within-network connectivity of the DMN. Another study also found that partial sleep deprivation was associated with reduction of functional connectivity in the DMN and its anticorrelated network (Sämann et al., 2010), which play a central role in processing cognitive functions dependent on internally constructed representations (Buckner & DiNicola, 2019). This disparity in findings may be, in part, attributable to the differences in sleep measures or even the imaging processing/modelling approaches (Lysen et al., 2020).

Using graph theoretical approach, a study involving healthy young adults (mean age = 21.1 and standard deviation = 1.9 years) also showed that small-world property (as measured by clustering coefficient and path length) was significantly enhanced in the sleep deprivation group compared to the sleep sufficient group (Liu, Li, Wang, & Lei, 2014). This implies a more optimal network topology and lesser wiring cost, which may be a compensatory effect (Liu et al., 2014). However, it seemed that there was no difference in small-world property between individuals with narcolepsy, which is a chronic sleep disorder with symptoms of excessive daytime sleepiness and the occurrence of rapid eye-movements (REM) and daytime sleep attacks, and controls (Xiao et al., 2019). These individuals showed altered local properties in the left putamen

and left posterior cingulate compared to controls instead (Xiao et al., 2019). Another study found that individuals with chronic insomnia disorder, which is characterised by difficulties falling asleep at bedtime, frequent awakenings in the middle of the night, and waking up too early in the morning (Kay & Buysse, 2017), showed disruptions in both global and local topological organisation of the brain functional connectome (Li et al., 2018). More specifically, these individuals showed decreased number of modules and hierarchy, increased assortativity, and altered nodal centrality in the DMN, dorsal attention, and sensory-motor networks (Li et al., 2018). While these studies show that sleep patterns may influence the functional topology of the brain, there is a paucity of literature in the ageing population.

2.5.2 The influence of exercise on functional brain networks

There is evidence showing that exercise may play a central role in ameliorating age-associated changes in brain structure and function (Hillman et al., 2006). Results from meta-analyses showed that aerobic exercises had general and selective effects that were beneficial to cognitive function in older adults (Colcombe & Kramer, 2003; Etnier, Nowell, Landers, & Sibley, 2006). Several studies have used RSFC to examine the plasticity of human brain networks in response to acute moderate-intensity exercise in a sample of healthy adults (Schmitt et al., 2019; Weng et al., 2017). Acute exercise increased the integration of attention and executive control networks as well as increased functional connectivity within the affect and reward network (ARN), which were brain regions associated with reward processing, learning and memory (Schmitt et al., 2019; Weng et al., 2017). In addition, pre-to-post comparisons after low intensity exercise revealed significant increase in RSFC in the frontoparietal network while high intensity exercise showed decrease RSFC in the sensorimotor and dorsal attention

networks and increase in left ARN (Schmitt et al., 2019). The findings suggest that different acute exercise intensities may have differential impact on the functional brain networks and cognitive responses. Other studies investigating the long-term effects of repeated exercise over several months showed stronger RSFC between the right parahippocampal gyrus and motor sensory, and mood regulating areas (Tozzi et al., 2016); as well as between DMN and primary motor regions associated with improved motor performance (McGregor et al., 2018). However, another study did not see any significant changes in intrinsic brain activity after six months of aerobic exercise (Flodin, Jonasson, Riklund, Nyberg, & Boraxbekk, 2017).

2.5.3 The influence of alcohol on functional brain networks

Alcohol consumption among older adults (aged between 60 and 69 years old) increased by 24% between 2001 and 2007 (Livingston, Callinan, Raninen, Pennay, & Dietze, 2018). It has been observed that alcohol acts to increase inhibitory neurotransmission, which decreases the responsiveness of other neurons to further stimuli (Lithari et al., 2012). Their effect on neurotransmitters, may, in part explain for some of the behavioural (do Canto-Pereira, David, Machado-Pinheiro, & Ranvaud, 2007), cognitive (De Cesarei, Codispoti, Schupp, & Stegagno, 2006), and affective stimuli processing (Curtin, Patrick, Lang, Cacioppo, & Birbaumer, 2001) changes seen when intoxicated. Therefore, understanding the neurophysiological mechanisms by which alcohol acts on the brain, thereby modifying behaviour, is imperative (Lithari et al., 2012).

Rs-fMRI studies have found a relationship between the intake of alcohol and cognitive, motor, and coordination dysregulation (Camchong, Stenger, & Fein, 2013; Chanraud, Pitel, Pfefferbaum, & Sullivan, 2011). Alcohol studies based on rs-fMRI observed

altered functional relationship and corresponding compensatory mechanisms among different brain regions associated to these deficits (Vergara, Liu, Claus, Hutchison, & Calhoun, 2017). Decreased functional connectivity in the left superior parietal gyrus and left interparietal sulcus of the dorsal attention network; and in the right superior frontal gyrus and right middle frontal gyrus of the default mode network were seen in individuals with alcohol-use disorder (Song, Chen, Wen, & Zhang, 2020). Significant decrease of functional connectivity in executive control, sensorimotor, visual, and subcortical networks was also observed in alcoholics compared to controls (Weiland et al., 2014). Interestingly, these regions also predicted relapse in alcoholics (Camchong et al., 2013). One study investigated whether moderate-heavy alcohol consumption was associated with increased age-related brain network changes in community-dwelling older adults (age range 65-80 years) compared to younger adults (age range 24-35 years) (Mayhugh et al., 2016). Their results revealed that alcohol consumption levels were not associated with overall changes in resting-state functional brain network topology in older adults. Taken together, findings suggest that alcoholic individuals may have an abnormal top-down attention modulation and cognition (Song et al., 2020), which may result in maladaptive decision making around alcohol use and relapse (Wilcox, Dekonenko, Mayer, Bogenschutz, & Turner, 2014). However, given the paucity of studies looking at community dwelling older adults, there is a need to study how alcohol consumption may accelerate age-related changes in functional connectivity.

2.5.3 The influence of smoking on functional brain networks

Nicotine is an addictive substance that has been known to enhance cognitive function during acute administration but cognitive impairment during acute withdrawal (Levin,

McClernon, & Rezvani, 2006). The mechanisms of cognitive enhancements are unknown but likely involve neuronal activation directly through nicotine cholinergic receptors (Poorthuis, Goriounova, Couey, & Mansvelder, 2009) and indirectly through the modulation of glutamate, GABA, dopamine or monoamine oxidase (MAO) inhibitors (Brody et al., 2004; Swan & Lessov-Schlaggar, 2007). Therefore, understanding nicotine's effects at a circuit level may be critical for the development of addiction treatment and the improvement of clinical outcomes.

Rs-fMRI studies have observed changes in the ventral and dorsal striatum (Sweitzer et al., 2016), frontostriatal region (Froeliger et al., 2015), prefrontal and limbic regions (Janes, Nickerson, Frederick Bde, & Kaufman, 2012), insula and parahippocampus (Ding & Lee, 2013), as well as widespread functional connectivity attenuation in the reward circuit (Shen et al., 2016) in smokers compared to non-smokers. In addition, the use of nicotine seems to have an enhancement effect on brain functional connectivity in motor, attention, and memory circuits (Jasinska, Zorick, Brody, & Stein, 2014). Decreased DMN and enhanced extra-striate activity with administered nicotine has been associated with an activity shift from internal to external information processing networks (Tanabe et al., 2011). It is possible that cholinergic agonist may have effect in mental disorders, including depression (Greicius et al., 2007) and schizophrenia (Zhou et al., 2007), associated with altered resting-state activity (Tanabe et al., 2011). Contrastingly, findings on nicotine effects during abstinence based on resting-state functional connectivity demonstrated a shift towards internal information processing represented by the DMN where the insula played a crucial role (Sutherland, McHugh, Pariyadath, & Stein, 2012). Given that the insula plays a significant role in the maintenance of tobacco dependence (Naqvi & Bechara, 2010) and has the highest

density of acetylcholine receptors within the human cortex (Picard et al., 2013), it is not surprising that the abnormal interactions due to nicotine addiction between brain networks of external and internal attention is regulated by a salience network anchored in the insula (Fedota & Stein, 2015). As evidence has it, nicotine plays a role in influencing the brain functional connectivity. However, there is a lack of studies investigating this in an older population, which warrants the need to determine if nicotine accelerates the process of functional brain network ageing.

2.6 Disease states

Disease states, including disorders such as depression, may influence the organisational properties of the brain functional network. Given that disease-states may be influenced by the inherent genetic make-up, it may be more holistic to consider the influence of both the genetics as well as the behavioural patterns of these phenotypes on brain functional topology.

2.6.1 The influence of major depressive disorder (MDD) on functional brain networks

Major depressive disorder (MDD) is characterised by pervasive sadness or irritability, disturbances in sleep, and withdrawal from pleasurable activities (Belmaker & Agam, 2008). It is the leading contributor to the global burden of disease due to its high prevalence, disabling consequences, and partial treatment response (Shen et al., 2020).

Due to the ambiguity of the aetiology of MDD, one assumption is that MDD results from a dysfunction in information-processing within the neuronal network rather than chemical imbalance in the brain's molecular structure (Castrén, 2005; Eickhoff & Grefkes, 2011; Leistedt & Linkowski, 2013). Previous studies found that MDD is

phenotypically correlated with brain functional networks (Gong & He, 2015; Jin et al., 2011; Meng et al., 2014; Ye et al., 2015; Zhang et al., 2011; Zhi et al., 2018). Networks including the default mode (DMN) (Yan et al., 2019; Zeng et al., 2012), affective (AN) (Zeng et al., 2012), and cortico-limbic (Hooley et al., 2009) networks have been associated with MDD. Others have reported reduction of functional connectivity in the hippocampus (Cao et al., 2012; Tahmasian et al., 2013), as well as from the posterior cingulate cortex to the caudate nucleus, thalamus, superior medial frontal gyrus, and superior frontal gyrus (Guo et al., 2013; Horn et al., 2010). Increased connectivity from the dorsomedial prefrontal cortex to the cognitive control network (CCN), DMN, and AN was also seen in MDD (Sheline, Price, Yan, & Mintun, 2010). The link between these regions may provide a potential mechanism to explain how symptoms of depression, including decreased focus, rumination, excessive self-focus, increased vigilance, and emotional, visceral, and autonomic dysregulation, may occur concomitantly and have synergistic effect (Sheline et al., 2010). Another study showed increased connectivity between the subgenual cingulate, thalamus, orbitofrontal cortex, and precuneus in MDD (Greicius et al., 2007).

Using graph theoretical approach, while Zhang et al. (2011) observed an increased in global efficiency and decreased nodal degree in MDD patients, Meng et al. (2014) showed a decrease in global efficiency and Jin et al. (2011) reported an increased nodal degree. This heterogeneity may, in part, be due to the differences in threshold used in binarised connectivity matrices (i.e. presence or absence of edge).

Importantly, given the heterogeneity in the definition of MDD, the difference in medicated or drug-naïve group, and the variations in the analysis method used for resting-state fMRI data, the results from MDD should be taken with extra caution.

2.7 Summary and gaps in the current literature

Rs-fMRI has gained advantages over other fMRI techniques due to its ease in signal acquisition and its application in the research and clinical setting has been growing over the past two decades (Lv et al., 2018). In addition, rs-fMRI has been widely used to characterise resting-state networks in both the healthy brain and in multiple disease states (Lee et al., 2013). There are several ways to analyse rs-fMRI data and each approach has implications with regards to the type of information that can be extracted from the data (Lv et al., 2018). Before the application of any of the analytical methods, preprocessing steps including realignment, removal of confounders (e.g. head motion and CSF signals), data normalisation, and smoothing, should be performed to ensure the reliability of the data. However, there is no single method currently considered a gold standard.

Given that the human brain is comprised of interconnected networks, this study is interested to study the properties of complex functional brain networks. These properties allow us to understand both the local and global organisation of neural networks, which may be important for providing a conceptual framework to help reduce the analytical brain complexity and underlying how network topology may be used to characterise and model vulnerabilities and resilience to ageing and brain diseases (Vecchio, Miraglia, & Maria Rossini, 2017).

Human functional network connectivity studies are a relatively new and growing field which offers a promising approach for elucidating the biological mechanisms underlying the functional organisation of the brain. However, the current functional network literature in association with genetics, environmental factors, and disease states is still in its infant stage. Findings are mixed and often lack validation, and cohorts are typically small. The differences in methodology used add to the inconsistencies in the literature. Due to the computational powers needed to study the brain at the level of voxels or small regions, current efforts have focused on quantifying these associations on either global summary measures of functional connectivity or large regions of interest (ROIs) (Reineberg et al., 2020). Therefore, in this thesis, I investigated the multifactorial processes that influence topology of the functional brain networks properties using graph theoretical measures.

Using genetics to investigate the functional networks may provide a better understanding of the underlying biological mechanisms contributing to the ageing brain. However, comprehensive modelling of the whole-brain and genome-wide data remains challenging due to the statistical and computational difficulties (Thompson et al., 2013). To address this issue, some studies have used a-priori biological information, such as examining candidate genes and biological pathways. However, this precludes the discovery of new genes associated with functional networks. In order to perform GWAS on RSFC, statistical methodologies of data reduction on imaging analysis can be performed. For instance, instead of binary connectivity matrix in graph theory analysis, using weighted connectivity matrix will not only provide a more holistic representation of the functional brain networks, it also allows for a more streamlined genetics analysis. Rather than performing GWAS on all different thresholds associated with binary

matrices, it might be more computationally feasible to run GWAS on a single weighted matrix. Importantly, there is a greater need for statistically and computationally powerful methods in order to cope with the high dimensionality of the imaging and genetics data and their covariates. Also, the increasing availability of whole genome sequencing data will add additional computational burden.

Using publicly available population-based datasets, such as the UK Biobank, that include both genetics and environmental factors, and imaging data are important to advance the field. It not only allows for better quality control and integrity of the data; it also provides researchers with the ability to replicate findings from other studies.

This review laid the foundation for the research in this thesis and highlighted areas where the research is lacking and/or inconsistent. Therefore, this thesis aims to address these gaps in the literature by examining genetics and environmental factors, as well as disease states contributing to the topological architecture of the functional brain networks using data from the UK Biobank. Integration of several lines of evidence is expected to extend current findings and potentially shed light on the neurobiological pathways and processes involved in the pathologies associated with the disruption of brain networks.

CHAPTER 3: HERITABILITY AND GENOME-WIDE ASSOCIATION STUDY OF FUNCTIONAL NETWORK TOPOLOGY IN THE AGEING BRAIN

Abstract

I investigated the genetics of weighted functional brain network graph theory measures from 18,445 participants of the UK Biobank (44-80 years). The eighteen measures studied showed low heritability (mean h^2_{SNP} =0.12) and were highly genetically correlated. One genome-wide significant locus was associated with strength of somatomotor and limbic networks. These intergenic variants were located near the *PAX8* gene on chromosome 2. Gene-based analyses identified five significantly associated genes for five of the network measures, which have been implicated in sleep duration, neuronal differentiation/development, cancer, and susceptibility to neurodegenerative diseases. Further analysis found that somatomotor network strength was phenotypically associated with sleep duration and insomnia. Single nucleotide polymorphism (SNP) and gene level associations with functional network measures were identified, which may help uncover novel biological pathways relevant to human brain functional network integrity and related disorders that affect it.

3.1 Introduction

During aging, the human brain undergoes functional changes which affect the integration of information within and between functional brain networks, and these have been shown to be associated with behavioural changes (Chan et al., 2014). By modelling large-scale brain networks using graph theory, defined by a collection of nodes (brain regions) and edges (magnitude of temporal correlation in functional magnetic resonance imaging (fMRI) activity between two brain regions) (Bertolero, Yeo, Bassett, & D'Esposito, 2018; Rubinov & Sporns, 2010), it is possible to investigate aging-related topological changes. Previous functional graph theory studies have mainly considered edge presence or absence represented as a binary variable (Cohen & D'Esposito, 2016; Geerligs et al., 2015; Song et al., 2014), which precludes information about variations in connectivity weights between networks. Given that connection weights exhibit high heterogeneity over several orders of magnitude (Markov et al., 2013), studying weighted brain networks may provide greater insights into their underlying hierarchy and organisational principles.

Genetics may play an important role in influencing changes in the functional topology of the aging brain. Graph theoretical brain functional measures are reported to be heritable (Fornito et al., 2011; Sinclair et al., 2015). However, to date, there has not been any population-based study investigating the genetic contribution to functional connectivity using graph theory measures. Studying the genetic architecture of graph theory brain functional measures has important implications (Thompson et al., 2013) - firstly, it can identify genes associated with network topology; and secondly, it may provide insights into the underlying biological mechanisms of macroscopic network topology in aging and how it alters during disease states.

This study addresses the question of how genetics influences the integrity of functional connectivity as measured by graph theory measures in resting-state fMRI (rs-fMRI) data. I assessed graph theory measures, including global efficiency, characteristic path length, Louvain modularity, transitivity, local efficiency and strength of default, dorsal attention, frontoparietal, limbic, salience, somatomotor, and visual networks, which are typically examined and found to change in aging (Song et al., 2014) as well as multiple neuropathological processes (Khazaee, Ebrahimzadeh, & Babajani-Feremi, 2015; Lebedev et al., 2014; Munilla et al., 2017). A UK Biobank sample comprising 18,445 participants of British ancestry was used in this study. I first estimated single nucleotide polymorphism (SNP) heritability (h^2). Subsequently, genome-wide association studies (GWAS) were performed to identify genetic variants associated with each graph theory measure. Gene-based association analysis was carried out to uncover gene-level associations, and the functional consequences of the significant genetic variants were explored.

3.2 Methods

3.2.1 Participants

Our study was approved by the UK Biobank in December 2018 (Application number: 45262). rs-fMRI data for 20,598 participants with British ancestry was downloaded in March 2019 (Sudlow et al., 2015). The imaging assessment took place at three different assessment centres with the majority assessed in Manchester, more recently scans were undertaken at Newcastle and Reading, UK. The UK Biobank study was conducted under approval from the NHS National Research Ethics Service (approval letter dated 17th June 2011, ref. 11/NW/0382), project 10279. All data and materials are available

via UK Biobank (http://www.ukbiobank.ac.uk). Only individuals with both genetics and rs-fMRI data were included in this study.

3.2.2 Image processing

Briefly, the UK Biobank structural T1-weighted MRI scans were acquired on three 3T Siemens Skyra MRI scanners (software platform VD13) at three sites (Reading, Newcastle, and Manchester) using a 32-channel receiving head coil and a 3D MPRAGE protocol (1.0 x 1.0 x 1.0 mm resolution, matrix 208 x 256 x 256, inversion time (TI)/repetition time (TR) = 880/2,000 ms, in-plane acceleration 2). An extensive overview of the data acquisition protocols and image processing carried out on behalf of the UK Biobank can be found elsewhere (Alfaro-Almagro et al., 2018). Rs-fMRI is based on a blood-oxygen level dependent (BOLD) signal which was obtained using an echo-planar imaging (EPI) sequence (TR = 0.735s, TE = 39 ms, FoV = 88 × 88 × 64, voxel resolution 2.4 × 2.4 × 2.4 mm) for the duration of ~6 mins (for more details, see https://biobank.ctsu.ox.ac.uk/crystal/crystal/docs/brain_mri.pdf). The images pre-processed by investigators affiliated with the UK Biobank (Alfaro-Almagro et al., 2018) were used. Briefly, motion correction, intensity normalisation, high-pass temporal filtering (Gaussian-weighted least-squares straight line fitting, with sigma=50.0s), echo-planar imaging (EPI) unwarping, and gradient distortion correction were performed. Subsequently, structured artefacts were removed by ICA+FIX processing (Independent component analysis followed by FMRIB's ICA-based X-noiseifier) (Beckmann & Smith, 2004; Griffanti et al., 2014; Salimi-Khorshidi et al., 2014). We removed participants with motion of > 2mm/degrees of translation/rotation. After image quality control and removal of participants with head motion outliers, we excluded 1,626 participants and 18,972 participants remained.

3.2.3 Graph theory analyses

The Schaefer atlas (Schaefer et al., 2018) was used as it met the following requirements: 1) it integrated both local gradient and global similarity approaches (i.e. Markov Random Field model) for parcellation, which showed greater homogeneity than four other previously published parcellations implying that it will not overestimate local connectivity of the regions; 2) it revealed neurobiologically meaningful features of the brain organisation; and 3) it was based of the Yeo 7-parcels atlas (Yeo et al., 2011) and provided a more fine-grained parcellation, which allowed us to look at an average of the parcels across the 7 networks for local efficiency and nodal strength. 3dNetCorr command from Analysis of Functional Neuroimages (AFNI) (Cox, 1996) was used to produce network adjacency matrix for each participant. The mean time-series for each region was correlated with the mean time-series for all other regions and extracted for each participant. Subsequently, using the derived network adjacency matrix, partial correlation, *r*, between all pairs of signals was computed to form a 400-by-400 (Schaefer atlas) connectivity matrix, which was then Fisher z-transformed. Self-connections and negative correlations were set to zero. The main network analysis was performed on positive weighted networks. Given that connection weights in brain networks can vary across magnitude, undirected weighted connectivity matrices were used instead of binary connectivity matrices. The higher the weight, the stronger the functional connectivity is between the brain regions (Fallani, Richiardi, Chavez, & Achard, 2014).

All graph theory measures were quantified by using the brain connectivity toolbox (BCT) (Rubinov & Sporns, 2010). Global-level measures included global efficiency, characteristic path length, transitivity, and Louvain modularity. A single value is

derived for each of these four measures and quantitatively represent the whole brain network. Network level measures, such as local efficiency and strength, were estimated for each node and averaged across all nodes within each network. Subsequently, I averaged the left-right hemisphere to derive a value for each node and averaged within each network to derive a value for each of the 7 networks.

To assess integration of information, I calculated global efficiency and characteristic path length (Deco, Tononi, Boly, & Kringelbach, 2015; Rubinov & Sporns, 2010). Global efficiency represents how effectively the information is transmitted at a global level and is the average inverse shortest path length while the latter measures the integrity of the network and how fast and easily information can flow within the network. To assess network segregation, which characterises the specialised processing of the brain at a local level, I calculated the Louvain modularity, transitivity, and local efficiency indices (Deco et al., 2015; Rubinov & Sporns, 2010). Louvain modularity is a community detection method, which iteratively transforms the network into a set of communities, each consisting of a group of nodes. Higher modularity values indicate denser within-modular connections but sparser connections between nodes that are in different modules. Transitivity refers to the sum of all the clustering coefficients around each node in the network and is normalised collectively. Local efficiency is a node-specific measure and is defined relative to the sub-graph comprising of the immediate neighbours of a node. Finally, strength (weighted degree) is described as the sum of all neighbouring edge weights (Rubinov & Sporns, 2010). High connectivity strength indicates stronger connectivity between the regions, which provides an estimation of functional importance of each network.

3.2.4 Genotype data in UK Biobank

Genetic data for approximately 500,000 individuals were available and full details on the genetics data used were described previously (Bycroft et al., 2018). The samples were collected from stored blood samples in the UK Biobank and genotyped either using the UK Bileve or the UK biobank axiom array. Genotyping was performed on 33 batches of ~4,700 samples by Affymetrix (High Wycombe, UK). Further details on the UK Biobank sample pre-processing are available here http://biobank.ctsu.ox.ac.uk/crystal/refer.cgi?id=155583.

An imputed data set was made available where the UK Biobank interim release was imputed to a reference set that consisted of > 92 million autosomal variants imputed from the Haplotype Reference Consortium (HRC) (McCarthy et al., 2016) and UK10K + 1000 Genomes resources reference panels. After SNP QC filters (MAF > 0.1% and imputation information score > 0.3), 9926107 SNPs were used in the GWAS analysis.

Further quality control measures were performed. Due to the confounds associated with population structure (Marchini, Cardon, Phillips, & Donnelly, 2004), only samples reported to have recent British ancestry were used in the GWAS analysis. Outliers, including those with high missingness, relatedness, quality control failure, and sex mismatch, were removed. The final UK Biobank sample, after genotyping quality control and including those with rs-fMRI data, was n = 18,445 participants.

3.2.4 Sleep behavioural data in UK Biobank

Self-reported sleep data, namely sleep duration and frequency of insomnia, were used. Sleep duration was recorded as the number of reported hours of sleep in every 24 hours

and frequency of insomnia was recorded as never/rarely, sometimes, or usually. More details can be found on http://biobank.ndph.ox.ac.uk/showcase/field.cgi?id=1160 and http://biobank.ndph.ox.ac.uk/showcase/field.cgi?id=1200.

3.3 Analysis

3.3.1 Potential confounds

In accordance with previous GWAS of brain imaging phenotypes in the UK Biobank (Elliott et al., 2018), I controlled for similar confounding variables in this study. In addition to age at scanning and sex (i.e. age, age^2, age × sex, age^2 × sex), covariates relating to imaging parameters and genetic ancestry were also included. These included: head motion from resting-state fMRI, head position (i.e. the exact location of the head in the scanner), volumetric scaling factor needed to normalise for head size, and the 10 genetic principal components.

3.3.2 SNP heritability

Heritability analysis, which is defined as the proportion of observed phenotypic variance explained by additive genetic factors of all common autosomal variants (Yang, Zeng, Goddard, Wray, & Visscher, 2017), estimates the relative contribution of genes and the environment on a phenotype. Using BOLT-REML (Loh et al., 2015) implemented in BOLT-LMM v2.3 (Loh, Kichaev, Gazal, Schoech, & Price, 2018), I estimated the heritability accounted by autosomal SNPs among the graph theory measures. BOLT-REML uses multiple component modelling to partition SNP heritability and applies Monte Carlo algorithm for variance component analysis.

3.3.3 Genome-wide association analysis

BOLT-LMM v2.3 (Loh et al., 2018) was used to conduct GWAS for the graph theory measures in the UK Biobank sample and adjusted for potential confounds. To correct for multiple hypothesis testing, I estimated the number of independent tests used based on Nyholt et al. method (Nyholt, 2004) and derived n = 6 independent tests for this study. The genome-wide significant threshold was set at $p < (5 \times 10^{-8} /6) = 8.33 \times 10^{-9}$. Quantile and Manhattan plots were also presented for each of the graph theory measure. Manhattan and QQ plots were made using the R-package (R Core Team, 2020). Locus Zoom (Pruim et al., 2010) was used for the visualisation of the nearest genes within a ±500-kilobase genomic region for the strength of somatomotor and limbic networks based on the hg19 UCSC Genome Browser assembly.

3.3.4 Linkage disequilibrium and Independent SNPs

The linkage disequilibrium plot of the associated genomic region was made using the LD plot function in the R package "gaston" (Perdry, 2020). To identify set of independent SNPs associated with each of the network measures a stepwise model selection method as implemented in the COJO (Yang et al., 2012) (cojo-slct) procedure of GCTA (Yang, Lee, Goddard, & Visscher, 2011) package with default parameters was used.

3.3.5 Multivariate association analysis

Multivariate association analysis was conducted using metaUSAT (Ray & Boehnke, 2018). The method uses summary statistics from individual studies and is suitable for correlated traits. MetaUSAT derives strength from two methods of multivariate association tests (score test and multivariate analysis variance test) as it uses convex

linear combination of two test statistics. Data-driven minimum p-value corresponding to the best-linear combination is obtained. The significant threshold was set as $p < (5 \times 10^{-8} /4) = 1.25 \times 10^{-8}$.

3.3.6 Gene-based association analysis and functional mapping

Gene-based association analysis was performed via MAGMA(de Leeuw, Mooij, Heskes, & Posthuma, 2015) (v1.07, https://ctg.cncr.nl/software/magma/). MAGMA uses 1000G reference panel for calculation of LD between the SNPs and gene coordinates based on NCBI build 37. SNPs were mapped to a gene if they were within ±5 kb of the gene co-ordinates. Gene-based association test statistic was derived using the default option, which is the sum of –log(SNP p-value). The Bonferroni correction was used for significance of the gene-based association tests (p-value of the gene-based tests / (number of independent tests × number of genes tested)). In other words, significant threshold was set as $p < 0.05/(6 \times 18319) = 4.56 \times 10^{-7}$.

3.3.7 Functional annotation

I performed lookups for variants that passed the suggestive GWAS threshold of $p < 5 \times 10^{-8}$ to investigate the previously reported associations with the other traits. NHGRI-EBI GWAS Catalogue (Buniello et al., 2019) included previous GWAS publications and SNPnexus (Dayem Ullah et al., 2018) included all other publications.

FUMA (Watanabe, Taskesen, van Bochoven, & Posthuma, 2017) gene2func online platform (version 1.3.4, http://fuma.ctglab.nl/) was used to explore the functional consequences of significant genes. All the genes in the GWAS analysis and the gene-based analysis after nominal significance were used as input (a total of 18 genes). Using

the FUMA platform, the GTEx v7 30 general tissue types data set was used for tissue specificity analyses. Differentially expressed gene (DEG) sets were pre-calculated by performing two-tailed t-test for any one of the tissue type against all others. Expression values were normalised (zero-mean) following a $\log_2$ transformation of expression values. Using the genes as background gene set, 2×2 enrichment sets were performed. Genes with p-value ≤ 0.05 after Bonferroni correction were defined as differentially expressed.

3.3.8 Genetic correlation estimation with LDSC

LD Hub (v1.9.1, http://ldsc. broadinstitute.org/ldhub/) was used to estimate the genetic correlation between graph theory measures and corresponding traits. Summary statistics were uploaded to LD hub where it calculates the genetic correlations using the LDSC software (v1.0.0, https:// github.com/bulik/ldsc).

3.3.9 Test of associations with graph theory measures

The graph theory measures were normalised using ranked transformation, rntransform() function in R from GeneABEL package (Karssen, van Duijn, & Aulchenko, 2016) and age were z-transformed for regression analysis. Regression model similar to GWAS analysis was used to test the association of self-reported sleep duration and frequency of insomnia variables with the graph theory measures. Only results with a two-tailed $p < 0.05/18$ (number of graph theory measures) were considered significant. Data management, derivation of summary statistics and other statistical analyses, and correlation plots were performed using R (V 4.0.0) software (R Core Team, 2020).

3.4. Results

3.4.1 Demographics and graph theory measures

After imaging and genetic pre-processing and quality control, 2,153 UK Biobank participants were excluded resulting in a final sample of 18,445 participants of British ancestry. There were 9,773 women and 8,672 men with a mean age (sd) of 62.47 (7.47). Eighteen weighted graph theory measures were derived by parcellating the rs-fMRI data using the Schaefer atlas (Schaefer et al., 2018), which is a fine-grained parcellation scheme based on Yeo-7 network. These 18 measures include: global efficiency and characteristic path length (network integration); modularity, transitivity, and local efficiency of 7 networks (network segregation); and strength of 7 networks. Supplementary Table A1 defines each of the measures and provides evidence of their association with aging and neuropathological diseases. Supplementary Table A2 shows the mean and standard deviation of the demographics and graph theory measures. Figure 3.1 shows the brain network reconstruction using rs-fMRI data.

Phenotypic correlations between the measures were examined (Supplementary Figure B1). High correlations were observed between the following measures: characteristic path length and modularity were negatively correlated with all other graph theory measures (r = -0.661 to -0.989); global efficiency and transitivity were positively correlated with local efficiency and strength of all the networks (r = 0.753 to 0.952); local efficiencies of networks were positively correlated with each other (r = 0.784 to 0.902); and strengths of networks were positively correlated with each other (r = 0.772 to 0.927).

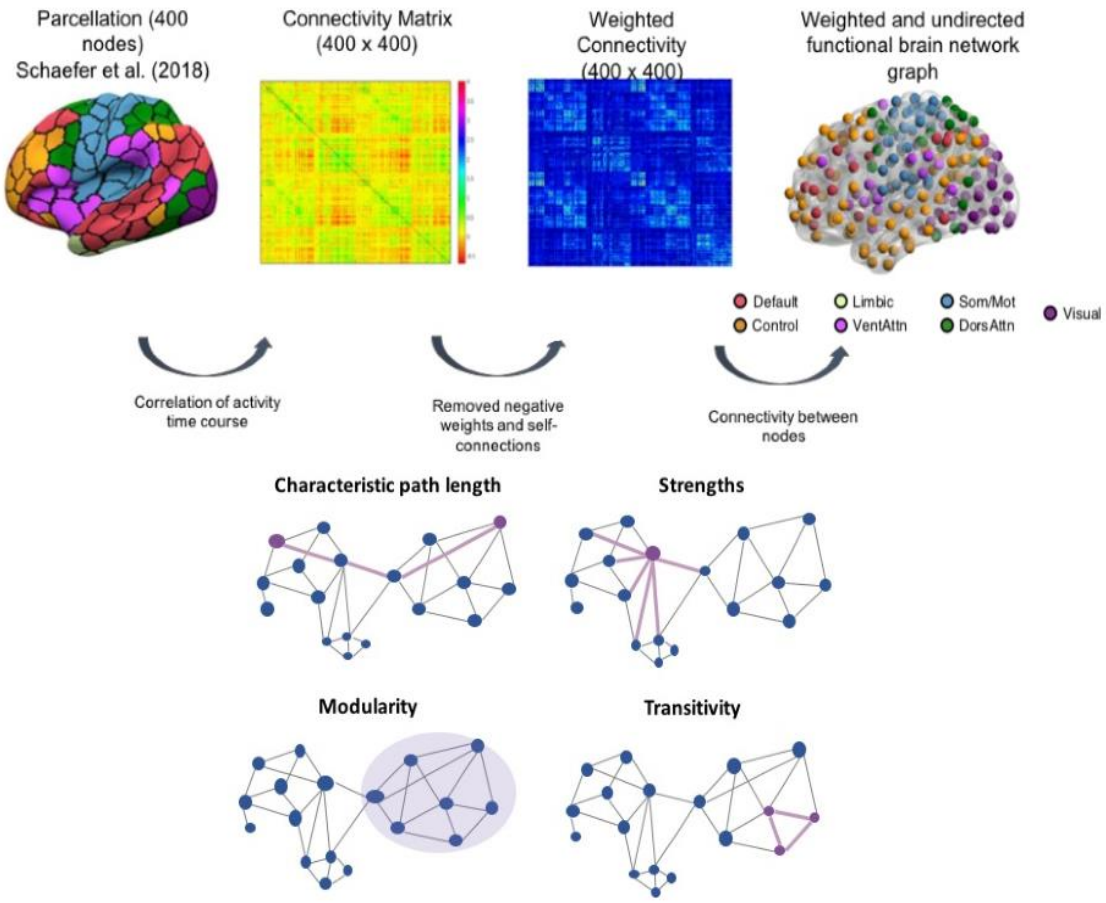

Figure 3.1 Schematic representation of brain network construction using graph theory analysis.

After pre-processing, the brain was divided into different parcels using the Schaefer et al. (2018) parcellation scheme. Subsequently, activity time course was extracted from each region to create the correlation matrix. I used the correlation matrix and removed all the self-connected and negative weights to derive a corresponding weighted undirected brain network matrix and functional brain network graph. Lastly, I used the network matrix to calculate the sets of topological graph theory measures.

3.4.2 SNP heritability estimates and genetic correlations

SNP heritability, h^2_{SNP}, was estimated using the proportion of variance in each graph theory measure that is explained by GWAS SNPs. All graph theory measures, except for strength of the visual network, were significantly heritable ($p < 0.05$), ranging from $h^2_{SNP} = 0.07$ for local efficiency of visual network to $h^2_{SNP} = 0.17$ for the strength of

limbic network, with a mean h^2_{SNP} of 0.12 (Supplementary Table A3; Figure 3.2A). Notably, higher h^2_{SNP} estimates (0.11-0.17) were observed for global efficiency, characteristic path length, transitivity, and strength of limbic, somatomotor, default, salience, and frontoparietal networks compared to the other measures. In addition, genetic and environmental correlations were examined. Strong genetic correlations between the network measures were observed. All measures were positively associated with each other with the exception of Louvain modularity and characteristic path length being negatively correlated with all other measures (Figure 3.2B).

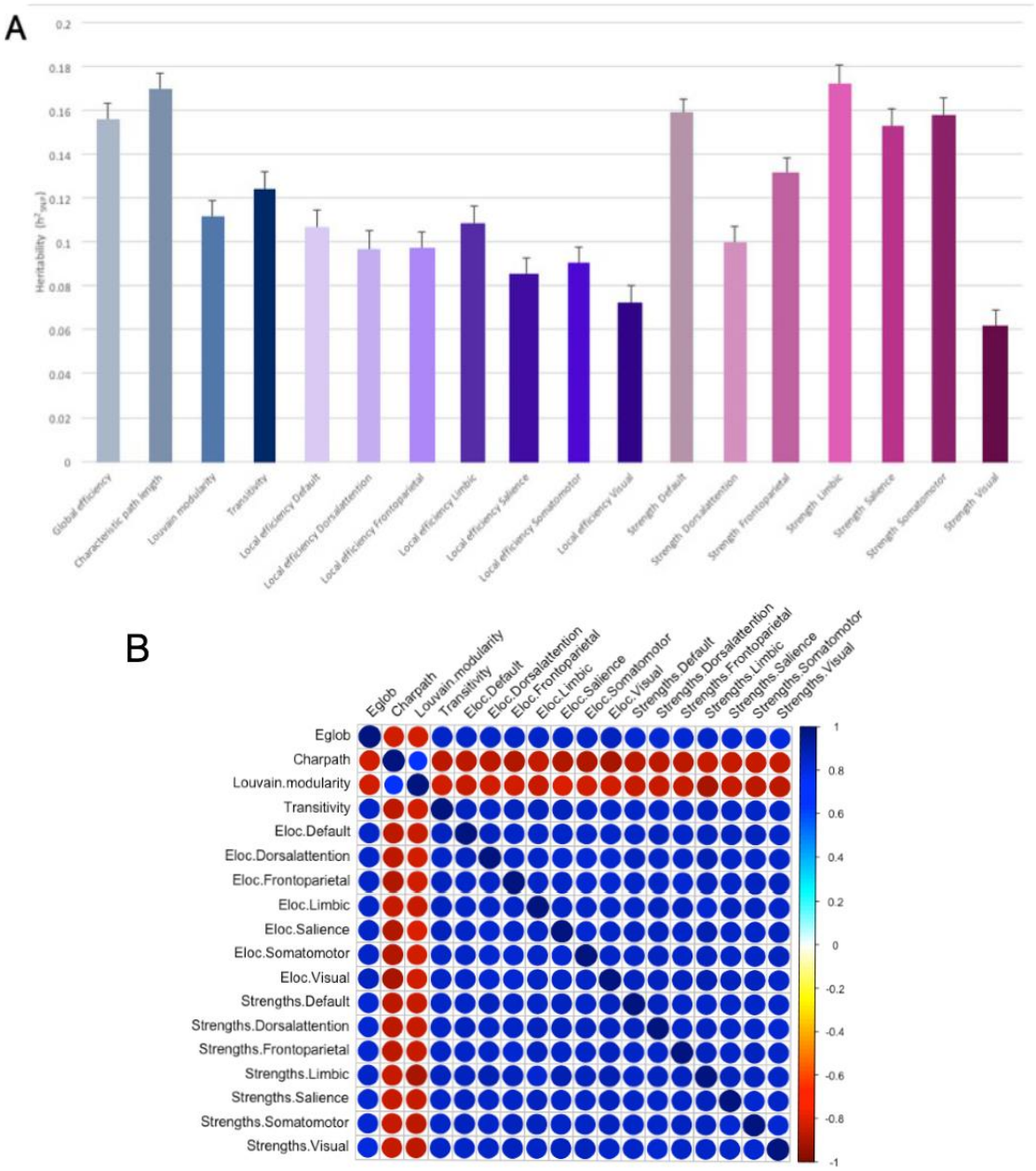

Figure 3.2 Genetic and environmental correlations between the 18 weighted graph theory measures. (A) represents the heritability estimates for each of the graph theory measures. Gray represents the network integration as characterised by global efficiency and characteristic path length; blue represents network segregation as characterised by Louvain modularity and transitivity; purple represents networks of local efficiency; and pink represents strength of the networks. (B) Genetic correlations were estimated using LDSC (https://github.com/bulik/ldsc). Strong genetic and environmental correlations between the network measures were observed (see Supplementary Table A4 for more details). Abbreviations: Eglob, global efficiency; Charpath, characteristic path length; Eloc, local efficiency.

3.4.3 Genome-wide association study

GWAS of the rs-fMRI data for each individual graph theory measure (n=18) were carried out using an additive genetic model adjusted for age, age^2, sex, age × sex, age^2 × sex, head motion from resting-state fMRI, head position, volumetric scaling factor needed to normalise for head size, genotyping array and 10 genetic principal components.

At the genome-wide significance level of $p < 5 \times 10^{-8}$ (unadjusted for the number of measures assessed), there were 31 SNPs significantly associated with nine of the 18 graph theory measures namely, global efficiency, characteristic path length, Louvain modularity, local efficiency of default and somatomotor networks, strength of default, limbic, salience, and somatomotor networks (Supplementary Table A4). Supplementary Figure B2 shows the Manhattan and quantile-quantile plots of all the 18 graph theory measures. However, after adjusting for the number of independent tests using this method (Nyholt, 2004) (n = 6 tests for this study; *p*-threshold = $5 \times 10^{-8}/6 = 8.33 \times 10^{-9}$), only fourteen variants from a single locus remained significant with strength of the somatomotor network (lead SNP: rs12616641), and one of which also was significant for strength of the limbic network (rs62158161) (Table 3.1; Figure 3.3A & 3.3B). All SNPs were located in an intergenic region near *PAX8* (Paired box gene 8) on chromosome 2 (BP 114065390 - 114092549) (Fig. 3.3C).

The conditional and joint association (COJO) analysis using the GWAS summary data of the network measures did not identify any additional SNPs apart from the top associated within each locus (Supplementary Table A4). There is high linkage

disequilibrium in the genomic region (114065390 – 114110568) on chromosome 2 (Supplementary Fig. B3).

Table 3.1 GWAS genome-wide significant results for brain functional network measures

SNP and measures	Chr	Function	Gene	A1/ A2	EAF	β	SE	*p*
Strength Limbic								
rs62158161	2	Intergenic	*PAX8*	C/T	0.749	0.069	0.012	*4.70E-09*
Strength Somatomotor								
rs62158160	2	Intergenic	*PAX8*	C/T	0.742	0.066	0.011	*6.90E-09*
rs62158161	2	Intergenic	*PAX8*	C/T	0.749	0.069	0.012	*2.40E-09*
rs62158166	2	Intergenic	*PAX8*	G/C	0.773	0.073	0.012	*1.20E-09*
rs62158168	2	Intergenic	*PAX8*	C/G	0.773	0.073	0.012	*1.20E-09*
rs12616641*	2	Intergenic	*PAX8*	C/A	0.774	0.073	0.012	*9.90E-10*
rs62158169	2	Intergenic	*PAX8*	C/T	0.784	0.072	0.012	*3.50E-09*
rs62158170	2	Intergenic	*PAX8*	A/G	0.784	0.073	0.012	*2.60E-09*
rs199993536	2	Intergenic	*PAX8*	T/A	0.783	0.072	0.012	*3.10E-09*
rs6737318	2	Intergenic	*PAX8*	A/G	0.779	0.070	0.012	*6.20E-09*
rs62158206	2	Intergenic	*PAX8*	T/C	0.779	0.071	0.012	*4.10E-09*
rs7556815	2	Intergenic	*PAX8*	G/A	0.780	0.071	0.012	*4.70E-09*
rs2863957	2	Intergenic	*PAX8*	C/A	0.779	0.071	0.012	*4.10E-09*
rs1823125	2	Intergenic	*PAX8*	A/G	0.779	0.071	0.012	*3.30E-09*
rs60873293	2	Intergenic	*PAX8*	G/T	0.779	0.070	0.012	*5.70E-09*

Linear regression models were adjusted for age, age^2, sex, age × sex, age^2 × sex, head motion from resting-state fMRI, head position, volumetric scaling factor needed to normalise for head size, and 10 genetic principal components. P values are two-tailed. Only results that survived Bonferroni correction ($p < 5 \times 10^{-8}/6$) were reported here. *Italics* represents significance.

*rs12616641 was the lead SNP.

Abbreviations: SNP, single nucleotide polymorphism; Chr, chromosome; A1, coded allele; A2, non-coded allele; EAF, effect allele frequency; β, beta; SE, standard error

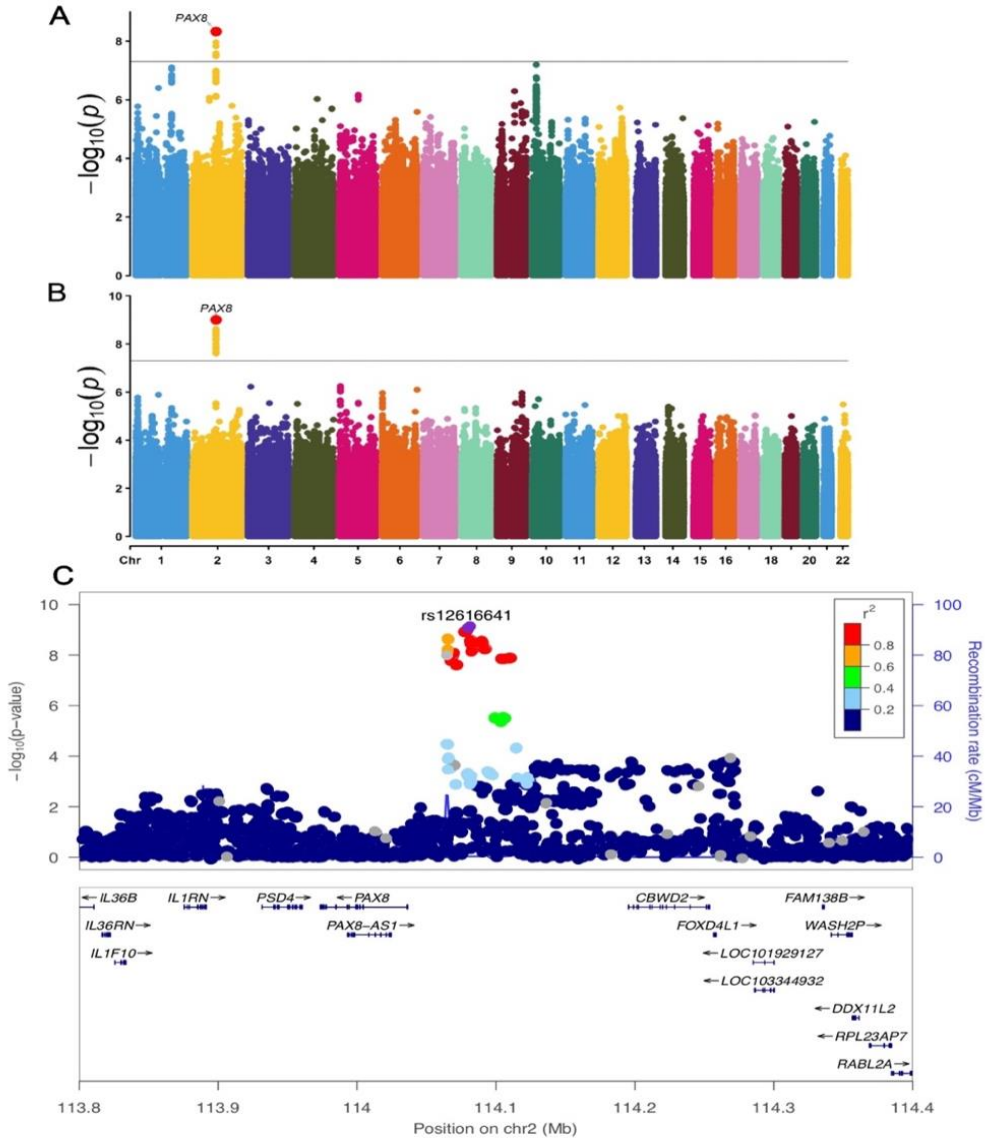

Figure 3.3 GWAS Manhattan Plots for strength of limbic and somatomotor networks and the locus zoom plot for the identified chromosome 2 region

(A) represents the Manhattan plot for strength of limbic network; (B) represents the Manhattan plot for strength of somatomotor network. For each of the Manhattan plots, each point represents a single genetic variant plotted according to its genomic position (x-axis) and its association with the relevant graph theory measure is shown by the corresponding –log10(P) values on the y-axis. Linear regression models were adjusted for age, age2, sex, age × sex, age2 × sex, head motion from resting-state fMRI, head position, volumetric scaling factor needed to normalise for head size, genotyping array and 10 genetic principal components. The black solid line represents the classical GWAS significance threshold of p < 5 × 10-8. (C) The Locus zoom plot showing the chromosome 2 locus significantly associated with both the strength of somatomotor and limbic networks. Rs12616641 is the lead SNP.

3.4.4 Multivariate association test

Since all network measures were highly correlated, to increase power a multivariate analysis using GWAS summary statistics from multiple network measures was performed. Based on their network properties, pooled summary statistics as implemented in metaUSAT (Ray & Boehnke, 2018) were obtained for (i) global efficiency and characteristic path length; (ii) modularity and transitivity; (iii) local efficiency of all networks; and (iv) strength across all networks. Multivariate analysis of the combined strength network measures yielded 31 significant associations at $p < 1.25 \times 10^{-8}$ (adjusted for four tests). Out of this, 23 were found in GWAS of somatomotor strength measure reported in Supplementary Table A4 and the remaining 8 SNPs were found for combined strength measure (Table 3.2). No additional hits were found in the multivariate analysis of the other three grouped measures.

Table 3.2 Multivariate SNP-based analyses for combined network strength measure

Measure	SNP	Chr	Function	Nearest gene	*p*
Combined Network Strength	rs145868127	2	ncRNA_exonic	*LOC101928386*	*3.92E-18*
	rs2680724	2	intergenic	*MIR3679*	*4.04E-18*
	rs62165320	2	intergenic	*AMER3*	*5.08E-18*
	rs2661030	2	intergenic	*LINC01826*	*5.33E-11*
	rs2661035	2	intergenic	*LINC01826*	*5.45E-11*
	rs1880544	2	ncRNA_exonic	*LINC01101*	*1.35E-10*
	rs2089478	2	intergenic	*LINC01826*	*1.56E-10*
	rs12474078	2	ncRNA_intronic	*LANCL1-AS1*	*2.50E-09*

Only results that survived Bonferroni correction ($p < 5 \times 10^{-8}/4 = 1.25 \times 10^{-8}$*) are reported. Italics* represents significance.

Abbreviations: SNP, single nucleotide polymorphism; Chr, chromosome; ncRNA, non-coding RNA; *LOC101928386*, Uncharacterised LOC101928386; *MIR3679*, MicroRNA 3679; *AMER3*, APC Membrane Recruitment Protein 3; *LINC01826*, Long Intergenic Non-Protein Coding RNA 1826; *LINC01101*, Long Intergenic Non-Protein Coding RNA 1101; *LANCL1-AS1*, LANCL1 Antisense RNA 1

3.4.5 Gene-based association analysis

Gene-based association analysis was performed using the software MAGMA(de Leeuw et al., 2015) (Table 3.3). Our results showed that five genes – *SLC25A33* (Solute Carrier Family 25 Member 33), *TMEM201* (Transmembrane Protein 201), *ZEB1* (Zinc Finger E-Box Binding Homeobox 1), *SH2B3* (SH2B Adaptor Protein 3), and *ATXN2* (Ataxin 2) – were associated with global efficiency, characteristic path length, and strength of default, dorsal attention, and somatomotor networks after adjusting for the number of independent tests (n = 6) and number of genes (n = 18,319) i.e. *p*-threshold < $0.05/(6 \times 18319) = 4.56 \times 10^{-7}$. Supplementary Table A5 describes the genes associated with the graph theory measures.

Table 3.3 Gene-based association analysis identified five significant gene-level associations for brain functional network measures

Gene	Graph theory measures	Chr	NSNPs	*p*
SLC25A33	Global efficiency	1	69	*5.64E-08*
	Characteristic path length	1	69	*5.23E-08*
TMEM201	Global efficiency	1	43	*1.83E-08*
	Characteristic path length	1	43	*1.48E-08*
	Strength Dorsal attention	1	43	*1.36E-07*
	Strength Somatomotor	1	43	*2.09E-07*
ZEB1	Global efficiency	10	323	*3.27E-07*
	Characteristic path length	10	323	*2.29E-07*
SH2B3	Strength Default	12	50	*2.95E-07*
ATXN2	Strength Default	12	149	*2.48E-07*

Gene-based association analysis was performed via MAGMA (de Leeuw et al., 2015), which uses 1000G reference panel for calculation of LD between the SNPs and gene coordinates based on NCBI build 37. Only genes that passed the Bonferroni correction ($p < 4.56 \times 10^{-7}$) are reported here. Italics represents significance. Abbreviations: Chr, chromosome; NSNP, number of single nucleotide polymorphisms; *SLC25A33*, Solute Carrier Family 25 Member 33; *TMEM201*, Transmembrane Protein 201; *ZEB1*, Zinc Finger E-Box Binding Homeobox 1; *SH2B3*, SH2B Adaptor Protein 3; *ATXN2*, Ataxin 2

3.4.6 Functional annotations

I assessed the potential functions of the 39 significant SNPs from the GWAS (n=31) and multivariate association tests (n=8) in SNPnexus (Dayem Ullah et al., 2018). The results showed that many of the network associated variants were associated with other phenotypes including sleep patterns, psychiatric disorders, coronary artery disease, cholesterol, and blood pressure (Supplementary Tables A6 and A7). None of the variants were found to be eQTLs.

Gene expression enrichment analysis of the list of significant genes in our results was subsequently performed using the Functional Mapping and Annotation (FUMA) platform (Watanabe et al., 2017). They were expressed in the brain but also across other tissue types (Supplementary Figure B4). Moreover, there was no enrichment in brain tissue types (Supplementary Table A8).

3.4.7 Genetic correlations with other traits

Given that the most robust GWAS result was observed for the strength of somatomotor network, I examined its genetic correlations with other traits via linkage disequilibrium (LD) score regression (LDSC) (Bulik-Sullivan et al., 2015) (Supplementary Table A9). Results showed that strength of somatomotor network was genetically correlated with other traits, such as nervous feelings, sleep traits, neuroticism, depressive symptoms, blood pressure, and education (unadjusted $p \leq 0.05$). However, none of them passed multiple comparisons correction.

3.4.8 Correlations with other associated traits

As the SNPs in our study have been associated with sleep and insomnia in previous GWAS studies (Supplementary Table A6), I explored the phenotypic correlations between the graph theory and sleep-related measures in the UK Biobank data (Supplementary Tables A10 and A11). Self-reported sleep duration and insomnia were significantly associated with the graph theory measures. Strength of somatomotor network showed the most significant association with sleep duration ($p = 8.33 \times 10^{-11}$) and insomnia ($p = 0.0019$).

3.5 Discussion

Functional graph theory measures reflect the underlying functional topography of the brain. To date, this is the first study investigating the genetics of weighted functional graph theory measures. I present h^2_{SNP} estimates and results from GWAS of graph theory measures using resting-state fMRI data from 18,445 UK Biobank participants. This study identified significant SNPs and gene associations that survived multiple correction testing with six of the 18 graph theory measures including global efficiency, characteristic path length, and strength of default, dorsal attention, limbic, and somatomotor networks. The novel contributions of this paper are the identification of new genetic associations at the variant, locus, and gene levels, providing insights into the genetic architecture of graph theory metrics using resting-state fMRI data.

Similar to the study by Elliot and colleagues (Elliott et al., 2018) who showed that resting-state fMRI connectivity edges had the lowest levels of h^2_{SNP}, I found low h^2_{SNP} across all the graph theory measures. This is in contrast to previous classical twin study design studies that have shown moderate to high heritability of 0.52 to 0.64 for global

efficiency, 0.47 to 0.61 for mean clustering coefficient, and 0.38 to 0.59 for modularity (Sinclair et al., 2015). One of the plausible explanations is that h^2_{SNP} typically provides smaller heritability estimates due to uncaptured rare genetic variants compared to those provided by the classic twin study design (Elliott et al., 2018). High genetic correlations observed between graph theory measures may be due to the high phenotypic correlations between the measures.

The GWAS results found that strength of limbic and somatomotor networks were associated with SNPs located in an intergenic region near *PAX8* (Paired box gene 8) on chromosome 2, which is the closest gene to the top SNP. The *PAX* gene family encodes transcription factors which are essential during development and tissue homeostasis (Blake & Ziman, 2014). Specifically, *PAX8* protein is considered as a master regulator for key cellular processes in DNA repair, replication, and metabolism (Ruiz-Llorente et al., 2012). It has also been shown to regulate several genes involved in the production of thyroid hormone (Pasca di Magliano, Di Lauro, & Zannini, 2000), essential for brain development and function such as neuronal differentiation, synaptogenesis, and dendritic proliferation (Bernal, 2007; Williams, 2008). A previous study has also linked reductions in intrinsic functional connectivity in the somatomotor network to participants with subclinical hypothyroidism compared to controls (Kumar et al., 2018). Interestingly, studies have also found subclinical thyroid dysfunction to be associated with sleep quality (Kim et al., 2019; Song et al., 2019). Other genes located in this intergenic region near PAX8 include CBWD2 and CHCHD5, which have also been associated with sleep duration in prior studies (Doherty et al., 2018; Veatch, Keenan, Gehrman, Malow, & Pack, 2017). Considering that this study also observed phenotypic correlations between sleep duration, insomnia and graph theory measures, it is possible

that variants in or near PAX8 and other genes in this region may play a role in the regulation of genes associated with functional brain network properties and sleep.

Results from multivariate SNP-based analyses from combined network strength measures found associations with SNPs on chromosome 2, which were associated with inflammation and oncogenesis. The majority of these SNPs were located in intergenic regions close to non-coding RNA genes. *LINC01826* (long intergenic non-protein coding RNA 1826) has been associated with inflammatory responses of the vascular endothelial cells, which are important in the development of cardio-cerebrovascular diseases (Lin et al., 2017). *MIR3679* (microRNA 3679) is a short non-coding RNA involved in post-transcriptional regulation of gene expression, which has been postulated to function as a tumor suppressor due to lower levels observed in patients with diffuse glioma than controls (Ohno et al., 2019). *LINC01101* (long intergenic non-protein coding RNA 1101), on the other hand, has been down-regulated in cervical cancer (Iancu et al., 2017). The identified genes may contribute to understanding the relationship between strength of brain networks and disease.

Gene-based association analysis showed associations with genes involved in neuronal differentiation/development, cancer, and susceptibility to neurodegenerative diseases. *ZEB1* has been implicated in neuronal glioblastoma (Yu, Liang, & Zhang, 2018) whereas *SLC25A33* has been associated with insulin/insulin-like growth factor 1 (IGF-1) necessary for metabolism, cell growth, and survival (Favre, Zhdanov, Leahy, Papkovsky, & O'Connor, 2010) and showed higher expression in transformed fibroblasts and cancer cell lines compared to non-transformed cells (Favre et al., 2010; Floyd et al., 2007). *TMEM201* mice, which undergo accelerated senescence, exhibited

an early onset age-related decline in antibody response and have a higher rate of mortality (Shimada & Hasegawa-Ishii, 2011). *ATXN2* belongs to a class of genes associated with microsatellite-expansion diseases, where an interrupted CAG repeat expansion has been associated with brain-related diseases including spinocerebellar ataxia type 2 (SCA2), frontotemporal lobar degeneration (FTLD), and amyotrophic lateral sclerosis (ALS) (Fournier et al., 2018; Lahut et al., 2012). A neighbouring gene *SH2B3* to *ATXN2* has also been implicated in increased ALS risk (Lahut et al., 2012). Consistent with previous studies that identified functional graph theory measures that were associated with the most common FTLD (behavioural variant of frontotemporal dementia) (Agosta et al., 2013; Reyes et al., 2018), I observed similar graph theory measures to be associated with the *ATXN2* gene. This implies that *ATXN2* may be involved in the relationship between the disruption of brain networks and neurological/neuromuscular disorders.

In addition, I observed that brain functional networks are associated with self-reported sleep traits. Consistent with a previous study showing that individuals with chronic insomnia also showed disrupted global and local properties of the brain involving networks such as default mode, dorsal attention, and sensory-motor (Li et al., 2018), I found that insomnia was most significantly associated with decreased strength of somatomotor network. Our study, therefore, supports the contention that sleep quality is related to certain functional brain networks. Given that I observed genes associated with these networks, it is possible that altered networks may be driving the sleep abnormality. The reverse is also possible, with sleep disturbance influencing the activity in the networks. The directionality of the relationship between brain networks and sleep traits may be determined using longitudinal data in future studies.

The strengths of this study include the well characterised sample and its large sample size, and uniform MRI methods. The results, however, should be interpreted with caution. While using weighted undirected matrix circumvents issues surrounding filtering/thresholding the connectivity matrix to maintain significant edge weights represented in a binary matrix, there are inherent difficulties associated with the interpretation of the results. As brain signals recorded from resting-state fMRI are typically noisy, it is possible that edge weights may be affected by non-neural contributions (Fallani et al., 2014). Despite this, with careful denoising of the resting-state fMRI data (Parkes, Fulcher, Yücel, & Fornito, 2018; Power, Plitt, Laumann, & Martin, 2017) and covarying for motion, it is possible to minimise the noise in the data. In addition, previous studies have suggested that stronger edge weights make greater contributions in the computation of graph metrics than lower weight connections (Drakesmith et al., 2015; Ginestet, Fournel, & Simmons, 2014). This implies that when evaluating weighted graphs, false positive connections based on lower correlations may have a less disruptive impact on the network topology (van den Heuvel et al., 2017). Given that the brain is a complex system with hierarchical network structure, studying weighted networks, as was done in this study, may provide a more holistic representation of the brain functional network. Future studies may benefit from investigating the genetic effects between binarised and weighted graph theory metrics. In order to get a stable covariance matrix, other studies have suggested the use of regularisation (Pervaiz, Vidaurre, Woolrich, & Smith, 2020; Thirion, Varoquaux, Dohmatob, & Poline, 2014). Moreover, it is important to consider that the number of nodes for the 400-by-400 Schaefer parcellation may not be optimum for the 500 number of time points of resting-state fMRI data. Therefore, future studies may consider using

regularisation in the derivation of the network matrix and a parcellation that consists of smaller number of nodes. Moreover, given the high correlations between the graph theory measures suggest that these measures may account for the same phenotype, or at least almost account for the same variability in the population, performing GWAS on each of these measures may not be necessary. However, these measures have shown to affect different disease states in older age. Importantly, this is an exploratory study and the findings presented are purely correlative. Despite so, the findings from the paper provide a new preliminary support for combining resting-state fMRI, graph theory methods, and GWAS to identify genetic variants associated with the various graph theory measures. It may also shed light to direct future studies in determining what graph theory imaging phenotypes should be included. In order to further understand the mechanisms about brain function at a more basic level, it may be useful for future studies to use developmental and adult human brain gene expression data to associate the expression of a single gene or genes with specific graph theory measures and phenotypes. Furthermore, given that the UK Biobank has recently released additional data, replication may be possible in the future.

In summary, this is the first study to investigate the genetics of weighted functional graph theory measures in a large and well characterised cohort. This study observed multiple SNPs and genes associated with weighted graph theory measures, which have been observed to be implicated in sleep duration, neuronal differentiation/development, cancer, and susceptibility to neurodegenerative diseases. Our findings may help in the identification of novel biological pathways relevant to human brain functional network integrity and disease.

Supplemental Tables for Chapter 3

Supplementary Table A1. Graph theory measures and their association with aging and aging-related diseases

Graph theory measures	Definition	Associations with ageing and ageing-related diseases	Implications	References
Global efficiency	How effectively the information is transmitted at a global level and is the average inverse shortest path length	Older age was associated with reduced global efficiency compared to younger participants	Ageing is associated with reduced network integration. Therefore, there may be a slower flow of information transmission within networks in older adults	Achard & Bullmore, 2007; Sun et al., 2012
Characteristic path length	Integrity of the network and how fast and easily information can flow within the network. It is the average of all the distances between every pair of nodes in the network	Older age was associated with longer characteristic path lengths compared to younger participants		Sala-Llonch et al., 2014
Louvain Modularity	Community detection method, which iteratively transforms the network into a set of communities, each consisting of a group of nodes. Higher modularity values indicate denser within-modular connections but sparser connections between nodes that are in different modules	Brain networks in the elderly showed decreased modularity (less distinct functional networks) but findings are mixed	Increasing age has been associated with decreasing segregation of the functional brain networks	Chan et al., 2014; Iordan et al., 2017

Transitivity	Total of all the clustering coefficients around each node in the network and is normalised collectively	Patients with Alzheimer's disesase (AD) showed lower normalised clustering coefficient (i.e. transitivity)		Supekar et al., 2008
Local efficiency	Node-specific measure and is defined relative to the sub-graph comprising of the immediate neighbours of a node	Ageing has been associated with decreased local efficiency		Iordan et al., 2017
Strength	Sum of all neighbouring edge weights. High connectivity strength indicates stronger connectivity between the regions	Age-related differences were observed in network-level functional connectivity such as increases in auditory network, decreases in connectivity in the visual, frontoparietal, dorsal attention, and salience network. However, findings are mixed.	In general, there appears to be selective vulnerability of the strengths of the networks in older adults.	Betzel et al., 2014; Geerligs et al., 2015; King et al., 2018; Onoda et al., 2012; Song et al., 2014; Tomasi & Volkow, 2012

Supplementary Table A2. Demographics and graph theory measures in the UK Biobank

Demographics	
Total N	18,445
Analysis	Discovery
Study design	Population-based
Ancestry	European
Age (years), mean (SD)	62.47 (7.47)
Age range (years)	44 - 80
n, % women	9773, 52.98%
Graph theory measures	
Global efficiency	0.358 (0.083)
Characteristic path length	3.606 (0.735)
Louvain Modularity	0.186 (0.062)
Transitivity	0.139 (0.044)
Local efficiency Default	0.482 (0.211)
Local efficiency Dorsal attention	0.595 (0.201)
Local efficiency Frontoparietal	0.564 (0.208)
Local efficiency Limbic	0.476 (0.215)
Local efficiency Salience	0.573 (0.197)
Local efficiency Somatomotor	0.557 (0.212)
Local efficiency Visual	0.519 (0.200)
Strength Default	98.353 (38.159)
Strength Dorsal attention	130.747 (43.352)
Strength Frontoparietal	111.522 (40.127)
Strength Limbic	50.490 (24.337)
Strength Salience	117.080 (43.991)
Strength Somatomotor	117.743 (49.511)
Strength Visual	123.486 (43.151)

Supplementary Table A3. Heritability estimates

Graph theory measures	**Genetic h^2_{SNP}**	**Genetic h^2_{SNP} S.E.**	**Non-genetic h^2_{SNP}**	**Non-genetic h^2_{SNP} S.E.**	**Estimated Genetic h^2_{SNP} P-value**
Global efficiency	0.155	0.032	0.845	0.032	2.40E-06
Characteristic path length	0.169	0.032	0.831	0.032	2.47E-07
Louvain modularity	0.111	0.031	0.889	0.031	0.001
Transitivity	0.124	0.031	0.876	0.031	1.50E-04
Local efficiency Default	0.107	0.031	0.893	0.031	0.001
Local efficiency Dorsal attention	0.097	0.031	0.903	0.031	0.003
Local efficiency Frontoparietal	0.096	0.031	0.904	0.031	0.003
Local efficiency Limbic	0.108	0.031	0.892	0.031	0.001
Local efficiency Salience	0.085	0.031	0.915	0.031	0.010
Local efficiency Somatomotor	0.089	0.031	0.911	0.031	0.007
Local efficiency Visual	0.072	0.031	0.928	0.031	0.026
Strength Default	0.157	0.031	0.843	0.031	1.44E-06
Strength Dorsal attention	0.099	0.031	0.901	0.031	0.003
Strength Frontoparietal	0.130	0.031	0.870	0.031	7.27E-05
Strength Limbic	0.172	0.031	0.828	0.031	1.17E-07
Strength Salience	0.153	0.032	0.847	0.032	3.77E-06
Strength Somatomotor	0.158	0.032	0.842	0.032	1.85E-06
Strength Visual	0.061	0.031	0.939	0.031	0.059

Abbreviations:h^2_{SNP}, single nucleotide polymorphism (SNP) heritability; S.E., standard error

Supplementary Table A4. GWAS results for the graph theory measures $p < 5 \times 10^{-8}$

SNP and graph theory measures	Chr	Position	Function	Nearest gene	A1/A2	EAF	β	SE	*p*
Global efficiency									
rs62158160	2	114065390	Intergenic	*PAX8*	C/T	0.742	0.064	0.011	2.60E-08
rs111789636	2	114065433	Intergenic	*PAX8*	A/C	0.732	0.063	0.011	3.60E-08
rs62158161[#]	2	114065572	Intergenic	*PAX8*	C/T	0.749	0.066	0.012	1.20E-08
rs62158166	2	114077218	Intergenic	*PAX8*	T/C	0.773	0.066	0.012	3.80E-08
rs62158168	2	114078381	Intergenic	*PAX8*	C/G	0.773	0.066	0.012	3.50E-08
rs12616641	2	114079248	Intergenic	*PAX8*	C/A	0.774	0.067	0.012	3.00E-08
Charpath									
rs62158160	2	114065390	Intergenic	*PAX8*	C/T	0.742	-0.064	0.011	2.60E-08
rs111789636	2	114065433	Intergenic	*PAX8*	A/C	0.732	-0.062	0.011	4.10E-08
rs62158161[#]	2	114065572	Intergenic	*PAX8*	C/T	0.749	-0.065	0.012	2.00E-08
Louvain Modularity									
rs12764517	10	91701705	Intronic	*LINC01375*	A/G	0.974	0.177	0.032	4.50E-08
Local efficiency Default									
rs147256540	11	94787430	Intergenic	*SRSF8*	T/G	0.99	-0.296	0.054	3.80E-08
Local efficiency Somatomotor									
rs147256540	11	94787430	Intergenic	*SRSF8*	T/G	0.99	-0.297	0.054	3.50E-08
Strength Default									
rs13176783	5	92676527	Intergenic	*NR2F1-AS1*	G/A	0.287	-0.062	0.011	4.00E-08
rs66954590[#]	5	92676616	Intergenic	*NR2F1-AS1*	C/A	0.288	-0.062	0.011	3.10E-08
rs6893744	5	92676659	Intergenic	*NR2F1-AS1*	T/C	0.287	-0.062	0.011	3.70E-08
Strength Limbic									
rs62158160	2	114065390	Intergenic	*PAX8*	C/T	0.742	0.066	0.012	1.10E-08
rs111789636	2	114065433	Intergenic	*PAX8*	A/C	0.732	0.065	0.011	1.50E-08

rs62158161*[#]	2	114065572	Intergenic	*PAX8*	C/T	0.749	0.069	0.012	4.70E-09
rs62158166	2	114077218	Intergenic	*PAX8*	G/C	0.773	0.067	0.012	3.30E-08
rs62158168	2	114078381	Intergenic	*PAX8*	C/G	0.773	0.067	0.012	3.10E-08
rs12616641	2	114079248	Intergenic	*PAX8*	C/A	0.774	0.068	0.012	2.60E-08
Strength Salience									
rs62158160	2	114065390	Intergenic	*PAX8*	C/T	0.742	0.064	0.011	2.60E-08
rs111789636	2	114065433	Intergenic	*PAX8*	A/C	0.732	0.063	0.011	2.90E-08
rs62158161	2	114065572	Intergenic	*PAX8*	C/T	0.749	0.065	0.012	2.00E-08
rs62158166	2	114077218	Intergenic	*PAX8*	G/C	0.773	0.068	0.012	1.40E-08
rs62158168	2	114078381	Intergenic	*PAX8*	C/G	0.773	0.068	0.012	1.30E-08
rs12616641[#]	2	114079248	Intergenic	*PAX8*	C/A	0.774	0.069	0.012	1.10E-08
rs62158169	2	114081827	Intergenic	*PAX8*	C/T	0.784	0.068	0.012	3.20E-08
rs62158170	2	114082175	Intergenic	*PAX8*	A/G	0.784	0.068	0.012	2.70E-08
rs199993536	2	114082628	Intergenic	*PAX8*	T/A	0.783	0.067	0.012	4.20E-08
Strength Somatomotor									
rs62158160*	2	114065390	Intergenic	*PAX8*	C/T	0.742	0.066	0.011	6.90E-09
rs111789636	2	114065433	Intergenic	*PAX8*	A/C	0.732	0.065	0.011	9.80E-09
rs62158161*	2	114065572	Intergenic	*PAX8*	C/T	0.749	0.069	0.012	2.40E-09
rs12615370	2	114068017	Intergenic	*PAX8*	T/G	0.751	0.065	0.012	1.60E-08
rs114068802	2	114068802	Intergenic	*PAX8*	G/C	0.75	0.065	0.012	2.00E-08
rs1964463	2	114069021	Intergenic	*PAX8*	A/G	0.749	0.066	0.012	1.00E-08
rs56163359	2	114071473	Intergenic	*PAX8*	T/C	0.751	0.065	0.012	2.50E-08
rs62158163	2	114071717	Intergenic	*PAX8*	T/C	0.751	0.065	0.012	2.40E-08
rs114073498	2	114073498	Intergenic	*PAX8*	A/G	0.751	0.065	0.012	2.50E-08
rs62158166*	2	114077218	Intergenic	*PAX8*	G/C	0.773	0.073	0.012	1.20E-09
rs62158168*	2	114078381	Intergenic	*PAX8*	C/G	0.773	0.073	0.012	1.20E-09
rs12616641*[#]	2	114079248	Intergenic	*PAX8*	C/A	0.774	0.073	0.012	9.90E-10
rs62158169*	2	114081827	Intergenic	*PAX8*	C/T	0.784	0.072	0.012	3.50E-09

rs62158170*	2	114082175	Intergenic	*PAX8*	A/G	0.784	0.073	0.012	2.60E-09
rs199993536*	2	114082628	Intergenic	*PAX8*	T/A	0.783	0.072	0.012	3.10E-09
rs6737318*	2	114083120	Intergenic	*PAX8*	A/G	0.779	0.07	0.012	6.20E-09
rs62158206*	2	114084596	Intergenic	*PAX8*	T/C	0.779	0.071	0.012	4.10E-09
rs7556815*	2	114085785	Intergenic	*PAX8*	G/A	0.78	0.071	0.012	4.70E-09
rs2863957*	2	114089551	Intergenic	*PAX8*	C/A	0.779	0.071	0.012	4.10E-09
rs1823125*	2	114090412	Intergenic	*PAX8*	A/G	0.779	0.071	0.012	3.30E-09
rs60873293*	2	114092549	Intergenic	*PAX8*	G/T	0.779	0.07	0.012	5.70E-09
rs56093896	2	114103966	Intergenic	*PAX8*	C/A	0.786	0.069	0.012	1.40E-08
rs62158211	2	114106139	Intergenic	*PAX8*	G/T	0.786	0.069	0.012	1.40E-08
rs4618068	2	114109355	Intergenic	*PAX8*	C/T	0.787	0.07	0.012	1.30E-08
rs1807282	2	114110036	Intergenic	*PAX8*	A/T	0.787	0.07	0.012	1.30E-08
rs62158213	2	114110568	Intergenic	*PAX8*	G/A	0.787	0.07	0.012	1.30E-08

* denotes SNPs that survived Bonferroni correction after adjusting for independent tests (n = 6) of $p < 5.00 \times 10\text{-}8/6$

[#] denotes SNPs that are Cojo lead SNPs

Abbreviations: SNP, single nucleotide polymorphism; Chr, chromosome; A1, coded allele; A2, non-coded allele; EFA, effect allele frequency; **β**, beta; SE, standard error ; PAX8, paired box gene 8; LINC01375, Long Intergenic Non-Protein Coding RNA 1375; SRSF8, Serine And Arginine Rich Splicing Factor 8; NR2F1-AS1, NR2F1 Antisense RNA 1

Supplementary Table A5. Description of genes influencing the graph theory measures

Gene	**Graph theory measures associated in the current study**	**Description and relevant phenotypes in humans and mammalian models**
SLC25A33	Global efficiency; Characteristic path length	Belongs to the SLC25 family of mitochondrial carrier proteins. Involved in the import/export pyrimidine nucleotides into and from mitochondria. Induced by IGF-1.
TMEM201	Global efficiency; Characteristic path length; Strength of Dorsal attention and Somatomotor networks	Involved in nuclear movement during fibroblast polarisation and migration.
ZEB1	Global efficiency; Characteristic path length	Encodes a zinc finger transcription factor, which likely plays a role in transcriptional repression of interleukin 2. An epithelial-mesenchymal transition (EMT) transcription factor that promotes invasion and metastasis in carcinomas.
SH2B3	Strength of Default network	Encodes a member of the SH2B adaptor family of proteins, which are involved in a range of signaling activities by growth factor and cytokine receptors. Neighbouring gene to *ATXN2* and has been implicated in increased ALS risk.
ATXN2	Strength of Default network	Belongs to a group of genes that is associated with microsatellite-expansion diseases, a class of neurological and neuromuscular disorders caused by expansion of short stretches of repetitive DNA. Associated with spinocerebellar ataxia type 2 (SCA2), frontotemporal lobar degeneration (FTLD), and amyotrophic lateral sclerosis (ALS).

Abbreviations: SLC25A33, Solute Carrier Family 25 Member 33; TMEM201, Transmembrane Protein 201; ZEB1, Zinc Finger E-Box Binding Homeobox 1; SH2B3, SH2B Adaptor Protein 3; ATXN2, Ataxin 2

Supplementary Table A6. Associations lookup from GWAS Catalogue

Variant name	Graph theory measures	Chr	Position	Associated variant risk allele	Associated gene with phenotype	P value	Phenotype description	Pubmed
rs1823125	Strength SM	2	113332835	G	*PAX8, LOC101927400, CBWD2*	1.00E-10	Sleep duration	30531941
rs2863957	Strength SM	2	113331974	C	*PAX8, LOC100130100*	3.00E-18	Sleep duration (short sleep)	30846698
rs62158169	Strength SM & SVAN	2	113324250	C	*CBWD2, FOXD4L1, PAX8*	1.00E-10	Depressive symptom sleep problems binary trait	30952852
rs62158170	Strength SM & SVAN	2	113324598	A	*PAX8-AS1*	6.00E-20	Sleep duration	30804566
rs62158170	Strength SM & SVAN	2	113324598	A	*PAX8/LOC100130100*	8.00E-13	Insomnia symptoms (never/rarely vs. usually)	30804566
rs62158170	Strength SM & SVAN	2	113324598	A	*PAX8/LOC100130100*	1.00E-16	Insomnia symptoms (never/rarely vs. sometimes/usually)	30804566
rs62158170	Strength SM & SVAN	2	113324598	A	*PAX8*	3.00E-13	Insomnia	30804565
rs62158170	Strength SM & SVAN	2	113324598	A	*PAX8*	1.00E-19	Insomnia	30804565
rs62158170	Strength SM & SVAN	2	113324598	A	*PAX8*	7.00E-15	Diastolic blood pressure	30224653
rs62158206	Strength SM	2	113327019	C	PAX8	3.00E-43	Sleep duration	30804565

rs62158206	Strength SM	2	113327019	T	PAX8	8.00E-09	Insomnia	30804565
rs62158211	Strength SM	2	113348562	G	*PAX8*	8.00E-13	Sleep traits (multi-trait analysis)	27992416
rs62158211	Strength SM	2	113348562	T	*PAX8*	1.00E-07	Sleep duration (oversleepers vs undersleepers)	27494321
rs62158211	Strength SM	2	113348562	G	*CHCHD5*	6.00E-17	Sleep duration	30531941
rs62158211	Strength SM	2	113348562	T	*PAX8*	5.00E-14	Sleep duration	30531941, 27494321
rs62158211	Strength SM	2	113348562	T	PAX8	1.00E-12	Sleep duration	30531941, 27494321
rs62158211	Strength SM	2	113348562	G	*PAX8*	2.00E-23	Sleep duration	30531941, 27494321
rs6737318	Strength SM	2	113325543	G	*PAX8, LOC100130100*	3.00E-13	Sleep duration (long sleep)	30846698
rs7556815	Strength SM	2	113328208	G	*PAX8-AS1*	2.00E-18	Sleep duration	30531941
rs7556815	Strength SM	2	113328208	A	*PAX8*	2.00E-54	Sleep duration	30846698

Abbreviations: PAX8, Paired box gene 8; LINC01375, Long Intergenic Non-Protein Coding RNA 1375; NR2F1-AS1, NR2F1 Antisense RNA 1; SRSF8, Serine And Arginine Rich Splicing Factor 8; LOC101927400, Uncharacterised LOC101927400; CBWD2, COBW Domain Containing 2; LOC100130100, Ig kappa chain V-I region Walker-like; FOXD4L1, Forkhead Box D4 Like 1; CHCHD5, Coiled-Coil-Helix-Coiled-Coil-Helix Domain Containing 5; SM, somatomotor network; SVAN, salience network

P-value shows the network associated variants significantly associated with other phenotypes including sleep duration, insomnia, depressive symptoms, and diastolic blood pressure

Supplementary Table A7. Associations lookup from SNPnexus

Variation ID	Chromosome	Phenotype	Gene	PubMed
rs12764517	10	Hirschsprung Disease	*RET*	19196962
rs12764517	10	Triglycerides	*ANK3*	17903299
rs12764517	10	Schizophrenia	*ANK3*	20185149
rs12764517	10	Bipolar Disorder	*ANK3*	18711365
rs12764517	10	Bipolar Disorder	*ANK3*	20351715
rs12764517	10	Bipolar Disorder	*ANK3*	22182935
rs12764517	10	Bipolar Disorder	*ANK3*	21926972
rs12764517	10	Creatinine	*ANK3*	17903292
rs12764517	10	Glomerular Filtration Rate	*ANK3*	17903292
rs12764517	10	Schizophrenia	*ANK3*	21926974
rs12764517	10	Cholesterol, LDL	*ANK3*	17903299
rs12764517	10	Cholesterol, LDL	*ANK3*	17903299
rs12764517	10	Cholesterol, LDL	*ANK3*	17903299
rs12764517	10	Cholesterol, LDL	*ANK3*	17903299
rs12764517	10	Cholesterol, LDL	*ANK3*	17903299
rs12764517	10	Cholesterol, LDL	*ANK3*	17903299
rs12764517	10	Cholesterol, LDL	*ANK3*	17903299
rs12764517	10	Cholesterol, LDL	*ANK3*	17903299
rs12764517	10	Coronary Artery Disease	*LIPA*	21378988
rs12764517	10	Coronary Artery Disease	*LIPA*	21606135
rs147256540	11	Attention Deficit Disorder with Hyperactivity	*NAV2*	18937294
rs147256540	11	HIV-1	*NAV2*	22174851
rs147256540	11	Bipolar Disorder	*HSP90AA2*	21254220
rs147256540	11	Gout	*SF1*	21768215
rs62158160	2	Respiratory Function Tests	*TPO*	17903307
rs62158160	2	C-Reactive Protein	*PTPRN2*	17903293
rs111789636	2	Respiratory Function Tests	*TPO*	17903307
rs111789636	2	C-Reactive Protein	*PTPRN2*	17903293

rs62158161	2	Respiratory Function Tests	*TPO*	17903307
rs62158161	2	C-Reactive Protein	*PTPRN2*	17903293
rs12615370	2	Respiratory Function Tests	*TPO*	17903307
rs12615370	2	C-Reactive Protein	*PTPRN2*	17903293
rs1964463	2	Respiratory Function Tests	*TPO*	17903307
rs1964463	2	C-Reactive Protein	*PTPRN2*	17903293
rs56163359	2	Respiratory Function Tests	*TPO*	17903307
rs56163359	2	C-Reactive Protein	*PTPRN2*	17903293
rs62158163	2	Respiratory Function Tests	*TPO*	17903307
rs62158163	2	C-Reactive Protein	*PTPRN2*	17903293
rs62158166	2	Respiratory Function Tests	*TPO*	17903307
rs62158166	2	C-Reactive Protein	*PTPRN2*	17903293
rs62158168	2	Respiratory Function Tests	*TPO*	17903307
rs62158168	2	C-Reactive Protein	*PTPRN2*	17903293
rs12616641	2	Respiratory Function Tests	*TPO*	17903307
rs12616641	2	C-Reactive Protein	*PTPRN2*	17903293
rs62158169	2	Respiratory Function Tests	*TPO*	17903307
rs62158169	2	C-Reactive Protein	*PTPRN2*	17903293
rs62158170	2	Respiratory Function Tests	*TPO*	17903307
rs62158170	2	C-Reactive Protein	*PTPRN2*	17903293
rs199993536	2	Respiratory Function Tests	*TPO*	17903307
rs199993536	2	C-Reactive Protein	*PTPRN2*	17903293
rs6737318	2	Respiratory Function Tests	*TPO*	17903307
rs6737318	2	C-Reactive Protein	*PTPRN2*	17903293
rs62158206	2	Respiratory Function Tests	*TPO*	17903307
rs62158206	2	C-Reactive Protein	*PTPRN2*	17903293
rs7556815	2	Respiratory Function Tests	*TPO*	17903307
rs7556815	2	C-Reactive Protein	*PTPRN2*	17903293
rs2863957	2	Respiratory Function Tests	*TPO*	17903307
rs2863957	2	C-Reactive Protein	*PTPRN2*	17903293
rs1823125	2	Respiratory Function Tests	*TPO*	17903307

rs1823125	2	C-Reactive Protein	*PTPRN2*	17903293
rs60873293	2	Respiratory Function Tests	*TPO*	17903307
rs60873293	2	C-Reactive Protein	*PTPRN2*	17903293
rs56093896	2	Respiratory Function Tests	*TPO*	17903307
rs56093896	2	C-Reactive Protein	*PTPRN2*	17903293
rs62158211	2	Respiratory Function Tests	*TPO*	17903307
rs62158211	2	C-Reactive Protein	*PTPRN2*	17903293
rs4618068	2	Respiratory Function Tests	*TPO*	17903307
rs4618068	2	C-Reactive Protein	*PTPRN2*	17903293
rs1807282	2	Respiratory Function Tests	*TPO*	17903307
rs1807282	2	C-Reactive Protein	*PTPRN2*	17903293
rs62158213	2	Respiratory Function Tests	*TPO*	17903307
rs62158213	2	C-Reactive Protein	*PTPRN2*	17903293
rs1880544	2	Respiratory Function Tests	*TPO*	17903307
rs1880544	2	C-Reactive Protein	*PTPRN2*	17903293
rs2089478	2	Respiratory Function Tests	*TPO*	17903307
rs2089478	2	C-Reactive Protein	*PTPRN2*	17903293
rs2661030	2	Respiratory Function Tests	*TPO*	17903307
rs2661030	2	C-Reactive Protein	*PTPRN2*	17903293
rs2661035	2	Respiratory Function Tests	*TPO*	17903307
rs2661035	2	C-Reactive Protein	*PTPRN2*	17903293
rs62165320	2	Respiratory Function Tests	*TPO*	17903307
rs62165320	2	C-Reactive Protein	*PTPRN2*	17903293
rs2680724	2	Respiratory Function Tests	*TPO*	17903307
rs2680724	2	C-Reactive Protein	*PTPRN2*	17903293
rs145868127	2	Respiratory Function Tests	*TPO*	17903307
rs145868127	2	C-Reactive Protein	*PTPRN2*	17903293
rs145868127	2	Carcinoma, Squamous Cell|Esophageal Neoplasms|	*GTDC1*	19826048
rs145868127	2	Tobacco Use Disorder	*GTDC1*	20379614
rs62158170	2	Insomnia symptoms (never/rarely vs. usually)	*PAX8/LOC100130100*	30804566
rs62158170	2	Insomnia symptoms (never/rarely vs. sometimes/usually)	*PAX8/LOC100130100*	30804566

rs62158170	2	Insomnia	None	30804565
rs62158170	2	Insomnia	NA	30804565
rs62158170	2	Sleep duration	*PAX8-AS1*	30531941
rs62158170	2	Diastolic blood pressure	*PAX8*	30224653
rs6737318	2	Sleep duration (long sleep)	*PAX8, LOC100130100*	30846698
rs62158206	2	Sleep duration	NA	30804565
rs62158206	2	Insomnia	NA	30804565
rs7556815	2	Sleep duration	None	30846698
rs7556815	2	Sleep duration	*PAX8-AS1*	30531941
rs2863957	2	Sleep duration (short sleep)	*PAX8, LOC100130100*	30846698
rs1823125	2	Sleep duration	*PAX8, LOC101927400, CBWD2*	25469926
rs62158211	2	Sleep duration	*CHCHD5*	30531941
rs62158211	2	Sleep duration	*None*	28604731
rs62158211	2	Sleep traits (multi-trait analysis)	*PAX8*	27992416
rs62158211	2	Sleep duration	*PAX8*	27992416
rs62158211	2	Sleep duration (oversleepers vs undersleepers)	*PAX8*	27494321
rs62158211	2	Sleep duration	*PAX8*	27494321

Abbreviations: RET, Ret Proto-Oncogene; ANK3, Ankyrin 3; LIPA, lipase A, lysosomal acid type; NAV2, Neuron navigator 2; HSP90AA2P, Heat Shock Protein 90 Alpha Family Class A Member 2; SF1, Splicing factor SF1; TPO, Thyroid Peroxidase; PTPRN2, Protein Tyrosine Phosphatase Receptor Type N2; GTDC1, Glycosyltransferase Like Domain Containing 1; PAX8, Paired box gene 8; LOC100130100, Ig kappa chain V-I region Walker-like; PAX8-AS1, PAX8 Antisense RNA 1; LOC101927400, Uncharacterised LOC101927400; CBWD2, COBW Domain Containing 2; CHCHD5, Coiled-Coil-Helix-Coiled-Coil-Helix Domain Containing 5

SNPs associated with the disease as reported in the study

Supplementary Table A8. Enrichment analysis from gene-based association results

GeneSet	**N genes**	**N overlap**	**p**	**genes**
Adipose_Subcutaneous	3668	4	0.16	*NR2F1-AS1, ZEB1, SH2B3, GPER1*
Adipose_Visceral_Omentum	3435	1	0.88	*SH2B3*
Adrenal_Gland	5041	3	0.58	*PAX8, SLC25A33, ZEB1*
Artery_Aorta	4241	5	0.09	*PAX8, SLC25A33, TMEM201, ZEB1*
Artery_Coronary	3006	4	0.09	*NR2F1-AS1, ZEB1, SH2B3, ACAN*
Artery_Tibial	4761	7	0.01	*PAX8, NR2F1-AS1, SLC25A33, TMEM201, ZEB1, ACAN, GPER1*
Bladder	948	1	0.43	*NR2F1-AS1*
Brain_Amygdala	9576	6	0.50	*PAX8, NR2F1-AS1, ZEB1, SH2B3, ATXN2, WTAP*
Brain_Anterior_cingulate_cortex_BA24	9101	5	0.64	*NR2F1-AS1, AMER3, SLC25A33, SH2B3, WTAP*
Brain_Caudate_basal_ganglia	9143	6	0.44	*AMER3, SLC25A33, ZEB1, SH2B3, ATXN2, WTAP*
Brain_Cerebellar_Hemisphere	8981	5	0.63	*NR2F1-AS1, AMER3, SH2B3, ATXN2, GPER1*
Brain_Cerebellum	8976	5	0.63	*NR2F1-AS1, AMER3, TMEM201, SH2B3, ATXN2*
Brain_Cortex	8420	6	0.36	*NR2F1-AS1, AMER3, SLC25A33, ZEB1, SH2B3, WTAP*
Brain_Frontal_Cortex_BA9	8222	5	0.54	*NR2F1-AS1, AMER3, SLC25A33, SH2B3, WTAP*
Brain_Hippocampus	9541	5	0.69	*PAX8, ZEB1, SH2B3, ATXN2, WTAP*
Brain_Hypothalamus	8506	6	0.37	*PAX8, NR2F1-AS1, AMER3, SLC25A33, SH2B3, WTAP*
Brain_Nucleus_accumbens_basal_ganglia	8939	4	0.81	*AMER3, ZEB1, SH2B3, WTAP*
Brain_Putamen_basal_ganglia	9598	6	0.50	*AMER3, SLC25A33, ZEB1, SH2B3, ATXN2, WTAP*
Brain_Spinal_cord_cervical_c-1	7371	4	0.65	*SLC25A33, SH2B3, WTAP, GPER1*
Brain_Substantia_nigra	8873	4	0.80	*PAX8, SLC25A33, SH2B3, WTAP*
Breast_Mammary_Tissue	2985	0	1.00	
Cells_Cultured_fibroblasts	6516	4	0.54	*NR2F1-AS1, ZEB1, SH2B3, GPER1*
Cells_EBV-transformed_lymphocytes	7523	3	0.85	*PAX8, SH2B3, GPER1*
Cervix_Ectocervix	197	0	1.00	

Cervix_Endocervix	1854	1	0.67	*ZEB1*
Colon_Sigmoid	3329	3	0.30	*PAX8, ZEB1, GPER1*
Colon_Transverse	3200	1	0.86	*NR2F1-AS1*
Esophagus_Gastroesophageal_Junction	2861	2	0.50	*PAX8, ZEB1*
Esophagus_Mucosa	5849	5	0.24	*SLC25A33, ZEB1, SH2B3, ATXN2, GPER1*
Esophagus_Muscularis	3091	2	0.55	*PAX8, ZEB1*
Fallopian_Tube	491	0	1.00	
Heart_Atrial_Appendage	9233	5	0.66	*NR2F1-AS1, ZEB1, ATXN2, WTAP, GPER1*
Heart_Left_Ventricle	10067	5	0.74	*SLC25A33, ZEB1, ATXN2, WTAP, GPER1*
Kidney_Cortex	6910	3	0.80	*PAX8, ZEB1, WTAP*
Kidney_Medulla	95	1	0.05	*PAX8*
Liver	9595	5	0.70	*TMEM201, ZEB1, SH2B3, ATXN2, WTAP*
Lung	5173	2	0.83	*SH2B3, GPER1*
Minor_Salivary_Gland	3769	4	0.17	*PAX8, ZEB1, SH2B3, GPER1*
Muscle_Skeletal	8051	5	0.52	*SLC25A33, TMEM201, SH2B3, ATXN2, GPER1*
Nerve_Tibial	6820	8	0.03	*NR2F1-AS1, LOC101928386, TMEM201, ZEB1, ATXN2, ACAN, GPER1*
Ovary	7253	4	0.64	*NR2F1-AS1, TMEM201, ATXN2, GPER1*
Pancreas	10415	7	0.40	*SLC25A33, TMEM201, ZEB1, SH2B3, ATXN2, WTAP, GPER1*
Pituitary	7125	3	0.82	*AMER3, TMEM201, ZEB1*
Prostate	4077	2	0.70	*PAX8, NR2F1-AS1*
Skin_Not_Sun_Exposed_Suprapubic	5468	5	0.20	*PAX8, SLC25A33, ZEB1, SH2B3, GPER1*
Skin_Sun_Exposed_Lower_leg	5315	4	0.37	*SLC25A33, ZEB1, SH2B3, GPER1*
Small_Intestine_Terminal_Ileum	4170	3	0.44	*NR2F1-AS1, SLC25A33, GPER1*
Spleen	6383	4	0.52	*PAX8, SLC25A33, ZEB1, SH2B3*
Stomach	3731	4	0.16	*PAX8, TMEM201, SH2B3, GPER1*
Testis	15330	6	0.95	*LINC01375, NR2F1-AS1, SLC25A33, TMEM201, ATXN2, GPER1*
Thyroid	6764	3	0.79	*PAX8, SH2B3, GPER1*
Uterus	6435	4	0.53	*NR2F1-AS1, TMEM201, ZEB1, ATXN2*

Vagina	3513	1	0.88	*SLC25A33*
Whole_Blood	9013	4	0.81	*SLC25A33, ZEB1, ATXN2, GPER1*

Analysis was performed using FUMA

Abbreviations: *NR2F1-AS1*, NR2F1 Antisense RNA 1; *ZEB1*, Zinc Finger E-Box Binding Homeobox 1; *GPER1*, G Protein-Coupled Estrogen Receptor 1; *PAX8*, Paired Box Gene 8; *SLC25A33*, Solute Carrier Family 25 Member 33; *TMEM201*, Transmembrane Protein 201; *SH2B3*, SH2B Adaptor Protein *3; ATXN*2, Ataxin 2; *ACAN*, aggrecan; *WTAP*, Wilms Tumor 1 Associated Protein; *LINC01375*, Long Intergenic Non-Protein Coding RNA 1375; *LOC101928386*, Uncharacterised LOC101928386; *AMER3*, APC Membrane Recruitment Protein 3

Supplementary Table A9. Genetic correlations with strengths of somatomotor network using LD hub (top 50)

Phenotype	**Category**	**rg**	**SE**	**z**	**h2 obs**	**h2 obs SE**	**h2 int**	**gcov int**	**h2 int SE**	**gcov int SE**	**Rg Padj**
Nervous feelings	ukbb	-0.271	0.076	-3.563	0.066	0.004	1.014	-0.002	0.012	0.005	0.240
Daytime dozing / sleeping (narcolepsy)	ukbb	0.284	0.091	3.108	0.049	0.003	1.009	0.002	0.009	0.006	0.311
Neuroticism	personality	-0.252	0.082	-3.082	0.091	0.008	0.986	0.001	0.013	0.005	0.311
Age at first live birth	ukbb	0.248	0.081	3.056	0.166	0.008	1.047	0.005	0.009	0.005	0.311
Transport type for commuting to job workplace: Cycle	ukbb	0.370	0.123	3.007	0.032	0.003	1.016	-0.005	0.007	0.004	0.311
Depressive symptoms	psychiatric	-0.328	0.114	-2.882	0.048	0.004	0.999	0.002	0.007	0.005	0.333
Qualifications: None of the above	ukbb	-0.221	0.078	-2.847	0.098	0.004	1.066	-0.004	0.012	0.005	0.333
Age at last live birth	ukbb	0.287	0.101	2.830	0.088	0.006	1.017	0.005	0.008	0.005	0.333
Systolic blood pressure_ automated reading	ukbb	-0.209	0.074	-2.807	0.128	0.005	1.067	0.006	0.015	0.006	0.333
Drive faster than motorway speed limit	ukbb	0.233	0.086	2.705	0.057	0.003	1.030	-0.001	0.009	0.005	0.392
Diastolic blood pressure_ automated reading	ukbb	-0.194	0.073	-2.675	0.136	0.006	1.066	0.004	0.016	0.006	0.392
Pulse wave reflection index	ukbb	0.360	0.136	2.648	0.055	0.005	1.008	-0.009	0.007	0.005	0.392
Number of depression episodes	ukbb	0.596	0.227	2.630	0.032	0.012	1.005	-0.008	0.006	0.004	0.392
Qualifications: O levels/GCSEs or equivalent	ukbb	0.236	0.092	2.567	0.049	0.003	1.017	0.001	0.009	0.005	0.441
Fractured/broken bones in last 5 years	ukbb	0.272	0.108	2.527	0.019	0.002	1.008	-0.011	0.008	0.005	0.459
Mineral and other dietary supplements: Glucosamine	ukbb	0.263	0.107	2.453	0.025	0.002	1.009	0.003	0.008	0.005	0.532
Friendships satisfaction	ukbb	-0.264	0.113	-2.329	0.062	0.005	0.998	-0.004	0.007	0.005	0.573
Illness_ injury	ukbb	0.279	0.120	2.316	0.014	0.002	1.011	-0.005	0.007	0.004	0.573

Happiness	ukbb	-0.249	0.108	-2.305	0.062	0.005	1.004	-0.002	0.008	0.005	0.573
Noisy workplace	ukbb	-0.242	0.106	-2.274	0.062	0.006	1.028	-0.003	0.007	0.004	0.573
Alzheimers disease	neurological	-0.475	0.209	-2.274	0.042	0.022	1.069	0.011	0.030	0.005	0.573
Number of days/week walked 10+ minutes	ukbb	-0.191	0.085	-2.258	0.042	0.002	1.010	0.007	0.007	0.005	0.573
Neuroticism score	ukbb	-0.155	0.069	-2.258	0.118	0.006	1.018	-0.006	0.013	0.005	0.573
Obesity class 1	anthropomet	-0.168	0.075	-2.250	0.218	0.012	1.017	0.010	0.011	0.005	0.573
Types of transport used (excluding work): Cycle	ukbb	0.236	0.106	2.227	0.025	0.002	1.026	0.000	0.007	0.005	0.573
Number of cigarettes previously smoked daily	ukbb	-0.220	0.099	-2.210	0.100	0.014	1.002	0.004	0.009	0.005	0.573
Tense / highly strung	ukbb	-0.164	0.075	-2.193	0.057	0.003	0.996	-0.001	0.010	0.005	0.573
Time spent using computer	ukbb	0.164	0.075	2.185	0.096	0.004	1.044	-0.010	0.009	0.006	0.573
Current employment status: Doing unpaid or voluntary work	ukbb	0.386	0.178	2.169	0.009	0.001	1.008	0.000	0.006	0.005	0.573
Vitamin and mineral supplements: Multivitamins +/- minerals	ukbb	0.224	0.104	2.147	0.024	0.002	1.008	-0.005	0.008	0.005	0.573
Number of self-reported cancers	ukbb	-0.478	0.223	-2.144	0.007	0.002	1.014	0.006	0.007	0.006	0.573
Mood swings	ukbb	-0.173	0.081	-2.130	0.071	0.003	1.017	-0.004	0.010	0.006	0.573
Obesity class 3	anthropomet	-0.264	0.125	-2.119	0.121	0.014	0.980	0.011	0.009	0.006	0.573
Non-cancer illness code_ self-reported: muscle or soft tissue injuries	ukbb	0.840	0.397	2.117	0.002	0.001	1.000	-0.007	0.007	0.004	0.573
Subjective well being	psychiatric	0.210	0.100	2.112	0.025	0.002	1.001	0.000	0.007	0.005	0.573
Qualifications: A levels/AS levels or equivalent	ukbb	0.159	0.075	2.111	0.097	0.004	1.053	0.005	0.012	0.006	0.573
Age completed full time education	ukbb	0.178	0.085	2.084	0.085	0.005	1.063	0.008	0.010	0.006	0.573
Diagnoses - main ICD10: N32 Other disorders of bladder	ukbb	-0.490	0.237	-2.070	0.004	0.001	0.989	0.005	0.006	0.004	0.573

Sleep duration	ukbb	-0.153	0.074	-2.060	0.071	0.004	1.024	-0.008	0.010	0.005	0.573
Vitamin and mineral supplements: Vitamin B	ukbb	0.366	0.179	2.046	0.007	0.002	1.000	-0.002	0.007	0.005	0.573
Non-cancer illness code_ self-reported: hypertension	ukbb	-0.153	0.075	-2.044	0.114	0.005	1.057	-0.004	0.017	0.006	0.573
Diagnoses - main ICD10: I10 Essential (primary) hypertension	ukbb	0.654	0.321	2.037	0.003	0.001	0.998	-0.010	0.006	0.004	0.573
Alcohol intake frequency.	ukbb	-0.162	0.080	-2.026	0.084	0.004	1.044	0.004	0.010	0.006	0.573
Wears glasses or contact lenses	ukbb	-0.231	0.114	-2.023	0.016	0.002	1.001	0.013	0.008	0.004	0.573
Vascular/heart problems diagnosed by doctor: High blood pressure	ukbb	-0.150	0.074	-2.018	0.116	0.005	1.062	-0.003	0.017	0.006	0.573
Other eye problems	ukbb	-0.285	0.141	-2.014	0.009	0.002	1.024	-0.003	0.007	0.005	0.573
Ever had prostate specific antigen (PSA) test	ukbb	0.250	0.125	1.997	0.034	0.003	1.004	-0.008	0.007	0.005	0.584
Average weekly spirits intake	ukbb	0.221	0.112	1.971	0.032	0.003	1.017	-0.004	0.008	0.005	0.601
Cancer diagnosed by doctor	ukbb	-0.405	0.206	-1.964	0.007	0.002	1.010	0.005	0.007	0.005	0.601

Abbreviations: rg, genetic correlation between two traits; SE, standard error; h2, heritability; h2 obs & h2 obs SE, observed scale h2 for trait 2 and standard error; h2 int & h2 int SE, single-trait LD Score regression intercept for trait 2 and standard error; gcov int & gcov int SE, cross-trait LD Score regression intercept and standard error; ICV, intracranial volume

Supplementary Table A10. Associations between graph theory measures and sleep duration in UK Biobank

Graph theory measures	**β**	**SE**	**t**	***p***
Eglob	-0.047	0.008	-6.181	6.52E-10
Charpath	0.048	0.008	6.240	4.47E-10
Modularity	0.009	0.008	1.188	0.235
Transitivity	-0.031	0.008	-3.985	6.77E-05
Eloc DMN	-0.026	0.008	-3.384	0.001
Eloc DAN	-0.019	0.008	-2.477	0.013
Eloc FPCN	-0.012	0.008	-1.528	0.127
Eloc LIMB	-0.029	0.008	-3.717	0.0002
Eloc SVAN	-0.022	0.008	-2.832	0.005
Eloc SM	-0.016	0.008	-2.101	0.036
Eloc VIS	-0.020	0.008	-2.624	0.009
Strength DMN	-0.033	0.008	-4.325	1.53E-05
Strength DAN	-0.036	0.008	-4.734	2.22E-06
Strength FPCN	-0.020	0.008	-2.645	0.008
Strength LIMB	-0.040	0.008	-5.253	1.51E-07
Strength SVAN	-0.039	0.008	-5.120	3.08E-07
Strength SM	-0.050	0.008	-6.498	8.33E-11
Strength VIS	-0.038	0.008	-4.930	8.31E-07

Abbreviations: β, beta; SE, standard error, t, t-value; *p*, p-value; Eglob, global efficiency; Charpath, characteristic path length; Eloc, local efficiency; DMN, strength of default mode network; DAN, strength of dorsal attention network; FPCN, strength of frontoparietal control network; LIMB, strength of limbic network; SVAN, strength of salience/ ventral attention network; SM, strength of somatomotor network; VIS, strength of visual network

Supplementary Table A11. Associations between graph theory measures and insomnia in UK Biobank

Graph theory measures	**β No insomnia vs Sometimes**	**β No insomnia vs Usually**	**SE No insomnia vs Sometimes**	**SE No insomnia vs Usually**	***p* No insomnia vs Sometimes**	***p* No insomnia vs Usually**
Eglob	-0.0505	-0.0531	0.0174	0.0201	0.0037	0.0083
Charpath	0.0491	0.0478	0.0174	0.0201	0.0047	0.0173
Modularity	0.0438	0.0739	0.0177	0.0204	0.0131	0.0003
Transitivity	-0.0505	-0.0546	0.0176	0.0203	0.0041	0.0072
Eloc DMN	-0.0377	-0.0357	0.0178	0.0205	0.0340	0.0824
Eloc DAN	-0.0493	-0.0589	0.0177	0.0205	0.0054	0.0040
Eloc FPCN	-0.0316	-0.0557	0.0177	0.0205	0.0741	0.0065
Eloc LIMB	-0.0372	-0.0360	0.0177	0.0205	0.0355	0.0781
Eloc SVAN	-0.0298	-0.0388	0.0177	0.0204	0.0921	0.0576
Eloc SM	-0.0378	-0.0399	0.0178	0.0205	0.0331	0.0521
Eloc VIS	-0.0446	-0.0633	0.0178	0.0206	0.0123	0.0021
Strength DMN	-0.0557	-0.0540	0.0176	0.0204	0.0016	0.0080
Strength DAN	-0.0530	-0.0694	0.0175	0.0202	0.0025	0.0006
Strength FPCN	-0.0384	-0.0572	0.0175	0.0202	0.0285	0.0048
Strength LIMB	-0.0430	-0.0242	0.0176	0.0203	0.0144	0.2332
Strength SVAN	-0.0400	-0.0447	0.0174	0.0201	0.0218	0.0266
Strength SM	-0.0540	-0.0576	0.0174	0.0201	0.0019	0.0042
Strength VIS	-0.0447	-0.0624	0.0177	0.0205	0.0116	0.0023

Abbreviations: β, beta; SE, standard error, t, t-value; *p*, p-value; Eglob, global efficiency; Charpath, characteristic path length; Eloc, local efficiency; DMN, strength of default mode network; DAN, strength of dorsal attention network; FPCN, strength of frontoparietal control network; LIMB, strength of limbic network; SVAN, strength of salience/ ventral attention network; SM, strength of somatomotor network; VIS, strength of visual network

Supplemental Figures for Chapter 3.

Supplementary Figure B1. Correlations between the graph theory measures in the UK Biobank sample (n = 18,445). Blue represents positive correlations whereas red represents negative correlations.

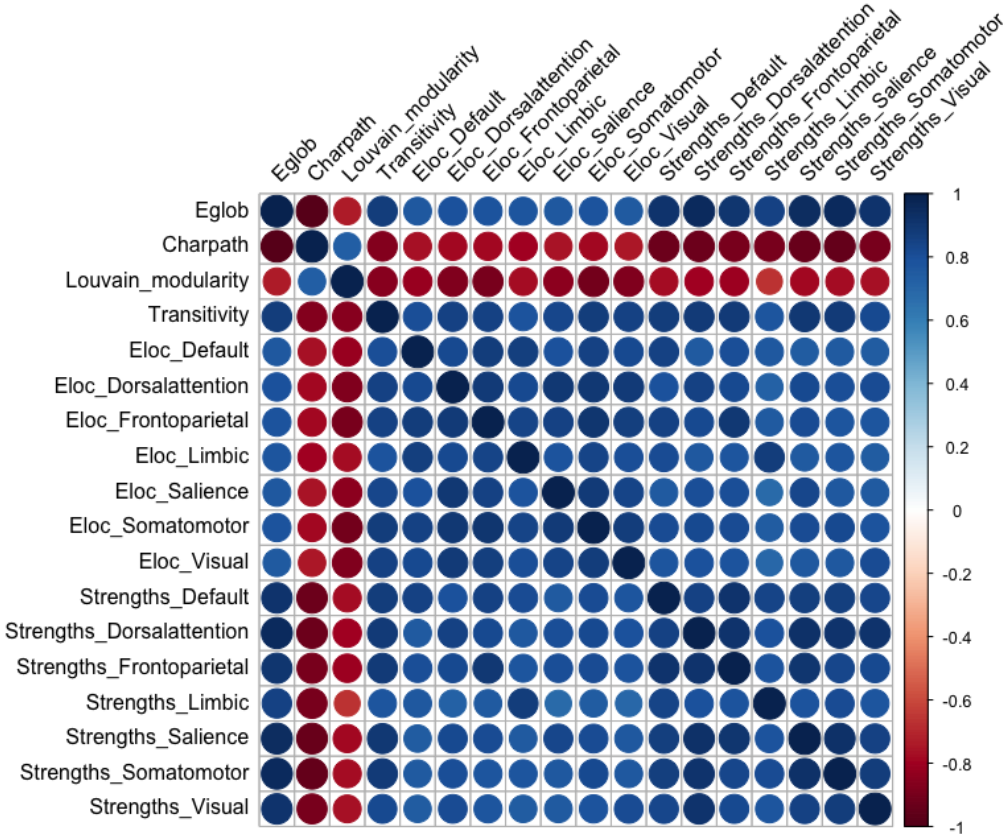

Abbreviations: Eglob, global efficiency; Charpath, characteristic path length; Eloc, local efficiency

Supplementary Figure B2. Manhattan and quantile-quantile (QQ) plots in the UK Biobank sample (n = 18,445).

In the Manhattan plots, each point represents a single genetic variant plotted according to its genomic position (x-axis) and its $-\log_{10}(P)$ for two-tailed associations with graph theory measures (y-axis). In QQ-plots, the line represents the expected null distribution and Lambda inflation factors (λ) are provided in each plot. Linear regression models were adjusted for age, age^2, sex, age × sex, age^2 × sex, head motion from resting-state fMRI, head position, volumetric scaling factor needed to normalise for head size, genotyping array, the 10 genetic principal components. The black solid line represents the classical GWAS significance threshold of $p < 5 \times 10^{-8}$. Genomic inflation factor (lambda gc) is between 1.013 to 1.046.

B2A. Global efficiency

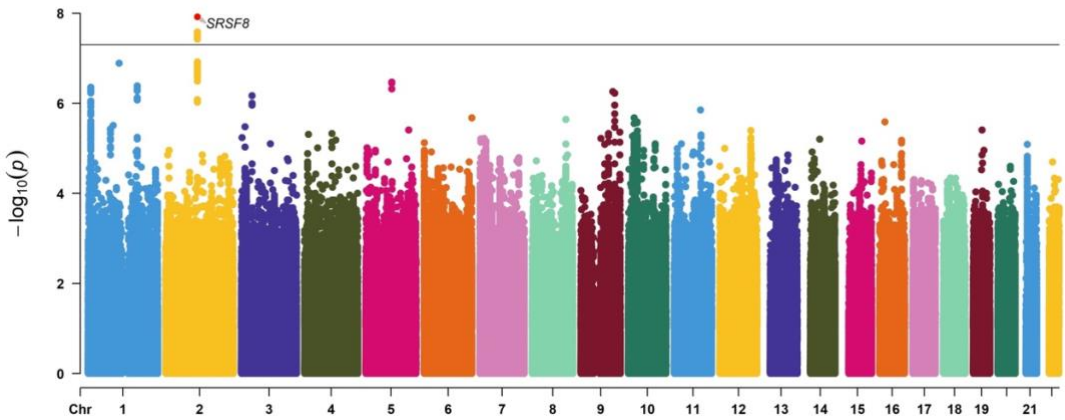

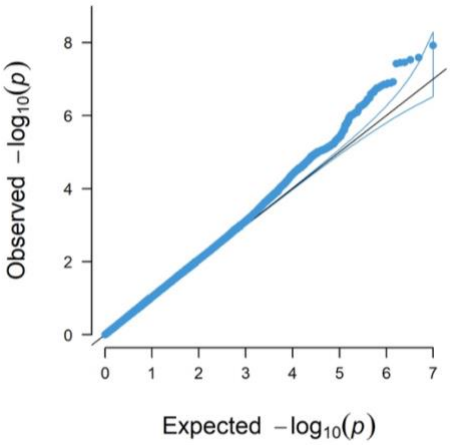

Lambda gc = 1.043

B2B. Characteristic path length

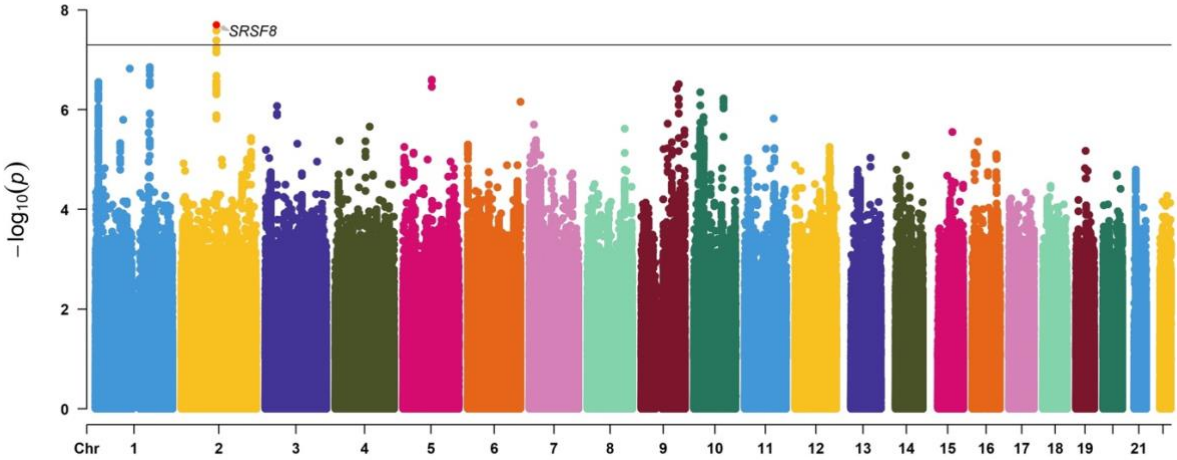

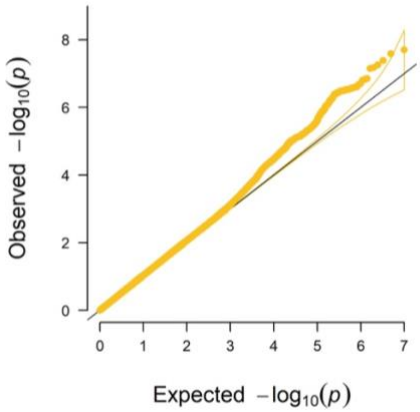

Lambda gc = 1.046

B2C. Louvain Modularity

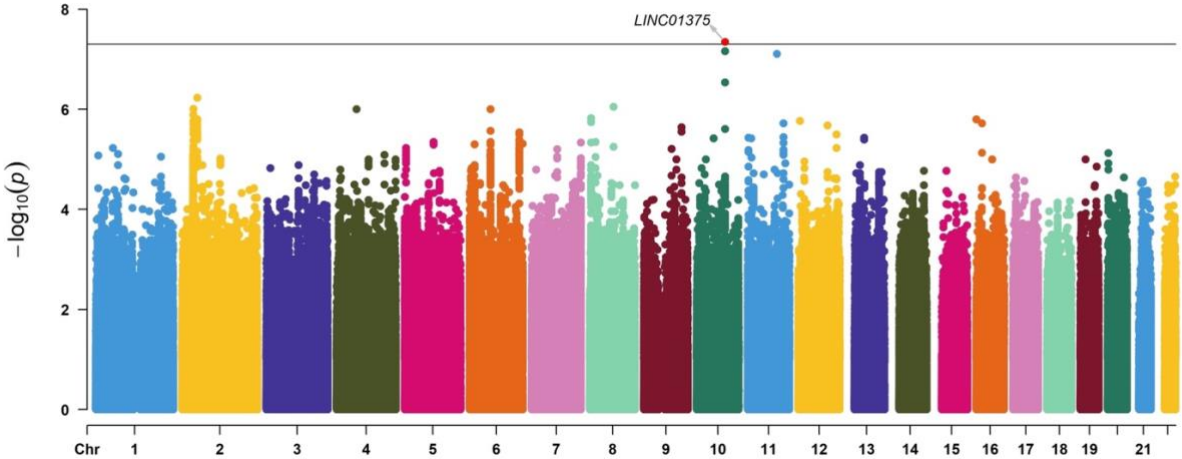

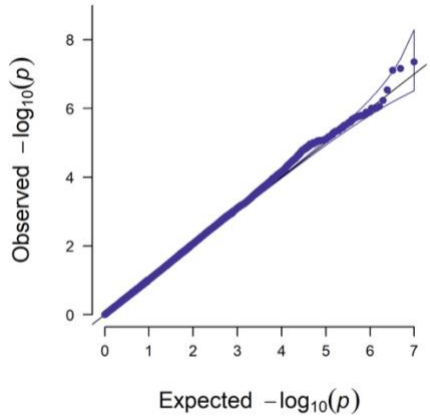

Lambda gc = 1.034

B2D. Transitivity

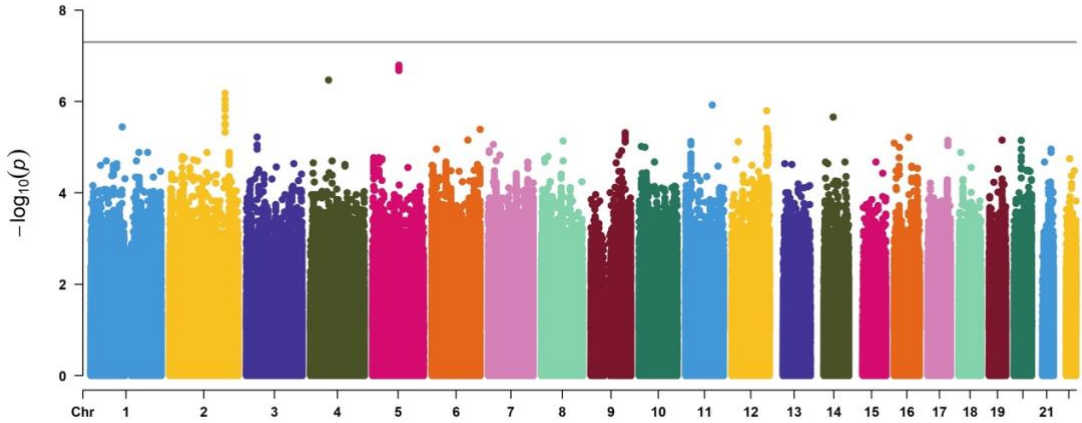

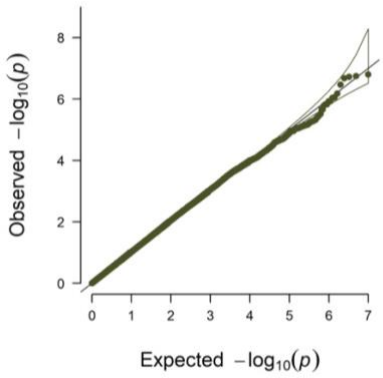

Lambda gc = 1.027

B2E. Local efficiency of default network

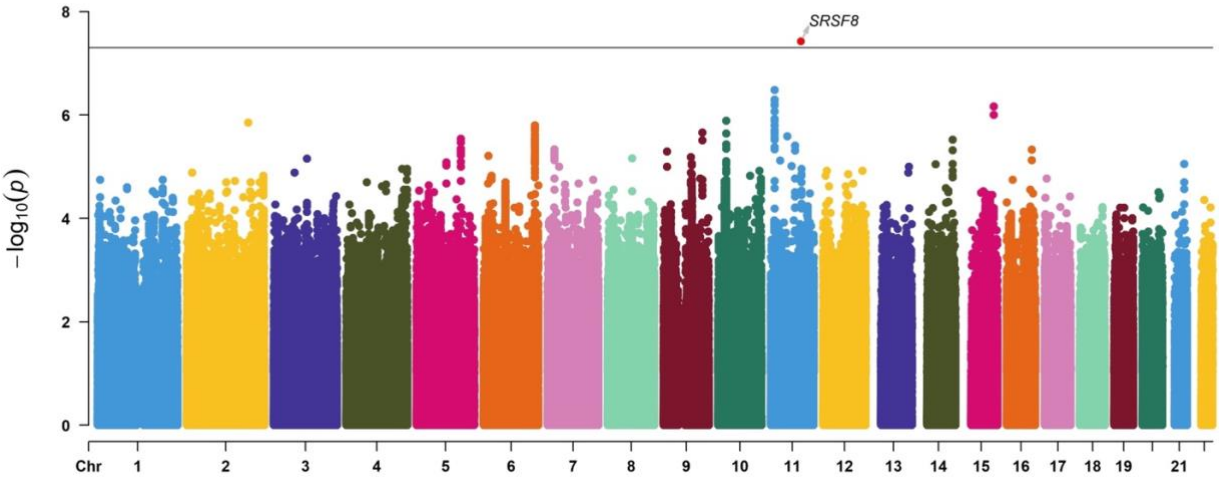

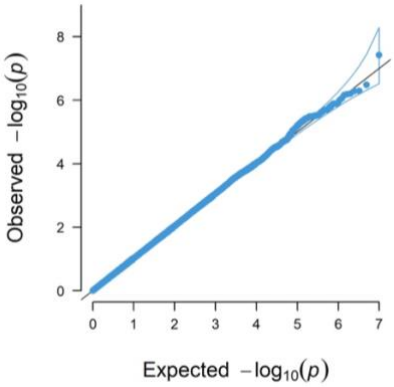

Lambda gc = 1.024

B2F. Local efficiency of dorsal attention network

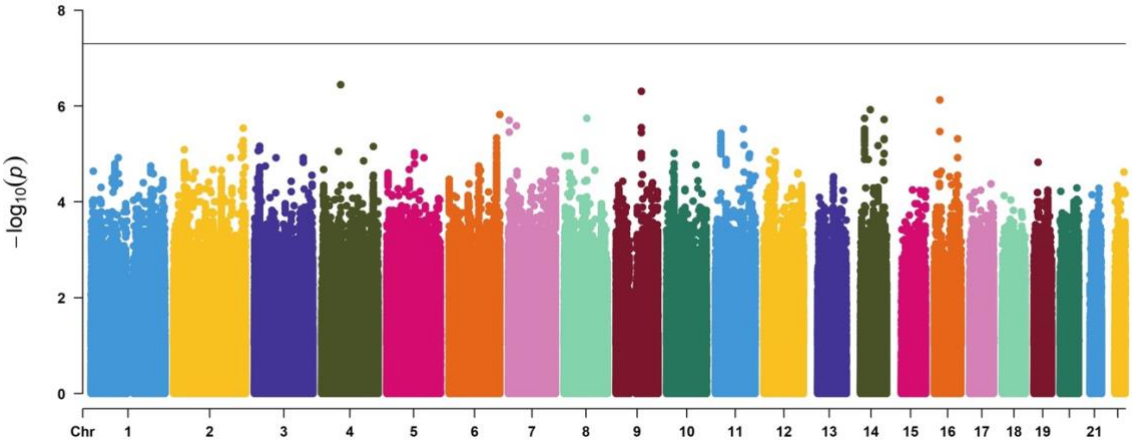

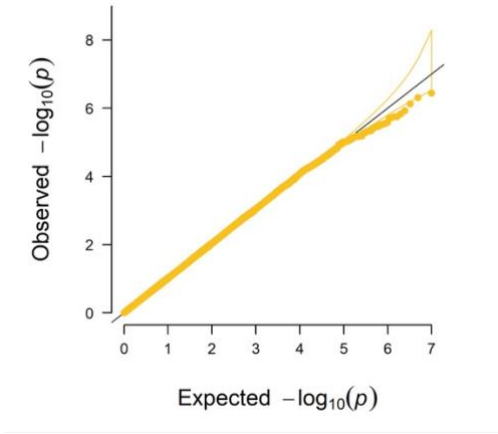

Lambda gc = 1.021

B2G. Local efficiency of frontoparietal network

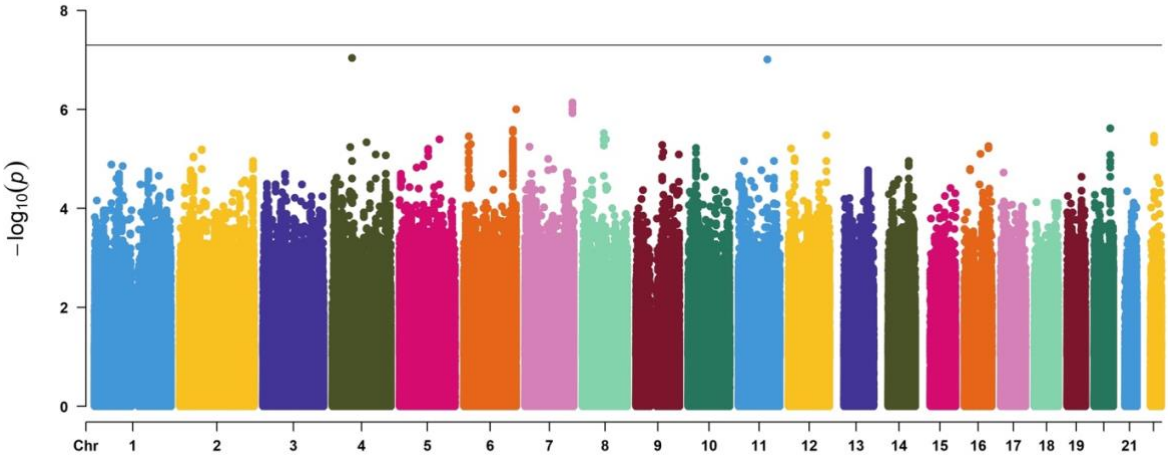

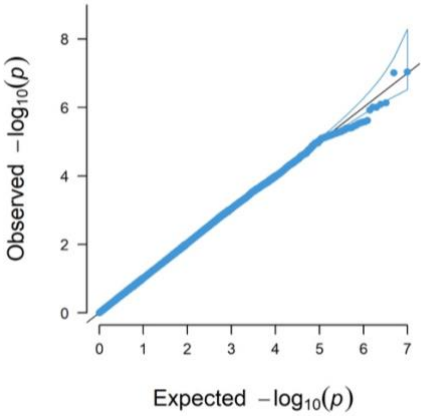

Lambda gc = 1.020

B2H. Local efficiency of limbic network

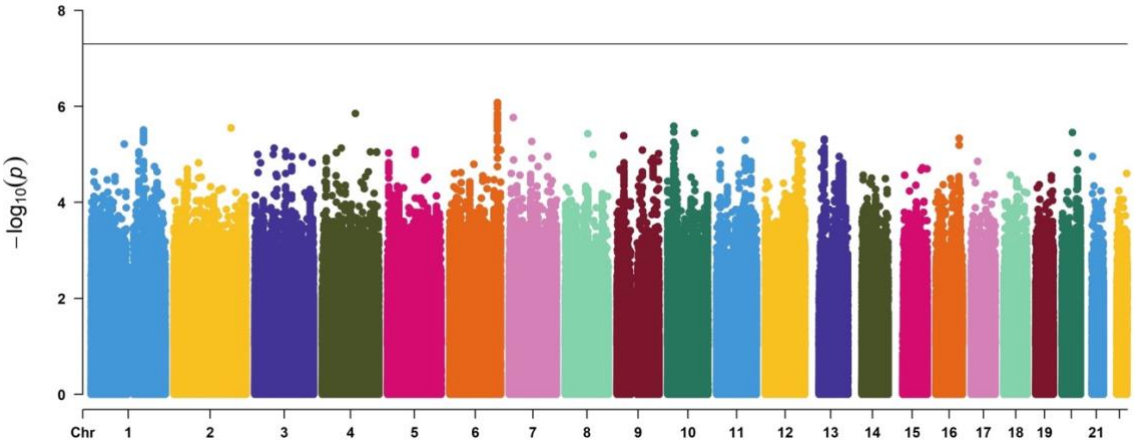

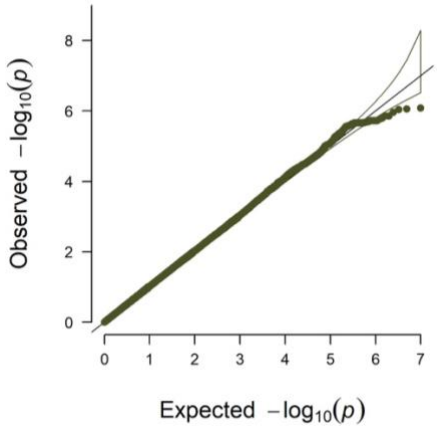

Lambda gc = 1.022

B2I. Local efficiency of salience network

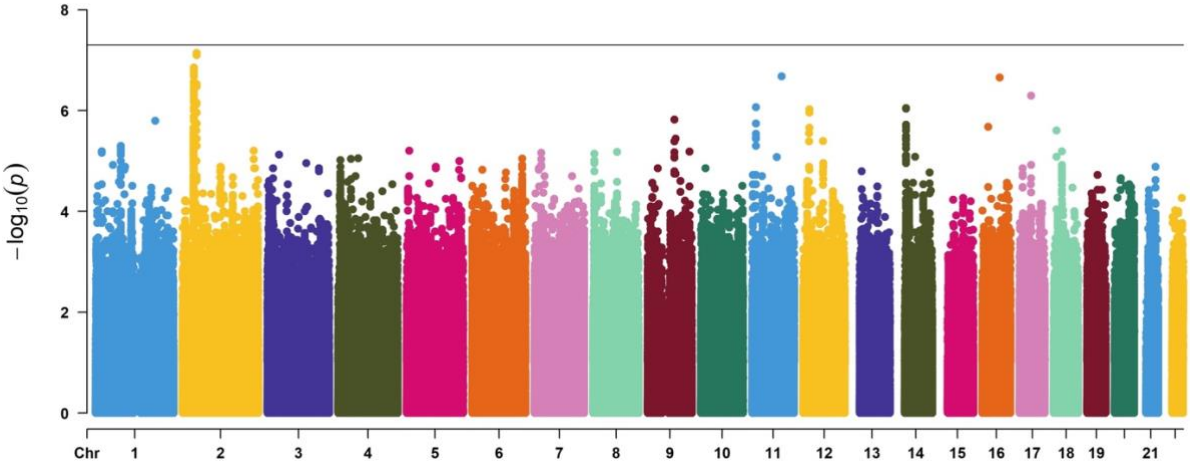

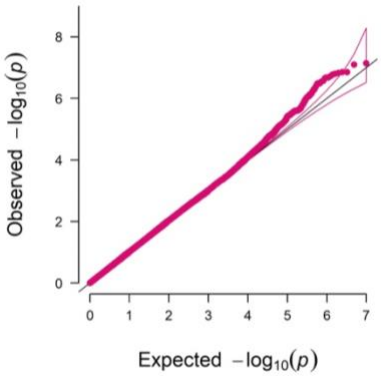

Lambda gc = 1.019

B2J. Local efficiency of somatomotor network

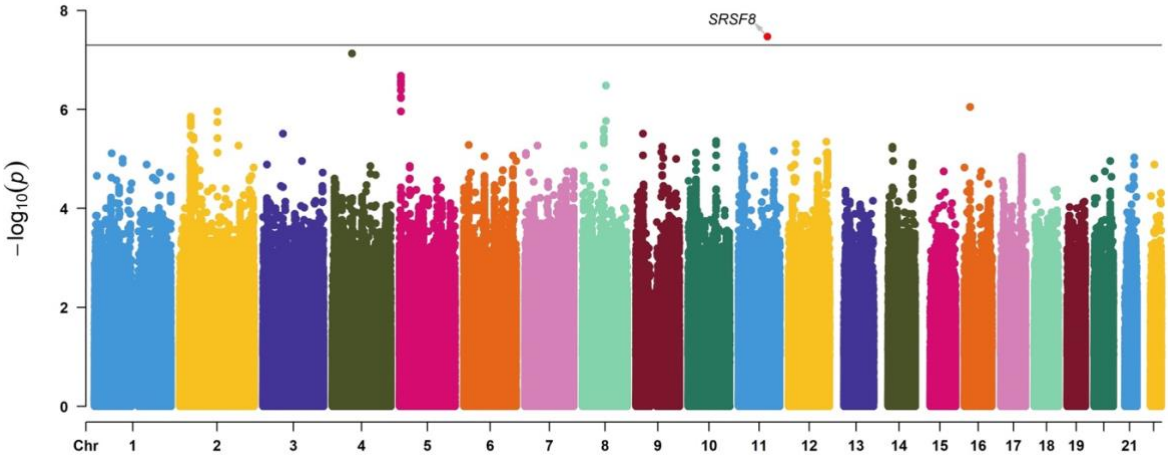

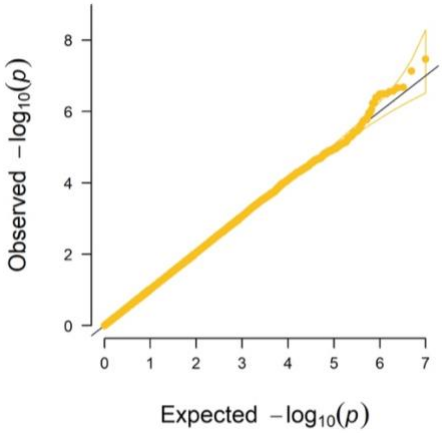

Lambda gc = 1.025

B2K. Local efficiency of visual network

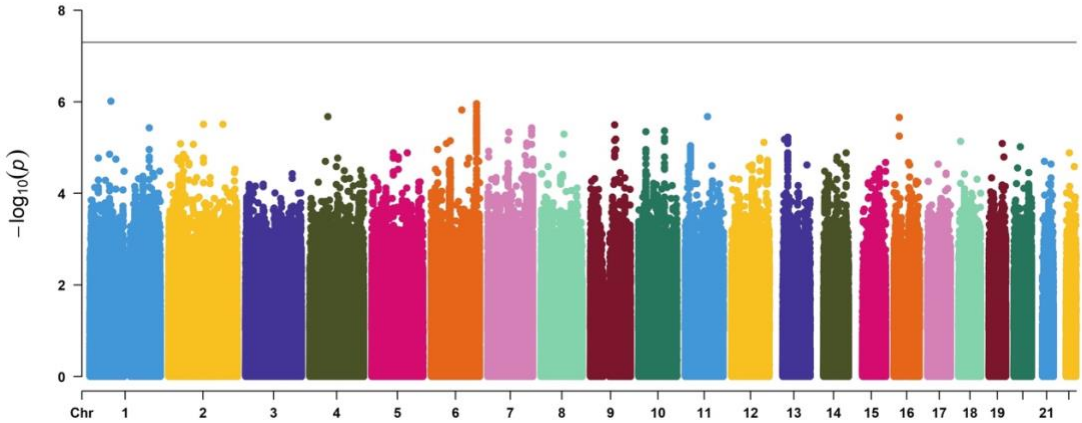

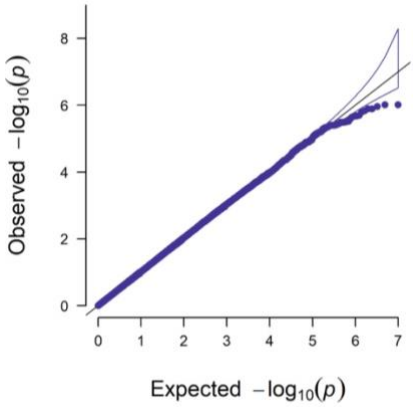

Lambda gc = 1.018

B2L. Strength of default network

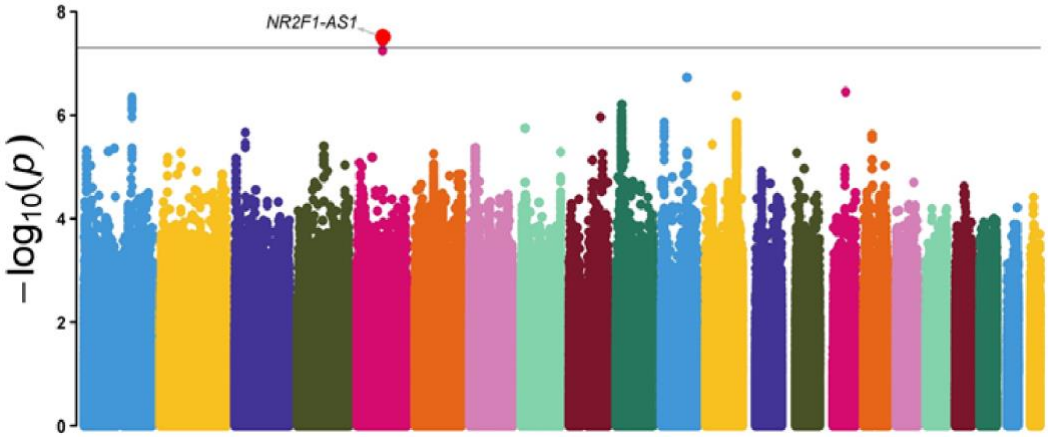

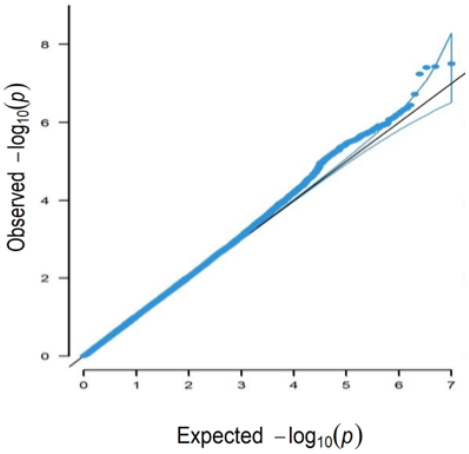

Lambda gc = 1.026

B2M. Strength of dorsal attention network

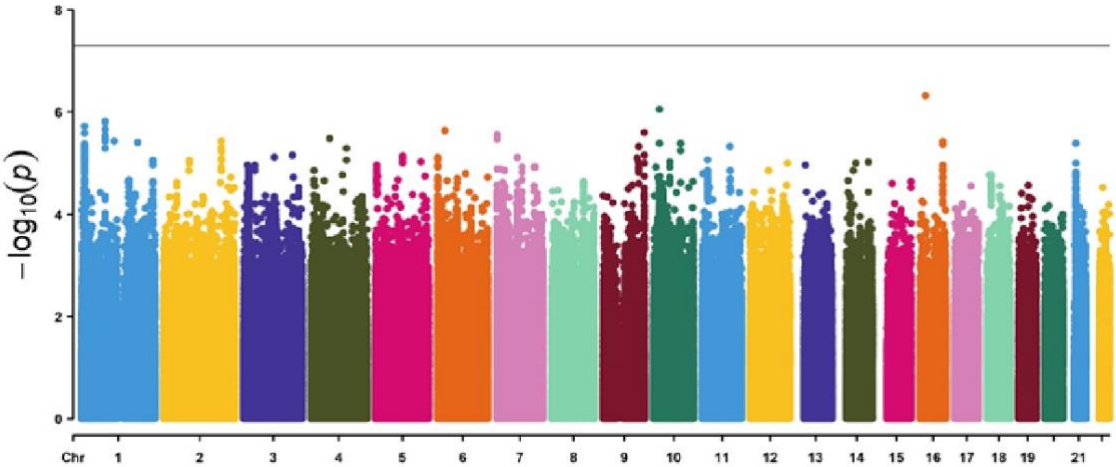

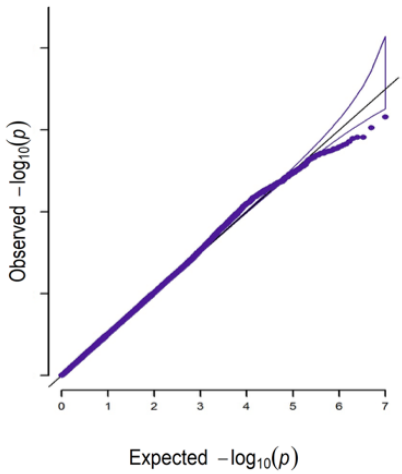

Lambda gc = 1.033

B2N. Strength of frontoparietal network

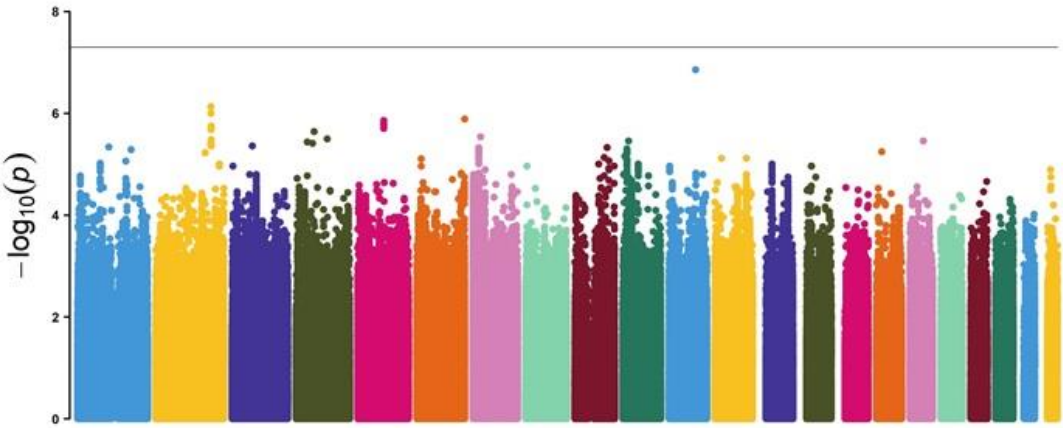

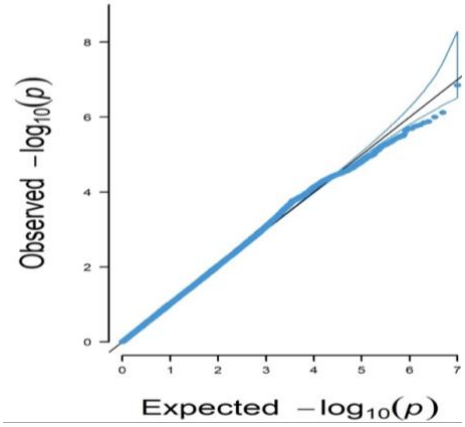

Lambda gc = 1.041

B2O. Strength of limbic network

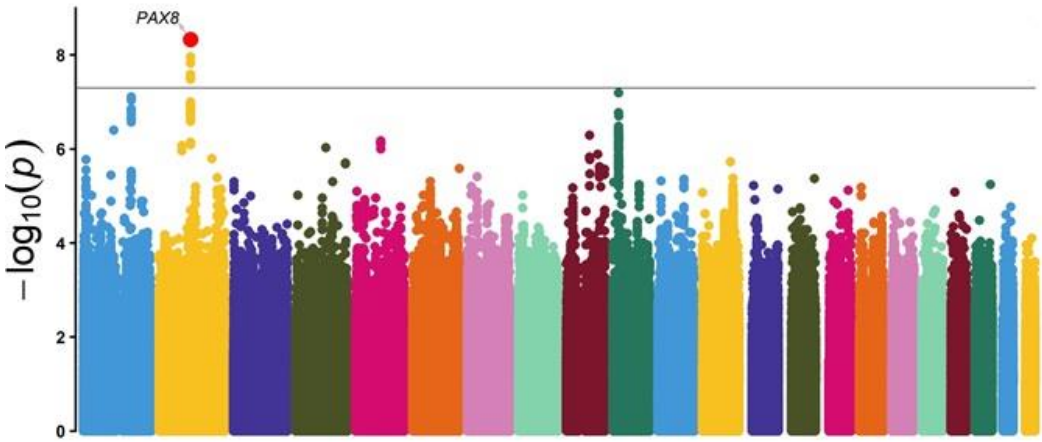

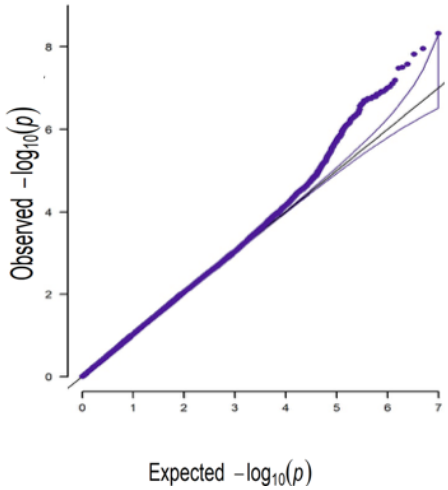

Lambda gc = 1.013

B2P. Strength of salience network

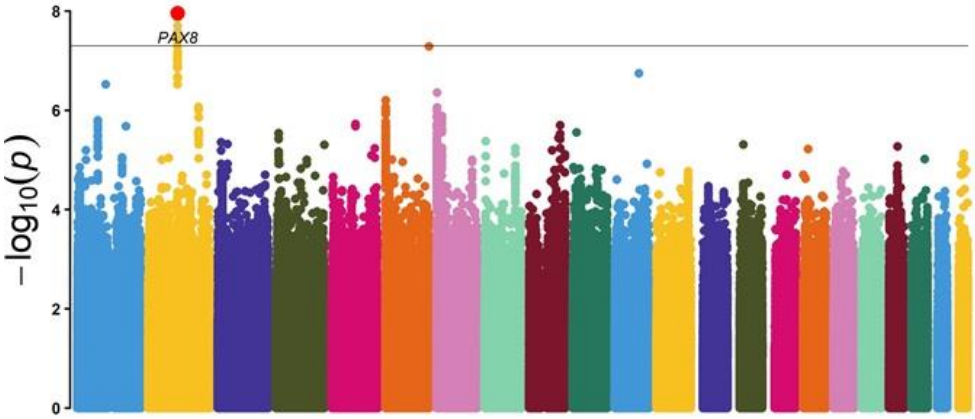

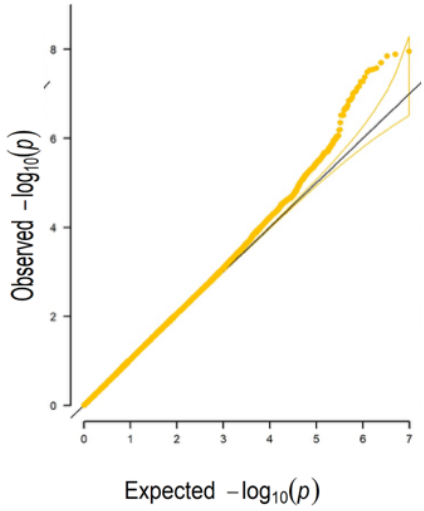

Lambda gc = 1.022

B2Q. Strength of somatomotor network

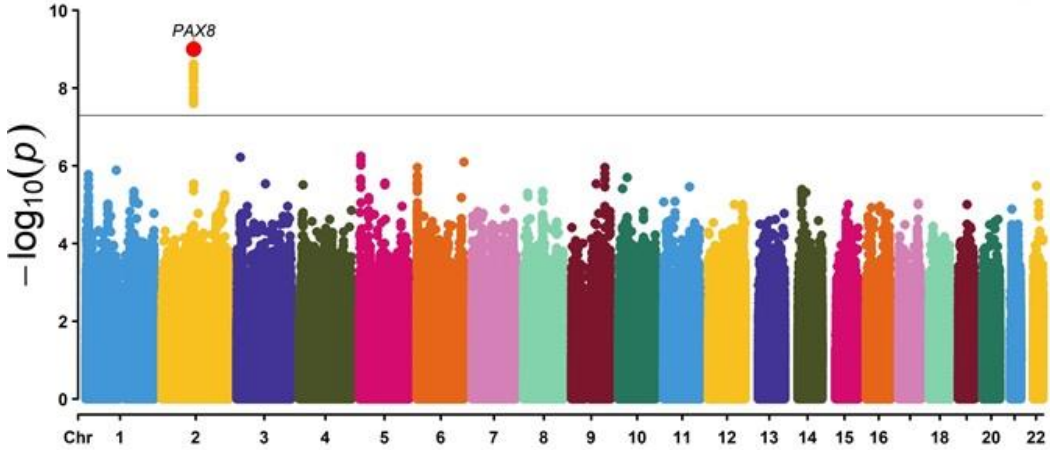

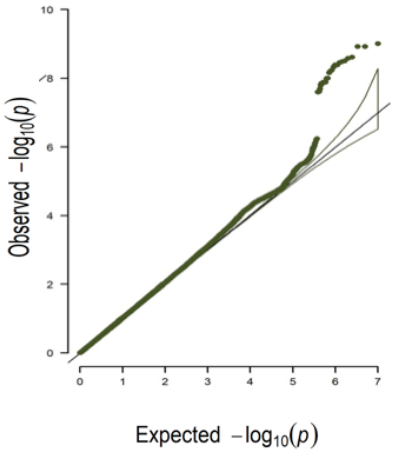

Lambda gc = 1.037

B2R. Strength of visual network

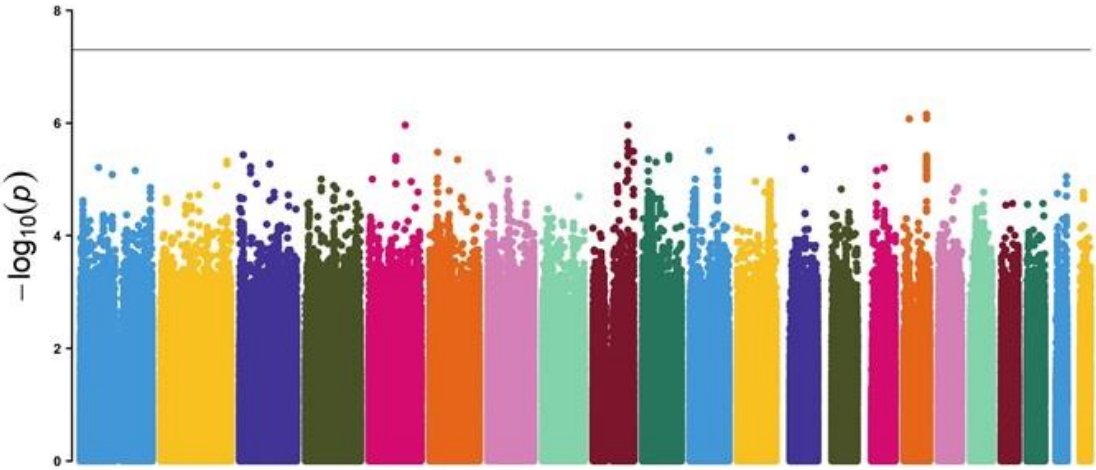

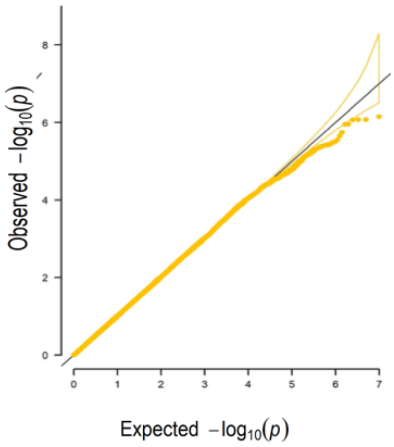

Lambda gc = 1.034

Supplementary Fig. B3. Linkage disequilibrium plot of the GWAS region on chromosome 2 associated with network measures.

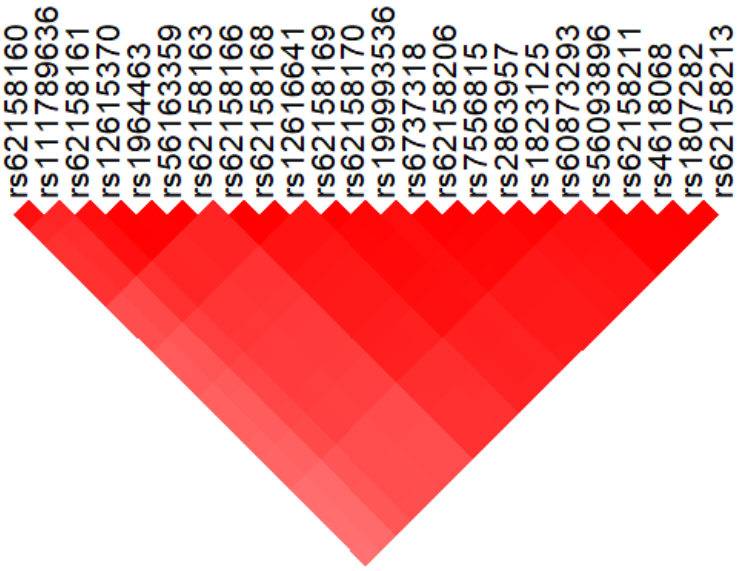

Supplementary Figure B4. Heat map of gene expression levels across tissues for the list of genes found in the gene-based association analysis using FUMA Gene2Func.

The colour bar represents the magnitude and direction of the gene expression – red represents higher expression of the genes compared to the cells filled in blue across tissue types.

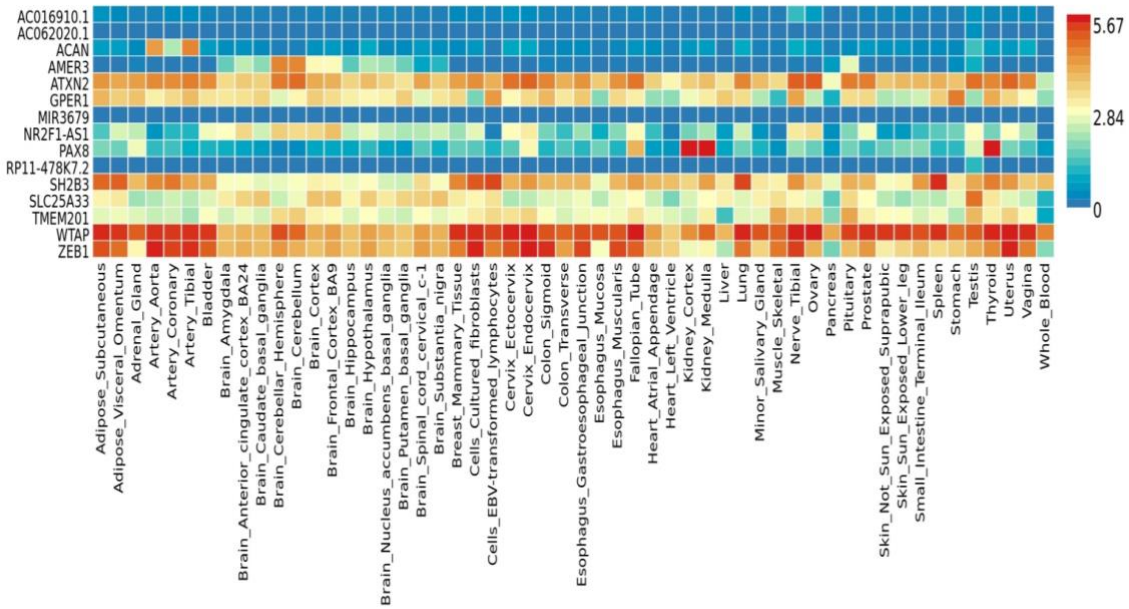

CHAPTER 4: AGE- AND SEX-RELATED TOPOLOGICAL ORGANISATION OF HUMAN BRAIN FUNCTIONAL NETWORKS AND THEIR RELATIONSHIP TO COGNITION

Abstract

Age and sex have been associated with changes in functional brain network topology and cognition in large population of older adults. However, findings from previous studies were mixed. We explored this question further by examining differences in 11 resting-state graph theory measures with respect to age, sex, and their relationships with cognitive performance in 17,127 UK Biobank participants (mean=62.83±7.41 years). Age was associated with an overall decrease in the effectiveness of network communication (i.e. integration) and loss of functional specialisation (i.e. segregation) of specific brain regions. Sex differences were also observed, with women showing more efficient networks which were less segregated than in men (FDR adjusted $p<.05$). Age-related changes were also more apparent in men than women, which suggests that men may be more vulnerable to cognitive decline with age. Interestingly, while network segregation and strength of limbic network were only nominally associated with cognitive performance, the network measures collectively were significantly associated with cognition (FDR adjusted $p \leq .002$). This may imply that individual measures may be inadequate to capture much of the variance in neural activity or its output and need further refinement. The complexity of the functional brain organisation may be shaped by an individual's age and sex, which ultimately may influence cognitive performance of older adults. Age and sex stratification may be used to inform clinical neuroscience research to identify older adults at risk of cognitive dysfunction.

4.1 Introduction

The brain is topographically organised into distinct networks. In the recent years, neuroscientists have examined networks to understand brain function rather than to assess the brain regions as was done classically. There are several approaches to mapping these brain networks, with one approach being resting-state functional magnetic resonance imaging (rs-fMRI). Rs-fMRI measures spontaneous brain activity as low-frequency fluctuations in bold oxygen level-dependent (BOLD) signals and is used to understand brain function (Wang et al., 2010b). In network models of rs-fMRI data, functional brain networks are summarised into a collection of nodes (i.e., brain regions) and edges (i.e., magnitude of temporal correlation in fMRI activity between regions) (Bertolero et al., 2018; Rubinov & Sporns, 2010). This network model can then be used to study the global and local properties of the functional brain networks (Table 4.1). There is evidence that adult human brains are organised into groups of specialised functional networks that are able to respond to various cognitive demands (Wang et al., 2010b). Therefore, studying the organisation of functional networks in the ageing brain may allow us to understand age-associated cognitive changes, even in the absence of brain disease (Burke & Barnes, 2006; Otte et al., 2015).

Reorganisation of the functional networks in the brain has been observed with ageing, and is also associated with changes in cognition (Betzel et al., 2014; Chan et al., 2014; Geerligs et al., 2015; Song et al., 2014; Zhang et al., 2016). Age-related alterations have been associated with a less efficient global network, decreased modularity, longer path lengths, and higher clustering coefficient, which may suggest a shift to more local organisation in older age (Achard & Bullmore, 2007; Geerligs et al., 2015; Wang, Li, Metzak, He, & Woodward, 2010c; Zhang et al., 2016). These topological functional

network changes occurred most pronouncedly in regions important for cognition. For instance, high clustering coefficients in some frontal, temporal, and parietal regions were related to lower performance in verbal and visual memory functions (Sala-Llonch et al., 2014). Declines in default mode network, which comprises of the medial and lateral parietal, medial prefrontal, and medial and lateral temporal cortices (Raichle, 2015), are reported in ageing and have been associated with memory consolidation (Murman, 2015). In addition, it has been observed that age has a mediating role in the correlation between local clustering coefficients and verbal memory learning scores (Sala-Llonch et al., 2014). Similarly, another study found that the relationship between aging and general decline in cognition could be mediated by changes in the functional connectivity measures such as path length (Bagarinao et al., 2019).

Previous studies have also shown sex differences in the organisation of brain functional networks using graph theory measures. Men showed network segregation (i.e., specialised processing of the brain at a local level) whereas women showed more network integration (i.e., how rapidly the brain can integrate specialised information at a global network level) (Zhang et al., 2016). Another study observed that men had a higher clustering coefficient in the right hemisphere than the left hemisphere (Tian et al., 2011), suggesting that men had greater specialisation of the right hemisphere. In addition, age-related differences in reorganisation of functional connectivity may also differ by sex, with men showing increasing between-network connectivity (Goldstone et al., 2016) while women exhibit smaller age-related decreases in the default mode and limbic networks (Scheinost et al., 2015). It is noteworthy that age-related changes in cognition also differ by sex. For instance, a recent study has observed that while women had significantly higher baseline global memory, executive function, and memory

performance than men, they showed significantly faster declines in the global memory and executive function (Levine et al., 2021). Another study found that older men had steeper rates of decline on measures of perceptuomotor speed and integration as well as visuospatial abilities (McCarrey, An, Kitner-Triolo, Ferrucci, & Resnick, 2016). Taken together, the findings show that sex may influence age-related functional reorganisation in the brain and improving our understanding of this may shed light onto why some cognitive abilities differ substantially by sex (Ritchie et al., 2018).

There is evidence to show that changes in cognition may be due to the changes in functional network connectivity. Segregated functional networks, for instance, seemed to be associated with better long-term episodic memory and fluid processing (Wig, 2017). However, there have been mixed findings regarding how resting-state functional connectivity differences relate to cognitive performance. One longitudinal study found age-related decline of within-network connectivity in default mode and executive control networks but without associations with cognitive decline, whereas an association of between-network connectivity of default mode

network and executive control network with processing speed was also observed (Ng et al., 2016). In contrast, another longitudinal study showed positive associations between within-network connectivity of the default mode network and memory performance (Persson, Pudas, Nilsson, & Nyberg, 2014).

One previous study has investigated the functional network architecture of older adults with respect to age, sex, and cognitive performance (attention, episodic and working memory, executive function, and language) in a cohort of 722 participants with ages between 55 and 85 years old (mean age of 67.1 years) (Stumme, Jockwitz, Hoffstaedter, Amunts, & Caspers, 2020). They found resting-state functional connectivity reorganisation with age, particularly in the visual and sensorimotor networks, which may suggest that these networks may mediate age-related differences in cognitive performance. In addition, the authors observed that men showed higher network integration whereas women showed more segregation, which may possibly facilitate sex-related differences in cognitive performance.

This study aims to extend previous work by firstly examining age, sex, and cognitive function in association with functional network properties but in a much larger sample of 17,127 UK Biobank participants. Additionally, a more extensive range of graph theory measures, which assess the global and local properties as well as the strength of the network, will be examined. These measures are namely global efficiency, characteristic path length, Louvain modularity, transitivity, and strength of default, dorsal attention, frontoparietal, limbic, salience, somatomotor, and visual networks, which are typically found to change with aging (Song et al., 2014) and are involved in

multiple neuropathological processes (Khazaee et al., 2015; Lebedev et al., 2014; Munilla et al., 2017).

4.2 Methods

4.2.1 Participants

Data from 20,598 participants of European ancestry with rs-fMRI scans from the UK Biobank (aged between 44 and 80 years old) (Sudlow et al., 2015) were accessed in March 2019. The imaging assessment took place at three different assessment centres: Manchester, Newcastle, and Reading, UK.

This project was approved by the NHS National Research Ethics Service (approval letter dated 17th June 2011, ref. 11/NW/0382), project 10279. All data and materials are available via UK Biobank (http://www.ukbiobank.ac.uk).

4.2.2 Image pre-processing and graph theory analyses

All participants underwent rs-fMRI scan on a Siemens Skyra 3T scanner (Siemens Medical Solutions, Erlangen, Germany). Rs-fMRI was obtained using a blood-oxygen level dependent (BOLD) sequence using an echo-planar imaging (EPI) sequence (TR = 0.735s, TE = 39 ms, FoV = 88 × 88 × 64, voxel resolution 2.4 × 2.4 × 2.4 mm), lasting for ~6 mins (for more details, see https://biobank.ctsu.ox.ac.uk/crystal/crystal/docs/brain_mri.pdf). I analysed the rs-fMRI data that was previously pre-processed by the UK Biobank (Alfaro-Almagro et al., 2018). The pre-processing steps involved: motion correction, intensity normalisation, high-pass temporal filtering (Gaussian-weighted least-squares straight line fitting, with sigma=50.0s), echo-planar imaging (EPI) unwarping, and gradient distortion correction.

ICA+FIX processing (Beckmann & Smith, 2004; Griffanti et al., 2014; Salimi-Khorshidi et al., 2014) was then used to remove structured artefacts. Participants with motion of > 2mm/degrees of translation/rotation were removed. Of the 20,598 participants of British ancestry with rs-fMRI scans provided by the UK Biobank (Sudlow et al., 2015), image pre-processing was successful for 19,820 participants.

The regions of interest (ROIs) used to construct the network properties were selected from the Schaefer atlas (Schaefer et al., 2018) corresponding to 100 cortical regions classified into seven resting-state networks including frontoparietal control (FPCN), default mode (DMN), dorsal attention (DAN), salience ventral attention (SVAN), limbic (LIMB), somatomotor (SM), and visual (VIS) networks. 3dNetCorr command from Analysis of Functional Neuroimaging (AFNI) (Cox, 1996) was used to produce network adjacency matrix for each participant. The mean time-series for each region was correlated with the mean time-series for all other regions and extracted for each participant. More details can be found in Miller et al. (2016). Subsequently, using the derived network adjacency matrix, partial correlation, *r*, between all pairs of signals was computed to form a 100-by-100 (Schaefer atlas) connectivity matrix, which was then Fisher z-transformed. To slightly improve the partial correlation coefficients, L2-regularisation was used (rho = 0.5 for Ridge Regression option in FSLNets). Self-connections and negative correlations were set to zero. As rs-fMRI can vary across magnitude, the use of undirected weighted matrices may provide a more comprehensive picture of the functional brain networks. The stronger the weights, the stronger the connections between nodes. In addition, I used undirected graph because in rs-fMRI, this study is unable to make inferences about the possible direction of information flow. However, undirected graph is useful as it allows us to identify existing connections

between specific pairs of network nodes (Fornito, Zalesky, & Bullmore, 2016). Therefore, I used weighted and undirected matrices in this study.

All graph theory measures were derived using the Brain Connectivity Toolbox (BCT) (Rubinov & Sporns, 2010). Functional integration can be assessed by global efficiency, which refers to the transmission of information at a global level, and characteristic path length, which is the average shortest distance between any two nodes in the network. To assess network segregation, which characterises the specialised processing of the brain at a local level, I calculated the Louvain modularity and transitivity. Louvain modularity is a community detection method, which iteratively transforms the network into a set of communities, each consisting of a group of nodes. Higher modularity values indicate denser within-modular connections but sparser connections between nodes that are in different modules. Transitivity refers to the sum of all the clustering coefficients around each node in the network and is normalised collectively. Finally, strength (weighted degree) is described as the sum of all neighbouring edge weights. High connectivity strength indicates stronger connectivity between the regions, which provides an estimation of functional importance of each network. Subsequently, I averaged the left-right hemisphere to derive a value for each node and averaged within each network to derive a value for each of the 7 networks for strength measures.

4.2.3 Cognition

Cognitive assessments were administered on a touchscreen computer and were acquired at the imaging visit (instance 2). Seven tests from the UK Biobank battery of tests were selected to represent three cognitive domains (Cox, Ritchie, Fawns-Ritchie, Tucker-Drob, & Deary, 2019; Kendall et al., 2017) namely processing speed, memory, and

executive function, in this study. All test scores were first z-transformed and then averaged to form domain scores. Processing speed domain included the following tests: “Reaction Time” (average time to correctly identify matches in a “snap”-like card game task), “Trail Making A” (time taken to complete a numeric path), and “Symbol Digit Substitution” (number of correct symbol number matches within the time limit). “Numeric Memory” (maximum number of digits remembered correctly) and “Pairs Matching” (number of incorrect visual matching) represented the memory domain whereas “Trail Making B” (time taken to complete an alphanumeric path) and “Fluid Intelligence” (total number of questions that required logic and reasoning correctly answered) formed the executive function domain. Global cognition was an average of the 3 domains. After including those with cognition data, the final sample in this study was 17,127 UK Biobank participants.

4.2.4 Statistical analyses

Statistical analyses were performed with R (V 4.0.0) (R Core Team, 2020). The graph theory measures were normalized using ranked transformation, rntransform() function in R from GeneABEL package (Karssen et al., 2016) and age was z-transformed for regression analysis. In line with previous studies (Elliott et al., 2018), we controlled for imaging covariates, including head size (intracranial volume), head motion from rs-fMRI, and volumetric scaling factor needed to normalize for head size, as well as scanning site and education. The network measures were residualised for imaging covariates and assessment centre and used in all subsequent analyses.

To explore age and sex-related changes in the networks, a multiple linear regression that modelled the targeted property of networks as the dependent variable and age, age^2, sex

(Female = 0, Male = 1), years of education, and age-by-sex and age^2-by-sex interactions as predictors was undertaken. In addition, separate multiple linear regressions were performed to study whether the network measures influenced cognitive functions (dependent variable) with covariates as in the previous model.

Penalised multiple regression with penalty parameters for the regression coefficients was done to further examine the joint effect of the network measures on cognitive functions after accounting for the same set of covariates in the univariate model. Since the network measures are correlated I used penalised regression analysis using glmnet algorithm as implemented in the R package caret (Kuhn, 2015). The glmnet uses two penalty functions with tuning parameters to shrink the beta coefficients in the generalised linear model (glm). I used elastic net glm model with default options to identify the optimum tuning parameter estimates. Network measures and the covariates with non-zero regression coefficient in the training step were fit with linear regression model. Likelihood ratio tests, p-values and the incremental r-square were computed by comparing the model with network measures (full model) against a model with only the covariates (base model). False discovery rate – adjusted p-values were obtained by using Benjamini and Hochberg (1995) procedure as implemented in the R function *p.adjust.*

4.3 Results

4.3.1 Sample characteristics

The current sample of 17,127 participants is a group of generally healthy middle-aged and older adults (range = 45.17 – 80.67 years, mean age = 62.83 ± 7.41 years) after including only samples with cognition and graph theory data. Of this sample 9,037 were

women and 8,090 were men, with an overall mean of 15.73 (± 4.74) years of education. Significant differences were observed for the demographics, graph theory measures, and memory scores between men and women (Table 4.1). Figure 4.1 shows the significant correlations between the network measures, except for transitivity, which was not significantly associated with any other measures.

4.3.2 Age- and sex- related differences in functional brain network

Figure 4.2 and Table 4.2 summarise the results of age- and sex- related differences on the graph theory measures. Global efficiency, Louvain modularity, and strength of all except for strength of default and salience networks decreased significantly with age, whereas characteristic path length and transitivity increased significantly with age.

Sex was significantly associated with all measures, except for transitivity. Men appeared to have lower global efficiency, transitivity, strengths of all the networks as well as longer characteristic path length compared to women. In addition, men showed increased Louvain modularity compared to women.

Age and sex interaction effects were negatively associated with Louvain modularity, and strength of visual, limbic, and default networks. This implies that age-related changes in these measures were more apparent in males than females.

4.3.3 Association of network measures with cognition

I studied whether the network influence on cognition after controlling for age, sex, and education. Although none of these results would survive correction for multiple testing, I report the results that were nominally significant. Louvain modularity showed positive

associations with global cognition whereas transitivity was negatively associated with memory. Strength of limbic network also showed negative associations with global cognition and memory (Supplementary Table C1).

I further examined this relationship to see if it is moderated by age and sex. However, none of the interaction effects between network measures and age or sex on cognition were significant (Supplementary Table C2).

Table 4.1 UK biobank sample characteristics and descriptive statistics (mean ± standard deviation) of graph theory measures and cognition measures in women and men

	Women	**Men**	***t***	***p***
Age, years (range)	62.21 ± 7.23 (45–80)	63.53 ± 7.55 (45-80)	-11.660	*< 0.001*
Education, years	15.44 ± 4.75	16.06 ± 4.70	-8.540	*< 0.001*
Graph theory measures				
Eglob	0.180 ± 1.010	-0.205 ± 0.952	25.573	*< 0.001*
Charpath	-0.199 ± 1.009	0.234 ± 0.904	-28.919	*< 0.001*
Louvain modularity	-0.086 ± 1.014	0.123 ± 0.964	-13.758	*< 0.001*
Transitivity	0.071 ± 0.989	-0.089 ± 0.992	10.544	*< 0.001*
DMN	0.191 ± 1.006	-0.227 ± 0.942	28.021	*< 0.001*
DAN	0.199 ± 1.005	-0.230 ± 0.945	28.643	*< 0.001*
FPCN	0.149 ± 1.019	-0.176 ± 0.950	21.499	*< 0.001*
LIMB	0.160 ± 0.991	-0.203 ± 0.973	24.158	*< 0.001*
SVAN	0.185 ± 1.010	-0.225 ± 0.935	27.415	*< 0.001*
SM	0.024 ± 1.026	-0.037 ± 0.923	3.992	*< 0.001*
VIS	0.194 ± 1.004	-0.222 ± 0.943	27.807	*< 0.001*
Cognition				
Memory	0.01 ± 0.943	0.11 ± 1.002	-4.604	*< 0.001*
Executive	0.12 ± 0.928	0.13 ± 0.990	-0.616	0.538
Processing speed	0.18 ± 0.945	0.14 ± 0.964	1.968	*0.049*
Global cognition	0.14 ± 0.917	0.16 ± 0.983	-1.178	0.239

Analysis were conducted using independent samples t-test for continuous variables. Graph theory measures and cognition are in z-scores i.e. negative value represents poorer score, except for characteristic path length. Abbreviations: *t*, *t*-value; *p*, *p*-value; Eglob, global efficiency; Charpath, characteristic path length; Vis, strength of visual network; SM, strength of somatomotor network; DAN, strength of dorsal attention network; SVAN, strength of salience network; LIMB, strength of limbic network; FPCN, strength of control network; DMN, strength of default network. *Italics* represents significance.

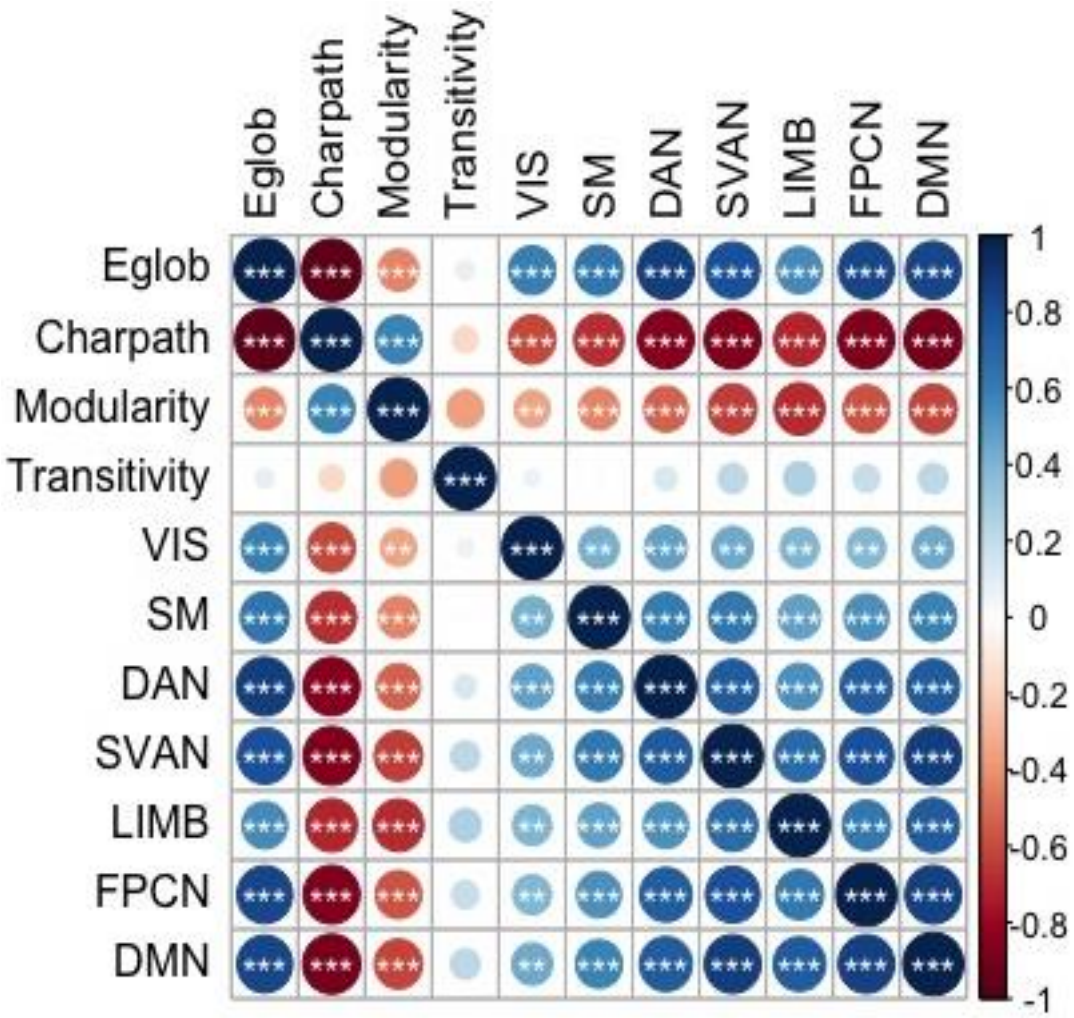

Figure 4.1 Correlations between the graph theory measures

* $p < 0.05$, ** $p < 0.01$, *** $p < 0.001$

Abbreviations: Speed, processing speed; Executive, executive function; Eglob, global efficiency; Charpath, characteristic path length; Vis, strength of visual network; SM, strength of somatomotor network; DAN, strength of dorsal attention network; SVAN, strength of salience network; LIMB, strength of limbic network; FPCN, strength of control network; DMN, strength of default network

Table 4.2 Age- and sex- related differences in graph theory measures

Graph theory measures	**β Age**	**SE Age**	**β Sex**	**SE Sex**	**β AgeXsex**	**SE AgeXsex**	***Padj* Age**	***Padj* Sex**	***Padj* AgeXsex**
Eglob	-0.108	0.011	-0.170	0.021	-0.014	0.016	*3.74E-21*	*1.29E-15*	0.391
Charpath	0.043	0.011	0.226	0.021	0.034	0.016	*1.67E-04*	*3.78E-26*	0.068
Louvain modularity	-0.181	0.011	0.166	0.021	0.046	0.016	*1.05E-57*	*2.96E-15*	*0.016*
Transitivity	0.072	0.011	-0.042	0.021	0.024	0.016	*4.55E-10*	*0.048*	0.179
DMN	0.004	0.011	-0.287	0.021	-0.044	0.016	0.772	*4.28E-41*	*0.016*
DAN	-0.055	0.011	-0.181	0.021	-0.006	0.016	*1.71E-06*	*2.27E-17*	0.681
FPCN	-0.025	0.011	-0.194	0.021	-0.015	0.016	*0.032*	*1.11E-19*	0.391
LIMB	0.142	0.011	-0.263	0.021	-0.043	0.016	*3.14E-36*	*3.04E-35*	*0.016*
SVAN	0.000	0.011	-0.223	0.021	-0.026	0.016	0.971	*2.29E-25*	0.145
SM	-0.093	0.011	-0.090	0.021	-0.031	0.016	*5.86E-16*	*2.27E-05*	0.093
VIS	-0.071	0.011	-0.106	0.021	-0.076	0.016	*5.12E-10*	*6.80E-07*	*1.21E-05*

β, Beta; SE, standard error; *Padj*, adjusted *p*-value; AgeXsex, age and sex interaction; Eglob; global efficiency; Charpath, characteristic path length; DMN, strength of default mode network; DAN, strength of dorsal attention network; FPCN, strength of frontoparietal control network; LIMB, strength of limbic network; SVAN, strength of salience/ventral attention network; SM, strength of somatomotor network; VIS, strength of visual network

Italics represents significance

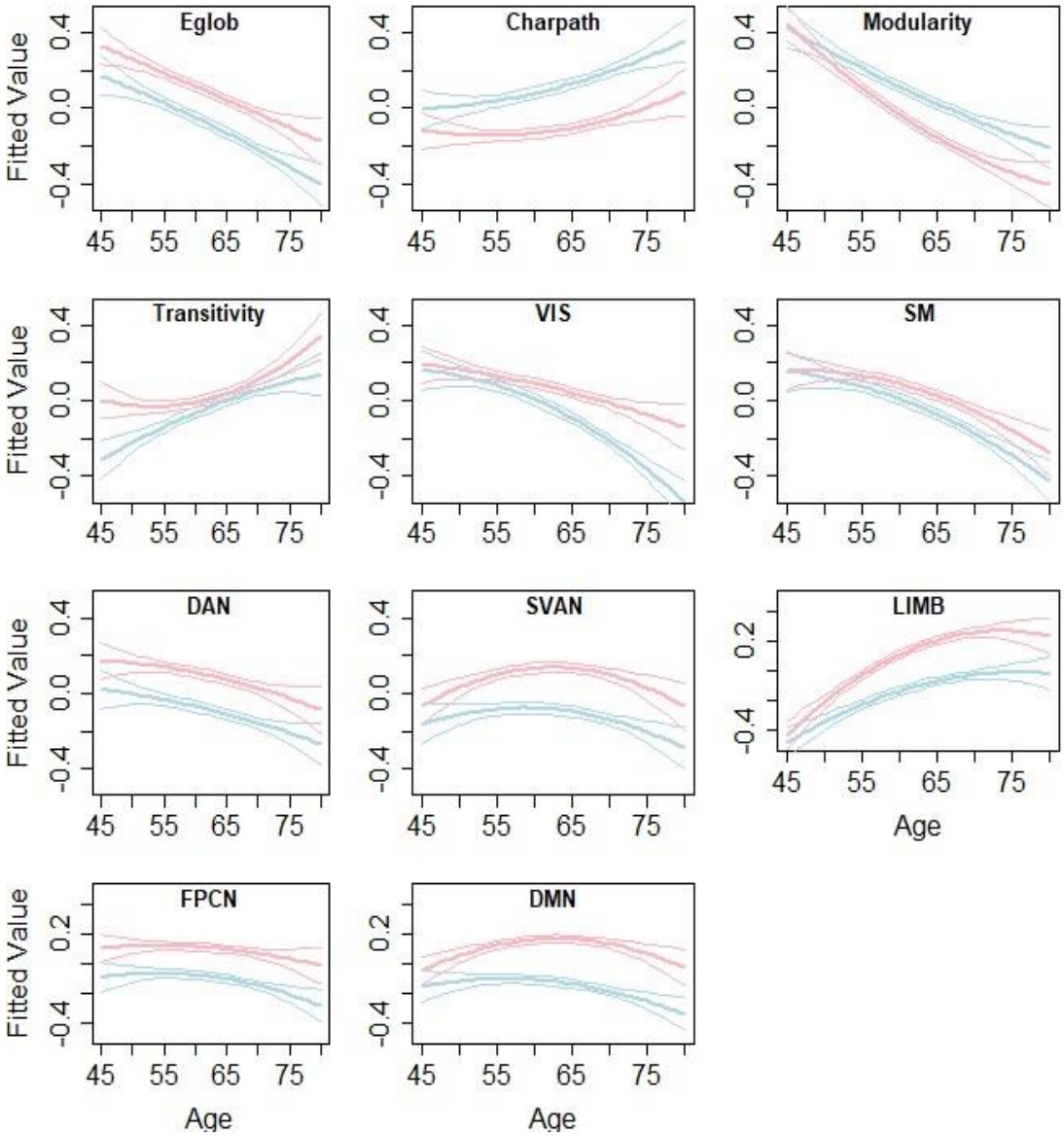

Figure 4.2 Age- and sex- related differences in the graph theory measures

Lines represent the fitted values for men (blue) and women (red) separately The middle line shows the fitted equation evaluated at the mean value of education for each sex, while the top and lower lines represent confidence bands. Abbreviations: Eglob, global efficiency; Charpath, characteristic path length; Vis, strength of visual network; SM, strength of somatomotor network; DAN, strength of dorsal attention network; SVAN, strength of salience network; LIMB, strength of limbic network; FPCN, strength of control network; DMN, strength of default network

4.3.4 *Multivariate analysis between network measures and cognition*

Given the significant correlations between the network measures, I further investigated whether the joint effect of the network measures contributed to cognition after controlling for age, sex, and education variables. Summary of the individual terms in the model are presented in the Supplementary table C3. I observed that while the R^2 difference between the base model (age, age^2, sex, and education) and the full model with the network measures was small, the joint effect of the network measures still significantly contributed to cognition (Table 4.3).

Table 4.3 Multivariate analysis of the joint effect of the network measures with cognitive function

Cognitive domains	df	LR	R^2 full model	R^2 base	R^2 diff	*Padj*
Processing speed	7	3.224	0.239	0.237	0.002	*0.002*
Executive function	9	3.503	0.132	0.128	0.004	*5.29E-04*
Memory	8	3.650	0.045	0.041	0.004	*5.29E-04*
Global cognition	3	4.480	0.188	0.184	0.004	*7.75E-05*

Abbreviations: df, number of network measures in the model; LR, likelihood ratio, diff, difference; Padj, adjusted p-value

Networks included in the final model:

Processing speed – Age, Age2, Sex, Education, Louvain Modularity, Transitivity, Strength of Visual Network, Strength of Somatomotor Network, Strength of Dorsal Attention Network, Strength of Salience Network, Strength of Limbic Network

Executive function - Age, Age2, Sex, Education, Louvain Modularity, Transitivity, Strength of Visual Network, Strength of Somatomotor Network, Strength of Dorsal Attention Network, Strength of Salience Network, Strength of Limbic Network, Strength of Control Network, Strength of Default Network

Memory - Age, Age2, Sex, Education, Global efficiency, Transitivity, Strength of Visual Network, Strength of Dorsal Attention Network, Strength of Salience Network, Strength of Limbic Network, Strength of Control Network, Strength of Default Network

Global cognition - Age, Age2, Sex, Education, Louvain Modularity, Transitivity, Strength of Visual Network, Strength of Somatomotor Network, Strength of Dorsal Attention Network, Strength of Limbic Network, Strength of Control Network, Strength of Default Network

Full model includes network measures and base model includes only covariate

Italics represents significance

4.4 Discussion

Changes to resting-state networks due to ageing arguably reflect more fundamental alterations or adaptations at the general level of brain function (Jockwitz & Caspers, 2021). Graph theoretical approaches may be the most integrative way to investigate resting-state functional connectivity (RSFC) as it studies connectivity at both nodal and systems levels (Jockwitz & Caspers, 2021). Therefore, in this study, I examined the topological age and sex relationship with functional brain networks, using graph theory measures, and cognition. I observed that most functional brain network measures showed decreasing strength of connectivity as well as reduced efficiency of communication and specialisation between the networks with ageing. However, the default mode and salience networks were an exception to this finding, with no significant results observed. In addition, there were significant sex differences in brain functional network topology where women showed greater efficiency of networks and network strength but less modularity than men. Further, age-related changes were more apparent in men than women. Lastly, the collective effect of the network measures contributed significantly to cognitive performance, with the highest correlation being with processing speed. However, no one network measure was significant after multiple testing adjustment.

I observed that global efficiency correlated negatively with age whereas characteristic path length correlated positively with age, which was similar to a previous study (Sala-Llonch et al., 2014). This suggests an overall age-related decrease in the effectiveness of the communication between brain regions. In addition, the finding that modularity decreases with age has also been reported previously (Song et al., 2014). This implies that increasing age is associated with a less differentiated functional modular structure,

which may be either due to the increase in between-network connections or the decrease in within-network connections or both (Chan et al., 2014; Song et al., 2014). At younger ages, functional brain networks are more segregated with every network being relatively specialised for distinct mental processes (Chan et al., 2014). The data suggest that there is some loss of functional specialisation of specific brain networks as the brain ages (Goh, 2011), which may be important for cognitive reserve and compensation in older adults. Furthermore, this study showed age-related decline in all of the other network strengths, excluding the DMN and salience network. However, results for other networks from previous studies are more complex. For instance, Betzel and colleagues (Betzel et al., 2014) found within-network decline for higher order control and attention networks but stability for visual and somatomotor networks, whilst another study (Song et al., 2014) showed increased global and local efficiency in the sensorimotor network in older compared to younger adults. Taken together, our data and others suggest age-related vulnerability in global network measures as well as specific network strengths.

Importantly, this study did not observe any age-related decline in the DMN and salience network. Prior works suggest that within-network posterior DMN connectivity, including angular gyrus, anterior cingulate cortex, precuneus, dorsal prefrontal, and inferior parietal lobe, decreases with age, (Betzel et al., 2014; Chan et al., 2014; Geerligs et al., 2015; Song et al., 2014; Stumme et al., 2020). In contrast, within the older adult population, DMN as a whole remains relatively stable (Jones et al., 2011; Stumme et al., 2020). This finding is important as it shows that anterior-posterior DMN has differential vulnerability to age-related changes. Moreover, the salience network seems to remain relatively stable throughout the lifespan (Chan et al., 2014; Varangis, Habeck, Razlighi, & Stern, 2019) as well as in older age (Siman-Tov et al., 2017;

Stumme et al., 2020). Interestingly, the DMN and salience network have also been implicated in age-related diseases such as Alzheimer's disease (AD) and depression. One study observed that individuals with AD showed moderate decrease of within-network DMN between the posterior cingulate cortex and right hippocampus as compared to healthy controls but no differences were evident for whole-network DMN (Grieder, Wang, Dierks, Wahlund, & Jann, 2018). Further, compared to older adult controls, individuals with AD showed significantly decreased within-network functional connectivity in the frontoinsular cortices and increased FC in medial prefrontal cortex in the salience network (He et al., 2014). Similarly, older adults with depression demonstrated higher within-network DMN in the left precuneus, subgenual anterior cingulate cortex (ACC), ventromedial prefrontal cortex, and lateral parietal regions than controls (Alexopoulos et al., 2012). In addition, regarding the salience network, within-network bilateral anterior insula showed decreased connectivity but bilateral ACC showed increased connectivity in middle-aged adults with depression compared to controls (Manoliu et al., 2014). These findings suggest that while the whole DMN may be preserved, within-network posterior DMN may be vulnerable to ageing and ageing-related diseases.

The topology of functional brain networks differed by sex. This study detected significant sex influence on all the assessed graph theory measures. Consistent with results from Zhang et al. (Zhang et al., 2016) showing that female brains facilitated functional integration in young adults, I found that in older individuals, women indeed had higher global efficiency and shorter characteristic path length than men. Similarly, congruent with previous findings, I also observed women had higher normalised clustering coefficients (i.e. transitivity) than men (Zhang et al., 2016). However, men

exhibited stronger Louvain modularity which suggests that there may be sex differences even within network segregation. It has previously been reported that women tend to exhibit overall higher within-network RSFC (Allen et al., 2011), which is consistent with our finding that women had higher network strengths than men. Similarly, consistent with previous findings that women show less age-related decreases in RSFC in the default and limbic network (Scheinost et al., 2015), I found that age-related changes in strengths of the limbic and default networks in addition to Louvain modularity and strength of visual network were more apparent in males than females. This suggests that ageing-related changes in the functional brain network are different in the two sexes and that this difference may in part account for the differential vulnerability in cognitive decline between men and women.

In this study, I saw that functional connectivity architecture in the brain has been associated with cognitive performance in older adults independent of age, sex, and education. I observed that decreased Louvain modularity was nominally associated with decline in global cognition and that decreased transitivity was nominally associated with decline in memory. Individuals with less segregated networks exhibited poorest memory ability after controlling for age, which may suggest that network segregation may be an age-invariant marker of individual differences in cognition (Chan et al., 2014). In addition, prior evidence from cognitive training interventions has shown that higher modularity at baseline in older adults was associated with greater cognitive training improvements, especially in sensory-motor processing (Gallen et al., 2016). Furthermore, given that the limbic network derived from the Schaefer parcellation comprises the orbitofrontal cortex and temporal pole, and these regions are associated with memory formation (Petrides, Alivisatos, & Frey, 2002) and executive function

(Robinson, Calamia, Gläscher, Bruss, & Tranel, 2014), it supports our finding that the strength of the limbic network showed negative associations with memory and executive function. While there is nominal significance between individual network measures and cognition, the joint effect of all the network measures contributed significantly to cognition after accounting for age, sex, and education. This suggests that cognitive decline observed in older adults may be partially explained by independent changes in brain functional network organisation. It also implies that individual network measures may be inadequate to capture much of the variance in neural activity and the functional output. Future studies are needed to combine various strategies to more holistically understand the network topology in relation to cognition.

The strengths of this study include a well-characterised large middle and older aged cohort, uniform imaging methods, the inclusion of a range of network measures associated with age and ageing-related diseases, and the examination of a number of cognitive domains. This is the largest study of its kind thus far. However, limitations should also be considered. Firstly, this study is cross-sectional, which precludes the ability to detect subtle changes in the functional brain topology over time within individuals. Secondly, while using weighted undirected matrix circumvents issues surrounding filtering/thresholding the connectivity matrix to maintain significant edge weights represented in a binary matrix, there are inherent difficulties associated with the interpretation of the results. As brain signals recorded from resting-state fMRI are typically noisy, it is possible that edge weights may be affected by non-neural contributions (De Vico Fallani, Richiardi, Chavez, & Achard, 2014). Despite this, with careful denoising of the resting-state fMRI data (Parkes et al., 2018; Power et al., 2017) and covarying for motion, it is possible to minimise the noise in the data. Given that I

have performed motion correction and included it as a covariate as well as performed regularisation on the imaging data, I am confident that the estimation of the partial correlation matrix derived for subsequent analysis of the graph theory measures is valid. Moreover, while I was only interested in investigating whole network functional connectivity, given the findings from DMN and salience network, it may be beneficial to look at individual nodes within the network to more holistically capture the nodal topology. Lastly, given the principles of neurobiology, I assumed that network properties influence cognition and not the other way around. This question needs to be examined longitudinally to confirm the directionality of the relationship.

In conclusion, in this large population-based study age was associated with decreased overall network integrity and specialised processing of the brain at a local level. Women had better functional network topology properties than men, with men tending to have denser within-network connections but sparser connections between-network connections. This work demonstrates the complexity of functional brain organisation that is shaped by age, sex and other factors, which ultimately may influence cognitive performance of older adults.

Supplemental Tables for Chapter 4

Supplementary Table C1. Results for network and cognition after controlling for age, sex, and education

Network measure (IV)	Cog Measure (DV)	β Network	SE Network	*P* Network	Adj *P* Network
Eglob	Processing speed	-0.014	0.010	0.149	0.414
Eglob	Executive function	0.011	0.011	0.323	0.570
Eglob	Memory	-0.010	0.011	0.331	0.570
Eglob	Global cognition	-0.004	0.010	0.700	0.850
Charpath	Processing speed	0.016	0.010	0.102	0.319
Charpath	Executive function	-0.006	0.011	0.585	0.809
Charpath	Memory	0.015	0.011	0.175	0.453
Charpath	Global cognition	0.008	0.010	0.400	0.652
Louvain modularity	Processing speed	0.024	0.010	0.017	0.095
Louvain modularity	Executive function	0.021	0.011	0.050	0.222
Louvain modularity	Memory	0.024	0.011	0.030	0.145
Louvain modularity	Global cognition	0.029	0.010	0.005	0.054
Transitivity	Processing speed	-0.011	0.010	0.249	0.548
Transitivity	Executive function	-0.003	0.010	0.759	0.850
Transitivity	Memory	-0.030	0.011	0.005	0.054
Transitivity	Global cognition	-0.017	0.010	0.084	0.309
VIS	Processing speed	0.003	0.010	0.750	0.850
VIS	Executive function	0.026	0.011	0.014	0.088
VIS	Memory	0.004	0.011	0.719	0.850
VIS	Global cognition	0.013	0.010	0.196	0.479
SM	Processing speed	-0.004	0.010	0.707	0.850

SM	Executive function	0.007	0.011	0.533	0.792
SM	Memory	-0.004	0.011	0.678	0.850
SM	Global cognition	-0.003	0.010	0.792	0.850
DAN	Processing speed	-0.025	0.010	0.009	0.069
DAN	Executive function	-0.003	0.011	0.780	0.850
DAN	Memory	-0.015	0.011	0.151	0.414
DAN	Global cognition	-0.017	0.010	0.100	0.319
SVAN	Processing speed	-0.005	0.010	0.588	0.809
SVAN	Executive function	0.000	0.011	0.983	0.983
SVAN	Memory	-0.020	0.011	0.069	0.275
SVAN	Global cognition	-0.008	0.010	0.441	0.693
LIMB	Processing speed	-0.026	0.010	0.009	0.069
LIMB	Executive function	-0.013	0.011	0.242	0.548
LIMB	Memory	-0.033	0.011	0.002	0.054
LIMB	Global cognition	-0.030	0.010	0.003	0.054
FPCN	Processing speed	-0.009	0.010	0.337	0.570
FPCN	Executive function	0.011	0.011	0.324	0.570
FPCN	Memory	-0.005	0.011	0.660	0.850
FPCN	Global cognition	0.001	0.010	0.949	0.971
DMN	Processing speed	-0.010	0.010	0.330	0.570
DMN	Executive function	0.012	0.011	0.262	0.549
DMN	Memory	-0.007	0.011	0.540	0.792
DMN	Global cognition	0.002	0.010	0.877	0.919

Abbreviations: β, beta; SE, standard error, *p*, *p*-value; Adj*p*, Adjusted *p*-value; Eglob, global efficiency; Charpath, characteristic path length; DMN, strength of default mode network; FPCN, strength of frontoparietal control network; LIMB, strength of limbic network; SVAN, strength of salience/ ventral attention network; SM, strength of somatomotor network; VIS, strength of visual network

Supplementary Table C2. Results for interaction between network measures and age-sex on cognition

Network measure (IV)	**CogMeasure (DV)**	**β AgeX Network**	**β SexX Network**	**SE AgeX Network**	**SE SexX Network**	**Adj *P* AgeX Network**	**Adj *P* SexX Network**
Eglob	Processing speed	0.003	-0.011	0.010	0.020	0.869	0.933
Eglob	Executive function	0.006	0.025	0.011	0.022	0.869	0.920
Eglob	Memory	0.010	-0.018	0.011	0.022	0.845	0.920
Eglob	Global cognition	0.006	0.001	0.010	0.020	0.869	0.997
Charpath	Processing speed	-0.003	0.007	0.010	0.020	0.869	0.956
Charpath	Executive function	0.000	-0.027	0.011	0.022	0.996	0.920
Charpath	Memory	-0.010	0.013	0.011	0.022	0.845	0.933
Charpath	Global cognition	-0.004	-0.006	0.010	0.020	0.869	0.956
Louvain modularity	Processing speed	0.011	0.011	0.010	0.020	0.845	0.933
Louvain modularity	Executive function	0.034	-0.011	0.011	0.022	0.104	0.933
Louvain modularity	Memory	0.011	-0.001	0.011	0.022	0.845	0.997
Louvain modularity	Global cognition	0.025	-0.001	0.010	0.021	0.223	0.997
Transitivity	Processing speed	-0.006	-0.003	0.010	0.019	0.869	0.997
Transitivity	Executive function	-0.020	0.026	0.011	0.021	0.414	0.920
Transitivity	Memory	-0.001	-0.014	0.011	0.021	0.992	0.933
Transitivity	Global cognition	-0.010	0.001	0.010	0.020	0.845	0.997
VIS	Processing speed	-0.001	0.038	0.010	0.020	0.992	0.792
VIS	Executive function	0.010	0.042	0.011	0.022	0.845	0.792
VIS	Memory	0.010	0.025	0.011	0.022	0.845	0.920
VIS	Global cognition	0.005	0.043	0.010	0.020	0.869	0.792
SM	Processing speed	0.024	0.006	0.010	0.020	0.223	0.956

SM	Executive function	0.018	0.024	0.011	0.022	0.637	0.920
SM	Memory	0.006	0.028	0.011	0.022	0.869	0.920
SM	Global cognition	0.020	0.025	0.010	0.020	0.414	0.920
DAN	Processing speed	-0.005	-0.016	0.010	0.020	0.869	0.920
DAN	Executive function	-0.005	0.018	0.011	0.022	0.869	0.920
DAN	Memory	0.000	-0.001	0.011	0.022	0.996	0.997
DAN	Global cognition	-0.007	0.004	0.010	0.020	0.869	0.997
SVAN	Processing speed	0.011	-0.019	0.010	0.020	0.845	0.920
SVAN	Executive function	-0.010	0.016	0.011	0.022	0.845	0.933
SVAN	Memory	0.010	-0.033	0.011	0.022	0.845	0.920
SVAN	Global cognition	0.003	-0.013	0.010	0.020	0.869	0.933
LIMB	Processing speed	-0.004	-0.006	0.010	0.020	0.869	0.956
LIMB	Executive function	-0.026	0.010	0.011	0.022	0.223	0.933
LIMB	Memory	0.008	0.000	0.011	0.022	0.869	0.997
LIMB	Global cognition	-0.011	0.004	0.011	0.021	0.845	0.997
FPCN	Processing speed	0.005	-0.028	0.010	0.020	0.869	0.920
FPCN	Executive function	0.000	0.017	0.011	0.022	0.996	0.920
FPCN	Memory	0.015	-0.021	0.011	0.022	0.845	0.920
FPCN	Global cognition	0.007	-0.011	0.010	0.020	0.869	0.933
DMN	Processing speed	0.004	-0.027	0.010	0.020	0.869	0.920
DMN	Executive function	-0.006	0.018	0.011	0.022	0.869	0.920
DMN	Memory	0.009	-0.017	0.011	0.022	0.869	0.920
DMN	Global cognition	0.001	-0.008	0.010	0.020	0.992	0.956

Abbreviations: β, beta; SE, standard error, *p*, *p*-value; Adj*p*, Adjusted *p*-value; Eglob, global efficiency; Charpath, characteristic path length; DMN, strength of default mode network; FPCN, strength of frontoparietal control network; LIMB, strength of limbic network; SVAN, strength of salience/ ventral attention network; SM, strength of somatomotor network; VIS, strength of visual network

Supplementary Table C3. Multivariate analysis between network measures and cognition

CogMeasure (DV)	**IV**	**β**	**SE**	**t.value**	***p***
Processing speed	Age	-0.444	0.011	-42.241	0
Processing speed	Age^2	-0.056	0.010	-5.589	2.38E-08
Processing speed	Sex	0.030	0.020	1.519	0.129
Processing speed	Education	0.019	0.002	8.931	5.31E-19
Processing speed	Louvain Modularity	0.016	0.015	1.101	0.271
Processing speed	Transitivity	-0.006	0.011	-0.543	0.587
Processing speed	VIS	0.021	0.012	1.827	0.068
Processing speed	SM	0.019	0.014	1.394	0.163
Processing speed	DAN	-0.046	0.015	-2.953	0.003
Processing speed	SVAN	0.030	0.017	1.762	0.078
Processing speed	LIMB	-0.028	0.015	-1.871	0.061
Executive function	Age	-0.213	0.011	-18.561	4.01E-75
Executive function	Age^2	-0.073	0.011	-6.737	1.74E-11
Executive function	Sex	0.046	0.022	2.146	0.032
Executive function	Education	0.050	0.002	22.036	0.000
Executive function	Louvain Modularity	0.041	0.016	2.524	0.012
Executive function	Transitivity	0.010	0.012	0.856	0.392
Executive function	VIS	0.041	0.013	3.260	0.001
Executive function	SM	0.016	0.015	1.044	0.297
Executive function	DAN	-0.034	0.018	-1.859	0.063
Executive function	SVAN	-0.020	0.022	-0.901	0.368

Executive function	LIMB	-0.040	0.017	-2.280	0.023
Executive function	FPCN	0.019	0.020	0.944	0.345
Executive function	DMN	0.057	0.026	2.241	0.025
Memory	Age	-0.159	0.012	-13.270	1.03E-39
Memory	Age^2	-0.042	0.011	-3.642	2.73E-04
Memory	Sex	0.120	0.023	5.223	1.81E-07
Memory	Education	0.017	0.002	7.037	2.15E-12
Memory	Global efficiency	-0.051	0.033	-1.552	0.121
Memory	Transitivity	-0.027	0.012	-2.313	0.021
Memory	VIS	0.028	0.015	1.905	0.057
Memory	DAN	-0.005	0.022	-0.206	0.836
Memory	SVAN	-0.034	0.023	-1.503	0.133
Memory	LIMB	-0.067	0.018	-3.765	1.68E-04
Memory	FPCN	0.029	0.023	1.264	0.206
Memory	DMN	0.087	0.028	3.067	0.002
Global cognition	Age	-0.339	0.011	-31.491	8.77E-204
Global cognition	Age^2	-0.071	0.010	-6.985	3.11E-12
Global cognition	Sex	0.081	0.020	4.012	6.09E-05
Global cognition	Education	0.036	0.002	16.701	1.92E-61
Global cognition	Louvain Modularity	0.021	0.015	1.407	0.160
Global cognition	Transitivity	-0.009	0.011	-0.860	0.390
Global cognition	VIS	0.033	0.012	2.774	0.006
Global cognition	SM	0.012	0.014	0.895	0.371
Global cognition	DAN	-0.048	0.017	-2.846	0.004
Global cognition	LIMB	-0.058	0.016	-3.543	3.98E-04
Global cognition	FPCN	0.012	0.019	0.663	0.507

Global cognition	DMN	0.055	0.022	2.462	0.014

Abbreviations: β, beta; SE, standard error, *p*, *p*-value; Adj*p*, Adjusted *p*-value; Eglob, global efficiency; Charpath, characteristic path length; DMN, strength of default mode network; FPCN, strength of frontoparietal control network; LIMB, strength of limbic network; SVAN, strength of salience/ ventral attention network; SM, strength of somatomotor network; VIS, strength of visual network

CHAPTER 5: ASSOCIATION OF SLEEP AND OTHER LIFESTYLE FACTORS, INCLUDING EXERCISE, ALCOHOL CONSUMPTION, AND SMOKING, WITH FUNCTIONAL NETWORK TOPOLOGY IN THE AGEING BRAIN

Abstract

Sleep and lifestyle factors, including exercise, alcohol consumption, and smoking, have been associated with changes in the brain's functional networks in older adults. However, findings from previous studies have been inconsistent. Here, I investigate how these factors influence functional networks, as well as their relationships with each other, in middle- to older-aged adults. The findings showed that self-reported sleep duration was associated with increasing strength of functional connectivity in several brain regions and better communication across the brain. Increased accelerometer-based nap duration was also associated with poorer specialised processing of the brain at a local level (i.e. reduced transitivity). In addition, exercise and alcohol consumption were related to global network segregation whereas smoking was associated with global network integration and specific network strengths. Furthermore, smoking also moderated the relationship between accelerometer-based nap hours and characteristic path length and strength of salience networks. In conclusion, these findings show that sleep and lifestyle factors are associated with distinct changes in the functional brain network properties.

5.1 Introduction

Sleep is an important human function. However, the mechanisms that regulate it remain to be elucidated. Along with other physiological alterations, sleep patterns change with ageing. Older people are more likely to have an earlier sleep onset, earlier morning wake signals, reduction of average sleep duration, and diminished sleep depth (Wolkove, Elkholy, Baltzan, & Palayew, 2007). Changes in sleep quality, quantity, and timing have been associated with brain function and psychiatric disorders (Fernandez-Mendoza & Vgontzas, 2013; He, Zhang, Li, Dai, & Shi, 2020; Spira, Chen-Edinboro, Wu, & Yaffe, 2014; Sterniczuk, Theou, Rusak, & Rockwood, 2013). Therefore, identifying the underlying brain functional changes associated with sleep patterns may contribute to the understanding of the association between sleep and disease states.

Various lifestyle factors, including exercise, alcohol intake, and smoking, have been shown to influence sleep. It has been postulated that regular physical activity and exercise may promote relaxation and energy expenditure in ways that may be beneficial to initiating and maintaining sleep (Dzierzewski et al., 2014), especially in older adults (Littman et al., 2007; Madden, Ashe, Lockhart, & Chase, 2014; Manjunath & Telles, 2005). Interestingly, a study investigating the directionality of this relationship using longitudinal data from the UK Biobank observed that sleep improvements overtime benefitted physical activity at follow-up while reduced physical activity was detrimental to sleep patterns at follow-up (Huang, Hamer, Duncan, Cistulli, & Stamatakis, 2021). This implies that there may be concurrent underlying mechanisms at play. In addition, some studies show that alcohol consumption affects sleep quality by momentarily increasing sleepiness but later causing frequent night-time and early morning

awakenings (Ebrahim, Shapiro, Williams, & Fenwick, 2013), whereas another study found no correlation between drinking pattern and sleep quality (Vinson et al., 2010). Furthermore, nicotine can stimulate the release of neurotransmitters, such as acetylcholine and norepinephrine, which may in turn inhibit gamma-aminobutyric acid (GABA) and sleep-promoting neurons (Saint-Mleux et al., 2004). Despite this, findings on the relationship between active smoking and sleep characteristics have been mixed, with some showing a positive association (McNamara et al., 2014; Riedel, Durrence, Lichstein, Taylor, & Bush, 2004; Zhang, Samet, Caffo, & Punjabi, 2006), and others showing nil (Jaehne et al., 2012; Liao et al., 2019) or a negative association (Wang et al., 2016). Given these inconsistencies, it is important to establish how other lifestyle factors may influence sleep patterns.

Using resting-state functional magnetic resonance imaging (rs-fMRI), studies have shown that sleep and other lifestyle factors affect the functional connectivity of the brain. Sleep deprivation has been associated with immediate widespread changes in functional connectivity during subsequent wakefulness (Nilsonne et al., 2017; Yeo, Tandi, & Chee, 2015). Others have shown that sleep quality or duration may affect intrinsic neural activity (Khalsa et al., 2016; Khazaie et al., 2017). Specifically, poor quality of sleep has been associated with alterations in functional connectivity of the default mode and attentional networks (Amorim et al., 2018). Individuals with chronic insomnia also showed disrupted global and local topological organisation of the brain (Li et al., 2018). Contrastingly, findings from large-scale population-based studies did not observe any associations between sleep quality and networks (Smith et al., 2016). Moreover, varying intensities of acute exercise may also have differential impacts on the brain functional networks. More specifically, low intensity exercise was associated

with decreased functional connectivity in the frontoparietal regions while high intensity exercise was associated with decreased functional connectivity in the sensorimotor and dorsal attention networks and increased activity in the left affect and reward networks (Schmitt et al., 2019). Dysfunctional alcohol consumption was associated with decreased functional connectivity in the executive control, sensorimotor, visual, and subcortical, regions that also predict relapse in alcoholics (Weiland et al., 2014). In addition, changes in the ventral and dorsal striatum (Sweitzer et al., 2016), frontostriatal region (Froeliger et al., 2015), prefrontal and limbic regions (Janes et al., 2012), insula and parahippocampus (Ding & Lee, 2013), as well as widespread functional connectivity attenuation in the reward circuit (Shen et al., 2016) were seen in smokers compared to non-smokers. Despite evidence showing that these lifestyle factors affect the functional brain networks, there is a paucity of studies looking at their influence in older populations. It, therefore, remains to be elucidated if variations in sleep and other lifestyle factors are related to functional connectivity in the older population.

In light of the uncertainty about how the above lifestyle factors influence sleep patterns, which may in turn alter the brain functional network topology, the aim of the present study was to examine these relationships in the UK Biobank participants. More specifically, I investigated how accelerometer-derived measures of sleep and rest-activity patterns, self-reported sleep duration, and other lifestyle factors influenced brain functional networks. I further determined whether physical activity as well as alcohol and smoking moderate functional brain networks through sleep.

5.2 Methods

5.2.1 Study population

The UK Biobank, which is a large prospective cohort study, included participants from the United Kingdom aged between 40 and 80 years old (Sudlow et al., 2015). Participants provided full informed consent to participate in UK Biobank and this project was approved by the NHS National Research Ethics Service (approval letter dated 17th June 2011, ref. 11/NW/0382), project 10279. All data and materials are available via UK Biobank (http://www.ukbiobank.ac.uk). This study included a total of 17,077 participants with self-reported sleep data, lifestyle factors, and imaging data in this study. As a subset, I also examined sleep patterns using accelerometer data.

5.2.2 Imaging data and network matrices

Brain images were acquired on Siemens Skyra 3.0T scanners (Siemens Medical Solutions, Germany) with a 32-channel head coil across three different assessment centres including Reading, Newcastle, and Manchester. I analysed the rs-fMRI data that was previously pre-processed by the UK Biobank (Alfaro-Almagro et al., 2018). The pre-processing steps involved: motion correction, intensity normalisation, high-pass temporal filtering (Gaussian-weighted least-squares straight line fitting, with sigma=50.0s), echo-planar imaging (EPI) unwarping, and gradient distortion correction. ICA+FIX processing (Beckmann & Smith, 2004; Griffanti et al., 2014; Salimi-Khorshidi et al., 2014) was then used to remove structured artefacts. I removed participants with motion of > 2mm/degrees of translation/rotation.

The Schaefer 7 network atlas (Schaefer et al., 2018) for 100 parcels was used for parcellation. Average time-series were extracted for the 100 functional parcels.

3dNetCorr command from Analysis of Functional Neuroimaging (AFNI) (Cox, 1996) was used to produce network adjacency matrix for each participant. The mean time-series for each region was correlated with the mean time-series for all other regions and extracted for each participant. More details can be found in Miller et al. (Miller et al., 2016).

Subsequently, using the derived network adjacency matrix, partial correlation, *r*, between all pairs of signals was computed to form a 100-by-100 (Schaefer atlas) connectivity matrix, which was then Fisher z-transformed. To slightly improve the partial correlation coefficients, L2-regularisation was applied (rho = 0.5 for Ridge Regression option in FSLNets). Self-connections and negative correlations were set to zero. As rs-fMRI can vary across magnitude, the use of undirected weighted matrices may provide a more comprehensive picture of the functional brain networks. The stronger the weights, the stronger the connections between nodes. While undirected graphs were unable to make inferences about the possible direction of information flow, they are useful as they allow us to identify existing connections between specific pairs of network nodes (Fornito et al., 2016). Therefore, I used weighted and undirected matrices in our study.

Brain Connectivity Toolbox (BCT) (Rubinov & Sporns, 2010) was used to derive the graph theory measures. Global-level metrics included global efficiency, characteristic path length, transitivity, and Louvain modularity. Network level measures, such as local efficiency and strengths, were estimated for each node and averaged across all nodes within each network.

To assess network segregation, which characterises the specialised processing of the brain at a local level, I calculated the Louvain modularity and transitivity (Deco et al., 2015). Louvain modularity is a community detection method, which iteratively transforms the network into a set of communities, each consisting of a group of nodes. Higher modularity values indicate denser within-modular connections but sparser connections between nodes that are in different modules. Transitivity refers to the total of all the clustering coefficients around each node in the network and is normalised collectively.

To assess integration of information, I calculated characteristic path length and global efficiency. Characteristic path length measures the integrity of the network and how fast and easily information can flow within the network. It is the average of all the distances between every pair of nodes in the network. Global efficiency represents how effectively the information is transmitted at a global level and is the average inverse shortest path length.

Finally, strength (weighted degree) is described as the sum of all neighbouring edge weights. High connectivity strength indicates stronger connectivity between the regions, which provides an estimation of functional importance of each network.

5.2.3 Activity-monitor devices

A Triaxial accelerometer device (Axivity AX3) was worn between 2.8 and 9.7 years after study baseline by 103,711 individuals from the UK Biobank for a continuous period up to 7 days. Quality control was performed by the UK Biobank (Doherty et al., 2017). Of these, individuals were excluded if the number of recording errors,

interrupted recording period, or duration of interrupted recording periods were greater than the variable's third quartile + 1.5 x IQR. In addition, participants were also excluded if the sleep period time (SPT)-window mean sleep duration was either too short (< 3 hours) or too long (> 12 hours) and mean number of sleep episodes was too low (≤5) or too high (≥30). This is to ensure that the extreme outliers that are not characteristic of normal sleep patterns were not included in subsequent analysis.

5.2.4 Accelerometer data processing and sleep measure derivations

Consistent with a previous study (Jones et al., 2019), I derived a total of six accelerometer-based measures of sleep and activity timing. These measures included sleep duration, sleep efficiency, daytime nap, the number of nocturnal sleep episodes, timing of the least-active 5 h (L5), and timing of the most-active 10 h (M10). All measures were derived by converting the raw accelerometer data (.cwa) files from the UK Biobank to .wav files using omconvert for signal calibration to gravitational acceleration (Doherty et al., 2017; van Hees et al., 2014) and interpolation (Doherty et al., 2017). Subsequently, the .wav files were processed with an open source R package GGIR (van Hees et al., 2018) to infer the non-wear time, and extract the z-angle across 5-s epochs from the time-series data for subsequent use in estimating the SPT window and sleep episodes within it. For more details on how each of these measures was derived, please refer to Jones et al. (2019) and https://cran.r-project.org/web/packages/GGIR/vignettes/GGIR.html#output-part-2. Only 6,740 participants with quality control acceptable accelerometer data with imaging data were included in the accelerometer data analyses.

5.2.5 Self-reported sleep measures

Self-reported sleep duration was also used. Sleep duration was recorded as the number of reported hours of sleep in every 24 hours. More details can be found in http://biobank.ndph.ox.ac.uk/showcase/field.cgi?id=1160.

5.2.6 Lifestyle factors

Exercise was quantified using the short-form International Physical Activity Questionnaire (IPAQ) (Hagströmer, Oja, & Sjöström, 2006), which measured the frequency and duration of light (Data-Fields: 864 and 874), moderate (Data-Fields: 884 and 894), and vigorous activities (Data-Fields: 904 and 914). Participants were categorised according to the World Health Organisation physical activity guidelines based on weekly Metabolic Equivalent of Task i.e. MET minutes/week into 3 groups: highly active, ≥ 1200; active, 600 to < 1200; inactive, < 600 (Huang et al., 2021). Other variables included smoking status (Data-Field: 20116), and number of packs of cigarettes a year (Data-Field: 20161), and frequency of alcohol intake (Data-Field: 1558). The responses for smoking were either currently smoking, previously smoked, and never smoked. For alcohol consumption, it was daily/almost daily, 3-4 times a week, once/twice a week, 1-3 times a month, special occasions only, or never. I recoded the variables where higher value/s reflected higher level/s of intake. Pack-years of smoking was calculated for individuals who had ever smoked.

5.2.7 Statistical analysis

All statistical analyses were performed using R version 3.5.1 software (The R Foundation, Vienna, Austria). To achieve normality of the graph theory measures and the sleep variables, normal transformation was applied using the R package.

In line with previous studies (Elliott et al., 2018), this study controlled for age, age^2, sex, age × sex (i.e. age and sex interaction), age^2 × sex (i.e. age^2 and sex interaction), head size (intracranial volume), head motion from rs-fMRI, and volumetric scaling factor needed to normalise for head size, as well as scanning site and years of education. The network measures were then residualised for subsequent analysis. The residuals included the age and sex variables and years of education.

Multiple linear regression models were performed to study the associations of sleep patterns and other lifestyle factors with functional network properties. False discovery rate-adjusted *p*-values were obtained by using Benjamini and Hochberg (Benjamini & Hochberg, 1995) procedure as implemented in the R function, *p.adjust.* Only results that reached significance level was set at $p < 0.05$ were reported in the main text.

In addition, I examined whether lifestyle factors moderated the influence of sleep patterns on functional network properties. The analysis was performed using the R package, mediation (Tingley, Yamamoto, Hirose, Keele, & Imai, 2014) and the p-values were obtained based on 100,000 stimulations.

5.3 Results

5.3.1 Demographics

Of the 17,077 participants, 9,014 (52.78%) were women and the mean (standard deviation) age was 62.33 (7.41) years. Table 5.1 shows descriptive statistics of the accelerometer-derived and self-reported sleep phenotypes as well as lifestyle factors such as exercise, alcohol, and smoking variables. Figure 5.1 shows correlation between

accelerometer-derived sleep variables and self-reported sleep duration. Accelerometer-based sleep duration and self-reported sleep duration showed weak positive correlations ($r^2 = 0.078$). Self-reported sleep duration was higher than that of accelerometer-based sleep duration.

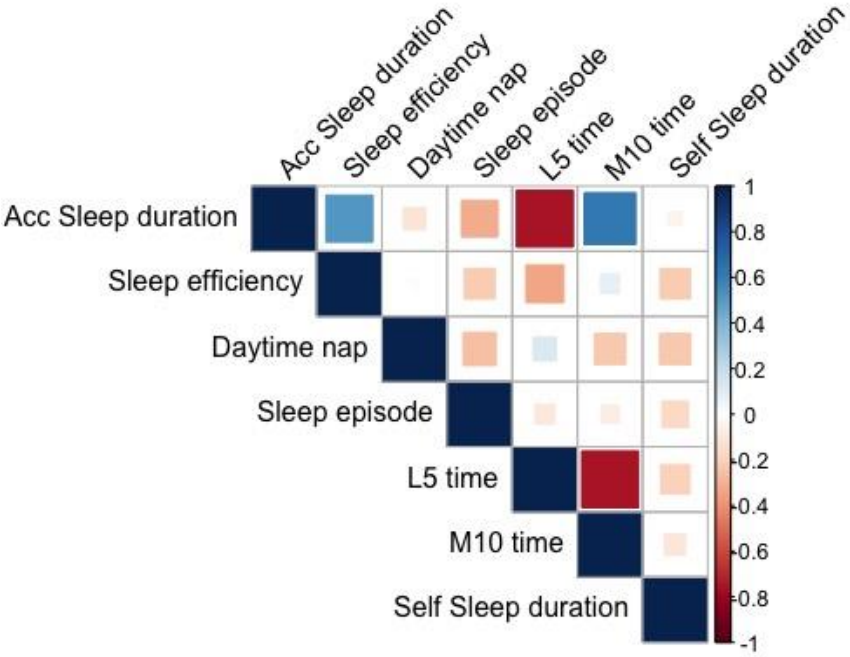

Figure 5.1 Correlations between accelerometer-based sleep variables and self-reported sleep duration

Abbreviations: Acc, accelerometer-based; L5, least-active 5 h; M10, timing of the most-active 10 h, Self, self-reported sleep duration. Blue represents positive correlations whereas red represents negative correlations.

Table 5.1 Descriptive statistics of demographics, self-reported sleep duration data and other lifestyle factors (n = 17,077); as well as sleep activity derived from accelerometer data (n = 6,740)

Demographics	
Age (years), mean (standard deviation)	62.33 (7.41)
Sex (n)	9014 women (52.8%), 8063 men (47.2%)
Education (years)	15.73 (4.74)
Accelerometer sleep data	
L5 timing (hours from previous midnight)	27.41 (6.21)
M10 timing (hours from previous midnight)	19.69 (1.92)
Sleep duration (hours)	4.83 (1.60)
Sleep efficiency (%)	89.76 (5.63)
Number of sleep episodes	15.56 (2.15)
Daytime napping	0.26 (0.16)
Self-reported sleep data	
Sleep duration (hours)	7.14 (1.10)
Exercise	
Physical activity (MET mins/week)	667.76 (767.50)
Physical activity level	
Inactive	10,590 (62.0%)
Active	3,985 (23.3%)
Highly active	2,505 (14.7%)
Smoking	
Smoking status	
Never	10,731 (63.0%)
Previous	5,687 (33.4%)
Current	627 (3.68%)
Pack years of smoking	19.05 (15.39)
Alcohol consumption	
Alcohol consumption	
Daily/ almost daily	2821 (16.6%)
3-4 times/ week	4,846 (28.4%)
1-2 times/ week	4,590 (26.9%)
1-3 times/ month	1,981 (11.6%)
Special occasions	1,759 (10.3%)
Never	1,048 (6.14%)

5.3.2 Association between sleep patterns and functional brain network measures

Accelerometer-based nap duration was negatively associated with transitivity (β = -0.043, SE = 0.012, *p*-adjusted = 0.010). In addition, self-reported sleep duration was negatively associated with characteristic path length and Louvain modularity but positively associated with transitivity, strength of default, control, limbic, and salience networks (Table 5.2).

Table 5.2 Associations between self-reported sleep duration and network measures

Graph theory measures	**β**	**SE**	***p***	***Padj***
Global efficiency	0.013	0.007	0.063	0.442
Characteristic path length	-0.024	0.007	0.001	*0.012*
Louvain Modularity	-0.054	0.007	5.44E-14	*6.58E-12*
Transitivity	0.028	0.007	8.19E-05	*0.002*
DMN	0.040	0.007	1.86E-08	*5.63E-07*
DAN	0.019	0.007	0.007	0.101
FPCN	0.049	0.007	1.07E-11	*4.30E-10*
LIMB	0.050	0.007	3.39E-12	*2.05E-10*
SVAN	0.027	0.007	1.36E-04	*0.003*
SM	-0.019	0.007	0.010	0.117
VIS	-0.014	0.007	0.056	0.442

Abbreviations: β, beta; SE, standard error, *p*, *p*-value; Padj, adjusted *p*-value; DMN, strength of default mode network; DAN, strength of dorsal attention network; FPCN, strength of control network; LIMB, strength of limbic network; SVAN, strength of salience network; SM, strength of somatomotor network; VIS, strength of visual network

Italics represents significance

5.3.3 Association between lifestyle factors and graph theory measures

Table 5.3 presents the significant association between lifestyle factors and graph theory measures. Increased physical activity was associated with decreased transitivity and increased strength of somatomotor network. Smoking status was positively associated

with global efficiency and strengths of all the networks as well as negatively associated with characteristic path length. Number of packets of cigarettes smoked in a year was associated positively associated with global efficiency and negatively associated with characteristic path length. Alcohol consumption was negatively associated with transitivity and positively associated with Louvain modularity. Supplementary table D1 presents results for all other associations.

Table 5.3 Associations between lifestyle factors and graph theory measures

Graph theory measures	β	SE	*p*	*Padj*
Physical activity status				
Transitivity	-0.038	0.011	0.000	*0.002*
SM	0.025	0.010	0.016	*0.047*
Smoking status				
Global efficiency	0.059	0.014	1.65E-05	*3.18E-04*
Characteristic path length	-0.059	0.014	2.17E-05	*3.18E-04*
DMN	0.035	0.014	0.012	*0.044*
DAN	0.056	0.014	4.91E-05	*0.001*
FPCN	0.039	0.014	0.005	*0.022*
LIMB	0.038	0.014	0.005	*0.022*
SVAN	0.055	0.014	6.46E-05	*0.001*
SM	0.052	0.014	1.72E-04	*0.001*
VIS	0.043	0.014	0.002	*0.008*
Packs per year				
Global efficiency	0.003	0.001	0.016	*0.047*
Characteristic path length	-0.003	0.001	0.016	*0.047*
Alcohol consumption				
Transitivity	-0.032	0.006	8.97E-09	*3.95E-07*
Louvain modularity	0.018	0.005	0.001	*0.005*

Abbreviations: β, beta; SE, standard error, *p*, *p*-value; *Padj*, adjuated *p*-value; DMN, strength of default mode network; DAN, strength of dorsal attention network; FPCN, strength of control network; LIMB, strength of limbic network; SVAN, strength of salience network; SM, strength of somatomotor network; VIS, strength of visual network

Italics represents significance

5.3.4 Moderation effect

I further examined if the relationship between self-reported sleep duration and graph theory measures was moderated by the significant lifestyle factors. Results showed that smoking status moderated accelerometer nap duration to affect characteristic path length and strength of salience network (Table 5.4). However, none of their interaction effects were significant (Supplementary Table D2).

Table 5.4 Moderation effect of lifestyle factors on sleep in affecting functional network properties

Networks	Sleep	LS	β Sleep	β LS	β LSxSleep	SE Sleep	SE LS	SE LSxSleep	AdjP Sleep	AdjP LS	AdjP LSxSleep
Charpath	Nap	Smoking status	-0.040	-0.161	0.365	0.098	0.046	0.154	0.847	*0.013*	0.390
SVAN	Nap	Smoking status	-0.024	0.153	-0.311	0.098	0.046	0.153	0.938	*0.017*	0.711

Abbreviations: β, beta; SE, standard error, Adj*p*, Adjusted p-value; LS, lifestyle factors; LSxSleep, interaction between lifestyle and sleep factors; Charpath, characteristic path length; SVAN, strength of salience/ ventral attention network. Italics *represents significance.*

5.4 Discussion

In this study, I investigated how sleep and various lifestyle factors, including physical activity, alcohol consumption, and smoking, influenced functional brain network properties in a large cohort of middle to older aged adults. The major findings were as follows. First, increased self-reported sleep duration was associated with greater strength of functional connectivity in several brain regions as well as efficiency of communication but with lower within-modular connections. Second, accelerometer derived nap was associated with transitivity. Next, physical activity and alcohol consumption were associated with global network segregation whereas smoking influenced global network integration and specific network strengths. Lastly, smoking status moderated the relationship between accelerometer nap hours, characteristic path length, and strength of salience network.

Global properties, including characteristic path length, transitivity, and Louvain modularity, as well as strength of functional connectivity between brain regions in DMN, FPCN, limbic, and salience networks, were associated with self-reported sleep duration. Previous studies have shown that sleep deprivation was associated with decreased DMN connectivity (De Havas, Parimal, Soon, & Chee, 2012; Sämann et al., 2010) and that cumulative amount of sleep was predictive of internetwork and intranetwork functional connectivity between DMN and salience network (Khalsa et al., 2016). Interestingly, there is evidence showing that even within the range of variability in self-reported sleep duration normally experienced by the majority of the healthy adults on weeknights, the accumulation of additional sleep was associated with greater functional connectivity within the DMN (Killgore, Schwab, & Weiner, 2012). This implies that even relatively minor differences in sleep duration may contribute

significantly to the differences in strength of functional connectivity in the DMN. Importantly, decreased DMN connectivity has been implicated in individuals with amnestic mild cognitive impairment (MCI) (Greicius, Srivastava, Reiss, & Menon, 2004; Sorg et al., 2007) and Alzheimer's disease (AD) (Greicius et al., 2004). Moreover, older adults with MCI with more sleep disturbances also showed decreased connectivity in the DMN (McKinnon et al., 2017; McKinnon et al., 2016). These findings suggest neural mechanisms implicated in disordered sleep may also result in memory dysfunction but the directionality has not been determined. However, to date, there is a lack of studies investigating how sleep duration affects functional network properties in healthy adults. Individuals with obstructive sleep apnoea, however, showed decreased transitivity and increased characteristic path length as well as decreased communication in DMN, salience, and control networks (Chen et al., 2018). Further, those with insomnia disorder showed decreased functional network connectivity in FPCN between anterior and posterior DMN (Dong et al., 2018). These findings suggest that disrupted global and regional properties of functional network may be potential biomarkers for sleep deprivation vulnerability (Yeo et al., 2015), however, more work needs to be done in healthy older adults in order to understand the underlying mechanisms.

In addition, increased derived nap hours were associated with reduced network segregation. One previous study has shown that daytime nap increased hippocampal activation during task-based fMRI encoding trials (Ong, Lau, Lee, van Rijn, & Chee, 2020). It is possible that increased activation is observed in specific regions within a network but there is an overall decrease in network connectivity. However, given that this is the first study showing the association between accelerometer sleep data and

functional network measures, more studies need to be undertaken in order to establish the significance.

Although some lifestyle habits may pose a risk to brain network integrity, others may be protective (Bittner et al., 2019). Here, this study show that the increasing frequency of physical activity is negatively associated with the efficiency in how the brain networks process information (i.e. decreased transitivity) and an increased strength of the somatomotor network. While there is an overall consensus that exercise has positive influence on the brain plasticity (Fernandes, Arida, & Gomez-Pinilla, 2017), findings are inconsistent on whether the influence are global or specific. For instance, while one study showed that exercise was associated with an increased overall efficiency of how information is integrated across the whole brain network (i.e. global efficiency) in older adults (Kawagoe, Onoda, & Yamaguchi, 2017), another showed that the associations were specific to the default and frontal executive networks rather than global (Voss et al., 2016). Further, there is evidence showing that an acute bout of exercise may increase neural processes underlying semantic memory activation in older adults but these associations were localised and did not reflect a widespread increase in overall brain activation (Won et al., 2019). These mixed findings may be, in part, due to the different intensity and frequency of the exercises examined in the different studies. Our current results are in the opposite direction to that in the previous studies. The reason is uncertain, but I speculate that older individuals who were more physically active may have recruited their global brain resources to protect the integrity of specific networks vulnerable to age-related declines.

I also observed graph theoretical measures differences in the topological organisation of functional networks in smokers compared to non-smokers, and a relationship with packs of cigarettes smoked per year. Similar to previous studies, this study showed increased network connectivity strength in the visual, frontoparietal, and motor areas in smokers compared to non-smokers (Bittner et al., 2019; Fedota & Stein, 2015; Janes et al., 2012). Moreover, increased coupling was observed between insula and dorsal anterior cingulate cortex, which are key nodes of the salience network (Seeley et al., 2007), which have been associated with smoking severity in a previous study (Hong et al., 2009). Interestingly, I saw an increase in global network integration, as reflected by increased global efficiency and reduced characteristic path length, associated with smoking. This association has been previously associated with attention-enhancing arising from acute administration of nicotine (Fedota & Stein, 2015; Hahn et al., 2009; Lim et al., 2010). Further, increased global efficiency was correlated with greater behavioural benefits of nicotine and increased frequency of smoking in acute nicotine administration in another study (Gießing, Thiel, Alexander-Bloch, Patel, & Bullmore, 2013). However, for chronic smokers, the associations were opposite (Lin, Wu, Zhu, & Lei, 2015). It is unclear why these patterns observed were similar to acute nicotine administration when this study was on chronic smokers. I assume that age may influence this since these previous studies on acute nicotine administration were performed in younger adults (aged 19 to 44 years). Further, I found that smoking status moderated accelerometer nap hours in influencing characteristic path length and strength of salience network. Previous studies have found that smoking affects sleep quality (Liao et al., 2019; Patterson et al., 2019). However, to date, none have examined how the relationship between smoking and sleep affects functional network measures. I

postulate that smoking may affect nap or the quality of sleep to affect the overall communication of network and specific network strength.

Additionally, greater alcohol consumption was associated with lower transitivity and higher Louvain modularity. Findings from a previous study on alcohol dependent middle-aged adults showed that reduced average clustering coefficient (i.e. transitivity) was associated with more severe alcohol use (Sjoerds et al., 2017). Given that reduced efficiency adversely affects cognition (van den Heuvel, Stam, Kahn, & Hulshoff Pol, 2009), it is possible that reduced transitivity due to alcohol consumption may be partly responsible for cognitive dysfunction seen in addicted individuals (Schulte et al., 2014; van Holst & Schilt, 2011). In addition, a previous study demonstrated that while community consistency (i.e. modularity) in DMN was similar between light and moderate-heavy drinkers, the latter showed significantly higher modularity in the central executive network compared to the former in older adults (Mayhugh et al., 2016). However, the study did not investigate overall modularity. As such, it is difficult to conclude how spatial specificity of functional communities is relevant to this group of older adults. I can only posit that the amount of alcohol consumed relates differentially within functional network segregation.

This study should be interpreted with caution due to its limitations. First, environmental influences often do not occur in isolation and are related to each other. Moreover, there are other factors, such as socialising and volunteering, that may confound the relationship between lifestyle factors and functional network properties that were not taken into consideration. Further, there is evidence to show the age influence on various sleep stages and wakefulness were associated with brain functional connectivity using

combined electroencephalography (EEG) and fMRI (Daneault et al., 2021). While this may increase our understanding of sleep and brain networks, it also represents a different construct and this study is also limited by the type of data available. However, future studies may consider investigating the influence of different sleep stages on the topological functional network properties in an ageing population. In addition, while I only investigated the physical activity status using the frequency and intensity of exercise, the type of exercise may also be important in understanding how physical activity helps with preserving the cognition. For example, previous studies have found that differential impacts on the brain functional connectivity depending on the type of exercises, such as aerobics or Tai Chi (Cui et al., 2021; Weng et al., 2017). Future studies may include this information for a more holistic understanding of how exercise affects functional connectivity. Furthermore, while self-report measurements have shown to have high reliability and validity, it may also be subjected to memory effects or social desirability bias (Bittner et al., 2019). Lastly, the cross-sectional design of this study makes it impossible to determine the causal directionality of the effects. Longitudinal data are needed to evaluate this in future studies.

In conclusion, in this large population-based study, I found that sleep and other lifestyle factors including, physical activity, smoking, and alcohol consumption, were associated with distinct differences in the brain functional network properties. There are important clinical implications of these results where self-report sleep assessments may be used to understand the brain function and cognition in older adults.

Supplemental Tables for Chapter 5

Supplementary Table D1. Associations between lifestyle factors and functional network measures

Networks	**Lifestyle**	**β**	**SE**	***p***	**Adj *P***
Eglob	Alcohol intake	0.009	0.006	0.110	0.186
Eglob	Smoking	0.059	0.014	1.65E-05	0.000
Eglob	Packs per year	0.003	0.001	0.016	0.047
Eglob	Physical activity	-0.016	0.010	0.122	0.199
Charpath	Alcohol intake	-0.007	0.006	0.208	0.286
Charpath	Smoking	-0.059	0.014	2.17E-05	3.14E-04
Charpath	Packs per year	-0.003	0.001	0.016	0.047
Charpath	Physical activity	0.015	0.010	0.156	0.237
Modularity	Alcohol intake	0.018	0.005	0.001	0.005
Modularity	Smoking	-0.009	0.014	0.525	0.564
Modularity	Packs per year	-0.002	0.001	0.066	0.121
Modularity	Physical activity	-0.008	0.010	0.457	0.529
Transitivity	Alcohol intake	-0.032	0.006	8.97E-09	3.95E-07
Transitivity	Smoking	0.012	0.014	0.385	0.484
Transitivity	Packs per year	8.65E-05	0.001	0.936	0.958
Transitivity	Physical activity	-0.038	0.011	0.000	0.002
DMN	Alcohol intake	0.007	0.006	0.185	0.262
DMN	Smoking	0.035	0.014	0.012	0.044
DMN	Packs per year	0.002	0.001	0.105	0.185
DMN	Physical activity	-0.020	0.010	0.060	0.115
DAN	Alcohol intake	0.003	0.006	0.620	0.649
DAN	Smoking	0.056	0.014	4.91E-05	0.001
DAN	Packs per year	0.002	0.001	0.030	0.078

DAN	Physical activity	-0.016	0.010	0.139	0.218
FPCN	Alcohol intake	0.007	0.006	0.183	0.262
FPCN	Smoking	0.039	0.014	0.005	0.022
FPCN	Packs per year	0.002	0.001	0.040	0.093
FPCN	Physical activity	-0.023	0.010	0.031	0.078
LIMB	Alcohol intake	0.004	0.005	0.497	0.551
LIMB	Smoking	0.038	0.014	0.005	0.022
LIMB	Packs per year	0.002	0.001	0.032	0.078
LIMB	Physical activity	-0.007	0.010	0.501	0.551
SVAN	Alcohol intake	-3.54E-05	0.006	0.995	0.995
SVAN	Smoking	0.055	0.014	6.46E-05	0.001
SVAN	Packs per year	0.002	0.001	0.045	0.094
SVAN	Physical activity	-0.009	0.010	0.402	0.491
SM	Alcohol intake	0.011	0.006	0.044	0.094
SM	Smoking	0.052	0.014	0.000	0.001
SM	Packs per year	0.002	0.001	0.053	0.105
SM	Physical activity	0.025	0.010	0.016	0.047
VIS	Alcohol intake	-0.006	0.006	0.305	0.394
VIS	Smoking	0.043	0.014	0.002	0.008
VIS	Packs per year	0.001	0.001	0.287	0.383
VIS	Physical activity	0.008	0.010	0.428	0.509

Abbreviations: β, beta; SE, standard error, *p*, *p*-value; Adj *P*, Adjusted *p*-value; Eglob, global efficiency; Charpath, characteristic path length; DMN, strength of default mode network; FPCN, strength of frontoparietal control network; LIMB, strength of limbic network; SVAN, strength of salience/ ventral attention network; SM, strength of somatomotor network; VIS, strength of visual network

Supplementary Table D2. Moderation effect of lifestyle factors on sleep variables in influencing network measures

Networks	**Sleep**	**LS**	**β Sleep**	**β LS**	**β LSxSleep**	**SE Sleep**	**SE LS**	**SE LSxSleep**	**Adj *P* Sleep**	**Adj *P* LS**	**Adj *P* LSxSleep**
Charpath	Nap	Smoking status	-0.040	-0.161	0.365	0.098	0.046	0.154	0.847	0.013	0.390
Charpath	Nap	Physical activity status	0.130	0.036	-0.098	0.094	0.034	0.111	0.401	0.583	0.791
Charpath	Nap	Alcohol intake	0.277	0.018	-0.057	0.249	0.020	0.071	0.505	0.639	0.838
Charpath	Sleep duration	Alcohol intake	-0.045	-0.058	0.007	0.016	0.035	0.005	0.023	0.370	0.752
Charpath	Sleep duration	Smoking status	-0.029	-0.143	0.012	0.009	0.090	0.013	0.007	0.370	0.766
Charpath	Sleep duration	Physical activity status	-0.029	-0.058	0.010	0.009	0.070	0.010	0.005	0.662	0.766
Modularity	Nap	Alcohol intake	-0.053	0.032	0.011	0.243	0.020	0.069	0.953	0.370	0.969
Modularity	Nap	Smoking status	-0.054	-0.025	0.142	0.096	0.045	0.150	0.781	0.767	0.766
Modularity	Nap	Physical activity status	0.032	0.008	-0.082	0.092	0.033	0.109	0.873	0.920	0.838

Modularity	Sleep duration	Physical activity status	-0.057	-0.093	0.012	0.009	0.070	0.010	4.18E-09	0.477	0.752
Modularity	Sleep duration	Alcohol intake	-0.044	0.034	-0.002	0.016	0.034	0.005	0.023	0.583	0.875
Modularity	Sleep duration	Smoking status	-0.053	-0.059	0.007	0.009	0.090	0.012	2.59E-08	0.739	0.875
Transitivity	Nap	Alcohol intake	-0.173	-0.039	0.031	0.245	0.020	0.070	0.762	0.270	0.875
Transitivity	Nap	Smoking status	-0.066	0.051	-0.054	0.096	0.045	0.151	0.764	0.578	0.902
Transitivity	Nap	Physical activity status	-0.055	-0.023	-0.058	0.093	0.033	0.109	0.781	0.729	0.875
Transitivity	Sleep duration	Physical activity status	0.015	-0.202	0.023	0.009	0.071	0.010	0.262	0.051	0.390
Transitivity	Sleep duration	Alcohol intake	0.023	-0.043	0.001	0.016	0.035	0.005	0.400	0.529	0.909
Transitivity	Sleep duration	Smoking status	0.031	0.095	-0.012	0.009	0.091	0.013	0.003	0.583	0.766
FPCN	Nap	Alcohol intake	-0.192	-0.009	0.032	0.250	0.020	0.071	0.730	0.814	0.875
FPCN	Sleep duration	Smoking status	0.054	0.143	-0.015	0.009	0.091	0.013	2.59E-08	0.370	0.766

FPCN	Sleep duration	Physical activity status	0.055	0.069	-0.013	0.009	0.070	0.010	1.04E-08	0.583	0.752
FPCN	Sleep duration	Alcohol intake	0.058	0.032	-0.003	0.016	0.035	0.005	0.002	0.613	0.838
DMN	Nap	Smoking status	-0.015	0.101	-0.227	0.097	0.046	0.153	0.959	0.204	0.752
DMN	Nap	Physical activity status	-0.114	-0.026	0.044	0.094	0.033	0.110	0.505	0.670	0.889
DMN	Nap	Alcohol intake	-0.207	-0.011	0.034	0.248	0.020	0.070	0.707	0.767	0.875
DMN	Sleep duration	Alcohol intake	0.056	0.049	-0.006	0.016	0.035	0.005	0.003	0.457	0.752
DMN	Sleep duration	Smoking status	0.042	0.089	-0.008	0.009	0.090	0.012	2.75E-05	0.583	0.875
DMN	Sleep duration	Physical activity status	0.044	0.049	-0.010	0.009	0.070	0.010	5.52E-06	0.728	0.766
LIMB	Nap	Smoking status	0.072	0.094	-0.193	0.096	0.045	0.150	0.731	0.233	0.752
LIMB	Nap	Physical activity status	-0.042	-0.036	0.109	0.092	0.033	0.109	0.828	0.583	0.766
LIMB	Nap	Alcohol intake	-0.135	-0.016	0.042	0.244	0.020	0.069	0.781	0.670	0.875

LIMB	Sleep duration	Physical activity status	0.054	0.095	-0.014	0.009	0.070	0.010	1.04E-08	0.477	0.752
LIMB	Sleep duration	Alcohol intake	0.038	-0.017	0.003	0.016	0.034	0.005	0.066	0.778	0.875
LIMB	Sleep duration	Smoking status	0.045	0.010	0.004	0.009	0.090	0.012	4.99E-06	0.965	0.909
SVAN	Nap	Smoking status	-0.024	0.153	-0.311	0.098	0.046	0.153	0.938	0.017	0.711
SVAN	Nap	Physical activity status	-0.148	-0.016	0.030	0.094	0.034	0.111	0.348	0.792	0.909
SVAN	Nap	Alcohol intake	-0.135	-0.007	0.001	0.249	0.020	0.071	0.781	0.877	0.992
SVAN	Sleep duration	Smoking status	0.035	0.201	-0.020	0.009	0.091	0.013	0.001	0.204	0.752
SVAN	Sleep duration	Alcohol intake	0.038	0.027	-0.004	0.016	0.035	0.005	0.073	0.670	0.838
SVAN	Sleep duration	Physical activity status	0.029	0.022	-0.004	0.009	0.070	0.010	0.005	0.891	0.875

Abbreviations: β, beta; SE, standard error, Adj *P*, Adjusted p-value; LS, lifestyle factors; LSxSleep, interaction between lifestyle and sleep factors; Charpath, characteristic path length; DMN, strength of default mode network; FPCN, strength of frontoparietal control network; LIMB, strength of limbic network; SVAN, strength of salience/ ventral attention network

CHAPTER 6: THE ASSOCIATION OF MAJOR DEPRESSIVE DISORDER PHENOTYPES AND ITS POLYGENIC RISK SCORE WITH FUNCTIONAL BRAIN NETWORKS

Abstract

Major depressive disorder (MDD) comprises a multitude of clinical symptoms, which suggest multiple disruptions of neural circuits. Therefore, in this present study, I aimed to investigate how phenotypic MDD and MDD polygenic risk scores (PRS_{MDD}) related to functional network properties in middle- to older-aged participants from the UK Biobank. Due to the heterogeneous nature of the disorder, I studied two depression phenotypes – namely, lifetime MDD and a broad category of 'mental disorder', which included individuals with mental health presentation to a physician for a non-psychotic psychiatric disorder. I observed that the broad mental disorder measure did not show any association with the graph theory measures. Individuals who met the criteria for lifetime depression showed reduced network integration, segregation, and strength compared to controls. In addition, PRS_{MDD} was associated with similar network disruption as with lifetime depression. Findings from this study provide insights into the biological and neural mechanisms underlying major depression.

6.1 Introduction

Major depressive disorder (MDD) is characterised by pervasive sadness or irritability, disturbances in sleep, and withdrawal from pleasurable activities (Belmaker & Agam, 2008). It is the leading contributor to the global burden of disease due to its high prevalence, disabling consequences, and partial treatment response (Shen et al., 2020). In the elderly, defined herein as those 60 years and above, MDD can cause considerable suffering and reduce their quality of life (Bohr et al., 2012). The diversity of the different depression symptoms may imply the existence of multiple disruptions of neural circuits in depression (Bezmaternykh et al., 2021). Furthermore, to date, there are no objective biomarkers to guide diagnosis and there are inconsistencies in the definition of depression (Harris et al., 2020). Therefore, understanding the biological correlates and the underlying brain networks involved in the pathogenesis of MDD may allow us to potentially develop effective treatments.

Previous studies found that MDD is phenotypically correlated with brain functional networks (Gong & He, 2015; Jin et al., 2011; Meng et al., 2014; Ye et al., 2015; Zhang et al., 2011; Zhi et al., 2018). More specifically, using graph theoretical approach, loss of small-worldness (Achard & Bullmore, 2007), significant reorganisation of community structures (Leistedt et al., 2009; Lord, Horn, Breakspear, & Walter, 2012; Zhang et al., 2011), and increased local efficiency and modularity (Ye et al., 2015) have been observed in MDD. Local brain regions such as default mode network (DMN) and executive control network (ECN) have also been shown to be significantly affected in MDD (Ye et al., 2015). However, the findings have not always been consistent - two studies observed that MDD was associated with decreased path length but not clustering coefficient (Leistedt et al., 2009; Zhang et al., 2011) whereas another showed no

difference in both path length and clustering coefficient but rather changes in community structure in MDD (Lord et al., 2012). This may be, in part, due to the differences in methodology and definition of MDD (Ye et al., 2015).

In addition, given that the heritability of MDD has been estimated at 37% in a meta-analysis of twin studies (Sullivan, Neale, & Kendler, 2000) and ranged up to 8.7% based on single-nucleotide polymorphisms (SNPs) (Wray et al., 2018), the functional alterations observed in MDD may be in part due to genetic influences (Lee, Shen, & Qiu, 2017). Genome-wide association and related studies have observed that risk of MDD is a result from the cumulative effects of many low-penetrance genetic variants (Lubke et al., 2012; Ripke et al., 2013). It has been shown that polygenic risk scores (PRS), which are derived as the weighted sums of risk alleles an individual carries for any particular disease or phenotype, hold great promise for supporting the identification of disease risks in different contexts (Halldorsdottir et al., 2019). For instance, higher depression PRS has been observed among adults who reported an early age onset (Wray et al., 2018). Thus, there may be value in understanding how genetic disposition using PRS, plays a role in the functional reorganisation of brain networks in MDD.

In this present study, I used graph theoretical approach to further understand how topological integrity of functional network connectivity is related to phenotypic MDD in a large sample of middle-aged to older participants from the UK Biobank. In addition, this study examined how MDD polygenic risk scores (PRS_{MDD}) influence functional brain networks.

6.2 Methods

6.2.1 Study population

The UK Biobank, which is a large prospective cohort study, included participants from the United Kingdom aged between 40 and 80 years old (Sudlow et al., 2015). Participants provided full informed consent to participate in UK Biobank and this project was approved by the NHS National Research Ethics Service (approval letter dated 17th June 2011, ref. 11/NW/0382), project 10279. All data and materials are available via the UK Biobank (http://www.ukbiobank.ac.uk).

This study was approved by the UK Biobank in December 2018 (Application number: 45262). After quality control filtering, including those with complete rs-fMRI, depression, and genetics data, and excluding those with other mental health issues, the final sample consisted of 16,613 participants.

6.2.2 Major Depressive Disorder Phenotypes

In this study, two depression phenotypes were examined.

The first phenotype analysed was lifetime depression based on the short form of the Composite International Diagnostic Interview (CIDI) short form (CIDI-SF) (Kessler, Andrews, Mroczek, Ustun, & Wittchen, 1998). It included a yes/no binary question to depressive feelings (Data-Field: 20446) or loss of interest (Data-Field: 20441) for more than two weeks. Participants who responded “Yes” were given follow up questions including feelings of worthlessness (Data-Field: 20450), tiredness (Data-Field: 20449), difficulty concentrating (Data-Field 20435), suicidal thoughts (Data-Field: 20437), changes in sleep patterns (Data-Field: 20532), and changes in weight (Data-Field:

20536). Cases were defined as those who answered “Yes” to the screening questions plus another four follow-up questions while the rest were defined as controls (Howard et al., 2020). This resulted in 13,071 controls and 3,542 cases. Participants were classified as subthreshold lifetime depression if they experienced fewer than five symptoms on the CIDI-SF (Xiang, Leggett, Himle, & Kales, 2018). Of the 13,071 controls categorised in lifetime depression, 2,807 of them had subthreshold depression.

The second phenotype was a broad category of mental disorder, which was defined as self-reported help-seeking behaviour for mental health issues, and was categorised as Broad Depression by Howard and colleagues (Howard et al., 2018). Using the definition defined by Howard et al. (Howard et al., 2018), cases were characterised as individuals who sought help for nerves, anxiety, tension, or depression from either a general practitioner or psychiatrist (Data-Field: 2090 and 2100). Controls were participants who did not fulfil the above-mentioned criteria. Participants identified with bipolar disorder, schizophrenia, or personality disorder were removed. This resulted in 11,256 controls and 5,357 cases.

In addition, I also investigated whether the number of depressive episodes was associated with functional network topology.

6.2.3 Imaging data pre-processing

Brain images were acquired on Siemens Skyra 3.0T scanner (Siemens Medical Solutions, Germany) with a 32-channel head coil across three different assessment centres including Reading, Newcastle, and Manchester. I analysed the rs-fMRI data that was previously pre-processed by the UK Biobank (Alfaro-Almagro et al., 2018), which

involved: motion correction, intensity normalisation, high-pass temporal filtering (Gaussian-weighted least-squares straight line fitting, with sigma=50.0s), echo-planar imaging (EPI) unwarping, and gradient distortion correction. ICA+FIX processing (Beckmann & Smith, 2004; Griffanti et al., 2014; Salimi-Khorshidi et al., 2014) was then used to remove structured artefacts. I removed participants with motion of > 2mm/degrees of translation/rotation.

6.2.4 Parcellation

The Schaefer 7 network atlas (Schaefer et al., 2018) for 100 parcels was used for parcellation. Average time-series were extracted for the 100 functional parcels. 3dNetCorr command from Analysis of Functional Neuroimaging (AFNI) (Cox, 1996) was used to produce network adjacency matrix for each participant. The mean time-series for each region was correlated with the mean time-series for all other regions and extracted for each participant. More details can be found in Miller et al. (Miller et al., 2016).

Subsequently, using the derived network adjacency matrix, partial correlation, *r*, between all pairs of signals was computed to form a 100-by-100 (Schaefer atlas) connectivity matrix, which was then Fisher z-transformed. To slightly improve the partial correlation coefficients, L2-regularisation was used (rho = 0.5 for Ridge Regression option in FSLNets). Self-connections and negative correlations were set to zero. As rs-fMRI can vary across magnitude, the use of undirected weighted matrices may provide a more comprehensive picture of the functional brain networks. The stronger the weights, the stronger the connections between nodes. In addition, I used undirected graph because in rs-fMRI, which is useful as it allows us to identify existing

connections between specific pairs of network nodes (Fornito et al., 2016). Therefore, I used weighted and undirected matrices in our study.

6.2.5 Network matrices

Brain Connectivity Toolbox (BCT) (Rubinov & Sporns, 2010) was used to derive the graph theory measures. Global-level metrics included global efficiency, characteristic path length, transitivity, and Louvain modularity. Network level measures, such as local efficiency and strengths, were estimated for each node and averaged across all nodes within each network.

To assess network segregation, which characterises the specialised processing of the brain at a local level, I calculated the Louvain modularity, transitivity, and local efficiency indices (Deco et al., 2015). Louvain modularity is a community detection method, which iteratively transforms the network into a set of communities, each consisting of a group of nodes. Higher modularity values indicate denser within-modular connections but sparser connections between nodes that are in different modules. Transitivity refers to the total of all the clustering coefficients around each node in the network and is normalised collectively. Local efficiency is a node-specific measure and is defined relative to the sub-graph comprising of the immediate neighbours of a node.

To assess integration of information, I calculated characteristic path length and global efficiency. Characteristic path length measures the integrity of the network and how fast and easily information can flow within the network. It is the average of all the distances between every pair of nodes in the network. Global efficiency represents how

effectively the information is transmitted at a global level and is the average inverse shortest path length.

Finally, strength (weighted degree) is described as the sum of all neighbouring edge weights. High connectivity strength indicates stronger connectivity between the regions, which provides an estimation of functional importance of each network.

6.2.6 Genotyping and imputation

DNA was extracted from stored blood samples, which were collected from participants on their visit to a UK Biobank assessment centre (Bycroft et al., 2018). Affymetrix UK Biobank Lung Exome Variant Evaluation (UK BiLEVE) Axiom array or Affymetrix UK Biobank Axiom array (Bycroft et al., 2018) were used to acquire the genetics data. Quality control (QC) was performed using the UK Biobank pipeline. Imputed data set was made available where the UK Biobank interim release was imputed to a reference set combining the UK10K haplotype and 1000 Genome Phase 3 reference panels. For more details, refer to http://biobank.ctsu.ox.ac.uk/crystal/refer.cgi?id=157020. Ten principal components generated by the UK Biobank were included as covariates in the statistical model to control for population stratification. For PRS calculation, only those SNPs that remained after QC filtering (MAF > 0.1%, imputation information score > 0.6) were used. I also only used samples with reported British ancestry and removed any samples with high genotype missing rate and relatedness.

6.2.7 Polygenic risk score (PRS) derivation

MDD PRS (PRS_{MDD}) were calculated as a weighted sum of risk alleles an individual carries for depression phenotype. The weights are the effect sizes observed in GWAS of

the relevant phenotype (Choi, Mak, & O'Reilly, 2020). For the current study, PRS derivations were based on the summary statistics obtained from previous depression GWAS from two cohorts, including the PGC (Wray et al., 2018) and the 23andMe discovery sample (Hyde et al., 2016). It was calculated using PRS-CS (Ge, Chen, Ni, Feng, & Smoller, 2019), which uses the Bayesian regression framework with continuous shrinkage priors to obtain posterior effect sizes of the summary statistics. In turn, it produces a pruned set of effect sizes using linkage disequilibrium (LD) among SNPs based on a reference panel (without the need to use thresholds based on the GWAS p-values). Subsequently, PLINK software was used to generate the PRS score (Chang et al., 2015).

6.2.8 Statistical analysis

All statistical analyses were performed using R version 3.5.1 software (The R Foundation, Vienna, Austria). The graph theory measures were normalised using ranked transformation, rntransform() function in R from GeneABEL package (Karssen et al., 2016) and age were z-transformed for regression analysis. In line with previous studies (Elliott et al., 2018), I controlled for imaging covariates, including head size (intracranial volume), head motion from rs-fMRI, and volumetric scaling factor needed to normalise for head size, as well as age, sex, age×sex, age^2, age^2×sex, and scanning site. In addition, as a previous study (Elliott et al., 2018) showed that rs-fMRI was associated with genetic factors, I controlled for ten genetic principal components. The network measures were residualised for subsequent analyses.

One-way analysis of variance (ANOVA) was performed to compare between the CIDI-SF lifetime depression groups (i.e. controls, subthreshold, and cases of lifetime

depression). Independent t-tests were used to examine the difference between individuals with mental disorders and controls. Further, using regression models, I compared the network measurements across the 3 groups of CIDI-SF depression phenotypes using pairwise comparisons while controlling for covariates. Logistic regression was then used to estimate the associations with functional network topology on mental disorders where the independent variables were the network properties and the dependent variable was the depression phenotype. In addition, linear regression model was used to study the influence of the number of depressive episodes as well as PRS_{MDD} on the graph theory measures.

False discovery rate adjusted p-values were obtained by using Benjamini and Hochberg (1995) procedure (Benjamini & Hochberg, 1995) as implemented in the R function *p*.adjust. Significance level was set at adjusted $p < 0.05$. Only results that passed the significance level are reported.

6.3 Results

6.3.1 Demographics

Of the 16,613 participants, 8,826 were women and 7,787 were men with mean (sd) age of 62.96 (7.43) years. Table 6.1 summarises the demographic information and the graph theory measures for the depression phenotypes. While participants with mental disorder did not differ from controls, subthreshold and cases of lifetime depression had significant differences compared to controls. More specifically, cases of lifetime depression were significantly younger, had lower global efficiency and strengths of all networks, longer characteristic path length, higher modularity, and higher PRS_{MDD} compared to subthreshold lifetime depression as well as controls. Individuals with

subthreshold depression were significantly older and had higher PRS_{MDD} compared to controls.

Table 6.1 Differences in demographics and graph theory measures between CIDI-SF lifetime depression, mental disorder, and controls

	CIDI-SF lifetime depression			Mental disorder	
	Controls (n = 10,264)	Subthreshold (n = 2,807)	Cases (n = 3,542)	Controls (n = 11,256)	Cases (n = 5,357)
Age	63.27 (7.52)	63.78 (7.20)*	61.44 (7.12)***$^{###}$	62.99 (7.38)	62.90 (7.51)
Sex (Women, %)	4885 (47.59%)	1520 (54.15%)***	2421 (68.35%)***$^{###}$	5,939 (52.76%)	2,887 (53.89%)
Eglob	0.037 (0.985)	0.022 (1.014)	-0.125 (0.968)***$^{###}$	-0.002 (0.991)	0.0055 (0.984)
Charpath	-0.036 (0.987)	-0.024 (1.016)	0.125 (0.967)***$^{###}$	0.003 (0.991)	-0.006 (0.986)
Louvain modularity	-0.023 (1.001)	-0.021 (0.984)	0.105 (0.980)***$^{###}$	0.007 (1.005)	-0.001 (0.974)
Transitivity	0.025 (0.991)	0.023 (1.002)	-0.117 (0.986)***$^{###}$	-0.008 (0.999)	-0.001 (0.981)
DMN	0.022 (0.996)	0.025 (1.013)	-0.114 (0.971)***$^{###}$	-0.011 (0.999)	0.002 (0.986)
DAN	0.041 (0.984)	0.026 (1.006)	-0.117 (0.971)***$^{###}$	0.001 (0.992)	0.013 (0.978)
FPCN	0.035 (0.992)	0.033 (1.013)	-0.119 (0.978)***$^{###}$	-0.0003 (0.997)	0.007 (0.990)
LIMB	0.028 (0.996)	0.014 (1.018)	-0.130 (0.965)***$^{###}$	-0.010 (0.995)	-0.002 (0.995)
SVAN	0.041 (0.988)	0.035 (1.006)	-0.121 (0.966)***$^{###}$	0.003 (0.991)	0.011 (0.984)
SM	0.028 (0.988)	0.018 (0.997)	-0.113 (0.978)***$^{###}$	-0.007 (0.993)	0.004 (0.980)
VIS	0.031 (0.980)	0.014 (1.015)	-0.106 (0.966)***$^{###}$	-0.001 (0.984)	-0.002 (0.986)
MDD PRS	-0.063 (1.012)	0.018 (0.972)***	0.168 (0.966)***$^{###}$	0.005 (0.995)	-0.010 (1.010)

* < 0.05, ** < 0.01, *** <0.001 compared to controls; $^{\#}$ <0.05, $^{\#\#}$ <0.01, $^{\#\#\#}$ <0.001 comparison between subthreshold and cases of lifetime depression

Abbreviations: Eglob; global efficiency; Charpath, characteristic path length; DMN, strength of default mode network; DAN, strength of dorsal attention network; FPCN, strength of frontoparietal control network; LIMB, strength of limbic network; SVAN, strength of salience/ventral attention network; SM, strength of somatomotor network; VIS, strength of visual network

6.3.2 Associations between depression phenotypes and graph theory measures

Table 6.2 summarises the pairwise comparisons between the CIDI-SF groups. Cases of CIDI-SF lifetime depression were negatively associated with global efficiency, transitivity, and strength of all the networks; and positively associated with characteristic path length and strength of visual network compared to controls. In contrast to cases, subthreshold CIDI-SF lifetime depression showed positive associations with global efficiency, transitivity, and strength of networks; and negative associations with Louvain modularity and characteristic path length. Mental disorder and the number of depressive episodes were not associated with any of the measures (Supplementary Tables E1 and E2).

Table 6.2 Associations between graph theory measures and CIDI-SF lifetime depression phenotype

Measures	β_1	SE_1	p_1	p_{adj1}	β_2	SE_2	p_2	p_{adj2}	β_3	SE_3	p_3	p_{adj3}
Eglob	-0.011	0.020	0.839	0.999	0.080	0.019	5.19E-05	*2.85E-04*	0.092	0.019	4.00E-04	*0.001*
Charpath	0.015	0.020	0.734	0.999	-0.081	0.019	5.17E-05	*2.85E-04*	-0.096	0.019	2.11E-04	*0.001*
Louvain modularity	0.019	0.021	0.637	0.999	-0.040	0.019	0.094	0.094	-0.058	0.019	0.046	*0.046*
Transitivity	-0.023	0.020	0.501	0.999	0.056	0.019	0.009	*0.010*	0.079	0.019	0.004	*0.005*
DMN	-0.023	0.020	0.515	0.999	0.060	0.019	0.005	*0.007*	0.083	0.019	0.002	*0.004*
DAN	-0.008	0.020	0.920	0.999	0.074	0.019	2.37E-04	*0.001*	0.082	0.019	0.002	*0.004*
FPCN	-0.018	0.020	0.651	0.999	0.058	0.019	0.006	*0.007*	0.076	0.019	0.005	*0.006*
LIMB	-0.005	0.021	0.965	0.999	0.076	0.019	2.05E-04	*0.001*	0.081	0.019	0.003	*0.004*
SVAN	-0.022	0.020	0.510	0.999	0.073	0.019	2.93E-04	*0.001*	0.095	0.019	2.26E-04	*0.001*
SM	-0.018	0.020	0.651	0.999	0.068	0.019	0.001	*0.002*	0.085	0.019	0.001	*0.003*
VIS	0.0001	0.020	0.999	0.999	0.080	0.019	7.79E-05	*2.86E-04*	0.080	0.019	0.003	*0.004*

Abbreviations**:** β, beta; SE, standard error; *p*, *p*-value; p_{adj}, adjusted p-value; 1, subthreshold lifetime depression versus controls; 2, cases lifetime depression verses controls; 3, subthreshold lifetime depression versus cases lifetime depression; Eglob, global efficiency; charpath, characteristic path length ; DMN, default mode network; DAN, dorsal attention network; FPCN, frontoparietal control network; LIMB, limbic network; SVAN, salience/ventral attention network; SM, somatomotor network; VIS, visual network

Italics represents significance

6.3.3 PRS$_{MDD}$

Global efficiency and strength of all the networks except for control network were negatively associated with PRS$_{MDD}$ whereas characteristic path length was positively associated with PRS$_{MDD}$ (Table 6.3).

Table 6.3 Associations between graph theory measures and PRS$_{MDD}$

Measures	**β**	**SE**	***p***	***Padj***
Eglob	-0.025	0.008	0.002	*0.007*
Charpath	0.024	0.008	0.003	*0.008*
Louvain modularity	0.006	0.008	0.467	0.467
Transitivity	-0.011	0.008	0.204	0.224
DMN	-0.024	0.008	0.004	*0.009*
DAN	-0.019	0.008	0.021	*0.033*
FPCN	-0.012	0.008	0.153	0.187
LIMB	-0.020	0.008	0.018	*0.033*
SVAN	-0.018	0.008	0.028	*0.039*
SM	-0.025	0.008	0.002	*0.007*
VIS	-0.026	0.008	0.002	*0.007*

Abbreviations: β, beta; SE, standard error; Padj, adjusted *p*-value; Eglob, global efficiency; Charpath, characteristic path length; DMN, strength of default mode network; DAN, strength of dorsal attention network; FPCN, strength of frontoparietal control network; LIMB, strength of limbic network; SVAN, strength of salience/ ventral attention network; SM, strength of somatomotor network; VIS, strength of visual network

Italics represents significance

6.4 Discussion

Depression is a heterogeneous mental health disorder that presents with a multitude of symptoms (Fried, 2017). Understanding the underlying biological mechanisms may provide valuable aetiological insights. The findings of the current study describe a

robust association between lifetime depression, genetics of MDD, and functional graph theory measures within a population-based sample. The main observations are that: (1) CIDI-SF lifetime depression phenotypes showed significant association with graph theory measures whereas mental disorders did not; (2) CIDI-SF lifetime depression phenotypes showed poorer network integration, segregation, and strengths as compared to controls; (3) Higher genetic load (PRS) for MDD was related to poorer network integration and strength.

One notable observation was that lifetime depression phenotypes seemed to be associated with the functional brain network properties rather than the mental disorders phenotype. There is evidence to show that the mental disorder phenotype, Broad depression, is likely to include a number of personality and psychiatric disorders (Howard et al., 2018) whereas the lifetime depression provides a more robust definition and is reported to be the gold standard for depression phenotypes in the UK Biobank (Glanville et al., 2021). Furthermore, it has been posited that genetic architecture differs between minimally defined and strictly defined depression phenotypes, where the former may yield associations with variants that may not be specific to MDD (Cai et al., 2020; Glanville et al., 2021). SNP-based heritability (h^2_{SNP}) for lifetime depression according to CIDI-SF was about 26% whereas it was 14% for broad depression (Cai et al., 2020). Findings by Wray and colleagues (Wray et al., 2018) showed that while these depression phenotypes had a high degree of shared genetic liability, pairwise genetic correlations showed that they differed significantly. This implies that there may be phenotype-specific genetic effects. Therefore, given their specific effects, it is not surprising that they showed differing associations with brain functional network properties.

In agreement with previous studies (Jiang et al., 2019b; Luo et al., 2015; Meng et al., 2014; Ye et al., 2015), I found reduced global efficiency, transitivity, and increased characteristic path length and modularity in individuals with lifetime depression compared to controls. This implies that the network architecture in individuals with MDD was less locally specialised and less globally integrated. Our results further indicated reduced functional network strengths in different brain regions. Similar to our findings, a study investigating functional connectivity differences in various seed regions in adults (mean age = 29.46) with MDD showed alterations in DMN, central executive, limbic, visual, somatomotor, ventral attention, dorsal attention networks (Liu et al., 2020). There is evidence to show that DMN provides the neural substrate for depressive rumination (Dutta, McKie, & Deakin, 2014; Hamilton, Farmer, Fogelman, & Gotlib, 2015; Yan et al., 2019) and predicts disease severity of MDD (Sambataro, Wolf, Pennuto, Vasic, & Wolf, 2014; Wang, Hermens, Hickie, & Lagopoulos, 2012). Other networks, including salience, control, and limbic networks, have also been shown to be relevant to MDD psychopathology due to their involvement in attention (Beevers, Clasen, Enock, & Schnyer, 2015), cognitive control (Stange et al., 2017), and emotional processing respectively (Dutta et al., 2014; Liu et al., 2020). These findings are supported by the neurocognitive model of MDD, which postulates that symptoms of MDD may be accounted for by disturbed connections of the control network with other networks involving attention, emotion, and internal mentation (Disner, Beevers, Haigh, & Beck, 2011; Kaiser, Andrews-Hanna, Wager, & Pizzagalli, 2015).

Higher genetic risk for MDD was also associated with disrupted network integration, segregation, and strengths. The contribution of an inherited genetic predisposition to the

occurrence of sporadic depression has been previously reported (Cao et al., 2021). One study found that higher genetic risk increased the risk of depression by 22% (Cao et al., 2021) and another showed that PRS may serve as an early indicator of clinically significant levels of depression in a youth cohort (Halldorsdottir et al., 2019). Given that this study observed PRS_{MDD} associated with these network properties, it is possible that higher genetic predisposition of depression alters networks that in turn, drive the depression phenotype. The reverse is also possible that depression phenotype influences the network topology. The directionality of the relationship between brain networks and MDD may be determined using longitudinal data in future studies.

The strengths of this work include the large sample size of UK Biobank participants, the use of standardised protocols for data collection, and the detailed depression phenotypes available. Some limitations should also be considered. Depression phenotype in the UK Biobank sample reflected lifetime history of depression based on CIDI-SF, which, although based on diagnostic criteria and well validated, is still limited by the reliance on retrospective self-report (de Nooij et al., 2020). Further, clinical assessments were not always concurrent with the MRI scan. There are some methodological limitations that should be considered. Although the use of weighted undirected networks resolves the issue on filtering/thresholding connectivity matrix to maintain significant edge weights represented in a binary matrix, it is possible that the edge weights may be affected by non-neural contributions (De Vico Fallani et al., 2014). However, with careful denoising and covarying for motion (Parkes et al., 2018; Power et al., 2017), it is possible to minimise the noise in the data. Furthermore, the limitation imposed by a cross-sectional design precludes the directionality of relationship between MDD phenotype, genotype, and functional brain network alterations over the disease course.

In summary, using graph theory measures, the present findings suggest that lifetime MDD and genetic predisposition to MDD relate to disruptions of the functional network properties among adults in their mid-late life. Using different clinical characteristics to define MDD show differential profiles of functional brain network alterations. This implies that depression phenotypes may differ quantitatively with respect to the construct they measure, which points to the importance of considering how depression is defined when conducting and interpreting the results. Together, these findings provide evidence of the underlying biological and neural mechanisms correlates of depression.

Supplemental Tables for Chapter 6

Supplementary Table E1. Logistic regression results for association between mental disorder and graph theory measures

Measures	**β**	**SE**	***t***	***p***
Eglob	0.019	0.018	1.093	0.274
Charpath	-0.021	0.018	-1.195	0.232
Louvain modularity	-0.018	0.017	-1.038	0.299
Transitivity	0.015	0.017	0.872	0.383
DMN	0.024	0.017	1.375	0.169
DAN	0.022	0.018	1.259	0.208
FPCN	0.019	0.017	1.079	0.280
LIMB	0.015	0.017	0.893	0.372
SVAN	0.020	0.018	1.144	0.252
SM	0.022	0.018	1.274	0.203
VIS	0.007	0.017	0.413	0.679

Abbreviations: β, beta; SE, standard error, t, t-value; *p*, p-value; Eglob, global efficiency; Charpath, characteristic path length; DMN, strength of default mode network; DAN, strength of dorsal attention network; FPCN, strength of frontoparietal control network; LIMB, strength of limbic network; SVAN, strength of salience/ ventral attention network; SM, strength of somatomotor network; VIS, strength of visual network

Supplementary Table E2. Results from linear regression associating the number of depressive episodes with graph theory measures

Measures	**β**	**SE**	**t**	***p***
Eglob	-0.00040	0.00047	-0.857	0.392
Charpath	0.00038	0.00047	0.794	0.427
Louvain modularity	-0.00036	0.00048	-0.757	0.449
Transitivity	0.00013	0.00048	0.278	0.781
DMN	-0.00008	0.00048	-0.175	0.861
DAN	-0.00041	0.00048	-0.862	0.389
FPCN	-0.00013	0.00048	-0.271	0.787
LIMB	-0.00051	0.00048	-1.064	0.288
SVAN	-0.00014	0.00047	-0.299	0.765
SM	-0.00024	0.00047	-0.508	0.611
VIS	-0.00009	0.00048	-0.184	0.854

Abbreviations: β, beta; SE, standard error, t, t-value; *p*, p-value; Eglob, global efficiency; Charpath, characteristic path length; DMN, strength of default mode network; DAN, strength of dorsal attention network; FPCN, strength of frontoparietal control network; LIMB, strength of limbic network; SVAN, strength of salience/ ventral attention network; SM, strength of somatomotor network; VIS, strength of visual network

CHAPTER 7: CONCLUSIONS AND FUTURE DIRECTIONS FOR RESEARCH

7.1 Review of thesis objectives and aims

The world's population is ageing, and there is an urgent need to understand the processes that distinguish healthy ageing from disability. Biologically, ageing is associated with declines at the molecular, cellular, and physiological levels. There is evidence to show that ageing is associated with decline in cognitive function that may be in part accounted for by changes in neural plasticity and function of the brain. However, depending on one's genetics, environment, and disease states, the impact of ageing differs markedly between individuals. Therefore, investigating how these factors influence the topology of functional networks in ageing may allow for a better distinction between healthy ageing and development of disease.

There are many determinants and correlates of brain ageing. For instance, an individual's genetics, age, sex, environmental factors such as sleep quality, physical activity, alcohol consumption, and smoking, as well as depression states all play a role in brain ageing (see Chapter 2). However, findings are either inconsistent or there is lack of studies investigating the associations of these factors with functional brain networks. Due to the multifactorial process of ageing, understanding the mechanistic underpinnings of brain functional network properties may help identify factors that may accelerate or slow down the brain ageing process. In addition, it may help to identify potential targets for preventive strategies to maintain brain health in older individuals.

Given that the human brain is composed of interconnected networks, studying the properties of both the local and global organisation of the neural networks may be important for characterising vulnerabilities and resilience to ageing and brain diseases. While human functional network connectivity studies offer a promising approach for

elucidating the biological mechanisms underlying the functional organisation of the brain, this field is still in its infancy. Therefore, in the thesis, I set out to examine the genetics, environmental factors, and disordered states that potentially influence the functional brain network properties in middle aged and older adults using samples from the UK Biobank. The specific aims of the research were to (i) to study the heritability and genetic variants associated with the graph theory measures; (ii) to examine the influence of age and sex on the graph theory properties, and how this relationship modifies cognitive performance; (iii) to study how sleep and lifestyle factors including exercise, alcohol, and smoking, influence graph theory measures; and (iv) to investigate how major depressive disorder (MDD) phenotype and genotype relate to the graph theory measures. These research aims were addressed in the four studies reported in the preceding chapters. Key findings of these studies are summarised below.

7.2 Summary of key findings

7.2.1 Genetics of functional brain network properties

Chapter 3 addressed the first research aims and examined the genetics of weighted functional brain network graph theory measures from 18,445 participants of the UK Biobank (44-80 years). To date, this is the first study investigating the genetics of weighted functional graph theory measures.

Eighteen graph theory measures, which were associated with ageing and other age-related neurodegenerative diseases, were derived from the rs-fMRI data. The eighteen measures studied showed low heritability (mean h^2_{SNP} =0.12) but were highly genetically correlated. This result was consistent with an earlier report by Elliott et al. (2018), which showed that rs-fMRI connectivity edges had the lowest h^2_{SNP}. This

implies that there is relatively low genetic predisposition to functional brain network properties.

This work identified significant SNPs and gene associations that survived multiple correction testing with six of the 18 graph theory measures, i.e. global efficiency, characteristic path length, and strength of default, dorsal attention, limbic, and somatomotor networks. More specifically, one genome-wide significant locus was associated with strength of somatomotor and limbic networks. These intergenic variants were located near the *PAX8* gene on chromosome 2. This gene is essential for brain development and functions and has been associated with sleep (Bernal, 2007; Doherty et al., 2018; Williams, 2008). Considering phenotypic correlations between sleep duration, insomnia, and the graph theory measures were observed, it is possible that variants in or near *PAX8* and other genes in this region may play a role in the regulation of genes associated with functional brain network properties and sleep. In a previous study by Stoykova and Gruss (1994), postnatal *PAX* gene expression patterns in the central nervous system were investigated in relationship to their embryonic expression profiles. They found that *PAX8* was active in the developing brain, especially in the intermediate zones of myelencephalon and metencephalon. This implies a role for *PAX8* in brain regionalisation. Given this evidence, it is possible that *PAX8* may influence somatomotor and limbic networks. However, due to the paucity of studies examining somatomotor and limbic networks and sleep, it is difficult to speculate further.
Gene-based analyses also identified five significantly associated genes for five of the network measures, which have been implicated in sleep duration, neuronal differentiation/development, cancer, and susceptibility to neurodegenerative diseases.

In summary, single nucleotide polymorphism (SNP) and gene level associations with functional network measures were identified, which may help uncover novel biological pathways relevant to human brain functional network integrity and related disorders that affect it.

7.2.2 Age and sex association with functional brain network properties

Age and sex have been associated with changes in functional brain network topology, which may in turn affect cognition in older adults. This study explored this question further in Chapter 4 by examining differences in 11 resting-state graph theory measures with respect to age, sex, and their relationships with cognitive performance in 17,127 UK Biobank participants (mean=62.83±7.41 years).

I found that age was associated with an overall decrease in the effectiveness of network communication (i.e. integration) and loss of functional specialisation (i.e. segregation) of specific brain regions. Sex differences were also observed, with women showing more efficient networks that were less segregated than men (FDR adjusted $p<.05$). Age-related changes were also more apparent in men than women, which may suggest that men may be more vulnerable to cognitive decline with age.

Network segregation and strength of limbic network were nominally associated with cognitive performance. Individuals with less segregated networks exhibited the poorest memory, suggesting that network segregation may be an age-invariant marker of individual differences in cognition (Chan et al., 2014). However, while the individual networks were nominally significant, the collective effect of all the network measures contributed significantly to cognition after accounting for age and sex, and education

(FDR adjusted $p \leq .002$). This suggests that cognitive decline observed in older adults may be partially explained by independent changes in brain functional network organisation. It may also imply that individual network measures may be inadequate to capture much of the variance in neural activity or its output and need further refinement.

Taken together, the data suggest that the complexity of functional brain organisation is related to an individual's age and sex, which may influence cognitive performance of older adults.

7.2.3 The association of sleep and other lifestyle factors with functional brain network properties

Sleep is an important human function that changes in quality and quantity as humans age. These changes have been associated with changes in the brain's functional networks. Other lifestyle factors, including exercise, alcohol intake, and smoking, have differential impact on the brain functional networks and have shown to influence sleep patterns. However, previous studies have been inconsistent in their findings and there is a paucity of studies looking at their influence in older population. Therefore, in Chapter 5, I studied how accelerometer-derived measures of sleep and rest-activity patterns, self-reported sleep duration, and other lifestyle factors influence brain functional networks, as well as their relationship with each other.

I observed that that increased self-reported sleep duration was associated with increasing strength of functional connectivity in several brain regions as well as efficiency of communication but decreasing within-modular connections. One important finding is the association between sleep duration and strength of the default mode

network connectivity, which has been implicated in neurodegenerative diseases such as mild cognitive impairment (MCI) and Alzheimer's disease. This may suggest that neural mechanisms implicated in disordered sleep may also result in memory dysfunction. In addition, I showed that accelerometer derived nap duration was associated with transitivity. However, due to the lack of nap studies in influencing resting-state fMRI, little can be concluded. Future studies should examine the relationship between accelerometer-based sleep data and functional brain networks to confirm this finding.

Lifestyle factors have also shown to influence functional brain network properties. I observed increasing frequency of physical activity have been associated with an overall reduction of efficiency in how the brain networks process information (i.e. decreased transitivity). This is contrary to previous studies. Further, I also showed differences in the topological organisation of functional networks in smokers compared to non-smokers. Interestingly, even though this study was on middle- to older-aged chronic smokers, results from this study were similar to other studies investigating acute nicotine smokers in younger adults. It is unclear why this may be but I postulate that age may have an influence on this finding. Moreover, greater alcohol consumption was associated with lower transitivity and higher Louvain modularity. Taken together, sleep and other lifestyle factors including, physical activity, smoking, and alcohol consumption, were associated with distinct changes in the brain functional network properties.

7.2.4 Depression and functional brain network properties

Major depressive disorder (MDD) comprises a multitude of clinical symptoms, which may suggest multiple disruptions of neural circuits. Therefore, in Chapter 6, I aimed to investigate how phenotypic MDD and MDD polygenic risk scores (PRS_{MDD}) influence the functional network properties in mid- and old- aged participants from the UK Biobank. Due to the heterogeneous nature of the disorder, I studied two depression phenotypes – namely, lifetime depression and mental disorders. It was observed that mental disorders did not show any association with the graph theory measures. Individuals who passed the criteria for lifetime depression showed reduced network integration, segregation, and strength compared to controls. Consistent with studies positing that genetic architecture differs between depression phenotypes (Cai et al., 2020; Glanville et al., 2021), I showed differing associations between depression phenotypes and brain functional network properties. In addition, our results further indicated reduced network strength in different brain regions that have been associated with depressive rumination (Yan et al., 2019), attention (Beevers et al., 2015), cognitive control (Stange et al., 2017), and emotional processing (Dutta et al., 2014). Furthermore, PRS_{MDD} showed similar network disruption as with the cases of lifetime depression where higher genetic risk for MDD was associated with disrupted network integration, segregation, and strengths. Therefore, findings from Chapter 6 show the biological and neural mechanisms underlying the different depression phenotypes.

7.3 The multifactorial process influencing functional brain network properties

Understanding the mechanisms that allow for the emergence of different complex functional network properties remain to be elucidated. Findings in this thesis highlight the potential role of genetics, environment, and disease-states on the underlying

alteration of functional brain network properties in a large sample of middle- and older-aged adults. While these factors seemingly affect the brain ageing process, they vary in their degree of influence. From the findings, it was observed that genetics have a small effect size on the functional brain network properties whereas environmental factors have greater associations with the network properties. One previous study has postulated that while major portions of the network systems were controlled by genetic factors as observed by the intermediate to high heritability, environmental factors influenced the interplay between networks (Yang et al., 2016). Findings from modelling studies for the evolution of complex networks may be able to explain this variation. It has been posited that adaptive rewiring of the brain networks drive changes within their given computational role to meet the new demands associated with the alteration of the brain networks (Rentzeperis & van Leeuwen, 2021). There are varying demands on plasticity depending on the brain region (Neville & Bavelier, 2000) or the triggering factor, including development (Sur & Leamey, 2001), learning (Plautz, Milliken, & Nudo, 2000), and ageing (Park & Bischof, 2013). Importantly, the robustness of the network is responsible for maintaining the function of the networks amidst the changes that are taking place in the brain, such as a centralised network that is adaptively rewired remains centralised (Rentzeperis & van Leeuwen, 2021). This implies that underlying biological mechanisms, such as genetics, may play a role in constraining the possible architecture of the network in the rewiring process due to environmental contributions without destroying the macroscopic topological features of the network (Rentzeperis & van Leeuwen, 2021). The versatility of functional brain networks may be due to the concomitant interplay of different mechanisms of genetics and the environment. However, more work needs to be done to understand if these neural changes are indicative of neural rewiring process due to the environmental factors.

7.4 Implications

Given that rs-fMRI allows for the indirect study of neural activity by assessing the hemodynamic relationship between blood flow and neural firing in the brain, it has been used to examine changes in functional signal amplitudes and connectivity associated with different cognitive conditions (Medaglia, 2017). Variations in intrinsic connectivity as measured by the organisation of the network properties using graph theoretical approach have identified associated cognitive functions and clinical syndromes (Medaglia, 2017). Studies that investigated topological changes across the lifespan identified changes in the number and strength of connections to balance out the wiring costs and communication efficiency over the lifespan (Bullmore & Sporns, 2012; Cao et al., 2014). Further, it has been reported that there is continuous reorganisation in the functional brain network with ageing, which may influence behavioural and cognitive variability throughout the lifespan. These imply that reconfiguration of networks may allow for more flexibility to meet the demands during different stages of life (Wang, Zuo, & He, 2010a). Consequentially, findings on how functional network properties change with age may allow us to distinguish normal ageing from pathological ageing. Applications of graph theory rs-fMRI have been used to examine the abnormalities in the organisation of intrinsic network properties in various pathological conditions. For instance, individuals with Alzheimer's disease showed significantly lower normalised clustering coefficient, which suggests disrupted local network connectivity, as compared to age-matched controls (Supekar et al., 2008). These findings show that graph theory rs-fMRI can capture specific changes in the features of the functional network properties associated with normal development, ageing, and pathology. Despite this, the unique theoretical value of graph theory rs-fMRI analysis

remains largely unknown (Medaglia, 2017). In other words, it remains unclear whether it is biologically and cognitively meaningful or whether it affords theoretical or predictive information (Medaglia, 2017). Nevertheless, cautious optimism for using graph theory rs-fMRI for some clinical purposes may be justified. For instance, the combination of graph theory and machine learning to develop models that identify disease states, including autism (Zhou, Yu, & Duong, 2014), Alzheimer's disease (Koch et al., 2012), schizophrenia (Fekete et al., 2013), and depression (Sacchet, Prasad, Foland-Ross, Thompson, & Gotlib, 2015), compared to controls have shown to have high sensitivity and specificity (Medaglia, 2017). Although these findings need to be validated and replicated in a clinical setting, it is crucial to credit the potential usefulness of graph theory rs-fMRI in capturing and monitoring the brain organisation under different mental conditions. Moreover, with the advancements in brain imaging techniques together with the concomitant use of multiple analytical approaches, it is possible that graph theory rs-fMRI may provide a holistic picture into the complexity of the functional brain networks.

7.5 Methodological and conceptual considerations and limitations

While there have been tremendous advances in genetics and rs-fMRI neuroimaging techniques and analysis in the past decade that have enhanced our understanding of the human brain, there still exist mechanistic issues associated with these techniques. In addition, given that ageing is a multifarious process, it is important to recognise that there are other factors that may have influenced the brain functional network properties besides the ones that have been covered in this thesis. Specific methodological limitations regarding each study have been addressed within their respective chapters.

In this section, I will discuss several broader methodological and conceptual issues and how these issues contribute to the gaps in the literature.

7.5.1 Processing and analysis of rs-fMRI data

Rs-fMRI has been widely used as a tool for mapping human brain function and multiple analytic techniques have been developed to examine the functional connectivity throughout the brain. However, there remains an inherent issue with the attained rs-fMRI signals and to date, there is also a lack of gold standard to process and analyse rs-fMRI data.

Rs-fMRI signals are easily contaminated by artefacts, such as the movement of head, physiological effects (e.g. respiration and cardiac pulsatility), and various imperfections in the MRI hardware (e.g. heating of imaging gradients) during the acquisition of the data, which can result in substantial errors in the functional connectivity estimates (Maknojia, Churchill, Schweizer, & Graham, 2019). While retrospective corrective methods have been developed to minimise the noise from these data, there is no standard protocol for researchers to follow. This means that researchers need to choose from a wide array of rs-fMRI pre-processing methods and this may contribute to the inconsistent findings in rs-fMRI literature.

In addition to the pre-processing methods, there are several approaches to analyse rs-fMRI data. Functional connectivity, which aims to establish the connection between two spatial regions of interest, is inferred using correlations among parameters of neuronal activity on which the majority of the analytic techniques are based on (Smitha et al., 2017). Using different number of nodes may also have different implications. For

instance, I used 400-by-400 connectivity unregularized matrix in Chapter 3 whereas 100-by-100 connectivity regularised matrix was used in the other Chapters. One reason for this change was the potential issue relating to inconsistencies in the estimates of parameters using partial correlations that could be mitigated by regularised partial correlation on timeseries. Changing the number of nodes may also increase robustness of the connectivity matrix. Furthermore, within one analytic technique, there are also numerous approaches one can undertake to analyse the data. In seed-based analysis, which is a model-based method where an a-priori selection of seed or region of interest (ROI) is required, the functional connectivity map derived is dependent on the size and region selected. Using graph theory analysis, one can also choose between weighted or unweighted and directed or undirected matrices; and the reliability of the matrices derived is heavily influenced by the rs-fMRI signals. In turn, the difference in analysis used may result in variability of the findings observed in rs-fMRI data.

7.5.2 The use of graph theory to examine functional network properties

Graph theory-based approaches, which model the brain as complex network represented by a collection of nodes and edges and can be summarised in the form of a connection/adjacency matrix, have been extensively used to study the functional brain network properties (Wang et al., 2010a). Functional graphs are dependent on the rs-fMRI time series and are often highly dense and variable across time (Sporns, 2018). In order to construct the adjacency matrix, one must define the nodes between which the edges are calculated and this is typically achieved by selecting a parcellation of rs-fMRI data voxels into coarse-grained units of parcels (Medaglia, 2017). The statistics of network analysis vary depending on the parcellation (Wang et al., 2009). While there is continued interest in the development of parcellations, there is no “perfect” parcellation.

Each relies either on statistical optimisation or anatomically-based boundary definitions coupled with the conceptual idea of what is biologically meaningful (Medaglia, 2017). As such, there needs to be careful selection and comparison of the parcellations and rationale behind selecting it. In addition, edges can either be binary or weighted, directed or undirected, depending on how interactions are estimated and they address different questions. Binary analyses focus on understanding the basic topology of the network in the simplest sense such as which regions are connected to each other. On the contrary, weighted analyses will also factor in variations in the strength of the connectivity, which may be able to provide a more accurate picture of the brain network since not all connections in the brain are equal in terms of information capacity. However, it may be more complex to interpret weighted networks. The direction of the graph is based on whether the edges between nodes carry directional information such as causal interaction (Farahani, Karwowski, & Lighthall, 2019b). While negative correlations (i.e. anticorrelations) may provide more information about neural ageing, there are inherent issues involving its interpretation given the known potential artifacts after global signal correction. To date, most graph theory analyses use undirected networks because of the technical constraints surrounding the interpretation of directional networks (Liao, Vasilakos, & He, 2017). Given that there is no gold standard for the derivation of graph theory that can account for signed weights, I used the same methods as previous studies looking at weighted graph theory measures.

7.5.3 Identifying genetic variants associated with imaging phenotypes

Combining multi-dimensional genetics and imaging to assess the impact of genetic variations on brain structure and function has allowed for better understanding of behavioural and brain functional alterations (Jiang, King, & Turner, 2019a). Despite its

potential, there are increasing concerns surrounding the lack of biological validation and replication in these studies (Bogdan et al., 2017). Firstly, there is a question about whether the neuroimaging phenotypes are comparable across studies. Specifically, the imaging data may be acquired using different scanners of differing strengths and the neuroimaging phenotypes may be derived differently, which may contribute to inconsistent results across studies. Secondly, over reporting of studies with large effect sizes looking at genetic associations with neural phenotypes may introduce publication bias, which misrepresents the robustness and biological importance of these genetic effects (Bogdan et al., 2017). Lastly, as most genetics studies are performed on samples with European origins, there is an issue of ancestry bias and the observed results may not be generalisable to other races/ethnicities.

7.6 Future avenues of research

Accounting for the findings from this thesis as well as the methodological and conceptual considerations discussed above, I highlight the potential future avenues of research.

1. While it was observed that multiple SNPs and genes were associated with weighted graph theory measures (Chapter 3), they require replication and validation in independent studies. Moreover, the high correlations between the graph theory measures may suggest that these measures may account for the same phenotype, or the same variability in the population. Therefore, performing GWAS on each of these measures may not be necessary. In order to further understand the mechanisms of brain function at a more basic level, it may be useful for future studies to use developmental and adult human brain gene expression data to associate the expression of a single gene or genes with

specific graph theory measures and phenotypes. Moreover, the finding that *PAX8* gene, which is involved in brain development and sleep, was related to somatomotor and limbic networks, may suggest that some aspects of functional connectivity patterns in these two networks are "wired" during development and may be important in older age when sleep patterns get disrupted. It would be interesting to study these networks across the lifespan.

2. Chapter 4 demonstrated that the complexity of the functional brain organisation is shaped by the individual's age and sex, which may contribute to the cognitive performance of older adults. The current assumption is that network properties influence cognition and not the other way around. Future studies should use longitudinal data to determine the directionality of this relationship as well as to study the age trajectory of this association.
3. In Chapter 5, it was observed that sleep duration as well as other lifestyle factors, including physical activity, alcohol consumption, and smoking status, influence functional brain network properties. While the directionality of this relationship may be bidirectional, causality cannot be inferred from this study due to its cross-sectional design. Moreover, even though this study is useful for understanding some environmental factors and their relationships with brain networks, it may be more beneficial to include a wider range of factors as well as undertaking multivariate analyses to evaluate their influence on functional brain networks. This may be a more holistic approach to identifying risk/protective factors underlying brain networks.
4. Findings in Chapter 6 suggest that lifetime MDD and genetic predisposition to MDD are associated with disruptions of the functional network properties among adults in their mid-late life. Different MDD phenotypes showed

differential profiles of functional brain network alterations. However, given the heterogeneity of depression and its measures as well as the limitation of reliance on retrospective self-report depression, future research should study the clinical symptom profiles and endophenotypes in relation to functional brain networks to further understand the underlying biological mechanisms behind the variability of depression symptoms. Another approach is to use Research Domain Criteria (RDoC) (https://www.nimh.nih.gov/research/research-funded-by-nimh/rdoc/about-rdoc), which serves to understand the varying degrees of dysfunction of mental health disorders, rather than using the diagnostic and statistical manual (DSM)-5 or other diagnostic categories, in order to study the changes of functional networks associated with the complexity of the disorder.

7.7 Concluding remarks

Functional neuronal connections provide the physical foundation for communication and activity across the different brain regions. Elucidating whether genetics and/or environmental factors contribute to the topological properties of the brain networks is important to understand the underlying mechanisms that govern the intrinsic functional architecture of the brain, which may in turn explain the individual variations in both behavioural and mental states. Studies presented in this thesis were designed to shed light on the influence of genetics, environmental factors, and depression disease states on the functional brain network properties. This thesis provides novel contributions to the field of neuroscience in the following ways:

1. This is the first study to investigate the genetics of weighted functional graph theory measures in a large and well characterised cohort. Our findings may help

in the identification of novel biological pathways relevant to human brain functional network integrity and disease.

2. I identified that age and sex contribute significantly to the functional brain network properties in cognitively healthy middle-aged and older adults. This allows for better understanding of the brain changes that occur in normal versus pathological ageing.
3. Through examining how sleep and other lifestyle factors affect the functional brain network topology, this study was able to elucidate that environmental factors play a role in shaping the functional integrity of the brain architecture. This can be useful in developing preventive strategies in order to maintain functional brain health.
4. By including different depression phenotypes, it was observed that different definitions have varying relationship strengths between depression and functional brain network properties. This emphasises the need to be aware of this variability when examining the associations between different depression phenotypes and functional network measures, as potentially it may contribute to inconsistencies of results observed between studies.

References

Achard, S., & Bullmore, E. (2007). Efficiency and Cost of Economical Brain Functional Networks. *PLOS Computational Biology, 3*(2), e17. doi:10.1371/journal.pcbi.0030017

Adhikari, B. M., Jahanshad, N., Shukla, D., Glahn, D. C., Blangero, J., Fox, P. T., . . . Kochunov, P. (2018). Comparison of heritability estimates on resting state fMRI connectivity phenotypes using the ENIGMA analysis pipeline. *Hum Brain Mapp, 39*(12), 4893-4902. doi:10.1002/hbm.24331

Agosta, F., Sala, S., Valsasina, P., Meani, A., Canu, E., Magnani, G., . . . Filippi, M. (2013). Brain network connectivity assessed using graph theory in frontotemporal dementia. *Neurology, 81*(2), 134-143. doi:10.1212/WNL.0b013e31829a33f8

Alexopoulos, G. S., Hoptman, M. J., Kanellopoulos, D., Murphy, C. F., Lim, K. O., & Gunning, F. M. (2012). Functional connectivity in the cognitive control network and the default mode network in late-life depression. *Journal of Affective Disorders, 139*(1), 56-65. doi:https://doi.org/10.1016/j.jad.2011.12.002

Alfaro-Almagro, F., Jenkinson, M., Bangerter, N. K., Andersson, J. L. R., Griffanti, L., Douaud, G., . . . Smith, S. M. (2018). Image processing and Quality Control for the first 10,000 brain imaging datasets from UK Biobank. *Neuroimage, 166*, 400-424. doi:10.1016/j.neuroimage.2017.10.034

Allen, E., Erhardt, E., Damaraju, E., Gruner, W., Segall, J., Silva, R., . . . Calhoun, V. (2011). A Baseline for the Multivariate Comparison of Resting-State Networks. *Frontiers in Systems Neuroscience, 5*(2). doi:10.3389/fnsys.2011.00002

Allen, L. S., Richey, M. F., Chai, Y. M., & Gorski, R. A. (1991). Sex differences in the corpus callosum of the living human being. *The Journal of neuroscience : the*

official journal of the Society for Neuroscience, 11(4), 933-942. doi:10.1523/jneurosci.11-04-00933.1991

Amorim, L., Magalhães, R., Coelho, A., Moreira, P. S., Portugal-Nunes, C., Castanho, T. C., . . . Santos, N. C. (2018). Poor Sleep Quality Associates With Decreased Functional and Structural Brain Connectivity in Normative Aging: A MRI Multimodal Approach. *Frontiers in Aging Neuroscience, 10*, 375-375. doi:10.3389/fnagi.2018.00375

Andrews-Hanna, J. R., Snyder, A. Z., Vincent, J. L., Lustig, C., Head, D., Raichle, M. E., & Buckner, R. L. (2007). Disruption of large-scale brain systems in advanced aging. *Neuron, 56*(5), 924-935. doi:10.1016/j.neuron.2007.10.038

Bagarinao, E., Watanabe, H., Maesawa, S., Mori, D., Hara, K., Kawabata, K., . . . Sobue, G. (2019). Reorganization of brain networks and its association with general cognitive performance over the adult lifespan. *Scientific Reports, 9*(1), 11352. doi:10.1038/s41598-019-47922-x

Beckmann, C. F., & Smith, S. M. (2004). Probabilistic independent component analysis for functional magnetic resonance imaging. *IEEE Trans Med Imaging, 23*(2), 137-152. doi:10.1109/tmi.2003.822821

Beevers, C. G., Clasen, P. C., Enock, P. M., & Schnyer, D. M. (2015). Attention bias modification for major depressive disorder: Effects on attention bias, resting state connectivity, and symptom change. *Journal of abnormal psychology, 124*(3), 463-475. doi:10.1037/abn0000049

Belmaker, R. H., & Agam, G. (2008). Major Depressive Disorder. *New England Journal of Medicine, 358*(1), 55-68. doi:10.1056/NEJMra073096

Benjamini, Y., & Hochberg, Y. (1995). Controlling the False Discovery Rate: A Practical and Powerful Approach to Multiple Testing. *Journal of the Royal*

Statistical Society: Series B (Methodological), 57(1), 289-300. doi:https://doi.org/10.1111/j.2517-6161.1995.tb02031.x

Bernal, J. (2007). Thyroid hormone receptors in brain development and function. *Nature Clinical Practice Endocrinology & Metabolism, 3*(3), 249-259. doi:10.1038/ncpendmet0424

Bertolero, M. A., Yeo, B. T. T., Bassett, D. S., & D'Esposito, M. (2018). A mechanistic model of connector hubs, modularity and cognition. *Nature Human Behaviour, 2*(10), 765-777. doi:10.1038/s41562-018-0420-6

Betzel, R. F., Byrge, L., He, Y., Goni, J., Zuo, X. N., & Sporns, O. (2014). Changes in structural and functional connectivity among resting-state networks across the human lifespan. *NeuroImage, 102 Pt 2*, 345-357. doi:10.1016/j.neuroimage.2014.07.067

Bezmaternykh, D. D., Melnikov, M. Y., Savelov, A. A., Kozlova, L. I., Petrovskiy, E. D., Natarova, K. A., & Shtark, M. B. (2021). Brain Networks Connectivity in Mild to Moderate Depression: Resting State fMRI Study with Implications to Nonpharmacological Treatment. *Neural Plasticity, 2021*, 8846097. doi:10.1155/2021/8846097

Bittner, N., Jockwitz, C., Mühleisen, T. W., Hoffstaedter, F., Eickhoff, S. B., Moebus, S., . . . Caspers, S. (2019). Combining lifestyle risks to disentangle brain structure and functional connectivity differences in older adults. *Nature Communications, 10*(1), 621. doi:10.1038/s41467-019-08500-x

Blake, J. A., & Ziman, M. R. (2014). Pax genes: regulators of lineage specification and progenitor cell maintenance. *Development, 141*(4), 737. doi:10.1242/dev.091785

Bogdan, R., Salmeron, B. J., Carey, C. E., Agrawal, A., Calhoun, V. D., Garavan, H., . . . Goldman, D. (2017). Imaging Genetics and Genomics in Psychiatry: A

Critical Review of Progress and Potential. *Biological psychiatry, 82*(3), 165-175. doi:10.1016/j.biopsych.2016.12.030

Bohr, I. J., Kenny, E., Blamire, A., O'Brien, J. T., Thomas, A. J., Richardson, J., & Kaiser, M. (2012). Resting-state functional connectivity in late-life depression: higher global connectivity and more long distance connections. *Front Psychiatry, 3*, 116. doi:10.3389/fpsyt.2012.00116

Brody, A. L., Olmstead, R. E., London, E. D., Farahi, J., Meyer, J. H., Grossman, P., . . . Mandelkern, M. A. (2004). Smoking-induced ventral striatum dopamine release. *Am J Psychiatry, 161*(7), 1211-1218. doi:10.1176/appi.ajp.161.7.1211

Brody, B. A., Kinney, H. C., Kloman, A. S., & Gilles, F. H. (1987). Sequence of central nervous system myelination in human infancy. I. An autopsy study of myelination. *J Neuropathol Exp Neurol, 46*(3), 283-301. doi:10.1097/00005072-198705000-00005

Buckner, R. L. (2004). Memory and executive function in aging and AD: multiple factors that cause decline and reserve factors that compensate. *Neuron, 44*(1), 195-208. doi:10.1016/j.neuron.2004.09.006

Buckner, R. L., & DiNicola, L. M. (2019). The brain's default network: updated anatomy, physiology and evolving insights. *Nature Reviews Neuroscience, 20*(10), 593-608. doi:10.1038/s41583-019-0212-7

Bulik-Sullivan, B., Finucane, H. K., Anttila, V., Gusev, A., Day, F. R., Loh, P.-R., . . . Genetic Consortium for Anorexia Nervosa of the Wellcome Trust Case Control, C. (2015). An atlas of genetic correlations across human diseases and traits. *Nature Genetics, 47*(11), 1236-1241. doi:10.1038/ng.3406

Bullmore, E., & Sporns, O. (2012). The economy of brain network organization. *Nature Reviews Neuroscience, 13*(5), 336-349.

Buniello, A., MacArthur, J. A. L., Cerezo, M., Harris, L. W., Hayhurst, J., Malangone, C., . . . Parkinson, H. (2019). The NHGRI-EBI GWAS Catalog of published genome-wide association studies, targeted arrays and summary statistics 2019. *Nucleic Acids Res, 47*(D1), D1005-d1012. doi:10.1093/nar/gky1120

Burke, S. N., & Barnes, C. A. (2006). Neural plasticity in the ageing brain. *Nat Rev Neurosci, 7*(1), 30-40. doi:10.1038/nrn1809

Bycroft, C., Freeman, C., Petkova, D., Band, G., Elliott, L. T., Sharp, K., . . . Marchini, J. (2018). The UK Biobank resource with deep phenotyping and genomic data. *Nature, 562*(7726), 203-209. doi:10.1038/s41586-018-0579-z

Cai, N., Revez, J. A., Adams, M. J., Andlauer, T. F. M., Breen, G., Byrne, E. M., . . . Consortium, M. D. D. W. G. o. t. P. G. (2020). Minimal phenotyping yields genome-wide association signals of low specificity for major depression. *Nature Genetics, 52*(4), 437-447. doi:10.1038/s41588-020-0594-5

Camchong, J., Stenger, A., & Fein, G. (2013). Resting-state synchrony in long-term abstinent alcoholics. *Alcohol Clin Exp Res, 37*(1), 75-85. doi:10.1111/j.1530-0277.2012.01859.x

Cao, M., Wang, J.-H., Dai, Z.-J., Cao, X.-Y., Jiang, L.-L., Fan, F.-M., . . . Dong, Q. (2014). Topological organization of the human brain functional connectome across the lifespan. *Developmental Cognitive Neuroscience, 7*, 76-93.

Cao, X., Liu, Z., Xu, C., Li, J., Gao, Q., Sun, N., . . . Zhang, K. (2012). Disrupted resting-state functional connectivity of the hippocampus in medication-naïve patients with major depressive disorder. *J Affect Disord, 141*(2-3), 194-203. doi:10.1016/j.jad.2012.03.002

Cao, Z., Yang, H., Ye, Y., Zhang, Y., Li, S., Zhao, H., & Wang, Y. (2021). Polygenic risk score, healthy lifestyles, and risk of incident depression. *Translational Psychiatry, 11*(1), 189. doi:10.1038/s41398-021-01306-w

Carter, A. R., Patel, K. R., Astafiev, S. V., Snyder, A. Z., Rengachary, J., Strube, M. J., . . . Corbetta, M. (2012). Upstream dysfunction of somatomotor functional connectivity after corticospinal damage in stroke. *Neurorehabil Neural Repair, 26*(1), 7-19. doi:10.1177/1545968311411054

Castrén, E. (2005). Is mood chemistry? *Nature Reviews Neuroscience, 6*(3), 241-246. doi:10.1038/nrn1629

Chan, M. Y., Park, D. C., Savalia, N. K., Petersen, S. E., & Wig, G. S. (2014). Decreased segregation of brain systems across the healthy adult lifespan. *Proceedings of the National Academy of Sciences, 111*(46), E4997. doi:10.1073/pnas.1415122111

Chang, C. C., Chow, C. C., Tellier, L. C., Vattikuti, S., Purcell, S. M., & Lee, J. J. (2015). Second-generation PLINK: rising to the challenge of larger and richer datasets. *Gigascience, 4*, 7. doi:10.1186/s13742-015-0047-8

Chanraud, S., Pitel, A. L., Pfefferbaum, A., & Sullivan, E. V. (2011). Disruption of functional connectivity of the default-mode network in alcoholism. *Cereb Cortex, 21*(10), 2272-2281. doi:10.1093/cercor/bhq297

Chen, L.-T., Fan, X.-L., Li, H.-J., Ye, C.-L., Yu, H.-H., Xin, H.-Z., . . . Yan, L.-P. (2018). Aberrant brain functional connectome in patients with obstructive sleep apnea. *Neuropsychiatric disease and treatment, 14*, 1059-1070. doi:10.2147/NDT.S161085

Choi, S. W., Mak, T. S.-H., & O'Reilly, P. F. (2020). Tutorial: a guide to performing polygenic risk score analyses. *Nature Protocols*. doi:10.1038/s41596-020-0353-1

Choi, S. W., Mak, T. S. H., & Reilly, P. (2018). A guide to performing Polygenic Risk Score analyses. *bioRxiv*, 416545. doi:10.1101/416545

Cohen, J. R., & D'Esposito, M. (2016). The Segregation and Integration of Distinct Brain Networks and Their Relationship to Cognition. *J Neurosci, 36*(48), 12083-12094. doi:10.1523/jneurosci.2965-15.2016

Colclough, G. L., Smith, S. M., Nichols, T. E., Winkler, A. M., Sotiropoulos, S. N., Glasser, M. F., . . . Woolrich, M. W. (2017). The heritability of multi-modal connectivity in human brain activity. *eLife, 6*, e20178. doi:10.7554/eLife.20178

Colcombe, S., & Kramer, A. F. (2003). Fitness effects on the cognitive function of older adults: a meta-analytic study. *Psychol Sci, 14*(2), 125-130. doi:10.1111/1467-9280.t01-1-01430

Cox, R. W. (1996). AFNI: software for analysis and visualization of functional magnetic resonance neuroimages. *Comput Biomed Res, 29*(3), 162-173.

Cox, S. R., Ritchie, S. J., Fawns-Ritchie, C., Tucker-Drob, E. M., & Deary, I. J. (2019). Structural brain imaging correlates of general intelligence in UK Biobank. *Intelligence, 76*, 101376. doi:https://doi.org/10.1016/j.intell.2019.101376

Cui, L., Tao, S., Yin, H.-C., Shen, Q.-Q., Wang, Y., Zhu, L.-N., & Li, X.-J. (2021). Tai Chi Chuan Alters Brain Functional Network Plasticity and Promotes Cognitive Flexibility. *Frontiers in psychology, 12*, 665419-665419. doi:10.3389/fpsyg.2021.665419

Curtin, J. J., Patrick, C. J., Lang, A. R., Cacioppo, J. T., & Birbaumer, N. (2001). Alcohol Affects Emotion Through Cognition. *Psychological Science, 12*(6), 527-531. doi:10.1111/1467-9280.00397

Damoiseaux, J. S. (2017). Effects of aging on functional and structural brain connectivity. *Neuroimage, 160*, 32-40. doi:10.1016/j.neuroimage.2017.01.077

Damoiseaux, J. S., Viviano, R. P., Yuan, P., & Raz, N. (2016). Differential effect of age on posterior and anterior hippocampal functional connectivity. *NeuroImage, 133*, 468-476. doi:10.1016/j.neuroimage.2016.03.047

Daneault, V., Orban, P., Martin, N., Dansereau, C., Godbout, J., Pouliot, P., . . . Carrier, J. (2021). Cerebral functional networks during sleep in young and older individuals. *Scientific Reports, 11*(1), 4905. doi:10.1038/s41598-021-84417-0

Dayem Ullah, A. Z., Oscanoa, J., Wang, J., Nagano, A., Lemoine, N. R., & Chelala, C. (2018). SNPnexus: assessing the functional relevance of genetic variation to facilitate the promise of precision medicine. *Nucleic Acids Research, 46*(W1), W109-W113. doi:10.1093/nar/gky399

de Carvalho, M. R., Dias, G. P., Cosci, F., de-Melo-Neto, V. L., Bevilaqua, M. C. d. N., Gardino, P. F., & Nardi, A. E. (2010). Current findings of fMRI in panic disorder: contributions for the fear neurocircuitry and CBT effects. *Expert Review of Neurotherapeutics, 10*(2), 291-303. doi:10.1586/ern.09.161

De Cesarei, A., Codispoti, M., Schupp, H. T., & Stegagno, L. (2006). Selectively attending to natural scenes after alcohol consumption: An ERP analysis. *Biological Psychology, 72*(1), 35-45. doi:https://doi.org/10.1016/j.biopsycho.2005.06.009

De Havas, J. A., Parimal, S., Soon, C. S., & Chee, M. W. (2012). Sleep deprivation reduces default mode network connectivity and anti-correlation during rest and

task performance. *NeuroImage, 59*(2), 1745-1751. doi:10.1016/j.neuroimage.2011.08.026

de Leeuw, C. A., Mooij, J. M., Heskes, T., & Posthuma, D. (2015). MAGMA: Generalized Gene-Set Analysis of GWAS Data. *PLOS Computational Biology, 11*(4), e1004219. doi:10.1371/journal.pcbi.1004219

de Nooij, L., Harris, M. A., Adams, M. J., Clarke, T.-K., Shen, X., Cox, S. R., . . . Whalley, H. C. (2020). Cognitive functioning and lifetime major depressive disorder in UK Biobank. *European Psychiatry, 63*(1), e28. doi:10.1192/j.eurpsy.2020.24

De Vico Fallani, F., Richiardi, J., Chavez, M., & Achard, S. (2014). Graph analysis of functional brain networks: practical issues in translational neuroscience. *Philos Trans R Soc Lond B Biol Sci, 369*(1653). doi:10.1098/rstb.2013.0521

Deco, G., Tononi, G., Boly, M., & Kringelbach, M. L. (2015). Rethinking segregation and integration: contributions of whole-brain modelling. *Nature Reviews Neuroscience, 16*(7), 430-439. doi:10.1038/nrn3963

Dennis, E. L., Jahanshad, N., McMahon, K. L., de Zubicaray, G. I., Martin, N. G., Hickie, I. B., . . . Thompson, P. M. (2013). Development of brain structural connectivity between ages 12 and 30: a 4-Tesla diffusion imaging study in 439 adolescents and adults. *Neuroimage, 64*, 671-684. doi:10.1016/j.neuroimage.2012.09.004

Dennis, E. L., & Thompson, P. M. (2014). Functional brain connectivity using fMRI in aging and Alzheimer's disease. *Neuropsychol Rev, 24*(1), 49-62. doi:10.1007/s11065-014-9249-6

Dennis, E. L., Thompson, P. M., & Jahanshad, N. (2019). Chapter 8 - Genetics of brain networks and connectivity. In B. C. Munsell, G. Wu, L. Bonilha, & P. J. Laurienti (Eds.), *Connectomics* (pp. 155-179): Academic Press.

Ding, X., & Lee, S. W. (2013). Changes of functional and effective connectivity in smoking replenishment on deprived heavy smokers: a resting-state FMRI study. *PloS one, 8*(3), e59331. doi:10.1371/journal.pone.0059331

Disner, S. G., Beevers, C. G., Haigh, E. A., & Beck, A. T. (2011). Neural mechanisms of the cognitive model of depression. *Nat Rev Neurosci, 12*(8), 467-477. doi:10.1038/nrn3027

do Canto-Pereira, L. H. M., David, I. d. P. A., Machado-Pinheiro, W., & Ranvaud, R. D. (2007). Effects of acute alcohol intoxication on visuospatial attention. *Human & Experimental Toxicology, 26*(4), 311-319. doi:10.1177/0960327106070490

Doherty, A., Jackson, D., Hammerla, N., Plötz, T., Olivier, P., Granat, M. H., . . . Wareham, N. J. (2017). Large Scale Population Assessment of Physical Activity Using Wrist Worn Accelerometers: The UK Biobank Study. *PloS one, 12*(2), e0169649. doi:10.1371/journal.pone.0169649

Doherty, A., Smith-Byrne, K., Ferreira, T., Holmes, M. V., Holmes, C., Pulit, S. L., & Lindgren, C. M. (2018). GWAS identifies 14 loci for device-measured physical activity and sleep duration. *Nature Communications, 9*(1), 5257. doi:10.1038/s41467-018-07743-4

Dong, X., Qin, H., Wu, T., Hu, H., Liao, K., Cheng, F., . . . Lei, X. (2018). Rest but busy: Aberrant resting-state functional connectivity of triple network model in insomnia. *Brain and behavior, 8*(2), e00876. doi:https://doi.org/10.1002/brb3.876

Drakesmith, M., Caeyenberghs, K., Dutt, A., Lewis, G., David, A. S., & Jones, D. K. (2015). Overcoming the effects of false positives and threshold bias in graph theoretical analyses of neuroimaging data. *NeuroImage, 118*, 313-333. doi:https://doi.org/10.1016/j.neuroimage.2015.05.011

Dutta, A., McKie, S., & Deakin, J. F. (2014). Resting state networks in major depressive disorder. *Psychiatry Res, 224*(3), 139-151. doi:10.1016/j.pscychresns.2014.10.003

Dzierzewski, J. M., Buman, M. P., Giacobbi, P. R., Jr., Roberts, B. L., Aiken-Morgan, A. T., Marsiske, M., & McCrae, C. S. (2014). Exercise and sleep in community-dwelling older adults: evidence for a reciprocal relationship. *J Sleep Res, 23*(1), 61-68. doi:10.1111/jsr.12078

Ebrahim, I. O., Shapiro, C. M., Williams, A. J., & Fenwick, P. B. (2013). Alcohol and sleep I: effects on normal sleep. *Alcohol Clin Exp Res, 37*(4), 539-549. doi:10.1111/acer.12006

Eickhoff, S. B., & Grefkes, C. (2011). Approaches for the integrated analysis of structure, function and connectivity of the human brain. *Clin EEG Neurosci, 42*(2), 107-121. doi:10.1177/155005941104200211

Elliott, L. T., Sharp, K., Alfaro-Almagro, F., Shi, S., Miller, K. L., Douaud, G., . . . Smith, S. M. (2018). Genome-wide association studies of brain imaging phenotypes in UK Biobank. *Nature, 562*(7726), 210-216. doi:10.1038/s41586-018-0571-7

Elliott, M. L., Knodt, A. R., Cooke, M., Kim, M. J., Melzer, T. R., Keenan, R., . . . Hariri, A. R. (2019). General functional connectivity: Shared features of resting-state and task fMRI drive reliable and heritable individual differences in

functional brain networks. *NeuroImage, 189*, 516-532. doi:https://doi.org/10.1016/j.neuroimage.2019.01.068

Etnier, J. L., Nowell, P. M., Landers, D. M., & Sibley, B. A. (2006). A meta-regression to examine the relationship between aerobic fitness and cognitive performance. *Brain Res Rev, 52*(1), 119-130. doi:10.1016/j.brainresrev.2006.01.002

Fallani, F. D. V., Richiardi, J., Chavez, M., & Achard, S. (2014). Graph analysis of functional brain networks: practical issues in translational neuroscience. *Philosophical Transactions of the Royal Society B: Biological Sciences, 369*(1653), 20130521. doi:doi:10.1098/rstb.2013.0521

Fallon, N., Chiu, Y., Nurmikko, T., & Stancak, A. (2016). Functional Connectivity with the Default Mode Network Is Altered in Fibromyalgia Patients. *PloS one, 11*(7), e0159198-e0159198. doi:10.1371/journal.pone.0159198

Farahani, F. V., Fafrowicz, M., Karwowski, W., Douglas, P. K., Domagalik, A., Beldzik, E., . . . Marek, T. (2019a). Effects of Chronic Sleep Restriction on the Brain Functional Network, as Revealed by Graph Theory. *Frontiers in Neuroscience, 13*(1087). doi:10.3389/fnins.2019.01087

Farahani, F. V., Karwowski, W., & Lighthall, N. R. (2019b). Application of Graph Theory for Identifying Connectivity Patterns in Human Brain Networks: A Systematic Review. *Frontiers in Neuroscience, 13*(585). doi:10.3389/fnins.2019.00585

Favre, C., Zhdanov, A., Leahy, M., Papkovsky, D., & O'Connor, R. (2010). Mitochondrial pyrimidine nucleotide carrier (PNC1) regulates mitochondrial biogenesis and the invasive phenotype of cancer cells. *Oncogene, 29*(27), 3964-3976. doi:10.1038/onc.2010.146

Fedota, J. R., & Stein, E. A. (2015). Resting-state functional connectivity and nicotine addiction: prospects for biomarker development. *Ann N Y Acad Sci, 1349*(1), 64-82. doi:10.1111/nyas.12882

Fekete, T., Wilf, M., Rubin, D., Edelman, S., Malach, R., & Mujica-Parodi, L. R. (2013). Combining classification with fMRI-derived complex network measures for potential neurodiagnostics. *PloS one, 8*(5), e62867. doi:10.1371/journal.pone.0062867

Fernandes, J., Arida, R. M., & Gomez-Pinilla, F. (2017). Physical exercise as an epigenetic modulator of brain plasticity and cognition. *Neuroscience and biobehavioral reviews, 80*, 443-456. doi:10.1016/j.neubiorev.2017.06.012

Fernandez-Mendoza, J., & Vgontzas, A. N. (2013). Insomnia and its impact on physical and mental health. *Current psychiatry reports, 15*(12), 418-418. doi:10.1007/s11920-013-0418-8

Fjell, A. M., Sneve, M. H., Grydeland, H., Storsve, A. B., & Walhovd, K. B. (2017). The Disconnected Brain and Executive Function Decline in Aging. *Cerebral Cortex, 27*(3), 2303-2317. doi:10.1093/cercor/bhw082

Fjell, A. M., Sneve, M. H., Storsve, A. B., Grydeland, H., Yendiki, A., & Walhovd, K. B. (2016). Brain Events Underlying Episodic Memory Changes in Aging: A Longitudinal Investigation of Structural and Functional Connectivity. *Cereb Cortex, 26*(3), 1272-1286. doi:10.1093/cercor/bhv102

Flodin, P., Jonasson, L. S., Riklund, K., Nyberg, L., & Boraxbekk, C. J. (2017). Does Aerobic Exercise Influence Intrinsic Brain Activity? An Aerobic Exercise Intervention among Healthy Old Adults. *Front Aging Neurosci, 9*, 267. doi:10.3389/fnagi.2017.00267

Floyd, S., Favre, C., Lasorsa, F. M., Leahy, M., Trigiante, G., Stroebel, P., . . . O'Connor, R. (2007). The insulin-like growth factor-I-mTOR signaling pathway induces the mitochondrial pyrimidine nucleotide carrier to promote cell growth. *Mol Biol Cell, 18*(9), 3545-3555. doi:10.1091/mbc.e06-12-1109

Foley, D. J., Monjan, A. A., Brown, S. L., Simonsick, E. M., Wallace, R. B., & Blazer, D. G. (1995). Sleep complaints among elderly persons: an epidemiologic study of three communities. *Sleep, 18*(6), 425-432. doi:10.1093/sleep/18.6.425

Fornito, A., Zalesky, A., Bassett, D. S., Meunier, D., Ellison-Wright, I., Yucel, M., . . . Bullmore, E. T. (2011). Genetic influences on cost-efficient organization of human cortical functional networks. *J Neurosci, 31*(9), 3261-3270. doi:10.1523/jneurosci.4858-10.2011

Fornito, A., Zalesky, A., & Bullmore, E. (2016). Chapter 3 - Connectivity Matrices and Brain Graphs. In A. Fornito, A. Zalesky, & E. T. Bullmore (Eds.), *Fundamentals of Brain Network Analysis* (pp. 89-113). San Diego: Academic Press.

Fournier, C., Anquetil, V., Camuzat, A., Stirati-Buron, S., Sazdovitch, V., Molina-Porcel, L., . . . Neuro, C. E. B. N. N. (2018). Interrupted CAG expansions in ATXN2 gene expand the genetic spectrum of frontotemporal dementias. *Acta Neuropathologica Communications, 6*(1), 41. doi:10.1186/s40478-018-0547-8

Franke, B., Stein, J. L., Ripke, S., Anttila, V., Hibar, D. P., van Hulzen, K. J. E., . . . Wellcome Trust Case Control, C. (2016). Genetic influences on schizophrenia and subcortical brain volumes: large-scale proof of concept. *Nature Neuroscience, 19*(3), 420-431. doi:10.1038/nn.4228

Fried, E. I. (2017). Moving forward: how depression heterogeneity hinders progress in treatment and research. *Expert Rev Neurother, 17*(5), 423-425. doi:10.1080/14737175.2017.1307737

Froeliger, B., McConnell, P. A., Stankeviciute, N., McClure, E. A., Kalivas, P. W., & Gray, K. M. (2015). The effects of N-Acetylcysteine on frontostriatal resting-state functional connectivity, withdrawal symptoms and smoking abstinence: A double-blind, placebo-controlled fMRI pilot study. *Drug Alcohol Depend, 156*, 234-242. doi:10.1016/j.drugalcdep.2015.09.021

Gallen, C. L., Baniqued, P. L., Chapman, S. B., Aslan, S., Keebler, M., Didehbani, N., & D'Esposito, M. (2016). Modular Brain Network Organization Predicts Response to Cognitive Training in Older Adults. *PloS one, 11*(12), e0169015-e0169015. doi:10.1371/journal.pone.0169015

Ge, T., Chen, C.-Y., Ni, Y., Feng, Y.-C. A., & Smoller, J. W. (2019). Polygenic prediction via Bayesian regression and continuous shrinkage priors. *Nature Communications, 10*(1), 1776. doi:10.1038/s41467-019-09718-5

Ge, T., Holmes, A. J., Buckner, R. L., Smoller, J. W., & Sabuncu, M. R. (2017). Heritability analysis with repeat measurements and its application to resting-state functional connectivity. *Proceedings of the National Academy of Sciences, 114*(21), 5521. doi:10.1073/pnas.1700765114

Geerligs, L., Renken, R. J., Saliasi, E., Maurits, N. M., & Lorist, M. M. (2015). A Brain-Wide Study of Age-Related Changes in Functional Connectivity. *Cereb Cortex, 25*(7), 1987-1999. doi:10.1093/cercor/bhu012

Giedd, J. N., Castellanos, F. X., Rajapakse, J. C., Vaituzis, A. C., & Rapoport, J. L. (1997). Sexual dimorphism of the developing human brain. *Prog Neuropsychopharmacol Biol Psychiatry, 21*(8), 1185-1201. doi:10.1016/s0278-5846(97)00158-9

Gießing, C., Thiel, C. M., Alexander-Bloch, A. F., Patel, A. X., & Bullmore, E. T. (2013). Human Brain Functional Network Changes Associated with Enhanced

and Impaired Attentional Task Performance. *The Journal of Neuroscience, 33*(14), 5903. doi:10.1523/JNEUROSCI.4854-12.2013

Ginestet, C. E., Fournel, A. P., & Simmons, A. (2014). Statistical network analysis for functional MRI: summary networks and group comparisons. *Front Comput Neurosci, 8*, 51. doi:10.3389/fncom.2014.00051

Glahn, D. C., Winkler, A. M., Kochunov, P., Almasy, L., Duggirala, R., Carless, M. A., . . . Blangero, J. (2010). Genetic control over the resting brain. *Proceedings of the National Academy of Sciences, 107*(3), 1223. doi:10.1073/pnas.0909969107

Glanville, K. P., Coleman, J. R. I., Howard, D. M., Pain, O., Hanscombe, K. B., Jermy, B., . . . Lewis, C. M. (2021). Multiple measures of depression to enhance validity of major depressive disorder in the UK Biobank. *BJPsych Open, 7*(2), e44. doi:10.1192/bjo.2020.145

Goh, J. O. (2011). Functional Dedifferentiation and Altered Connectivity in Older Adults: Neural Accounts of Cognitive Aging. *Aging and disease, 2*(1), 30-48.

Goldstein, J. M., Seidman, L. J., Horton, N. J., Makris, N., Kennedy, D. N., Caviness, V. S., Jr., . . . Tsuang, M. T. (2001). Normal sexual dimorphism of the adult human brain assessed by in vivo magnetic resonance imaging. *Cereb Cortex, 11*(6), 490-497. doi:10.1093/cercor/11.6.490

Goldstone, A., Mayhew, S. D., Przezdzik, I., Wilson, R. S., Hale, J. R., & Bagshaw, A. P. (2016). Gender Specific Re-organization of Resting-State Networks in Older Age. *Frontiers in Aging Neuroscience, 8*, 285-285. doi:10.3389/fnagi.2016.00285

Gong, G., Rosa-Neto, P., Carbonell, F., Chen, Z. J., He, Y., & Evans, A. C. (2009). Age- and Gender-Related Differences in the Cortical Anatomical Network. *The*

Journal of Neuroscience, 29(50), 15684. doi:10.1523/JNEUROSCI.2308-09.2009

Gong, Q., & He, Y. (2015). Depression, neuroimaging and connectomics: a selective overview. *Biological psychiatry, 77*(3), 223-235. doi:10.1016/j.biopsych.2014.08.009

Grady, C., Sarraf, S., Saverino, C., & Campbell, K. (2016). Age differences in the functional interactions among the default, frontoparietal control, and dorsal attention networks. *Neurobiology of aging, 41*, 159-172. doi:10.1016/j.neurobiolaging.2016.02.020

Grayson, D. S., & Fair, D. A. (2017). Development of large-scale functional networks from birth to adulthood: A guide to the neuroimaging literature. *Neuroimage, 160*, 15-31. doi:10.1016/j.neuroimage.2017.01.079

Greicius, M. D., Flores, B. H., Menon, V., Glover, G. H., Solvason, H. B., Kenna, H., . . . Schatzberg, A. F. (2007). Resting-state functional connectivity in major depression: abnormally increased contributions from subgenual cingulate cortex and thalamus. *Biological psychiatry, 62*(5), 429-437. doi:10.1016/j.biopsych.2006.09.020

Greicius, M. D., Srivastava, G., Reiss, A. L., & Menon, V. (2004). Default-mode network activity distinguishes Alzheimer's disease from healthy aging: evidence from functional MRI. *Proc Natl Acad Sci U S A, 101*(13), 4637-4642. doi:10.1073/pnas.0308627101

Grieder, M., Wang, D. J. J., Dierks, T., Wahlund, L.-O., & Jann, K. (2018). Default Mode Network Complexity and Cognitive Decline in Mild Alzheimer's Disease. *Frontiers in Neuroscience, 12*, 770-770. doi:10.3389/fnins.2018.00770

Griffanti, L., Salimi-Khorshidi, G., Beckmann, C. F., Auerbach, E. J., Douaud, G., Sexton, C. E., . . . Smith, S. M. (2014). ICA-based artefact removal and accelerated fMRI acquisition for improved resting state network imaging. *Neuroimage, 95*, 232-247. doi:10.1016/j.neuroimage.2014.03.034

Guo, W., Liu, F., Dai, Y., Jiang, M., Zhang, J., Yu, L., . . . Xiao, C. (2013). Decreased interhemispheric resting-state functional connectivity in first-episode, drug-naive major depressive disorder. *Prog Neuropsychopharmacol Biol Psychiatry, 41*, 24-29. doi:10.1016/j.pnpbp.2012.11.003

Gur, R. C., Richard, J., Calkins, M. E., Chiavacci, R., Hansen, J. A., Bilker, W. B., . . . Gur, R. E. (2012). Age group and sex differences in performance on a computerized neurocognitive battery in children age 8-21. *Neuropsychology, 26*(2), 251-265. doi:10.1037/a0026712

Gur, R. C., Turetsky, B. I., Matsui, M., Yan, M., Bilker, W., Hughett, P., & Gur, R. E. (1999). Sex Differences in Brain Gray and White Matter in Healthy Young Adults: Correlations with Cognitive Performance. *The Journal of Neuroscience, 19*(10), 4065. doi:10.1523/JNEUROSCI.19-10-04065.1999

Hagmann, P., Cammoun, L., Gigandet, X., Meuli, R., Honey, C. J., Wedeen, V. J., & Sporns, O. (2008). Mapping the structural core of human cerebral cortex. *PLoS Biol, 6*(7), e159. doi:10.1371/journal.pbio.0060159

Hagströmer, M., Oja, P., & Sjöström, M. (2006). The International Physical Activity Questionnaire (IPAQ): a study of concurrent and construct validity. *Public Health Nutrition, 9*(6), 755-762. doi:10.1079/PHN2005898

Hahn, B., Ross, T. J., Wolkenberg, F. A., Shakleya, D. M., Huestis, M. A., & Stein, E. A. (2009). Performance effects of nicotine during selective attention, divided

attention, and simple stimulus detection: an fMRI study. *Cerebral cortex (New York, N.Y. : 1991), 19*(9), 1990-2000. doi:10.1093/cercor/bhn226

Halldorsdottir, T., Piechaczek, C., Soares de Matos, A. P., Czamara, D., Pehl, V., Wagenbuechler, P., . . . Binder, E. B. (2019). Polygenic Risk: Predicting Depression Outcomes in Clinical and Epidemiological Cohorts of Youths. *American Journal of Psychiatry, 176*(8), 615-625. doi:10.1176/appi.ajp.2019.18091014

Halpern, D. F., Benbow, C. P., Geary, D. C., Gur, R. C., Hyde, J. S., & Gernsbacher, M. A. (2007). The Science of Sex Differences in Science and Mathematics. *Psychological science in the public interest : a journal of the American Psychological Society, 8*(1), 1-51. doi:10.1111/j.1529-1006.2007.00032.x

Hamilton, J. P., Farmer, M., Fogelman, P., & Gotlib, I. H. (2015). Depressive Rumination, the Default-Mode Network, and the Dark Matter of Clinical Neuroscience. *Biological psychiatry, 78*(4), 224-230. doi:10.1016/j.biopsych.2015.02.020

Harris, M. A., Cox, S. R., de Nooij, L., Barbu, M. C., Adams, M. J., Shen, X., . . . Whalley, H. C. (2020). The Influence of Phenotyping Method on Structural Neuroimaging Associations with Depression in UK Biobank. *medRxiv*, 2020.2012.2018.20248488. doi:10.1101/2020.12.18.20248488

He, Q., Zhang, P., Li, G., Dai, H., & Shi, J. (2020). The association between insomnia symptoms and risk of cardio-cerebral vascular events: A meta-analysis of prospective cohort studies. *European Journal of Preventive Cardiology, 24*(10), 1071-1082. doi:10.1177/2047487317702043

He, X., Qin, W., Liu, Y., Zhang, X., Duan, Y., Song, J., . . . Yu, C. (2013). Age-related decrease in functional connectivity of the right fronto-insular cortex with the

central executive and default-mode networks in adults from young to middle age. *Neurosci Lett, 544*, 74-79. doi:10.1016/j.neulet.2013.03.044

He, X., Qin, W., Liu, Y., Zhang, X., Duan, Y., Song, J., . . . Yu, C. (2014). Abnormal salience network in normal aging and in amnestic mild cognitive impairment and Alzheimer's disease. *Human Brain Mapping, 35*(7), 3446-3464. doi:https://doi.org/10.1002/hbm.22414

Hillman, C. H., Motl, R. W., Pontifex, M. B., Posthuma, D., Stubbe, J. H., Boomsma, D. I., & de Geus, E. J. C. (2006). Physical activity and cognitive function in a cross-section of younger and older community-dwelling individuals. *Health Psychol, 25*(6), 678-687. doi:10.1037/0278-6133.25.6.678

Hong, L. E., Gu, H., Yang, Y., Ross, T. J., Salmeron, B. J., Buchholz, B., . . . Stein, E. A. (2009). Association of nicotine addiction and nicotine's actions with separate cingulate cortex functional circuits. *Arch Gen Psychiatry, 66*(4), 431-441. doi:10.1001/archgenpsychiatry.2009.2

Hooley, J. M., Gruber, S. A., Parker, H. A., Guillaumot, J., Rogowska, J., & Yurgelun-Todd, D. A. (2009). Cortico-limbic response to personally challenging emotional stimuli after complete recovery from depression. *Psychiatry Res, 172*(1), 83-91. doi:10.1016/j.pscychresns.2009.02.001

Horn, D. I., Yu, C., Steiner, J., Buchmann, J., Kaufmann, J., Osoba, A., . . . Walter, M. (2010). Glutamatergic and resting-state functional connectivity correlates of severity in major depression - the role of pregenual anterior cingulate cortex and anterior insula. *Front Syst Neurosci, 4*. doi:10.3389/fnsys.2010.00033

Howard, D. M., Adams, M. J., Shirali, M., Clarke, T.-K., Marioni, R. E., Davies, G., . . . andMe Research, T. (2018). Genome-wide association study of depression

phenotypes in UK Biobank identifies variants in excitatory synaptic pathways. *Nature Communications, 9*(1), 1470. doi:10.1038/s41467-018-03819-3

Howard, D. M., Folkersen, L., Coleman, J. R. I., Adams, M. J., Glanville, K., Werge, T., . . . McIntosh, A. M. (2020). Genetic stratification of depression in UK Biobank. *Translational Psychiatry, 10*(1), 163. doi:10.1038/s41398-020-0848-0

Huang, B. H., Hamer, M., Duncan, M. J., Cistulli, P. A., & Stamatakis, E. (2021). The bidirectional association between sleep and physical activity: A 6.9 years longitudinal analysis of 38,601 UK Biobank participants. *Prev Med, 143*, 106315. doi:10.1016/j.ypmed.2020.106315

Huang, C. C., Hsieh, W. J., Lee, P. L., Peng, L. N., Liu, L. K., Lee, W. J., . . . Lin, C. P. (2015). Age-related changes in resting-state networks of a large sample size of healthy elderly. *CNS Neurosci Ther, 21*(10), 817-825. doi:10.1111/cns.12396

Huttenlocher, P. R. (1979). Synaptic density in human frontal cortex - developmental changes and effects of aging. *Brain Research, 163*(2), 195-205. doi:10.1016/0006-8993(79)90349-4

Hyde, C. L., Nagle, M. W., Tian, C., Chen, X., Paciga, S. A., Wendland, J. R., . . . Winslow, A. R. (2016). Identification of 15 genetic loci associated with risk of major depression in individuals of European descent. *Nat Genet, 48*(9), 1031-1036. doi:10.1038/ng.3623

Iancu, I. V., Anton, G., Botezatu, A., Huica, I., Nastase, A., Socolov, D. G., . . . Plesa, A. (2017). LINC01101 and LINC00277 expression levels as novel factors in HPV-induced cervical neoplasia. *Journal of cellular and molecular medicine, 21*(12), 3787-3794. doi:10.1111/jcmm.13288

Jaehne, A., Unbehaun, T., Feige, B., Lutz, U. C., Batra, A., & Riemann, D. (2012). How smoking affects sleep: A polysomnographical analysis. *Sleep Medicine, 13*(10), 1286-1292. doi:https://doi.org/10.1016/j.sleep.2012.06.026

Janes, A. C., Nickerson, L. D., Frederick Bde, B., & Kaufman, M. J. (2012). Prefrontal and limbic resting state brain network functional connectivity differs between nicotine-dependent smokers and non-smoking controls. *Drug Alcohol Depend, 125*(3), 252-259. doi:10.1016/j.drugalcdep.2012.02.020

Jasinska, A. J., Zorick, T., Brody, A. L., & Stein, E. A. (2014). Dual role of nicotine in addiction and cognition: a review of neuroimaging studies in humans. *Neuropharmacology, 84*, 111-122. doi:10.1016/j.neuropharm.2013.02.015

Jiang, W., King, T. Z., & Turner, J. A. (2019a). Imaging Genetics Towards a Refined Diagnosis of Schizophrenia. *Frontiers in Psychiatry, 10*(494). doi:10.3389/fpsyt.2019.00494

Jiang, X., Shen, Y., Yao, J., Zhang, L., Xu, L., Feng, R., . . . Wang, J. (2019b). Connectome analysis of functional and structural hemispheric brain networks in major depressive disorder. *Translational Psychiatry, 9*(1), 136. doi:10.1038/s41398-019-0467-9

Jin, C., Gao, C., Chen, C., Ma, S., Netra, R., Wang, Y., . . . Li, D. (2011). A preliminary study of the dysregulation of the resting networks in first-episode medication-naive adolescent depression. *Neurosci Lett, 503*(2), 105-109. doi:10.1016/j.neulet.2011.08.017

Jockwitz, C., & Caspers, S. (2021). Resting-state networks in the course of aging—differential insights from studies across the lifespan vs. amongst the old. *Pflügers Archiv - European Journal of Physiology*. doi:10.1007/s00424-021-02520-7

Jones, D. T., Machulda, M. M., Vemuri, P., McDade, E. M., Zeng, G., Senjem, M. L., . . . Jack, C. R., Jr. (2011). Age-related changes in the default mode network are more advanced in Alzheimer disease. *Neurology, 77*(16), 1524-1531. doi:10.1212/WNL.0b013e318233b33d

Jones, S. E., van Hees, V. T., Mazzotti, D. R., Marques-Vidal, P., Sabia, S., van der Spek, A., . . . Wood, A. R. (2019). Genetic studies of accelerometer-based sleep measures yield new insights into human sleep behaviour. *Nature Communications, 10*(1), 1585. doi:10.1038/s41467-019-09576-1

Kaiser, R. H., Andrews-Hanna, J. R., Wager, T. D., & Pizzagalli, D. A. (2015). Large-Scale Network Dysfunction in Major Depressive Disorder: A Meta-analysis of Resting-State Functional Connectivity. *JAMA Psychiatry, 72*(6), 603-611. doi:10.1001/jamapsychiatry.2015.0071

Karssen, L. C., van Duijn, C. M., & Aulchenko, Y. S. (2016). The GenABEL Project for statistical genomics. *F1000Research, 5*, 914-914. doi:10.12688/f1000research.8733.1

Kawagoe, T., Onoda, K., & Yamaguchi, S. (2017). Associations among executive function, cardiorespiratory fitness, and brain network properties in older adults. *Scientific Reports, 7*, 40107-40107. doi:10.1038/srep40107

Kay, D. B., & Buysse, D. J. (2017). Hyperarousal and Beyond: New Insights to the Pathophysiology of Insomnia Disorder through Functional Neuroimaging Studies. *Brain Sci, 7*(3). doi:10.3390/brainsci7030023

Kendall, K. M., Rees, E., Escott-Price, V., Einon, M., Thomas, R., Hewitt, J., . . . Kirov, G. (2017). Cognitive Performance Among Carriers of Pathogenic Copy Number Variants: Analysis of 152,000 UK Biobank Subjects. *Biological psychiatry, 82*(2), 103-110. doi:10.1016/j.biopsych.2016.08.014

Kessler, R. C., Andrews, G., Mroczek, D., Ustun, B., & Wittchen, H.-U. (1998). The World Health Organization Composite International Diagnostic Interview short-form (CIDI-SF). *International Journal of Methods in Psychiatric Research, 7*(4), 171-185. doi:https://doi.org/10.1002/mpr.47

Khalsa, S., Mayhew, S. D., Przezdzik, I., Wilson, R., Hale, J., Goldstone, A., . . . Bagshaw, A. P. (2016). Variability in Cumulative Habitual Sleep Duration Predicts Waking Functional Connectivity. *Sleep, 39*(1), 87-95. doi:10.5665/sleep.5324

Khazaee, A., Ebrahimzadeh, A., & Babajani-Feremi, A. (2015). Identifying patients with Alzheimer's disease using resting-state fMRI and graph theory. *Clin Neurophysiol, 126*(11), 2132-2141. doi:10.1016/j.clinph.2015.02.060

Khazaie, H., Veronese, M., Noori, K., Emamian, F., Zarei, M., Ashkan, K., . . . Rosenzweig, I. (2017). Functional reorganization in obstructive sleep apnoea and insomnia: A systematic review of the resting-state fMRI. *Neuroscience & Biobehavioral Reviews, 77*, 219-231. doi:https://doi.org/10.1016/j.neubiorev.2017.03.013

Killgore, W. D. S., Schwab, Z. J., & Weiner, M. R. (2012). Self-reported nocturnal sleep duration is associated with next-day resting state functional connectivity. *NeuroReport, 23*(13). Retrieved from https://journals.lww.com/neuroreport/Fulltext/2012/09120/Self_reported_nocturnal_sleep_duration_is.1.aspx

Kim, W., Lee, J., Ha, J., Jo, K., Lim, D. J., Lee, J. M., . . . Kim, M. H. (2019). Association between Sleep Duration and Subclinical Thyroid Dysfunction Based on Nationally Representative Data. *J Clin Med, 8*(11). doi:10.3390/jcm8112010

Koch, W., Teipel, S., Mueller, S., Benninghoff, J., Wagner, M., Bokde, A. L., . . . Meindl, T. (2012). Diagnostic power of default mode network resting state fMRI in the detection of Alzheimer's disease. *Neurobiology of aging, 33*(3), 466-478. doi:10.1016/j.neurobiolaging.2010.04.013

Korgaonkar, M. S., Ram, K., Williams, L. M., Gatt, J. M., & Grieve, S. M. (2014). Establishing the resting state default mode network derived from functional magnetic resonance imaging tasks as an endophenotype: A twins study. *Hum Brain Mapp, 35*(8), 3893-3902. doi:10.1002/hbm.22446

Kuhn, M. (2015). *caret: Classification and Regression Training*.

Kumar, M., Modi, S., Rana, P., Kumar, P., Kanwar, R., Sekhri, T., . . . Khushu, S. (2018). Alteration in intrinsic and extrinsic functional connectivity of resting state networks associated with subclinical hypothyroid. *J Neuroendocrinol*. doi:10.1111/jne.12587

Lahut, S., Ömür, Ö., Uyan, Ö., Ağım, Z. S., Özoğuz, A., Parman, Y., . . . Başak, A. N. (2012). ATXN2 and its neighbouring gene SH2B3 are associated with increased ALS risk in the Turkish population. *PloS one, 7*(8), e42956-e42956. doi:10.1371/journal.pone.0042956

Lebedev, A., Westman, E., Simmons, A., Lebedeva, A., Siepel, F., Pereira, J., & Aarsland, D. (2014). Large-scale resting state network correlates of cognitive impairment in Parkinson's disease and related dopaminergic deficits. *Frontiers in systems neuroscience, 8*(45). doi:10.3389/fnsys.2014.00045

Lee, A., Shen, M., & Qiu, A. (2017). Psychiatric polygenic risk associates with cortical morphology and functional organization in aging. *Translational Psychiatry, 7*(12), 1276. doi:10.1038/s41398-017-0036-z

Lee, M. H., Smyser, C. D., & Shimony, J. S. (2013). Resting-state fMRI: a review of methods and clinical applications. *AJNR Am J Neuroradiol, 34*(10), 1866-1872. doi:10.3174/ajnr.A3263

Leistedt, S. J., Coumans, N., Dumont, M., Lanquart, J. P., Stam, C. J., & Linkowski, P. (2009). Altered sleep brain functional connectivity in acutely depressed patients. *Hum Brain Mapp, 30*(7), 2207-2219. doi:10.1002/hbm.20662

Leistedt, S. J., & Linkowski, P. (2013). Brain, networks, depression, and more. *Eur Neuropsychopharmacol, 23*(1), 55-62. doi:10.1016/j.euroneuro.2012.10.011

Levin, E. D., McClernon, F. J., & Rezvani, A. H. (2006). Nicotinic effects on cognitive function: behavioral characterization, pharmacological specification, and anatomic localization. *Psychopharmacology (Berl), 184*(3-4), 523-539. doi:10.1007/s00213-005-0164-7

Levine, D. A., Gross, A. L., Briceño, E. M., Tilton, N., Giordani, B. J., Sussman, J. B., . . . Galecki, A. T. (2021). Sex Differences in Cognitive Decline Among US Adults. *JAMA Netw Open, 4*(2), e210169. doi:10.1001/jamanetworkopen.2021.0169

Li, Z., Chen, R., Guan, M., Wang, E., Qian, T., Zhao, C., . . . Li, Y. (2018). Disrupted brain network topology in chronic insomnia disorder: A resting-state fMRI study. *NeuroImage: Clinical, 18*, 178-185. doi:https://doi.org/10.1016/j.nicl.2018.01.012

Liao, X., Vasilakos, A. V., & He, Y. (2017). Small-world human brain networks: perspectives and challenges. *Neuroscience & Biobehavioral Reviews, 77*, 286-300.

Liao, Y., Xie, L., Chen, X., Kelly, B. C., Qi, C., Pan, C., . . . Tang, J. (2019). Sleep quality in cigarette smokers and nonsmokers: findings from the general

population in central China. *BMC public health, 19*(1), 808-808. doi:10.1186/s12889-019-6929-4

Lim, J., Wu, W.-C., Wang, J., Detre, J. A., Dinges, D. F., & Rao, H. (2010). Imaging brain fatigue from sustained mental workload: an ASL perfusion study of the time-on-task effect. *NeuroImage, 49*(4), 3426-3435. doi:10.1016/j.neuroimage.2009.11.020

Lin, F., Wu, G., Zhu, L., & Lei, H. (2015). Altered brain functional networks in heavy smokers. *Addiction biology, 20*(4), 809-819.

Lin, Z., Ge, J., Wang, Z., Ren, J., Wang, X., Xiong, H., . . . Zhang, Q. (2017). Let-7e modulates the inflammatory response in vascular endothelial cells through ceRNA crosstalk. *Sci Rep, 7*, 42498. doi:10.1038/srep42498

Lithari, C., Klados, M. A., Pappas, C., Albani, M., Kapoukranidou, D., Kovatsi, L., . . . Papadelis, C. L. (2012). Alcohol Affects the Brain's Resting-State Network in Social Drinkers. *PloS one, 7*(10), e48641. doi:10.1371/journal.pone.0048641

Littman, A. J., Vitiello, M. V., Foster-Schubert, K., Ulrich, C. M., Tworoger, S. S., Potter, J. D., . . . McTiernan, A. (2007). Sleep, ghrelin, leptin and changes in body weight during a 1-year moderate-intensity physical activity intervention. *Int J Obes (Lond), 31*(3), 466-475. doi:10.1038/sj.ijo.0803438

Liu, H., Li, H., Wang, Y., & Lei, X. (2014). Enhanced brain small-worldness after sleep deprivation: a compensatory effect. *Journal of Sleep Research, 23*(5), 554-563. doi:10.1111/jsr.12147

Liu, Y., Chen, Y., Liang, X., Li, D., Zheng, Y., Zhang, H., . . . Qiu, S. (2020). Altered Resting-State Functional Connectivity of Multiple Networks and Disrupted Correlation With Executive Function in Major Depressive Disorder. *Frontiers in Neurology, 11*(272). doi:10.3389/fneur.2020.00272

Livingston, M., Callinan, S., Raninen, J., Pennay, A., & Dietze, P. M. (2018). Alcohol consumption trends in Australia: Comparing surveys and sales-based measures. *Drug Alcohol Rev, 37 Suppl 1*, S9-s14. doi:10.1111/dar.12588

Loh, P.-R., Bhatia, G., Gusev, A., Finucane, H. K., Bulik-Sullivan, B. K., Pollack, S. J., . . . Price, A. L. (2015). Contrasting genetic architectures of schizophrenia and other complex diseases using fast variance-components analysis. *Nature Genetics, 47*(12), 1385-1392. doi:10.1038/ng.3431

Loh, P.-R., Kichaev, G., Gazal, S., Schoech, A. P., & Price, A. L. (2018). Mixed-model association for biobank-scale datasets. *Nature Genetics, 50*(7), 906-908. doi:10.1038/s41588-018-0144-6

López-Otín, C., Blasco, M. A., Partridge, L., Serrano, M., & Kroemer, G. (2013). The hallmarks of aging. *Cell, 153*(6), 1194-1217. doi:10.1016/j.cell.2013.05.039

Lord, A., Horn, D., Breakspear, M., & Walter, M. (2012). Changes in community structure of resting state functional connectivity in unipolar depression. *PloS one, 7*(8), e41282. doi:10.1371/journal.pone.0041282

Lowsky, D. J., Olshansky, S. J., Bhattacharya, J., & Goldman, D. P. (2014). Heterogeneity in healthy aging. *J Gerontol A Biol Sci Med Sci, 69*(6), 640-649. doi:10.1093/gerona/glt162

Lubke, G. H., Hottenga, J. J., Walters, R., Laurin, C., de Geus, E. J., Willemsen, G., . . . Boomsma, D. I. (2012). Estimating the genetic variance of major depressive disorder due to all single nucleotide polymorphisms. *Biological psychiatry, 72*(8), 707-709. doi:10.1016/j.biopsych.2012.03.011

Luo, Q., Deng, Z., Qin, J., Wei, D., Cun, L., Qiu, J., . . . Xie, P. (2015). Frequency Dependant Topological Alterations of Intrinsic Functional Connectome in Major Depressive Disorder. *Scientific Reports, 5*(1), 9710. doi:10.1038/srep09710

Lv, H., Wang, Z., Tong, E., Williams, L. M., Zaharchuk, G., Zeineh, M., . . . Wintermark, M. (2018). Resting-State Functional MRI: Everything That Nonexperts Have Always Wanted to Know. *AJNR Am J Neuroradiol, 39*(8), 1390-1399. doi:10.3174/ajnr.A5527

Lysen, T. S., Zonneveld, H. I., Muetzel, R. L., Ikram, M. A., Luik, A. I., Vernooij, M. W., & Tiemeier, H. (2020). Sleep and resting-state functional magnetic resonance imaging connectivity in middle-aged adults and the elderly: A population-based study. *Journal of Sleep Research, 29*(5), e12999. doi:https://doi.org/10.1111/jsr.12999

Madden, K. M., Ashe, M. C., Lockhart, C., & Chase, J. M. (2014). Sedentary behavior and sleep efficiency in active community-dwelling older adults. *Sleep Sci, 7*(2), 82-88. doi:10.1016/j.slsci.2014.09.009

Maknojia, S., Churchill, N. W., Schweizer, T. A., & Graham, S. J. (2019). Resting State fMRI: Going Through the Motions. *Frontiers in Neuroscience, 13*(825). doi:10.3389/fnins.2019.00825

Manjunath, N. K., & Telles, S. (2005). Influence of Yoga and Ayurveda on self-rated sleep in a geriatric population. *Indian J Med Res, 121*(5), 683-690.

Manoliu, A., Meng, C., Brandl, F., Doll, A., Tahmasian, M., Scherr, M., . . . Sorg, C. (2014). Insular dysfunction within the salience network is associated with severity of symptoms and aberrant inter-network connectivity in major depressive disorder. *Frontiers in Human Neuroscience, 7*, 930-930. doi:10.3389/fnhum.2013.00930

Marchini, J., Cardon, L. R., Phillips, M. S., & Donnelly, P. (2004). The effects of human population structure on large genetic association studies. *Nat Genet, 36*(5), 512-517. doi:10.1038/ng1337

Markov, N. T., Ercsey-Ravasz, M., Lamy, C., Ribeiro Gomes, A. R., Magrou, L., Misery, P., . . . Kennedy, H. (2013). The role of long-range connections on the specificity of the macaque interareal cortical network. *Proceedings of the National Academy of Sciences, 110*(13), 5187. doi:10.1073/pnas.1218972110

Mayhew, A. J., & Meyre, D. (2017). Assessing the Heritability of Complex Traits in Humans: Methodological Challenges and Opportunities. *Curr Genomics, 18*(4), 332-340. doi:10.2174/1389202918666170307161450

Mayhugh, R. E., Moussa, M. N., Simpson, S. L., Lyday, R. G., Burdette, J. H., Porrino, L. J., & Laurienti, P. J. (2016). Moderate-Heavy Alcohol Consumption Lifestyle in Older Adults Is Associated with Altered Central Executive Network Community Structure during Cognitive Task. *PloS one, 11*(8), e0160214. doi:10.1371/journal.pone.0160214

McCarrey, A. C., An, Y., Kitner-Triolo, M. H., Ferrucci, L., & Resnick, S. M. (2016). Sex differences in cognitive trajectories in clinically normal older adults. *Psychology and Aging, 31*(2), 166-175. doi:10.1037/pag0000070

McCarthy, S., Das, S., Kretzschmar, W., Delaneau, O., Wood, A. R., Teumer, A., . . . Durbin, R. (2016). A reference panel of 64,976 haplotypes for genotype imputation. *Nat Genet, 48*(10), 1279-1283. doi:10.1038/ng.3643

McDonald, P. (2016). Ageing in Australia

Population changes and responses. In H. A. L. Kendig, P. McDonald, & J. Piggott (Eds.), *Population Ageing and Australia's Future* (pp. 65-84): ANU Press.

McGregor, K. M., Crosson, B., Krishnamurthy, L. C., Krishnamurthy, V., Hortman, K., Gopinath, K., . . . Nocera, J. R. (2018). Effects of a 12-Week Aerobic Spin Intervention on Resting State Networks in Previously Sedentary Older Adults. *Frontiers in psychology, 9*, 2376-2376. doi:10.3389/fpsyg.2018.02376

McKinnon, A. C., Duffy, S. L., Cross, N. E., Terpening, Z., Grunstein, R. R., Lagopoulos, J., . . . Naismith, S. L. (2017). Functional Connectivity in the Default Mode Network is Reduced in Association with Nocturnal Awakening in Mild Cognitive Impairment. *J Alzheimers Dis, 56*(4), 1373-1384. doi:10.3233/jad-160922

McKinnon, A. C., Lagopoulos, J., Terpening, Z., Grunstein, R., Hickie, I. B., Batchelor, J., . . . Naismith, S. L. (2016). Sleep disturbance in mild cognitive impairment is associated with alterations in the brain's default mode network. *Behav Neurosci, 130*(3), 305-315. doi:10.1037/bne0000137

McNamara, J. P., Wang, J., Holiday, D. B., Warren, J. Y., Paradoa, M., Balkhi, A. M., . . . McCrae, C. S. (2014). Sleep disturbances associated with cigarette smoking. *Psychol Health Med, 19*(4), 410-419. doi:10.1080/13548506.2013.832782

Medaglia, J. D. (2017). Graph Theoretic Analysis of Resting State Functional MR Imaging. *Neuroimaging clinics of North America, 27*(4), 593-607. doi:10.1016/j.nic.2017.06.008

Meier, J., Tewarie, P., Hillebrand, A., Douw, L., van Dijk, B. W., Stufflebeam, S. M., & Van Mieghem, P. (2016). A Mapping Between Structural and Functional Brain Networks. *Brain connectivity, 6*(4), 298-311. doi:10.1089/brain.2015.0408

Meng, C., Brandl, F., Tahmasian, M., Shao, J., Manoliu, A., Scherr, M., . . . Sorg, C. (2014). Aberrant topology of striatum's connectivity is associated with the number of episodes in depression. *Brain, 137*(Pt 2), 598-609. doi:10.1093/brain/awt290

Meunier, D., Achard, S., Morcom, A., & Bullmore, E. (2009). Age-related changes in modular organization of human brain functional networks. *Neuroimage, 44*(3), 715-723. doi:10.1016/j.neuroimage.2008.09.062

Miller, K. L., Alfaro-Almagro, F., Bangerter, N. K., Thomas, D. L., Yacoub, E., Xu, J., . . . Smith, S. M. (2016). Multimodal population brain imaging in the UK Biobank prospective epidemiological study. *Nature Neuroscience, 19*(11), 1523-1536. doi:10.1038/nn.4393

Miranda-Dominguez, O., Feczko, E., Grayson, D. S., Walum, H., Nigg, J. T., & Fair, D. A. (2018). Heritability of the human connectome: A connectotyping study. *Netw Neurosci, 2*(2), 175-199. doi:10.1162/netn_a_00029

Montembeault, M., Joubert, S., Doyon, J., Carrier, J., Gagnon, J. F., Monchi, O., . . . Brambati, S. M. (2012). The impact of aging on gray matter structural covariance networks. *Neuroimage, 63*(2), 754-759. doi:10.1016/j.neuroimage.2012.06.052

Munilla, J., Ortiz, A., Górriz, J. M., Ramírez, J., , t. A. s. D. N. I., Weiner, M. W., . . . Ravdin, L. (2017). Construction and Analysis of Weighted Brain Networks from SICE for the Study of Alzheimer's Disease. *Frontiers in Neuroinformatics, 11*(19). doi:10.3389/fninf.2017.00019

Murman, D. L. (2015). The Impact of Age on Cognition. *Seminars in hearing, 36*(3), 111-121. doi:10.1055/s-0035-1555115

Naqvi, N. H., & Bechara, A. (2010). The insula and drug addiction: an interoceptive view of pleasure, urges, and decision-making. *Brain Struct Funct, 214*(5-6), 435-450. doi:10.1007/s00429-010-0268-7

Neville, H., & Bavelier, D. (2000). Specificity and plasticity in neurocognitive development in humans. New cognitive neurosciences, 2nd edn, ed. by MS Gazzaniga, 83–98. In: Cambridge, MA: MIT Press.

Ng, K. K., Lo, J. C., Lim, J. K. W., Chee, M. W. L., & Zhou, J. (2016). Reduced functional segregation between the default mode network and the executive control network in healthy older adults: A longitudinal study. *NeuroImage, 133*, 321-330. doi:10.1016/j.neuroimage.2016.03.029

Nilsonne, G., Tamm, S., Schwarz, J., Almeida, R., Fischer, H., Kecklund, G., . . . Åkerstedt, T. (2017). Intrinsic brain connectivity after partial sleep deprivation in young and older adults: results from the Stockholm Sleepy Brain study. *Sci Rep, 7*(1), 9422. doi:10.1038/s41598-017-09744-7

Nyholt, D. R. (2004). A simple correction for multiple testing for single-nucleotide polymorphisms in linkage disequilibrium with each other. *American journal of human genetics, 74*(4), 765-769. doi:10.1086/383251

Ohno, M., Matsuzaki, J., Kawauchi, J., Aoki, Y., Miura, J., Takizawa, S., . . . Ochiya, T. (2019). Assessment of the Diagnostic Utility of Serum MicroRNA Classification in Patients With Diffuse Glioma. *JAMA Network Open, 2*(12), e1916953-e1916953. doi:10.1001/jamanetworkopen.2019.16953

Ong, J. L., Lau, T. Y., Lee, X. K., van Rijn, E., & Chee, M. W. L. (2020). A daytime nap restores hippocampal function and improves declarative learning. *Sleep, 43*(9). doi:10.1093/sleep/zsaa058

Onoda, K., Ishihara, M., & Yamaguchi, S. (2012). Decreased functional connectivity by aging is associated with cognitive decline. *J Cogn Neurosci, 24*(11), 2186-2198. doi:10.1162/jocn_a_00269

Otte, W. M., van Diessen, E., Paul, S., Ramaswamy, R., Subramanyam Rallabandi, V. P., Stam, C. J., & Roy, P. K. (2015). Aging alterations in whole-brain networks during adulthood mapped with the minimum spanning tree indices: the interplay of density, connectivity cost and life-time trajectory. *Neuroimage, 109*, 171-189. doi:10.1016/j.neuroimage.2015.01.011

Park, D. C., & Bischof, G. N. (2013). The aging mind: neuroplasticity in response to cognitive training. *Dialogues in clinical neuroscience, 15*(1), 109-119. doi:10.31887/DCNS.2013.15.1/dpark

Parkes, L., Fulcher, B., Yücel, M., & Fornito, A. (2018). An evaluation of the efficacy, reliability, and sensitivity of motion correction strategies for resting-state functional MRI. *NeuroImage, 171*, 415-436. doi:https://doi.org/10.1016/j.neuroimage.2017.12.073

Pasca di Magliano, M., Di Lauro, R., & Zannini, M. (2000). Pax8 has a key role in thyroid cell differentiation. *Proc Natl Acad Sci U S A, 97*(24), 13144-13149. doi:10.1073/pnas.240336397

Patterson, F., Grandner, M. A., Malone, S. K., Rizzo, A., Davey, A., & Edwards, D. G. (2019). Sleep as a Target for Optimized Response to Smoking Cessation Treatment. *Nicotine & tobacco research : official journal of the Society for Research on Nicotine and Tobacco, 21*(2), 139-148. doi:10.1093/ntr/ntx236

Perdry, H., Dandine-Roulland, C., Bandyopadhyay, D., Kettner, L. . (2020). Gaston: Genetic Data Handling (QC, GRM, LD, PCA) & Linear Mixed Models. Retrieved from https://CRAN.R-project.org/package=gaston

Perry, A., Wen, W., Lord, A., Thalamuthu, A., Roberts, G., Mitchell, P. B., . . . Breakspear, M. (2015). The organisation of the elderly connectome. *Neuroimage, 114*, 414-426. doi:10.1016/j.neuroimage.2015.04.009

Persson, J., Pudas, S., Nilsson, L. G., & Nyberg, L. (2014). Longitudinal assessment of default-mode brain function in aging. *Neurobiology of aging, 35*(9), 2107-2117. doi:10.1016/j.neurobiolaging.2014.03.012

Pervaiz, U., Vidaurre, D., Woolrich, M. W., & Smith, S. M. (2020). Optimising network modelling methods for fMRI. *NeuroImage, 211*, 116604-116604. doi:10.1016/j.neuroimage.2020.116604

Petrides, M., Alivisatos, B., & Frey, S. (2002). Differential activation of the human orbital, mid-ventrolateral, and mid-dorsolateral prefrontal cortex during the processing of visual stimuli. *Proceedings of the National Academy of Sciences, 99*(8), 5649. doi:10.1073/pnas.072092299

Picard, F., Sadaghiani, S., Leroy, C., Courvoisier, D. S., Maroy, R., & Bottlaender, M. (2013). High density of nicotinic receptors in the cingulo-insular network. *NeuroImage, 79*, 42-51. doi:10.1016/j.neuroimage.2013.04.074

Plautz, E. J., Milliken, G. W., & Nudo, R. J. (2000). Effects of repetitive motor training on movement representations in adult squirrel monkeys: role of use versus learning. *Neurobiology of learning and memory, 74*(1), 27-55.

Poorthuis, R. B., Goriounova, N. A., Couey, J. J., & Mansvelder, H. D. (2009). Nicotinic actions on neuronal networks for cognition: general principles and long-term consequences. *Biochemical pharmacology, 78*(7), 668-676. doi:10.1016/j.bcp.2009.04.031

Power, J. D., Fair, D. A., Schlaggar, B. L., & Petersen, S. E. (2010). The development of human functional brain networks. *Neuron, 67*(5), 735-748. doi:10.1016/j.neuron.2010.08.017

Power, J. D., Plitt, M., Laumann, T. O., & Martin, A. (2017). Sources and implications of whole-brain fMRI signals in humans. *NeuroImage, 146*, 609-625. doi:10.1016/j.neuroimage.2016.09.038

Pruim, R. J., Welch, R. P., Sanna, S., Teslovich, T. M., Chines, P. S., Gliedt, T. P., . . . Willer, C. J. (2010). LocusZoom: regional visualization of genome-wide association scan results. *Bioinformatics, 26*(18), 2336-2337. doi:10.1093/bioinformatics/btq419

Raichle, M. E. (2015). The Brain's Default Mode Network. *Annual Review of Neuroscience, 38*(1), 433-447. doi:10.1146/annurev-neuro-071013-014030

Ray, D., & Boehnke, M. (2018). Methods for meta-analysis of multiple traits using GWAS summary statistics. *Genetic Epidemiology, 42*(2), 134-145. doi:10.1002/gepi.22105

Reineberg, A. E., Hatoum, A. S., Hewitt, J. K., Banich, M. T., & Friedman, N. P. (2020). Genetic and Environmental Influence on the Human Functional Connectome. *Cereb Cortex, 30*(4), 2099-2113. doi:10.1093/cercor/bhz225

Rentzeperis, I., & van Leeuwen, C. (2021). Adaptive Rewiring in Weighted Networks Shows Specificity, Robustness, and Flexibility. *Frontiers in Systems Neuroscience, 15*(13). doi:10.3389/fnsys.2021.580569

Reyes, P., Ortega-Merchan, M. P., Rueda, A., Uriza, F., Santamaria-García, H., Rojas-Serrano, N., . . . Matallana, D. (2018). Functional Connectivity Changes in Behavioral, Semantic, and Nonfluent Variants of Frontotemporal Dementia. *Behavioural neurology, 2018*, 9684129-9684129. doi:10.1155/2018/9684129

Riedel, B. W., Durrence, H. H., Lichstein, K. L., Taylor, D. J., & Bush, A. J. (2004). The relation between smoking and sleep: the influence of smoking level, health,

and psychological variables. *Behav Sleep Med, 2*(1), 63-78. doi:10.1207/s15402010bsm0201_6

Ripke, S., Wray, N. R., Lewis, C. M., Hamilton, S. P., Weissman, M. M., Breen, G., . . . Sullivan, P. F. (2013). A mega-analysis of genome-wide association studies for major depressive disorder. *Mol Psychiatry, 18*(4), 497-511. doi:10.1038/mp.2012.21

Ritchie, S. J., Cox, S. R., Shen, X., Lombardo, M. V., Reus, L. M., Alloza, C., . . . Deary, I. J. (2018). Sex Differences in the Adult Human Brain: Evidence from 5216 UK Biobank Participants. *Cereb Cortex, 28*(8), 2959-2975. doi:10.1093/cercor/bhy109

Robinson, H., Calamia, M., Gläscher, J., Bruss, J., & Tranel, D. (2014). Neuroanatomical correlates of executive functions: a neuropsychological approach using the EXAMINER battery. *Journal of the International Neuropsychological Society : JINS, 20*(1), 52-63. doi:10.1017/S135561771300060X

Rosazza, C., & Minati, L. (2011). Resting-state brain networks: literature review and clinical applications. *Neurol Sci, 32*(5), 773-785. doi:10.1007/s10072-011-0636-y

Rubinov, M., & Sporns, O. (2010). Complex network measures of brain connectivity: Uses and interpretations. *NeuroImage, 52*(3), 1059-1069. doi:https://doi.org/10.1016/j.neuroimage.2009.10.003

Ruiz-Llorente, S., Carrillo Santa de Pau, E., Sastre-Perona, A., Montero-Conde, C., Gómez-López, G., Fagin, J. A., . . . Santisteban, P. (2012). Genome-wide analysis of Pax8 binding provides new insights into thyroid functions. *BMC genomics, 13*, 147-147. doi:10.1186/1471-2164-13-147

Sacchet, M. D., Prasad, G., Foland-Ross, L. C., Thompson, P. M., & Gotlib, I. H. (2015). Support vector machine classification of major depressive disorder using diffusion-weighted neuroimaging and graph theory. *Front Psychiatry, 6*, 21. doi:10.3389/fpsyt.2015.00021

Saint-Mleux, B., Eggermann, E., Bisetti, A., Bayer, L., Machard, D., Jones, B. E., . . . Serafin, M. (2004). Nicotinic Enhancement of the Noradrenergic Inhibition of Sleep-Promoting Neurons in the Ventrolateral Preoptic Area. *The Journal of Neuroscience, 24*(1), 63. doi:10.1523/JNEUROSCI.0232-03.2004

Sala-Llonch, R., Junqué, C., Arenaza-Urquijo, E. M., Vidal-Piñeiro, D., Valls-Pedret, C., Palacios, E. M., . . . Bartrés-Faz, D. (2014). Changes in whole-brain functional networks and memory performance in aging. *Neurobiology of aging, 35*(10), 2193-2202. doi:10.1016/j.neurobiolaging.2014.04.007

Salimi-Khorshidi, G., Douaud, G., Beckmann, C. F., Glasser, M. F., Griffanti, L., & Smith, S. M. (2014). Automatic denoising of functional MRI data: combining independent component analysis and hierarchical fusion of classifiers. *Neuroimage, 90*, 449-468. doi:10.1016/j.neuroimage.2013.11.046

Sämann, P. G., Tully, C., Spoormaker, V. I., Wetter, T. C., Holsboer, F., Wehrle, R., & Czisch, M. (2010). Increased sleep pressure reduces resting state functional connectivity. *Magma, 23*(5-6), 375-389. doi:10.1007/s10334-010-0213-z

Sambataro, F., Wolf, N. D., Pennuto, M., Vasic, N., & Wolf, R. C. (2014). Revisiting default mode network function in major depression: evidence for disrupted subsystem connectivity. *Psychol Med, 44*(10), 2041-2051. doi:10.1017/s0033291713002596

Sánchez-Castañeda, C., de Pasquale, F., Caravasso, C. F., Marano, M., Maffi, S., Migliore, S., . . . Squitieri, F. (2017). Resting-state connectivity and modulated

somatomotor and default-mode networks in Huntington disease. *CNS Neuroscience & Therapeutics, 23*(6), 488-497. doi:https://doi.org/10.1111/cns.12701

Schaefer, A., Kong, R., Gordon, E. M., Laumann, T. O., Zuo, X. N., Holmes, A. J., . . . Yeo, B. T. T. (2018). Local-Global Parcellation of the Human Cerebral Cortex from Intrinsic Functional Connectivity MRI. *Cereb Cortex, 28*(9), 3095-3114. doi:10.1093/cercor/bhx179

Scheinost, D., Finn, E. S., Tokoglu, F., Shen, X., Papademetris, X., Hampson, M., & Constable, R. T. (2015). Sex differences in normal age trajectories of functional brain networks. *Hum Brain Mapp, 36*(4), 1524-1535. doi:10.1002/hbm.22720

Schmitt, A., Upadhyay, N., Martin, J. A., Rojas, S., Strüder, H. K., & Boecker, H. (2019). Modulation of Distinct Intrinsic Resting State Brain Networks by Acute Exercise Bouts of Differing Intensity. *Brain plasticity (Amsterdam, Netherlands), 5*(1), 39-55. doi:10.3233/BPL-190081

Schulte, M. H., Cousijn, J., den Uyl, T. E., Goudriaan, A. E., van den Brink, W., Veltman, D. J., . . . Wiers, R. W. (2014). Recovery of neurocognitive functions following sustained abstinence after substance dependence and implications for treatment. *Clin Psychol Rev, 34*(7), 531-550. doi:10.1016/j.cpr.2014.08.002

Seeley, W. W., Menon, V., Schatzberg, A. F., Keller, J., Glover, G. H., Kenna, H., . . . Greicius, M. D. (2007). Dissociable intrinsic connectivity networks for salience processing and executive control. *The Journal of neuroscience : the official journal of the Society for Neuroscience, 27*(9), 2349-2356. doi:10.1523/jneurosci.5587-06.2007

Seidler, R. D., Bernard, J. A., Burutolu, T. B., Fling, B. W., Gordon, M. T., Gwin, J. T., . . . Lipps, D. B. (2010). Motor control and aging: links to age-related brain

structural, functional, and biochemical effects. *Neuroscience and biobehavioral reviews, 34*(5), 721-733. doi:10.1016/j.neubiorev.2009.10.005

Sheline, Y. I., Price, J. L., Yan, Z., & Mintun, M. A. (2010). Resting-state functional MRI in depression unmasks increased connectivity between networks via the dorsal nexus. *Proc Natl Acad Sci U S A, 107*(24), 11020-11025. doi:10.1073/pnas.1000446107

Shen, J., Qin, W., Xu, Q., Xu, L., Xu, J., Zhang, P., . . . Yu, C. (2017). Modulation of APOE and SORL1 genes on hippocampal functional connectivity in healthy young adults. *Brain Struct Funct, 222*(6), 2877-2889. doi:10.1007/s00429-017-1377-3

Shen, W., Tu, Y., Gollub, R. L., Ortiz, A., Napadow, V., Yu, S., . . . Kong, J. (2019). Visual network alterations in brain functional connectivity in chronic low back pain: A resting state functional connectivity and machine learning study. *NeuroImage: Clinical, 22*, 101775. doi:https://doi.org/10.1016/j.nicl.2019.101775

Shen, X., Howard, D. M., Adams, M. J., Hill, W. D., Clarke, T.-K., Adams, M. J., . . . Major Depressive Disorder Working Group of the Psychiatric Genomics, C. (2020). A phenome-wide association and Mendelian Randomisation study of polygenic risk for depression in UK Biobank. *Nature Communications, 11*(1), 2301. doi:10.1038/s41467-020-16022-0

Shen, Z., Huang, P., Qian, W., Wang, C., Yu, H., Yang, Y., & Zhang, M. (2016). Severity of dependence modulates smokers' functional connectivity in the reward circuit: a preliminary study. *Psychopharmacology (Berl), 233*(11), 2129-2137. doi:10.1007/s00213-016-4262-5

Shi, L., Chen, S. J., Ma, M. Y., Bao, Y. P., Han, Y., Wang, Y. M., . . . Lu, L. (2018). Sleep disturbances increase the risk of dementia: A systematic review and meta-analysis. *Sleep Med Rev, 40*, 4-16. doi:10.1016/j.smrv.2017.06.010

Shimada, A., & Hasegawa-Ishii, S. (2011). Senescence-accelerated Mice (SAMs) as a Model for Brain Aging and Immunosenescence. *Aging and disease, 2*(5), 414-435. Retrieved from https://pubmed.ncbi.nlm.nih.gov/22396891

https://www.ncbi.nlm.nih.gov/pmc/articles/PMC3295080/

Siman-Tov, T., Bosak, N., Sprecher, E., Paz, R., Eran, A., Aharon-Peretz, J., & Kahn, I. (2017). Early Age-Related Functional Connectivity Decline in High-Order Cognitive Networks. *Frontiers in Aging Neuroscience, 8*(330). doi:10.3389/fnagi.2016.00330

Sinclair, B., Hansell, N. K., Blokland, G. A., Martin, N. G., Thompson, P. M., Breakspear, M., . . . McMahon, K. L. (2015). Heritability of the network architecture of intrinsic brain functional connectivity. *Neuroimage, 121*, 243-252. doi:10.1016/j.neuroimage.2015.07.048

Sjoerds, Z., Stufflebeam, S. M., Veltman, D. J., Van den Brink, W., Penninx, B. W. J. H., & Douw, L. (2017). Loss of brain graph network efficiency in alcohol dependence. *Addiction biology, 22*(2), 523-534. doi:https://doi.org/10.1111/adb.12346

Smith, S., Vidaurre, D., Glasser, M., Winkler, A., McCarthy, P., Robinson, E., & Van Essen, D. (2016). Second beta-release of the HCP Functional Connectivity MegaTrawl. *See https://db. humanconnectome. org/megatrawl/HCP820_MegaTrawl_April2016. pdf*.

Smitha, K. A., Akhil Raja, K., Arun, K. M., Rajesh, P. G., Thomas, B., Kapilamoorthy, T. R., & Kesavadas, C. (2017). Resting state fMRI: A review on methods in

resting state connectivity analysis and resting state networks. *Neuroradiol J, 30*(4), 305-317. doi:10.1177/1971400917697342

Song, J., Birn, R. M., Boly, M., Meier, T. B., Nair, V. A., Meyerand, M. E., & Prabhakaran, V. (2014). Age-related reorganizational changes in modularity and functional connectivity of human brain networks. *Brain Connect, 4*(9), 662-676. doi:10.1089/brain.2014.0286

Song, L., Lei, J., Jiang, K., Lei, Y., Tang, Y., Zhu, J., . . . Tang, H. (2019). The Association Between Subclinical Hypothyroidism and Sleep Quality: A Population-Based Study. *Risk management and healthcare policy, 12*, 369-374. doi:10.2147/RMHP.S234552

Song, Z., Chen, J., Wen, Z., & Zhang, L. (2020). Abnormal functional connectivity and effective connectivity between the default mode network and attention networks in patients with alcohol-use disorder. *Acta Radiologica, 62*(2), 251-259. doi:10.1177/0284185120923270

Sorg, C., Riedl, V., Mühlau, M., Calhoun, V. D., Eichele, T., Läer, L., . . . Wohlschläger, A. M. (2007). Selective changes of resting-state networks in individuals at risk for Alzheimer's disease. *Proc Natl Acad Sci U S A, 104*(47), 18760-18765. doi:10.1073/pnas.0708803104

Speed, D., Cai, N., the, U. C., Johnson, M. R., Nejentsev, S., & Balding, D. J. (2017). Reevaluation of SNP heritability in complex human traits. *Nature Genetics, 49*, 986. doi:10.1038/ng.3865

https://www.nature.com/articles/ng.3865#supplementary-information

Spira, A. P., Chen-Edinboro, L. P., Wu, M. N., & Yaffe, K. (2014). Impact of sleep on the risk of cognitive decline and dementia. *Curr Opin Psychiatry, 27*(6), 478-483. doi:10.1097/yco.0000000000000106

Sporns, O. (2018). Graph theory methods: applications in brain networks. *Dialogues in clinical neuroscience, 20*(2), 111-121. doi:10.31887/DCNS.2018.20.2/osporns

Spreng, R. N., & Schacter, D. L. (2012). Default network modulation and large-scale network interactivity in healthy young and old adults. *Cereb Cortex, 22*(11), 2610-2621. doi:10.1093/cercor/bhr339

Spreng, R. N., Shoemaker, L., & Turner, G. R. (2017). Chapter 8 - Executive Functions and Neurocognitive Aging. In E. Goldberg (Ed.), *Executive Functions in Health and Disease* (pp. 169-196). San Diego: Academic Press.

Stange, J. P., Bessette, K. L., Jenkins, L. M., Peters, A. T., Feldhaus, C., Crane, N. A., . . . Langenecker, S. A. (2017). Attenuated intrinsic connectivity within cognitive control network among individuals with remitted depression: Temporal stability and association with negative cognitive styles. *Hum Brain Mapp, 38*(6), 2939-2954. doi:10.1002/hbm.23564

Sterniczuk, R., Theou, O., Rusak, B., & Rockwood, K. (2013). Sleep disturbance is associated with incident dementia and mortality. *Curr Alzheimer Res, 10*(7), 767-775. doi:10.2174/15672050113109990134

Stoykova, A., & Gruss, P. (1994). Roles of Pax-genes in developing and adult brain as suggested by expression patterns. *J Neurosci, 14*(3 Pt 2), 1395-1412. doi:10.1523/jneurosci.14-03-01395.1994

Stumme, J., Jockwitz, C., Hoffstaedter, F., Amunts, K., & Caspers, S. (2020). Functional network reorganization in older adults: Graph-theoretical analyses of age, cognition and sex. *NeuroImage, 214*, 116756. doi:https://doi.org/10.1016/j.neuroimage.2020.116756

Sudlow, C., Gallacher, J., Allen, N., Beral, V., Burton, P., Danesh, J., . . . Collins, R. (2015). UK biobank: an open access resource for identifying the causes of a

wide range of complex diseases of middle and old age. *PLoS Med, 12*(3), e1001779. doi:10.1371/journal.pmed.1001779

Sullivan, P. F., Neale, M. C., & Kendler, K. S. (2000). Genetic epidemiology of major depression: review and meta-analysis. *Am J Psychiatry, 157*(10), 1552-1562. doi:10.1176/appi.ajp.157.10.1552

Supekar, K., Menon, V., Rubin, D., Musen, M., & Greicius, M. D. (2008). Network analysis of intrinsic functional brain connectivity in Alzheimer's disease. *PLoS Comput Biol, 4*(6), e1000100. doi:10.1371/journal.pcbi.1000100

Sur, M., & Leamey, C. A. (2001). Development and plasticity of cortical areas and networks. *Nature Reviews Neuroscience, 2*(4), 251-262.

Sutherland, M. T., McHugh, M. J., Pariyadath, V., & Stein, E. A. (2012). Resting state functional connectivity in addiction: Lessons learned and a road ahead. *NeuroImage, 62*(4), 2281-2295. doi:10.1016/j.neuroimage.2012.01.117

Swan, G. E., & Lessov-Schlaggar, C. N. (2007). The effects of tobacco smoke and nicotine on cognition and the brain. *Neuropsychol Rev, 17*(3), 259-273. doi:10.1007/s11065-007-9035-9

Sweitzer, M. M., Geier, C. F., Addicott, M. A., Denlinger, R., Raiff, B. R., Dallery, J., . . . Donny, E. C. (2016). Smoking Abstinence-Induced Changes in Resting State Functional Connectivity with Ventral Striatum Predict Lapse During a Quit Attempt. *Neuropsychopharmacology, 41*(10), 2521-2529. doi:10.1038/npp.2016.56

Tahmasian, M., Knight, D. C., Manoliu, A., Schwerthöffer, D., Scherr, M., Meng, C., . . . Sorg, C. (2013). Aberrant intrinsic connectivity of hippocampus and amygdala overlap in the fronto-insular and dorsomedial-prefrontal cortex in

major depressive disorder. *Front Hum Neurosci, 7*, 639. doi:10.3389/fnhum.2013.00639

Tanabe, J., Nyberg, E., Martin, L. F., Martin, J., Cordes, D., Kronberg, E., & Tregellas, J. R. (2011). Nicotine effects on default mode network during resting state. *Psychopharmacology (Berl), 216*(2), 287-295. doi:10.1007/s00213-011-2221-8

Tang, Y., Jiao, X., Wang, J., Zhu, T., Zhou, J., Qian, Z., . . . Wang, J. (2019). Dynamic Functional Connectivity Within the Fronto-Limbic Network Induced by Intermittent Theta-Burst Stimulation: A Pilot Study. *Frontiers in Neuroscience, 13*(944). doi:10.3389/fnins.2019.00944

R Core Team (2020). R: A language and environment for statistical computing. R Foundation for Statistical Computing, Vienna, Austria.

Thirion, B., Varoquaux, G., Dohmatob, E., & Poline, J. B. (2014). Which fMRI clustering gives good brain parcellations? *Front Neurosci, 8*, 167. doi:10.3389/fnins.2014.00167

Thompson, P. M., Ge, T., Glahn, D. C., Jahanshad, N., & Nichols, T. E. (2013). Genetics of the connectome. *Neuroimage, 80*, 475-488. doi:10.1016/j.neuroimage.2013.05.013

Tian, L., Wang, J., Yan, C., & He, Y. (2011). Hemisphere- and gender-related differences in small-world brain networks: a resting-state functional MRI study. *NeuroImage, 54*(1), 191-202. doi:10.1016/j.neuroimage.2010.07.066

Tingley, D., Yamamoto, T., Hirose, K., Keele, L., & Imai, K. (2014). mediation: R Package for Causal Mediation Analysis. *2014, 59*(5), 38. doi:10.18637/jss.v059.i05

Tomasi, D., & Volkow, N. D. (2012a). Gender differences in brain functional connectivity density. *Hum Brain Mapp, 33*(4), 849-860. doi:10.1002/hbm.21252

Tomasi, D., & Volkow, N. D. (2012b). Laterality patterns of brain functional connectivity: gender effects. *Cerebral cortex (New York, N.Y. : 1991), 22*(6), 1455-1462. doi:10.1093/cercor/bhr230

Tozzi, L., Carballedo, A., Lavelle, G., Doolin, K., Doyle, M., Amico, F., . . . Frodl, T. (2016). Longitudinal functional connectivity changes correlate with mood improvement after regular exercise in a dose-dependent fashion. *Eur J Neurosci, 43*(8), 1089-1096. doi:10.1111/ejn.13222

United Nations Department of Economic and Social Affairs, P. D. (2019). World Population Ageing 2019 (ST/ESA/SER.A/444).

van den Heuvel, M. P., de Lange, S. C., Zalesky, A., Seguin, C., Yeo, B. T. T., & Schmidt, R. (2017). Proportional thresholding in resting-state fMRI functional connectivity networks and consequences for patient-control connectome studies: Issues and recommendations. *NeuroImage, 152*, 437-449. doi:10.1016/j.neuroimage.2017.02.005

van den Heuvel, M. P., & Hulshoff Pol, H. E. (2010). Exploring the brain network: A review on resting-state fMRI functional connectivity. *European Neuropsychopharmacology, 20*(8), 519-534. doi:https://doi.org/10.1016/j.euroneuro.2010.03.008

van den Heuvel, M. P., Stam, C. J., Kahn, R. S., & Hulshoff Pol, H. E. (2009). Efficiency of functional brain networks and intellectual performance. *The Journal of neuroscience : the official journal of the Society for Neuroscience, 29*(23), 7619-7624. doi:10.1523/jneurosci.1443-09.2009

van Hees, V. T., Fang, Z., Langford, J., Assah, F., Mohammad, A., da Silva, I. C., . . . Brage, S. (2014). Autocalibration of accelerometer data for free-living physical activity assessment using local gravity and temperature: an evaluation on four

continents. *J Appl Physiol (1985), 117*(7), 738-744. doi:10.1152/japplphysiol.00421.2014

van Hees, V. T., Sabia, S., Jones, S. E., Wood, A. R., Anderson, K. N., Kivimäki, M., . . . Weedon, M. N. (2018). Estimating sleep parameters using an accelerometer without sleep diary. *Scientific Reports, 8*(1), 12975. doi:10.1038/s41598-018-31266-z

van Holst, R. J., & Schilt, T. (2011). Drug-related decrease in neuropsychological functions of abstinent drug users. *Curr Drug Abuse Rev, 4*(1), 42-56. doi:10.2174/1874473711104010042

Varangis, E., Habeck, C. G., Razlighi, Q. R., & Stern, Y. (2019). The Effect of Aging on Resting State Connectivity of Predefined Networks in the Brain. *Frontiers in Aging Neuroscience, 11*(234). doi:10.3389/fnagi.2019.00234

Veatch, O. J., Keenan, B. T., Gehrman, P. R., Malow, B. A., & Pack, A. I. (2017). Pleiotropic genetic effects influencing sleep and neurological disorders. *The Lancet. Neurology, 16*(2), 158-170. doi:10.1016/S1474-4422(16)30339-8

Vecchio, F., Miraglia, F., & Maria Rossini, P. (2017). Connectome: Graph theory application in functional brain network architecture. *Clinical Neurophysiology Practice, 2*, 206-213. doi:https://doi.org/10.1016/j.cnp.2017.09.003

Vemuri, P., Jones, D. T., & Jack, C. R., Jr. (2012). Resting state functional MRI in Alzheimer's Disease. *Alzheimers Res Ther, 4*(1), 2. doi:10.1186/alzrt100

Vergara, V. M., Liu, J., Claus, E. D., Hutchison, K., & Calhoun, V. (2017). Alterations of resting state functional network connectivity in the brain of nicotine and alcohol users. *NeuroImage, 151*, 45-54. doi:10.1016/j.neuroimage.2016.11.012

Vinson, D. C., Manning, B. K., Galliher, J. M., Dickinson, L. M., Pace, W. D., & Turner, B. J. (2010). Alcohol and sleep problems in primary care patients: a

report from the AAFP National Research Network. *Ann Fam Med, 8*(6), 484-492. doi:10.1370/afm.1175

Visscher, P. M., Hill, W. G., & Wray, N. R. (2008). Heritability in the genomics era — concepts and misconceptions. *Nature Reviews Genetics, 9*, 255. doi:10.1038/nrg2322

Voss, M. W., Weng, T. B., Burzynska, A. Z., Wong, C. N., Cooke, G. E., Clark, R., . . . Kramer, A. F. (2016). Fitness, but not physical activity, is related to functional integrity of brain networks associated with aging. *NeuroImage, 131*, 113-125. doi:https://doi.org/10.1016/j.neuroimage.2015.10.044

Wang, J., Wang, L., Zang, Y., Yang, H., Tang, H., Gong, Q., . . . He, Y. (2009). Parcellation-dependent small-world brain functional networks: a resting-state fMRI study. *Hum Brain Mapp, 30*(5), 1511-1523. doi:10.1002/hbm.20623

Wang, J., Zuo, X., & He, Y. (2010a). Graph-based network analysis of resting-state functional MRI. *Frontiers in Systems Neuroscience, 4*(16). doi:10.3389/fnsys.2010.00016

Wang, J., Zuo, X., & He, Y. (2010b). Graph-based network analysis of resting-state functional MRI. *Front Syst Neurosci, 4*, 16. doi:10.3389/fnsys.2010.00016

Wang, L., Hermens, D. F., Hickie, I. B., & Lagopoulos, J. (2012). A systematic review of resting-state functional-MRI studies in major depression. *J Affect Disord, 142*(1-3), 6-12. doi:10.1016/j.jad.2012.04.013

Wang, L., Li, Y., Metzak, P., He, Y., & Woodward, T. S. (2010c). Age-related changes in topological patterns of large-scale brain functional networks during memory encoding and recognition. *Neuroimage, 50*(3), 862-872. doi:10.1016/j.neuroimage.2010.01.044

Wang, Y. M., Chen, H. G., Song, M., Xu, S. J., Yu, L. L., Wang, L., . . . Lu, L. (2016). Prevalence of insomnia and its risk factors in older individuals: a community-based study in four cities of Hebei Province, China. *Sleep Med, 19*, 116-122. doi:10.1016/j.sleep.2015.10.018

Watanabe, K., Taskesen, E., van Bochoven, A., & Posthuma, D. (2017). Functional mapping and annotation of genetic associations with FUMA. *Nature Communications, 8*(1), 1826. doi:10.1038/s41467-017-01261-5

Weiland, B. J., Sabbineni, A., Calhoun, V. D., Welsh, R. C., Bryan, A. D., Jung, R. E., . . . Hutchison, K. E. (2014). Reduced left executive control network functional connectivity is associated with alcohol use disorders. *Alcohol Clin Exp Res, 38*(9), 2445-2453. doi:10.1111/acer.12505

Weng, T. B., Pierce, G. L., Darling, W. G., Falk, D., Magnotta, V. A., & Voss, M. W. (2017). The Acute Effects of Aerobic Exercise on the Functional Connectivity of Human Brain Networks. *Brain plasticity (Amsterdam, Netherlands), 2*(2), 171-190. doi:10.3233/BPL-160039

Wig, G. S. (2017). Segregated Systems of Human Brain Networks. *Trends in Cognitive Sciences, 21*(12), 981-996. doi:https://doi.org/10.1016/j.tics.2017.09.006

Wilcox, C. E., Dekonenko, C. J., Mayer, A. R., Bogenschutz, M. P., & Turner, J. A. (2014). Cognitive control in alcohol use disorder: deficits and clinical relevance. *Reviews in the neurosciences, 25*(1), 1-24. doi:10.1515/revneuro-2013-0054

Williams, G. R. (2008). Neurodevelopmental and neurophysiological actions of thyroid hormone. *J Neuroendocrinol, 20*(6), 784-794. doi:10.1111/j.1365-2826.2008.01733.x

Wolkove, N., Elkholy, O., Baltzan, M., & Palayew, M. (2007). Sleep and aging: 1. Sleep disorders commonly found in older people. *Canadian Medical Association Journal, 176*(9), 1299. doi:10.1503/cmaj.060792

Won, J., Alfini, A. J., Weiss, L. R., Michelson, C. S., Callow, D. D., Ranadive, S. M., . . . Smith, J. C. (2019). Semantic Memory Activation After Acute Exercise in Healthy Older Adults. *Journal of the International Neuropsychological Society : JINS, 25*(6), 557-568. doi:10.1017/s1355617719000171

World Health, O. (2015). *World report on ageing and health*. Geneva: World Health Organization.

Wray, N. R., Ripke, S., Mattheisen, M., Trzaskowski, M., Byrne, E. M., Abdellaoui, A., . . . the Major Depressive Disorder Working Group of the Psychiatric Genomics, C. (2018). Genome-wide association analyses identify 44 risk variants and refine the genetic architecture of major depression. *Nature Genetics, 50*(5), 668-681. doi:10.1038/s41588-018-0090-3

Wu, K., Taki, Y., Sato, K., Kinomura, S., Goto, R., Okada, K., . . . Fukuda, H. (2012). Age-related changes in topological organization of structural brain networks in healthy individuals. *Hum Brain Mapp, 33*(3), 552-568. doi:10.1002/hbm.21232

Wu, Z., Chen, F., Yu, F., Wang, Y., & Guo, Z. (2018). A meta-analysis of obstructive sleep apnea in patients with cerebrovascular disease. *Sleep Breath, 22*(3), 729-742. doi:10.1007/s11325-017-1604-4

Xiang, X., Leggett, A., Himle, J. A., & Kales, H. C. (2018). Major Depression and Subthreshold Depression among Older Adults Receiving Home Care. *The American Journal of Geriatric Psychiatry, 26*(9), 939-949. doi:https://doi.org/10.1016/j.jagp.2018.05.001

Xiao, F., Lu, C., Zhao, D., Zou, Q., Xu, L., Li, J., . . . Han, F. (2019). Independent Component Analysis and Graph Theoretical Analysis in Patients with Narcolepsy. *Neuroscience Bulletin, 35*(4), 743-755. doi:10.1007/s12264-018-0307-6

Yan, C.-G., Chen, X., Li, L., Castellanos, F. X., Bai, T.-J., Bo, Q.-J., . . . Zang, Y.-F. (2019). Reduced default mode network functional connectivity in patients with recurrent major depressive disorder. *Proceedings of the National Academy of Sciences, 116*(18), 9078. doi:10.1073/pnas.1900390116

Yang, J., Ferreira, T., Morris, A. P., Medland, S. E., Madden, P. A. F., Heath, A. C., . . . Meta-analysis, C. (2012). Conditional and joint multiple-SNP analysis of GWAS summary statistics identifies additional variants influencing complex traits. *Nature Genetics, 44*(4), 369-375. doi:10.1038/ng.2213

Yang, J., Lee, S. H., Goddard, M. E., & Visscher, P. M. (2011). GCTA: a tool for genome-wide complex trait analysis. *American journal of human genetics, 88*(1), 76-82. doi:10.1016/j.ajhg.2010.11.011

Yang, J., Zeng, J., Goddard, M. E., Wray, N. R., & Visscher, P. M. (2017). Concepts, estimation and interpretation of SNP-based heritability. *Nature Genetics, 49*, 1304. doi:10.1038/ng.3941

https://www.nature.com/articles/ng.3941#supplementary-information

Yang, Y.-L., Deng, H.-X., Xing, G.-Y., Xia, X.-L., & Li, H.-F. (2015). Brain functional network connectivity based on a visual task: visual information processing-related brain regions are significantly activated in the task state. *Neural regeneration research, 10*(2), 298-307. doi:10.4103/1673-5374.152386

Yang, Z., Zuo, X. N., McMahon, K. L., Craddock, R. C., Kelly, C., de Zubicaray, G. I., . . . Wright, M. J. (2016). Genetic and Environmental Contributions to

Functional Connectivity Architecture of the Human Brain. *Cereb Cortex, 26*(5), 2341-2352. doi:10.1093/cercor/bhw027

Ye, M., Yang, T., Qing, P., Lei, X., Qiu, J., & Liu, G. (2015). Changes of Functional Brain Networks in Major Depressive Disorder: A Graph Theoretical Analysis of Resting-State fMRI. *PloS one, 10*(9), e0133775-e0133775. doi:10.1371/journal.pone.0133775

Yeo, B. T., Krienen, F. M., Sepulcre, J., Sabuncu, M. R., Lashkari, D., Hollinshead, M., . . . Buckner, R. L. (2011). The organization of the human cerebral cortex estimated by intrinsic functional connectivity. *J Neurophysiol, 106*(3), 1125-1165. doi:10.1152/jn.00338.2011

Yeo, B. T., Tandi, J., & Chee, M. W. (2015). Functional connectivity during rested wakefulness predicts vulnerability to sleep deprivation. *NeuroImage, 111*, 147-158. doi:10.1016/j.neuroimage.2015.02.018

Yu, W., Liang, S., & Zhang, C. (2018). Aberrant miRNAs Regulate the Biological Hallmarks of Glioblastoma. *NeuroMolecular Medicine, 20*(4), 452-474. doi:10.1007/s12017-018-8507-9

Zeng, L. L., Shen, H., Liu, L., Wang, L., Li, B., Fang, P., . . . Hu, D. (2012). Identifying major depression using whole-brain functional connectivity: a multivariate pattern analysis. *Brain, 135*(Pt 5), 1498-1507. doi:10.1093/brain/aws059

Zhang, C., Cahill, N. D., Arbabshirani, M. R., White, T., Baum, S. A., & Michael, A. M. (2016). Sex and Age Effects of Functional Connectivity in Early Adulthood. *Brain Connect, 6*(9), 700-713. doi:10.1089/brain.2016.0429

Zhang, J., Wang, J., Wu, Q., Kuang, W., Huang, X., He, Y., & Gong, Q. (2011). Disrupted brain connectivity networks in drug-naive, first-episode major

depressive disorder. *Biological psychiatry, 70*(4), 334-342. doi:10.1016/j.biopsych.2011.05.018

Zhang, L., Samet, J., Caffo, B., & Punjabi, N. M. (2006). Cigarette smoking and nocturnal sleep architecture. *Am J Epidemiol, 164*(6), 529-537. doi:10.1093/aje/kwj231

Zhi, D., Calhoun, V. D., Lv, L., Ma, X., Ke, Q., Fu, Z., . . . Sui, J. (2018). Aberrant Dynamic Functional Network Connectivity and Graph Properties in Major Depressive Disorder. *Frontiers in Psychiatry, 9*(339). doi:10.3389/fpsyt.2018.00339

Zhou, Y., Liang, M., Tian, L., Wang, K., Hao, Y., Liu, H., . . . Jiang, T. (2007). Functional disintegration in paranoid schizophrenia using resting-state fMRI. *Schizophr Res, 97*(1-3), 194-205. doi:10.1016/j.schres.2007.05.029

Zhou, Y., Yu, F., & Duong, T. (2014). Multiparametric MRI characterization and prediction in autism spectrum disorder using graph theory and machine learning. *PloS one, 9*(6), e90405. doi:10.1371/journal.pone.0090405

Zhu, W., Wen, W., He, Y., Xia, A., Anstey, K. J., & Sachdev, P. (2012). Changing topological patterns in normal aging using large-scale structural networks. *Neurobiol Aging, 33*(5), 899-913. doi:10.1016/j.neurobiolaging.2010.06.022

Appendix A. Publications for Chapter 2

Neuroscience and Biobehavioral Reviews 113 (2020) 98–110

Contents lists available at ScienceDirect

Neuroscience and Biobehavioral Reviews

journal homepage: www.elsevier.com/locate/neubiorev

Review article

Genetic influence on ageing-related changes in resting-state brain functional networks in healthy adults: A systematic review

Heidi Foo[a,*], Karen A. Mather[a,b], Jiyang Jiang[a], Anbupalam Thalamuthu[a], Wei Wen[a], Perminder S. Sachdev[a,c]

[a] Centre for Healthy Brain Aging, CHeBA, School of Psychiatry, University of New South Wales Medicine, Kensington, New South Wales, 2052, Sydney, Australia
[b] Neuroscience Research Australia, Randwick, New South Wales, 2031, Sydney, Australia
[c] Neuropsychiatric Institute, Euroa Centre, Prince of Wales Hospital, Randwick, New South Wales, 2031, Sydney, Australia

ARTICLE INFO

Keywords:
Resting-state functional magnetic resonance imaging (rs-fMRI)
Resting-state functional connectivity (RSFC)
Genetics
Heritability
Alzheimer's disease
Candidate genes
Genome-wide association studies (GWAS)
Epigenetics
Ageing-related brain changes

ABSTRACT

This systematic review examines the genetic and epigenetic factors associated with resting-state functional connectivity (RSFC) in healthy human adult brains across the lifespan, with a focus on genes associated with Alzheimer's disease (AD). There were 58 studies included. The key findings are: (i) genetic factors have a low to moderate contribution; (ii) the *apolipoprotein E ε2/3/4* polymorphism was the most studied genetic variant, with the *APOE-ε4* allele most consistently associated with deficits of the default mode network, but there were insufficient studies to determine the relationships with other AD candidate risk genes; (iii) a single genome-wide association study identified several variants related to RSFC; (iv) two epigenetic independent studies showed a positive relationship between blood DNA methylation of the *SLC6A4* promoter and RSFC measures. Thus, there is emerging evidence that genetic and epigenetic variation influence the brain's functional organisation and connectivity over the adult lifespan. However, more studies are required to elucidate the roles genetic and epigenetic factors play in RSFC measures across the adult lifespan.

1. Introduction

The ageing human brain undergoes complex functional changes, which are associated with changes in cognition (Chan et al., 2014; Shen et al., 2017). These include significant age effects on the functional organisation of brain networks (Huang et al., 2015). Functional connectivity reflects the magnitude of temporal correlations in neural activity and may occur between pairs of anatomically unconnected brain regions (Rubinov and Sporns, 2010). Resting-state functional connectivity (RSFC) measures are commonly derived from resting-state functional magnetic resonance imaging (rs-fMRI) data, which examine the synchronisation of neural activity between regions by measuring the blood oxygen level-dependent (BOLD) signal fluctuations that occur at low frequencies (< 0.1 Hz), where participants are scanned in the absence of a stimulus or task (Lv et al., 2018; Rosazza and Minati, 2011). Characterising resting-state functional changes in the ageing brain may increase our understanding of age-associated cognitive changes, even in the absence of disease (Burke and Barnes, 2006; Otte et al., 2015)

Many studies have explored the effect of age on RSFC either by using region of interest-based correlations (i.e. seed-based) or data-driven reduction techniques (i.e. independent component analysis - ICA), or whole brain approaches (i.e. graph theoretical analysis) (Grayson and Fair, 2017; Lee et al., 2013). Within graph theory, quantitative measures on topological properties of networks, such as small-worldness, highly-connected hubs, and modularity (Otte et al., 2015; Perry et al., 2015; Rubinov and Sporns, 2010), can be calculated. Although these analytical approaches vary in their underlying assumptions and interpretation, it is assumed that functional connectivity measures the same neurophysiological processes (Thompson et al., 2013). Using these techniques – including seed-based, ICA, and graph theory – several resting-state networks (RSNs), which are strong functionally linked sub-networks during rest (van den Heuvel and Hulshoff Pol, 2010), have been identified. These networks include but are not exclusive to the default mode, salience, frontoparietal control, somatosensory, and dorsal attention networks (Lee et al., 2013). Patterns of functional connectivity within and between major RSNs are regarded as intrinsic properties of brain function as they strongly predict patterns of co-activation during common processing tasks (Chan et al., 2014; Grayson and Fair, 2017). More specifically, the default mode network (DMN) has been involved in cognitive control and higher cognitive demands for working memory. Frontoparietal control and dorsal

* Corresponding author at: Centre for Healthy Brain Aging, CHeBA, School of Psychiatry, UNSW Medicine, Kensington, 2052, Sydney, Australia.
E-mail address: heidi.foo@student.unsw.edu.au (H. Foo).

https://doi.org/10.1016/j.neubiorev.2020.03.011
Received 7 August 2019; Received in revised form 8 February 2020; Accepted 9 March 2020
Available online 10 March 2020
0149-7634/

attention networks are implicated in attention, memory, and executive functions (Jiang et al., 2018; Vantansever et al., 2017).

Evidence from neurodevelopmental studies of RSFC shows strong functional connectivity with nearby brain regions and that selected local correlations tend to weaken while correlations with more distant brain regions tend to strengthen across childhood and adolescence (Power et al., 2010). The observed changes in functional connectivity may be due to synaptic pruning (Huttenlocher, 1979) and myelination that occur throughout early life (Brody et al., 1987). Due to the constant state of alterations in the brain that accompany neurodevelopment, this review will only consider ageing-related changes in adults above 20 years old.

Ageing-related changes in resting-state functional connectivity have been observed. Older adults showed lower within-network connectivity and decreased functional connectivity in the DMN compared to younger adults (Damoiseaux, 2017; Dennis and Thompson, 2014). Previous studies have also shown ageing-related decrease in connectivity in the salience and visual networks as well as between DMN and visual networks (Onoda et al., 2012). In addition, findings from graph theoretical approach demonstrate that normal ageing is associated with reduced global and local efficiency, increased local network clustering, and reduced centrality of hub regions (Achard and Bullmore, 2007; Dennis et al., 2013; Geerligs et al., 2015; Gong et al., 2009; Hagmann et al., 2008; Meunier et al., 2009; Montembeault et al., 2012; Otte et al., 2015; Spreng and Schacter, 2012; Wu et al., 2012; Zhu et al., 2012). On average, functional connections within RSNs decrease while connections between RSNs tend to increase with age (Betzel and Bassett, 2017). This ageing-related decrease in connectivity is mainly found in the high-function networks, including DMN, cingulo-opercular, and fronto-parietal control networks, while the primary function networks, such as somatomotor and visual networks, are mainly preserved (Geerligs et al., 2015).

Genetics may play a crucial role in influencing changes in the resting-brain functional organisational properties observed in ageing. Brain functional connectivity can be studied as endophenotypes for characterising disorders that are not yet observable (Dennis et al., 2019). There is evidence to show that brain measures, including RSFC, are heritable (Buckner, 2004; Glahn et al., 2010). Besides genetics, epigenetic factors may also play a role contributing to ageing-related brain functional connectivity changes. Therefore, studying epigenetics and RSFC may increase our understanding of the underlying biological mechanisms that influence functional specialisation across various brain regions in the ageing brain.

Importantly, ageing-related diseases disrupt the brain's functional connectivity, which may result in cognitive decline. Late-onset Alzheimer's disease is the most common form of dementia with high heritability (60–80 %, Gatz et al., 2006). There is evidence that AD risk genes may also be good candidates for brain-related phenotypes, such as RSFC. Previous animal studies have demonstrated that although mice with human apolipoprotein E epsilon 4 lack the classical AD pathological changes, they have impairments in hippocampal-dependent behaviours (e.g. memory tasks) and show changes in neuronal morphology (DiBattista et al., 2016). This implies that AD-related genes may affect the brain in normal ageing and early before the onset of clinical AD. Therefore, investigating how AD genes affect functional connectivity in humans may potentially allow for better understanding of changes in functional network topology with ageing and the development of disease.

Moreover, the study of epigenetics may contribute to our understanding of how environmental factors affect gene expression, which may influence ageing-related brain changes (Papenberg et al., 2015). During ageing, alterations of epigenetic patterns, including a gradual decrease in global DNA methylation, are observed. Knowledge of the influence of internal and external factors on the epigenome may lead to strategies targeting epigenome modifications that may slow down the ageing process and age-related disease (Sierra et al., 2015).

The review will summarise published research on heritability and genetic association studies, with a focus on AD risk genes, and genome-wide association studies (GWAS) of functional connectivity and graph theory measures using rs-fMRI in healthy adults. In addition, epigenetic studies are also reviewed. Finally, suggestions to advance this field are provided.

2. Method

Studies related to the genetics of rs-fMRI were retrieved from PubMed®, Medline ®, and Scorpus©, published until April 2019, using search criteria based on combinations of the following keywords: brain, brain network*, resting-state fMRI, heritability, *APOE*-ε4, clusterin (*CLU*), bridging integrator 1 (*BIN1*), phosphatidylinositol-binding clathrin assembly protein (*PICALM*), kidney and brain expressed protein (*KIBRA*), and sortilin-related receptor (*SORL1*), GWAS, epigenetics, and healthy, ageing or age-related, adults. Further reports were identified by manually searching the citations from the retrieved references. Studies were only included if they meet the following criteria: published in English in a peer-reviewed journal; carried out on healthy individuals; original investigations of genetic and epigenetic factors; examined functional connectivity using rs-fMRI, and the age group was specified. Studies with participants aged 20 years and above were included. Conference abstracts were excluded. Two investigators independently screened the abstracts of retrieved references and assessed full-text for eligibility. Disagreement was resolved through consensus.

3. Results

3.1. Study selection

As shown in Fig. 1, the literature search retrieved 383 records. Six additional references were found after reviewing the reference lists of included articles. After removing duplicates, 333 unique references were screened. Of which, 276 references were excluded after title and abstract screening. These articles included studies involving task-based fMRI, electroencephalogram, diffusion weighted imaging, participants below the age of 20 years old, and those who included pathology. As a result, 58 studies that assessed genetics/epigenetics and functional connectivity using rs-fMRI met inclusion criteria for the systematic review.

3.2. Heritability/genetic correlation

Heritability analysis estimates the relative influence of genes and the environment on a particular phenotype. It is defined as the proportion of the observed variation in a particular trait that can be attributed to genetic versus environmental factors. Classical heritability studies include twin, family, and adoption studies. Alternatively, SNP heritability (h^2_{SNP}), uses SNP data, commonly provided by genome-wide genotyping to assess genetic similarity between individuals (Mayhew and Meyre, 2017; Speed et al., 2017). Trait heritability (h^2) of less than 0.30 is considered as low, 0.30 to 0.60 as moderate, and above 0.60 as high (Visscher et al., 2008). A significant h^2 estimate implies that a trait is significantly influenced by genetic factors, making it an appropriate target for genetic analyses (Thompson et al., 2013).

As shown in Table 1 and Fig. 2, heritability of functional connectivity measures has been assessed by a number of studies, although many of them have examined different RSN properties. The majority of studies observed significant heritability. Using a twin study design, one study found that within-network connectivity in DMN, sensory-somatomotor, dorsal attention, and visual networks were more heritable than averaged between-network connectivity as a whole (Reineberg et al., 2018). Functional connectivity within DMN as a whole was moderately heritable (h^2: 30 %–42 %) in both family and twin studies in middle-aged adults (Glahn et al., 2010). Other networks, including

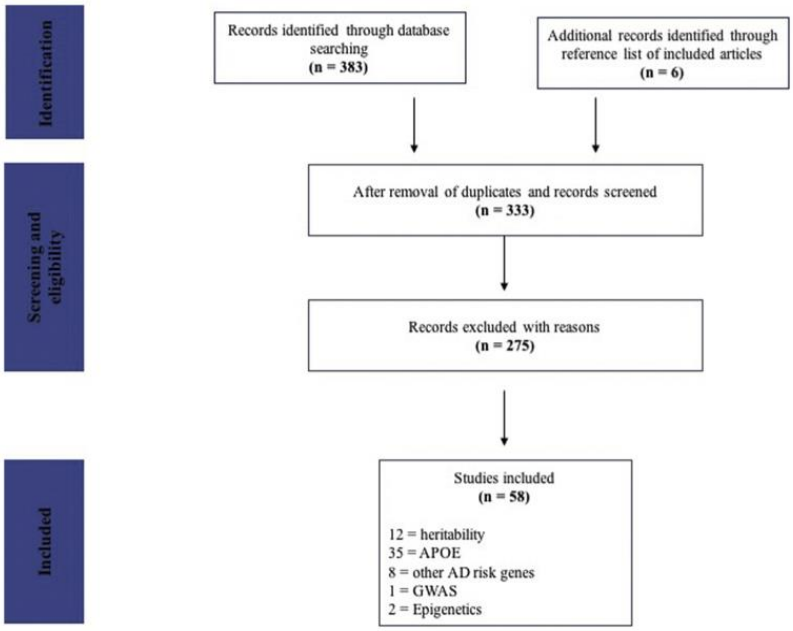

Fig. 1. Systematic search: Diagram showing the selection process of retrieving articles and results using the search criteria.

precuneus-dorsal posterior cingulate network, visual network, fronto-parietal, dorsal attention network, auditory, executive control, and salience, showed low-to-strong heritability (h^2: 20 %–80 %) in both young and middle-aged twins (Ge et al., 2017; Miranda-Dominguez et al., 2017; Yang et al., 2016). Using both twins and family cohorts of young and middle-aged adults, h^2 estimates were low-to-moderate across various regions within networks such as auditory, frontoparietal, visual, executive control, salience, and attention (Adhikari et al., 2018). Middle-aged adults had weakly-to-moderately heritable (h^2: 10%–42%) connectivity of subcomponents of DMN in a family study (Glahn et al., 2010). Moderate heritability was observed for connectivity between the posterior cingulate cortex and inferior parietal cortex (h^2 = 41 %) (Korgaonkar et al., 2014), and connectivity between DMN and sensory/somatomotor networks was also moderately heritable (h^2 = 36 %) (Reineberg et al., 2018). Graph theoretical measures in twin studies showed low heritability for connection strength (h^2: 15 %–18 %) (Colclough et al., 2017), moderate heritability (h^2 = 60 %) for cost-efficiency (Fornito et al., 2011), and moderate heritability (h^2: 38%–64%) for mean clustering coefficient, modularity, global efficiency, and small worldness (Sinclair et al., 2015). Interestingly, one twin study observed higher estimated within-network heritability when leveraging shared features across both rs-fMRI and task-based fMRI than rs-fMRI alone (Elliott et al., 2019). Using genome-wide genotyping to estimate h^2_{SNP}, one study found that 235 of 1771 rs-fMRI image-derived phenotypes IDPs showed low to moderate h^2_{SNP} (Elliott et al., 2018). Importantly, h^2_{SNP} typically provides smaller heritability estimates relative to those provided by the classic design. Taken together, however, these studies appear to suggest a low to moderate genetic contribution for resting-state functional connectivity phenotypes.

3.3. AD candidate gene analysis and RSFC

Candidate genes are chosen based on prior hypothesis and/or biological relevance to the phenotype under consideration (Kanchibhotla et al., 2013; Patnala et al., 2013). Few have been investigated in relation to RSFC.

As suggested in a review by Karch and Goate (2015), we examine some of the more commonly investigated AD-risk genes and their polymorphisms – *APOE-ε4*, *CLU (rs11136000)*, *BIN1 (rs744373)*, *PICALM (rs3851179* and *rs541458)*, *KIBRA (rs17070145)*, and *SORL1 (rs2070045)* – and their influence on ageing-related changes in RSFC in healthy adults (Tables 2 and 3).

3.3.1. APOE-ε4

Table 2 summarises the studies studying *APOE* in RSFC. The *APOE-ε2/3/4* polymorphism is one of the most commonly studied variants in ageing due to the high risk of late-onset AD in ε4 carriers; the odds ratio for AD for ε4 homozygotes is 14.9 (Farrer et al., 1997). Evidence has shown that the ApoE protein is important in brain lipid homeostasis (Huang and Mahley, 2014) and synapse formation (Mauch et al., 2001), and that the *APOE-ε4* allele is associated with localised brain functional alterations (Luo et al., 2016). The relationship between the *APOE-ε4* allele and RSFC has been well studied (Chiesa et al., 2017) across adulthood in different populations.

Most consistently, across adulthood, studies showed decreased DMN connectivity (Damoiseaux et al., 2012; Goveas et al., 2013; Liang et al., 2017) in the posterior cingulate cortex/precuneus, orbital and middle frontal cortex, and inferior parietal lobe (Chen et al., 2015; D'Angelo et al., 2012; Heise et al., 2014; Liang et al., 2017; Lu et al., 2017; Ma et al., 2016; Sheline et al., 2010; Su et al., 2017; Wang et al., 2012). In addition, increased DMN connectivity (Su et al., 2015) in the medial temporal lobe (MTL), parahippocampus, hippocampus, and prefrontal cortex in *APOE-ε4* carriers compared to non-carriers across adulthood were also observed (Matura et al., 2014; Patel et al., 2013; Shu et al., 2016; Song et al., 2015; Westlye et al., 2011; Wu et al., 2016; Ye et al., 2017), with the exception of Yan et al. (2015) showing decreased hippocampal connectivity. In addition, while one study showed that *APOE* status did not predict baseline connectivity or change in connectivity (Staffaroni et al., 2018), another study demonstrated that in *APOE-ε4* non-carriers with a family history of AD, there was a reduction in functional connectivity of DMN in older adults (Wang et al., 2012). This suggests that disruptions to the DMN may be an early

Table 1
Studies examining the heritability of functional connectivity using rs-fMRI in healthy adults.

Measure	Method	Total sample size	Sex	Age (years); M (SD)/ age range (years)	Ethnicity	Heritability (h^2) results	Reference (year)
5 nodes within DMN	Seed based correlation	277 from 2 cohorts: (1) twin cohort (250 twins: 79 MZ & 46 DZ); (2) 27 unrelated/nontwins	(1) 96 M & 154 F; (2) 15 M & 12 F	39.7 (12.8)	European ancestry	Posterior cingulate cortex - R inferior parietal cortex (PCC-RIPC) connectivity - 41 % Other measures n.s.	Korgaonkar et al. (2014)
AN, DMN, FPN, VN, ECN, SN, AttN, SMN	Seed-based & dual-regression	2 cohorts: (1) GOBS (334 individuals - 29 extended pedigrees); (2) HCP (518 - MZ, DZ, non-twin siblings)	GOBS: 124 M & 210 F; HCP: 240 M & 278F	GOBS: 47.9 (13.2); HCP: 28.7 (3.7)	GOBS: Mexican-Americans; HCP: Mainly Caucasians	20 % –40 % across the 8 networks	Adhikari et al. (2018)
1 cm spherical ROIs drawn from each of the 264 functional areas	Power parcellation, ROI	2 cohorts: (1) LTS (251 - 102 MZ pairs, 91 DZ pairs, 34 MZ twin singletons, 45 DZ twin singleton); (2) HCP (442 - 136 MZ pairs, 75 DZ pairs)	LTS: 97 M & 154 F; HCP: 171 M & 271 F	LTS: 28.7 (0.63); HCP: 29.2 (3.46)	LTS & HCP: Mainly Caucasians	36 % for DMN to sensory/SMN connection as a whole	Reineberg et al. (2018)
DMN (8 anatomical regions)	Dual-regression, ICA	GOBS: 333 individuals - 29 pedigrees	123 M & 210 F	48.38 (12.9)	Mexican-American	42.4 % as a whole	Glahn et al. (2010)
PCN, VN, DMN, FPN, SN, SMN, DAN	ICA	QTIM: 105 - 80 DZ, 25 singletons	51 M & 54F	19-29	Caucasians	5/7 networks heritable (i.e. PCN, VN, DMN, FPN, DAN) h^2 = 23.3% - 65.2%	Yang et al. (2016)
Network edges. SNP heritability estimated.	ICA	UK Biobank: 8428 (unrelated individuals)	4045 M & 4383F	40-69	English	235/1771 functional connectivity edges heritable	Elliott et al. (2018)
39 cortical regions (network nodes)	Parcellation from resting-state 100-dimensional group ICA decomposition	HCP: 820 - MZ & DZ twin pairs	Information not available	22 – 35	Mainly Caucasians	15.0 %–18.0 % for connection strength between components of nodes (eg. DMN, motor network, VN, DAN)	Colclough et al. (2017)
7 network parcellations (i.e. VN, SMN, DAN, salience ventral attention, limbic, control, DMN) split into 51 spatially contiguous regions across 2 hemispheres	Yeo seven-network parcellation	2 cohorts: (1) HCP (528 - 92 MZ, 46 DZ twin pairs, 250 full siblings, 56 singletons); (2) GSP (809 unrelated younger subjects)	HCP: 203 M & 325 F; GSP: 362 M & 447F	HCP: 29.21 (3.47); GSP: 20.84 (2.77)	Mainly Caucasians	~ 45.0 %–80.0 % for all network parcellations	Ge et al. (2017)
12 functional networks (i.e. auditory, cingulo-opercular, cingulo-parietal, DMN, DAN, FPN, retrosplenial temporal, SN, SMN hand, SMN mouth, VAN, & VN) into 333 ROIs	Gordon parcellation	2 cohorts: (1) longitudinal study in Oregon (159); (2) HCP (198 – MZ, DZ, non-twin siblings)	HCP: 89 M & 109 F	HCP: 28.4 (3.50)	Mainly Caucasians	~ 20 % across the whole brain; driven by high-order systems including the FPN, DAN, VAN, cingulo-opercular, & DMN	Miranda-Dominguez et al. (2017)
Network edges	Power and Yeo parcellation	2 cohorts: HCP (298 - MZ, DZ, full siblings); (2) Dunedin Study (591)	Information not available	HCP: 25–35; Dunedin Study: 45	Mainly Caucasians	Within-network heritability ↑ from 22 % in rs-fMRI to 28 % when combining task-based fMRI & rs-fMRI at 40 minutes scan time	Elliott et al. (2019)
Network cost-efficiency (global & regional communication efficiency, connection distance, connection density)	1041 cortical regions parcellated, graph theory	58 - 16 MZ & 13 DZ twin pairs	28 M & 30 F	40.48 (11.77)	Caucasians	60 % in network-cost efficiency	Fornito et al. (2011)
Mean clustering coefficient, global efficiency, modularity, & rich club coefficient	AAL template, 116 regions, graph theory	QTIM: 591 - 84 MZ & 89 DZ twin pairs, 246 single twins	MZ: 23 M & 61 F; DZ: 34 M & 55 F; single twins information not provided	23.0 (2.5)	Caucasians	47 % – 61 % for mean clustering coefficient; 38%–59% for modularity; 52 %–64 % for global efficiency; 51 – 59% for small worldness	Sinclair et al. (2015)

L, left; R, right; fMRI, functional magnetic resonance imaging; Rs-fMRI, resting-state functional magnetic resonance imaging; ROI, region of interest; LAN, auditory network; AttN, attention network; DAN, dorsal attention network; DMN, default mode network; ECN, executive control network; FPN, fronto-parietal network; PCN, posterior cingulate network; SMN, sensorimotor network; SN, salience network; VAN, ventral attention network; VN, visual network; ICA, independent component analysis; MZ, monozygotic; DZ, dizygotic; GOBS, Genetics of brain structure and function study; HCP, Human connectome project; GSP, Genomics superstruct project; LTS, Colorado longitudinal twin study; QTIM, Queenland Twin Imaging study; USA, United States of America; UK, United Kingdom; n.s., no significant results.

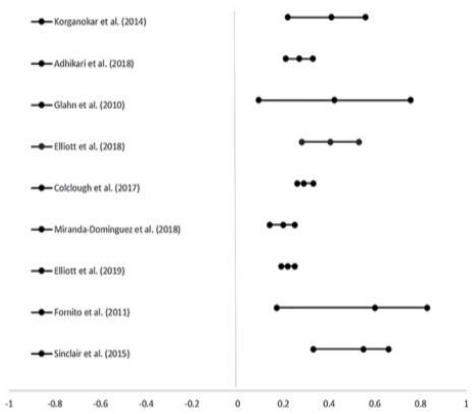

Measures	h^2 [95%-CI]
PCC-RIPC	0.41 [0.22, 0.5
Mean FC	0.27 [0.21, 0.33]
DMN	0.42 [0.09, 0.76]
Mean of significant netmat ICA	0.42 [0.28, 0.53]
fMRI connectivity	0.29 [0.26, 0.33]
Whole brain FC	0.20 [0.14, 0.25]
10 minutes resting-state fMRI scan time	0.22 [0.19, 0.25]
Network cost efficiency	0.60 [0.17, 0.83]
Global efficiency	0.49 [0.31, 0.57]

Fig. 2. Forest plot showing the heritability estimates of various resting-state network measures from 9 studies. Three of the 12 reported studies did not report confidence intervals and/or standard errors, which precluded them from being added into the forest plot. Note that non-significant heritability results are not included.
Abbreviations: PCC-RIPC, posterior cingulate cortex-right inferior parietal/temporal cortex; FC, functional connectivity, DMN, default mode network, ICA, independent component analysis.

pathophysiological marker of AD that may be influenced by other genetic factors besides *APOE*-ε4.

Other brain regions have also shown differences in RSFC between *APOE*-ε4 carriers and non-carriers across adulthood however, the findings are mixed. Young *APOE*-ε4 carriers aged between 20 and 29 years old showed increased functional connectivity within the sensorimotor network (Filippini et al., 2009) and visual network (Dowell et al., 2016). Whereas middle aged *APOE*-ε4 carriers aged between 45 and 54 years old showed decreased connectivity in the posterior cingulate/precuneus (Patel et al., 2013), frontal, thalamus, and basal ganglia regions (Li et al., 2014), increased connectivity was observed in superior temporal gyrus, supramarginal gyrus, insula (Patel et al., 2013), salience (Goveas et al., 2013), and the anterior hippocampal networks (Trachtenberg et al., 2012). Older *APOE*-ε4 carriers aged between 63 and 89 years old showed increased connectivity in the salience network (Liang et al., 2017; Machulda et al., 2011), anterior and posterior cingulate cortex (Cai et al., 2017; Matura et al., 2014), medial prefrontal cortex (Cai et al., 2017), inferior and superior frontal gyri (Yang et al., 2014), inferior and middle temporal gyrus (Matura et al., 2014; McKenna et al., 2016), precuneus, and visual network (McKenna et al., 2016). However, one study observed an opposite effect in BOLD signal reduction in the precuneus and posterior cingulate regions (Yang et al., 2014). Another longitudinal study has also shown decreased connectivity between executive control and salience networks at baseline and reduced functional segregation between executive control and DMN at follow up in elderly *APOE*-ε4 carriers compared to non-carriers (Ng et al., 2018).

Using a graph theoretical approach, *APOE*-ε4 carriers had significantly lower global and local efficiency, and less resilience to targeted node failure of RSN compared to non-carriers in middle-aged adults (Korthauer et al., 2018). Reduction of both node efficiency in the middle temporal lobe and regional efficiency in the parahippocampal gyrus was observed in older *APOE*-ε4 carriers compared to non-carriers (Chen et al., 2015). This finding suggests that network-level vulnerabilities are present in those at increased genetic risk of AD (Korthauer et al., 2018). Eigenvector centrality values showed reductions in the left medial temporal lobe, left lingual gyrus and visual cortex in middle-aged adults (Wink et al., 2018) whereas another study showed increases in the left middle frontal gyrus in older *APOE*-ε4 carriers (Luo et al., 2017). Moreover, older *APOE*-ε4 carriers who had a decline in episodic memory performance also showed altered anterior-posterior brain functional connectivity (Quevenco et al., 2017).

Collectively, the most consistent finding observed was in relation to decreased DMN connectivity in *APOE*-ε4 carriers compared to non-carriers across adulthood. Results for other networks, all of which had fewer studies were mixed, with no consistent patterns observed where the influence of *APOE*-ε4 on RSFC does not follow a fixed pattern of increased/decreased connectivity from younger to older adults.

3.3.2. Other AD risk genes

Table 3 summarises the association results from other AD risk genes that have been investigated with resting-state functional networks. However, there are very few studies reported (n = 9). The most studies have been performed for *KIBRA rs17070145* (n = 3), with one finding a significant interaction between *KIBRA* and *APOE* polymorphisms (Zhang et al., 2017). Two or less studies have been reported for *CLU*, *PICALM*, *SORL1* and *BIN1* variants. Four of the nine studies examined hippocampal connectivity whereas the rest focused on either specific networks or voxel-wise connectivity. Thus, currently it is very difficult to make any conclusions from these studies due to methodological differences and lack of studies. The details of these studies are briefly discussed below.

Studies in the Chinese cohort showed that younger adult *CLU rs11136000* C-allele carriers compared to CLU *rs11136000* T-allele carriers showed increased hippocampal connectivity (Zhang, Qin et al., 2015). Conversely reductions in hippocampal connectivity in *BIN1 rs744373* G-allele carriers (Zhang, Yu et al., 2015) and *PICALM rs3851179* G-allele carriers (Zhang, Qin et al., 2015) were observed. Older Caucasian *KIBRA rs17070145* T-allele carriers compared to non-T-allele carriers also showed decreased hippocampal connectivity (Witte et al., 2016).

In younger Chinese adults, *SORL1 rs2070045* G allele carriers had lower functional connectivity density in the inferior temporal gyrus than non-carriers (Shen et al., 2016) as well as decreased functional connectivity between the hippocampus and middle temporal gyrus (Shen et al., 2017). Moreover, stronger synchronisation patterns in the DMN and executive control network (ECN) were seen in young Chinese *KIBRA rs17070145* C-allele carriers compared to non-carriers (Wang et al., 2013). An epistatic interaction between *APOE* ε4 and *KIBRA rs17070145* polymorphisms was observed in the functional connectivity density in the dorsolateral prefrontal cortex (Zhang et al., 2017). Whereas reduced functional connectivity between the hippocampus and inferior frontal gyrus was observed in the interactive effects between variants in the *APOE* and *SORL1 rs2070045* genes in young Chinese healthy adults (Shen et al., 2017). In another Chinese study, the *PICALM* risk allele T (rs541458) showed decreased functional connectivity in the left superior parietal gyrus and left fronto-parietal network in the less than 65 years old age group compared to those 65 years and above (Liu et al., 2018). The result suggests that age may modulate the relationship between the *PICALM* rs541458

Table 2
Studies examining the *apolipoprotein E gene (APOE) ε2/3/4* polymorphism and functional connectivity using rs-fMRI in healthy adults.

Measure	Method	Total sample size & Gender	Age (years); M (SD)/ age range (years)	Ethnicity	Results	Reference (year)
Precuneus to 9 ROIs	Seed-based	ADRC: 100 (28 M & 72 F)	61.23 (8.0)	Mainly Caucasians	*ε4+* ↓ precuneus FC	Sheline et al. (2010)
DMN, SN	Seed-based	Mayo Clinic: 56 (35 M & 21 F)	70-89	Mainly Caucasians	In phase connectivity: *ε4+* ↓ posterior DMN, ↑ SN	Machulda et al. (2011)
Bilateral precuneus	Seed-based	ADRC: 99 (28 M & 71 F)	60.95 (7.95)	Mainly Caucasians	*ε4+* vs *ε4-* functional connectivity differences between precuneus & other ROIs	D'Angelo et al. (2012)
DMN	Seed-based	ADRC: 348 (138 M & 210 F)	69 (9.5)	Mainly Caucasians	↓ FC within DMN (PCC-MTL) in *ε4-* with family history of Alzheimer's disease	Wang et al. (2012)
DMN, ECN, SN	Seed-based	Wisconsin Medical School: 46 (15 M & 31 F)	53.45 (5.7)	Mainly Caucasians	*ε4+* ↓ DMN & ECN, ↑ SN functional connectivity	Goveas et al. (2013)
Hippocampal functional connectivity	Seed-based	Oxford: 86 (37 M & 49 F)	63.92 (10.47)	English	Female *ε4+:* ↓ FC between the hippocampus & precuneus/ PCC	Heise et al. (2014)
Papez circuit using hippocampus seed	Seed-based	Wisconsin Medical School: 48 (15 M & 31 F)	53.45 (5.7)	Mainly Caucasians	*ε4+* ↓ FC in frontal, cingulate, thalamus, & basal ganglia regions	Li et al. (2014)
PCC	Seed-based	Goethe-University: 63 (22 M & 41 F)	65.9 (6.7)	German	*ε4+* ↑ connectivity between PCC & L-hemispheric MTG	Matura et al. (2014)
13 ROIs in relation to DMN	Seed-based	Xuanwu Hospital Capital Medical University: 49 (19 M & 30 F)	74.02 (4.69)	Chinse	*ε4+* ↑ connectivity – L parahippocampal gyrus & R superior frontal cortex, L parahippocampal gyrus & medial PFC; ↓ connectivity between cerebellar tonsils & retrosplenial	Song et al. (2015)
105 ROIs	Seed-based	ADNI: 36 (10 M & 26 F)	69.72 (13.21)	Mainly Caucasians	*ε4-:* stronger connectivity in 7 ROIs (precuneus, bilateral primary visual cortex, bilateral retrosplenial cortex, bilateral secondary visual cortex)	McKenna et al. (2016)
PCC	Seed-based	ZhongDa Hospital: 129 (62 M & 67 F)	68.50 (6.63)	Chinese	*ε4+* ↓ DMN in bilateral ACC/R dorsolateral prefrontal cortex; ↓ FC with age	Shu et al. (2016)
DMN (9 ROIs), SN (6 ROIs)	Seed-based	ADNI: 32 (15 M & 17 F)	63.63 (5.73)	Mainly Caucasians	*ε4+* ↓ DMN, ↑ SN FC	Liang et al. (2017)
DMN (5 ROIs)	Seed-based	CUHK: 38 (14 M & 24 F)	69.94 (4.38)	Chinese	*ε4+* ↓ interhemispheric RFCS, esp. R hippocampus & L inferior parietal lobular	Lu et al. (2017)
DMN (3 ROIs)	Seed-based	Jinling Hospital: 83 (49 M & 34 F)	24.1 (2.5)	Chinese	*ε4+* ↓ functional connectivity in the L SFC & bilateral PCu, PCC, & MCC	Su et al. (2017)
Bilateral hippocampal networks	Seed-based	ZhongDa Hospital: 104 (54 M & 50 F)	68.58 (6.37)	Chinese	*ε4+* ↑ FC between the L hippocampus & R frontal regions longitudinally	Ye et al. (2017)
DMN, VC, SM	ICA, dual regression	Oxford: 36 (21 M & 15 F)	28.5 (4.4)	English	*ε4+* ↑ sensorimotor FC	Filippini et al. (2009)
DMN	ICA, dual regression	Norway: 95 (34 M & 61 F)	63.8 (7.2)	Norwegian	*ε4+* ↑ hippocampal synchronisation in RSN spanning the posterior DMN	Westlye et al. (2011)
30 components subdivided into sub-networks	ICA, dual regression	UCSF: 131 (60 M & 71 F)	70.5 (6.9)	Mainly Caucasians	*ε4+* ↓ DMN connectivity compared to *ε3* homozygotes	Damoiseaux et al. (2012)
10 RSNs	ICA, dual regression, ROI	Oxford: 77 (39 M & 38 F)	45.95 (4.63)	English	*ε4-:* ↑ connectivity in most regions except widespread ↓ connectivity between the AN & frontal, temporal, & parietal regions & basal ganglia	Trachtenberg et al. (2012)
DMN	ICA	Yale University: 36 (15 M & 21 F)	45.0 (8.05)	Mainly Caucasians	*ε4+* ↓ PCC/precuneus, ↑ STG, SMG, & insula	Patel et al. (2013)
DMN	ICA	Jinling Hospital: 76 (34 M & 42 F)	23.7 (2.8)	Chinese	*ε4+* ↑ DMN compared to *ε2* & *ε3*	Su et al. (2015)
DMN, ECN, HCN	Seed-based, ICA	Taipei Medical University: 17 (7 M & 10 F)	48.05 (12.6)	Chinese	*ε4+* ↓ HPN connectivity in the L parahippocampal gyrus	Yan et al. (2015)
20 ICAs	ICA, dual regression	University of Sussex: Young: 98 (34 M & 64 F); Mid: 78 (34 M & 44 F)	Young: 20.0 (2.0); Mid: 51.0 (3.0)	English	Young: *ε4+* showed ↑ connectivity within the medial visual network compared to *ε4-;* n.s. for middle-age *ε4+*	Dowell et al. (2016)
DMN, including PCC, precuneus, PFC, inferior parietal lobule	ICA	BABRI: 100 (41 M & 59 F)	64.5 (6.9)	Chinese	*ε4+* ↑ FC in R PCC; ↓ FC in superior medial frontal gyrus, L medial frontal gyrus in anterior DMN, & cingulate gyrus	Ma et al. (2016)
ECN, SN, DMN	ICA	USCD: 29 (8 M & 21 F)	50 - 65	Mainly Caucasians	*ε4+* ↑ FC inferior parietal lobe, L middle frontal gyrus, L MTL, posterior lobe of cerebellum, & supplemental motor area	Wu et al. (2016)

(*continued on next page*)

Table 2 (*continued*)

Measure	Method	Total sample size & Gender	Age (years); M (SD)/ age range (years)	Ethnicity	Results	Reference (year)
Voxel-wise	Multiscale entropy	Taiwan: 212 (107 M & 105 F)	Younger: 27.2 (4.3); Older: 68.4 (6.5)	Chinese	Older *ε4+*: ↓ BOLD complexity in precuneus/PCC; ↑ FC in superior & inferior frontal gyrus	Yang et al. (2014)
Voxel-wise	ALFF, ReHo	ADNI: 42 (19 M & 23 F)	73.94 (4.55)	Mainly Caucasians	*ε4+* ↓ precuneus, ↑ ACC & mPFC	Cai et al. (2017)
Homotopic RSFC	Voxel-mirrored homotopic connectivity	ADNI: 35 (17 M & 18 F)	76.63 (5.89)	Mainly Caucasians	*ε4+* ↓ inter-hemispheric RSFC in the bilateral MTL & orbital frontal cortex	Luo et al. (2016)
DMN, ECN, SN	Arslan and Yeo parcellation, internetwork and intranetwork FC	Duke-NUS: 122 (61 M & 61 F)	70.11 (5.62)	Chinese	*ε4+* Cross-sectional: ↓ FC between ECN & SN; longitudinally: Reduced segregation of ECN-DMN	Ng et al. (2018)
Global efficiency & local efficiency	AAL atlas, graph theory	BABRI: 75 (36 M & 39 F)	65.86 (7.46)	Chinese	*ε4+* ↓ node efficiency in MTL regions, ↓ regional efficiency in R PHG	Chen et al. (2015)
Eigenvector centrality	Graph theory	ADNI: 35 (17 M & 18 F)	76.63 (5.89)	Mainly Caucasians	*ε4+* ↓ eigenvector centrality in MTL, LG; ↑ L MFG	Luo et al. (2017)
Dynamic functional connectivity patterns, node strength	Sliding-window approach, AAL atlas, graph theory	Zurich: 37 (24 M & 13 F)	74.0 (6.0)	Swiss-German	*ε4+* & decline episodic performance: alterations in global connectivity, anterior-posterior network, & between parieto-temporal & fronto-occipital	Quevenco et al. (2017)
DMN, modularity	Brainnetome atlas, graph theory	UCSF MAC: 111 at baseline (65 M & 46 F)	69.3 (6.7)	Mainly Caucasians	*APOE* status did not predict baseline connectivity or change in connectivity	Staffaroni et al. (2018)
Global efficiency, local efficiency, betweenness centrality, eigenvector centrality	Graph theory	Wisconsin Medical School: 76 (32 M & 44 F)	49.9 (6.0)	Caucasians	*ε4+* ↓ global & local efficiency of the integrated rsSC	Korthauer et al. (2018)
Eigenvector centrality	Graph theory	GAP: 261 (110 M & 151 F)	56.4 (6.7)	Spanish	*ε4+* ↓ eigenvector centrality in visual cortex	Wink et al. (2018)

APOE ε4 +, APOE ε4 carriers; APOE ε4-, APOE ε4 non-carriers; AAL, automated anatomical labelling; ROI, region of interest; RSN, Resting-state networks; RSFC, resting-state functional connectivity; rsSC, resting-state structural connectome; ACC, anterior cingulate cortex; AFC, amygdala functional connectivity; AHN, anterior hippocampal network; AN, auditory network; DMN, default mode network; ECN, executive control network; HPN, hippocampal network; lFPN, left frontal-parietal network; LG, lingual gyrus; MFG, middle frontal gyrus; MPFC, medial prefrontal cortex; MTG, middle temporal gyrus; MTL, medial temporal lobe; PCC/PCu, posterior cingulate cortex/precuneus; PHG, parahippocampal gyrus; PHN, posterior hippocampal network; SFC, superior frontal cortex; SN, salience network; SM, sensorimotor; STG, superior temporal gyrus; SMG, supramarginal gyrus; VC, visual cortex; ALFF, amplitude of low frequency fluctuations; ICA, independent component analysis; ReHo, regional homogeneity; ADNI, Alzheimer's disease neuroimaging initiative; ARDC, Knight Alzheimer's disease research centre; BABRI, Beijing Ageing Brain Rejuvenation Initiative; CUHK, Chinese University of Hong Kong; Duke-NUS, Duke-National University of Singapore; GAP, Gipuzkoa Alzheimer's project; UCSF, UCSD, University of California San Diego; University of California San Francisco; USCF MAC, University of San Francisco Memory and Aging Center; USA, United States of America; UK, United Kingdom; n.s., no significant results.

Table 3
Studies examining the relationship of other candidate genes and functional connectivity using rs-fMRI in healthy adults.

Gene/SNP	Measure	Method	Total sample size (Gender)	Age (years); M (SD)/ age range (years)	Ethnicity	Results	Reference (year)
KIBRA rs17070145	20 components including anterior DMN, posterior DMN, ECN, SMN, VN	ICA	Tianjin Medical School: 288 (133 M & 155 F)	22.7 (2.5)	Chinese	*KIBRA C-allele*: ↑ synchronisation in DMN & ECN	Wang et al. (2013)
KIBRA rs17070145	Hippocampus	Seed-based	Berlin: 140 (69 M & 71 F)	63.0 (6.9)	German	*KIBRA T-allele*: ↓ FC of L hippocampus	Witte et al. (2016)
CLU rs11136000 & *PICALM rs3851179*	Hippocampal regions	Seed-based	Tianjin Medical School: 283 (129 M & 154 F)	22.7 (2.5)	Chinese	*CLU*: positive rsFC between hippocampus & MTL & AG, negative rsFC of bilateral hippocampi & L MCC; *PICALM*: negative rsFC between the hippocampus & precuneus & SFG	Zhang et al. (2015a)
BIN1 rs744373	Hippocampal regions	Seed-based	University of Electronic Science and Technology of China: 360 (186 M & 174 F)	19.41 (1.09)	Chinese	↓ hippocampal–dorsolateral prefrontal cortex connectivity	Zhang et al. (2015b)
SORL1 rs2070045	Voxel-wise	FDC	Tianjin Medical School: 275 (129 M & 149 F)	22.7 (2.3)	Chinese	*SORL1 G-allele*: ↓ FCD than the protective TT carriers.	Shen et al. (2016)
APOE & *SORL1 rs2070045*	Hippocampus	Seed-based	Tianjin Medical School: 287 (134 M & 153 F)	22.7 (2.4)	Chinese	*SORL1 G-allele*: ↓ rsFC between the hippocampus & middle temporal gyrus; interaction effects *APOE* & *SORL1*: negative rsFC between the hippocampus & inferior frontal gyrus	Shen et al. (2017)
APOE & *KIBRA rs17070145*	Voxel-wise	FDC	Tianjin Medical School: 267 (118 M & 149 F)	22.8 (2.5)	Chinese	*APOE* x *KIBRA* interaction: ↓ FCD in the L parahippocampal gyrus & the R middle temporal gyrus & ↑ FCD in the bilateral middle occipital gyri	Zhang et al. (2017)
PICALM rs541458	DMN, FPN	ICA	BABRI: 638 (221 M & 417 F)	50-82	Chinese	*PICALM-T*: ↓ L SPG within the L FPN in the < 65 years but ↑ connectivity in the ≥ 65 years	Liu et al. (2018)

APOE, apolipoprotein; Bridging integrator 1 (BIN1); CLU, clusterin; PICALM, phosphatidylinositol-binding clathrin assembly protein; SORL1, sortilin-related receptor 1; AD, Alzheimer's disease; rsFC, resting-state functional connectivity; AG, angular gyri; DPFC, dorsolateral prefrontal cortex; ECN, executive control network; FDC, functional connectivity density; FPN, fronto-parietal network; MCC, mid-cingulate cortex; MPFC, medial prefrontal cortex; MTL, middle temporal lobe; PCC, posterior cingulate cortex; SFG, superior frontal gyrus; SMN, sensorimotor network; SPG, superior parietal gyrus; VN, visual network; ICA, independent component analysis; FDC, Functional connectivity density; BABRI, Beijing Ageing Brain Rejuvenation Initiative.

polymorphism and resting-state functional networks, although this finding requires replication. As most of these studies were performed in the Chinese population, replication studies should be done in the other ethnicities to ascertain whether these findings are also applicable to other races.

3.4. Genome wide association studies (GWAS)

GWAS use a hypothesis-free approach to systematically test multiple genetic variants across the genome. It has been used to identify many genetic variants, commonly SNPs, associated with a wide range of traits (Choi et al., 2018).

However, thus far, there has only been one GWAS investigating the genetics of rs-fMRI. This was performed in 8428 adults aged between 40 and 69 years old using the United Kingdom (UK) Biobank data (Elliott et al., 2018). They used group-ICA to identify the major RSNs and estimated network matrices for all participants. Their findings demonstrated several SNPs, including rs60873293, rs35124509, rs2279829, rs7442779, rs2274224, and rs11596664 were associated with RSN measures. This study highlights the potential contributions of genetic variation in influencing resting-state functional connectivity in mid-late life.

Due to the paucity of literature, more GWAS are required to identify further loci. Independent replication of the aforementioned results is required to confirm the relationships between previously identified genetic variants and resting-state functional connectivity measures in adults over the lifespan. The influence of ethnicity should also be examined.

3.5. Epigenetics associated with ageing-related changes in functional connectivity

Epigenetics refers to any changes in gene expression that are independent of any changes in the deoxyribonucleic acid (DNA) sequence itself (Hwang et al., 2017; Zhao et al., 2016). It is influenced by not only the environment but also by genetic and sporadic processes. Epigenetic processes include DNA methylation, non-coding RNAs and histone modifications. However, to date, there have been only two epigenetic studies, both of which investigated changes in resting-state functional networks and DNA methylation of the serotonin transporter gene (*SLC6A4*) in young adults (Ismaylova et al., 2017; Muehlhan et al., 2015). Blood-derived *SLC6A4* promoter methylation was associated with amygdaloid resting state functional coupling with key brain regions of the salience network (Muehlhan et al., 2015) and stronger right lateral parietal-frontal pole and occipital resting-state functional connectivity (Ismaylova et al., 2017) in young adults. Whereas buccal-derived *SLC6A4* promoter methylation was associated with greater resting-state functional connectivity between right lateral parietal, anterior cingulate cortex, and medial prefrontal cortex (Ismaylova et al., 2017). As *SLC64A* genetic variation has previously been related to late-life depression (Lam et al., 2018) these results show that DNA methylation levels in the SLC64A promoter may be important in detecting changes in resting-state functional connectivity with implications for psychopathological disease resilience/susceptibility.

4. Discussion

Determining the relative contribution of genes to the maintenance and/or disruption of RSFC is of much interest in the field of imaging genetics. This systematic review provides a comprehensive synthesis of previous studies that have assessed the relationship of genetics (i.e. heritability, AD risk gene association studies and GWAS) and epigenetic factors with RSFC in healthy adults.

Given the complex relationship between BOLD fMRI measures – including blood flow, blood volume, and oxygen metabolism – and the molecular mechanisms that control neuronal firing patterns, the exact biological mechanisms contributing to signal variation of rs-fMRI remain unclear. Establishing heritability of RSFC is therefore important in order to justify further genetic studies and to improve our understanding of the biological pathways involved (Fornito et al., 2011; Glahn et al., 2010; Korgaonkar et al., 2014). Our review found low to moderate heritability estimates reported for RSFC measures in healthy adults from a range of ages, implying significant genetic underpinnings for variability in RSFC measures across brain regions in cognitively unimpaired populations. Interestingly, Reineberg et al. (2018) demonstrated higher heritability of within network than between network properties, suggesting that genetic influence on the connectivity of regions involved in the same process may be driving functional brain organisation (Reineberg et al., 2018). As demonstrated by Elliott et al. (2019), heritability estimates increase when combining both rs-fMRI and task-based fMRI data, thus future studies should investigate the genetic influence on functional connections both at rest and when in active states. There may be potential age effects on the heritability of resting-state networks. The heritability findings summarised here are from a ranges of age. To our knowledge there are no studies that have investigated the effects of age on heritability of resting-state networks. Therefore, future studies should consider investigating this.

Genetic association studies have shown how specific AD-related genetic variation may alter the RSFC patterns in adults. In *APOE*-ε4 carriers compared to non-carriers, the most consistent result across adulthood was decreased connectivity in the precuneus/ posterior cingulate, with the exception of one study showing an increase (Matura et al., 2014). This result is consistent with the observation that AD patients also show disruption of connectivity in the same regions (Mevel et al., 2011). This suggests that *APOE*-ε4 may affect the precuneus/posterior cingulate cortex connectivity very early in the disease process. In addition, increases in DMN connectivity within the MTL and hippocampus may be due to the existence of potential compensatory mechanisms in *APOE*-ε4 carriers that may be located in various regions within the DMN. There is evidence to show that cognitive reserve, which relates to the capacity of the brain to cope with neuropathology, modulates the effect of *APOE*-ε4 on brain function (Mevel et al., 2011; Stern, 2002). Other resting-brain functional connectivity patterns associated with *APOE*-ε4 seem to have distinct effects in young, middle-aged, and older age groups. Antagonistic pleiotropy, which is a concept positing that certain genes may influence survival differently at different stages in life, may be able to account for the variations in the results observed between these genetic studies (Tuminello and Han, 2011). More specifically, it seems that younger *APOE*-ε4 carriers exhibit compensatory neural mechanisms whereas *APOE*-ε4 has deleterious effects at older ages (Tuminello and Han, 2011). The relationships between other AD risk genes, including *CLU*, *BIN1*, *PICALM*, *KIBRA*, and *SORL1*, and RSFC is inconclusive due to the limited number of studies, most of which have been performed in Chinese cohorts.

Findings from a GWAS investigating imaging phenotypes found several SNPs to be associated with RSFC measures (Elliott et al., 2018). A reported variant for middle temporal sulcus nodes and edges, rs35124509, is a non-synonymous SNP located in the EPH Receptor A3 (*EPHA3*) gene and is also an eQTL for *EPHA3*. Notably, the product of this gene has been associated with the regulation of cell migration, axon guidance, and trans-axonal signaling (Gallarda et al., 2008; Shi et al., 2010). Another SNP identified from the RSFC GWAS, namely rs2279829 (Elliott et al., 2018), which is located in the 3' untranslated region of the gene *ZIC4*, has been linked to brain development and is associated with parietal lobe volume and a rare brain disease, Dandy-Walker Malformation (van der Lee et al., 2019). SNPs close to or located in other genes were also identified, including *PLCE1*, *NR2F1*-AS1 and *INPP5A*. Many of these polymorphisms had not been previously identified in regards to RSFC measures or other neuroimaging/brain phenotypes. Identification of these variants may have implications in the maintenance and/or disruption of RSFC observed across adulthood.

Epigenetics is an emerging field in the study of brain function. Thus

far, there have only been two studies that investigated the relationship between epigenetic variation and RSFC (Ismaylova et al., 2017; Muehlhan et al., 2015). Their findings showed that variation in DNA methylation in the *SLC64A* gene promoter was associated with connectivity patterns (Ismaylova et al., 2017; Muehlhan et al., 2015). More studies on epigenetic mechanisms are necessary to improve our understanding of the contribution of epigenetic factors underlying the functional organisation of the brain.

Methodological considerations are important to understand the significance of the findings of this review. Firstly, there is considerable heterogeneity in the way functional connectivity in rs-fMRI is defined and analysed. This may, in part, account for the mixed findings observed. For instance, Hayasaka and Laurienti (2010) demonstrated that small-worldness may be better approximated using single voxel seeds instead of larger ROI seeds as voxel-based networks had higher relative clustering than using region-based networks. This implies that different resting-state functional connectivity analysis methods may result in disparate findings (Cole et al., 2010). Additionally, parcellation methods, which include anatomical (e.g. automated anatomical labelling), cytoarchitecture (e.g. Brodmann areas), random, and connectivity-based parcellations, are another source of this heterogeneity. Although there is evidence to show that connectivity-driven parcellations better reflect the underlying rs-fMRI connectivity compared to the other methods, to date, there has not been a gold standard parcellation method for the generation and evaluation of resting-state functional connectivity (Arslan et al., 2018). Furthermore, most previous studies studying genetics of functional connectivity using the graph theory approach used binarised connectivity matrices (i.e. presence or absence of edge). However, this precludes the information about variations in connectivity weights between the functional networks (Markov et al., 2013). Secondly, most studies investigating the genetic influence on resting-brain functional connectivity are cross-sectional in nature. This precludes the understanding of how genetics may affect the trajectory of RSFC across the adult lifespan as well as whether the observed connectivity patterns were ageing-related or subclinical disease related. Thirdly, sample characteristics, such as sample size and ethnic heterogeneity, are important considerations in imaging genetics. Gaining sufficient effect sizes to detect the true genotypic effect on brain functional connectivity is important. As allele frequencies can differ between ethnic populations, accounting for ancestral heritage is imperative to avoid spurious associations between a polymorphism and imaging phenotype (Casey et al., 2010). Consequently, these considerations may have effect the reproducibility of findings across different studies.

5. Conclusion and future directions

Connectome genetics is a relatively new and growing field which offers a promising approach for elucidating the biological mechanisms underlying the functional organisation of the brain.

The current connectome literature has a number of limitations. One suggestion that emerged from our review is that the limitations of parcellation methods may be overcome by a recent method known as "gradient analysis" in rs-fMRI. This method estimates and delineates continuous changes in functional connectivity patterns across neighbouring voxels within a region of interest (O'Rawe et al., 2019). Another novel imaging method is multiscale network analysis that can study the brain networks at different spatial and temporal resolution from neurons to large-scale brain areas (Betzel and Bassett, 2017). This allows for the comprehensive study of the network architecture and how it varies over ageing.

Using genetics to investigate the connectome may provide a better understanding of the underlying biological mechanisms contributing to the ageing brain. However, comprehensive modeling of the whole-brain and genome-wide data remains challenging due to the statistical and computational difficulties (Thompson et al., 2013). To address this issue, some studies used a-priori biological information, such as examining candidate genes and biological pathways. However, this precludes the discovery of new genes associated with functional networks. In order to perform GWAS on RSFC, statistical methodologies of data reduction on imaging analysis can be performed. For instance, instead of binary connectivity matrix in graph theory analysis, using weighted connectivity matrix will not only provide a more holistic representation of the functional brain networks, it allows for a more streamlined genetics analysis. Rather than performing GWAS on all different thresholds associated with binary matrices, it might be more computationally feasible to run GWAS on a single weighted matrix. Importantly, there is a greater need for statistically and computationally powerful methods in order to cope with the high dimensionality of the imaging and genetics data and their covariates. Also, the increasing availability of whole genome sequencing data will add additional computational burden.

Publicly available population-based datasets that include both genetics/epigenetics and imaging data are important to advance the field. It not only allows for better quality control and integrity of the data; it also provides researchers with the ability to replicate findings from other studies. Harmonisation of methods across studies by collaboration between research groups or through neuroimaging/genetic consortiums may prove fruitful in facilitating more consistent results across studies and advancing the field.

Future work should be longitudinal with comprehensive phenotyping and careful consideration of the neuroimaging methods used to examine how ageing-related changes in functional connectivity are influenced by genetic and epigenetic factors, and whether this is related to age-related disease.

Financial support and sponsorship

This research did not receive any specific grant from funding agencies in the public, commercial, or not-for-profit sectors.

Declaration of Competing Interest

There are no conflicts of interests.

Acknowledgement

Many thanks to the UNSW Scientia Scholarship Program for their support to HF.

Appendix A. Supplementary data

Supplementary material related to this article can be found, in the online version, at doi:https://doi.org/10.1016/j.neubiorev.2020.03.011.

References

Achard, S., Bullmore, E., 2007. Efficiency and cost of economical brain functional networks. PLoS Comput. Biol. 3, e17. https://doi.org/10.1371/journal.pcbi.0030017.

Adhikari, B.M., Jahanshad, N., Shukla, D., Glahn, D.C., Blangero, J., Fox, P.T., Reynolds, R.C., Cox, R.W., Fieremans, E., Veraart, J., Novikov, D.S., Nichols, T.E., Hong, L.E., Thompson, P.M., Kochunov, P., 2018. Comparison of heritability estimates on resting state fMRI connectivity phenotypes using the ENIGMA analysis pipeline. Hum. Brain Mapp. 39, 4893–4902. https://doi.org/10.1002/hbm.24331.

Arslan, S., Ktena, S.I., Makropoulos, A., Robinson, E.C., Rueckert, D., Parisot, S., 2018. Human brain mapping: a systematic comparison of parcellation methods for the human cerebral cortex. NeuroImage 170, 5–30. https://doi.org/10.1016/j.neuroimage.2017.04.014.

Betzel, R.F., Bassett, D.S., 2017. Multi-scale brain networks. Neuroimage 160, 73–83. https://doi.org/10.1016/j.neuroimage.2016.11.006.

Brody, B.A., Kinney, H.C., Kloman, A.S., Gilles, F.H., 1987. Sequence of central nervous system myelination in human infancy. I. An autopsy study of myelination. J. Neuropathol. Exp. Neurol. 46, 283–301.

Buckner, R.L., 2004. Memory and executive function in aging and AD: multiple factors that cause decline and reserve factors that compensate. Neuron 44, 195–208. https://

doi.org/10.1016/j.neuron.2004.09.006.
Burke, S.N., Barnes, C.A., 2006. Neural plasticity in the ageing brain. Nature reviews. Neuroscience 7, 30–40. https://doi.org/10.1038/nrn1809.
Cai, S., Jiang, Y., Wang, Y., Wu, X., Ren, J., Lee, M.S., Lee, S., Huang, L., 2017. Modulation on brain gray matter activity and white matter integrity by APOE ε4 risk gene in cognitively intact elderly: a multimodal neuroimaging study. Behav. Brain Res. 322, 100–109. https://doi.org/10.1016/j.bbr.2017.01.027.
Casey, B.J., Soliman, F., Bath, K.G., Glatt, C.E., 2010. Imaging genetics and development: challenges and promises. Hum. Brain Mapp. 31, 838–851. https://doi.org/10.1002/hbm.21047.
Chan, M.Y., Park, D.C., Savalia, N.K., Petersen, S.E., Wig, G.S., 2014. Decreased segregation of brain systems across the healthy adult lifespan. Proc. Natl. Acad. Sci. 111, E4997. https://doi.org/10.1073/pnas.1415122111.
Chen, Y., Chen, K., Zhang, J., Li, X., Shu, N., Wang, J., Zhang, Z., Reiman, E.M., 2015. Disrupted functional and structural networks in cognitively normal elderly subjects with the APOE varepsilon4 allele. Neuropsychopharmacology 40, 1181–1191. https://doi.org/10.1038/npp.2014.302.
Chiesa, P.A., Cavedo, E., Lista, S., Thompson, P.M., Hampel, H., 2017. Revolution of resting-state functional neuroimaging genetics in Alzheimer's disease. Trends Neurosci. 40, 469–480. https://doi.org/10.1016/j.tins.2017.06.002.
Choi, S.W., Mak, T.S.H., Reilly, P., 2018. A guide to performing polygenic risk score analyses. bioRxiv 416545. https://doi.org/10.1101/416545.
Colclough, G.L., Smith, S.M., Nichols, T.E., Winkler, A.M., Sotiropoulos, S.N., Glasser, M.F., Van Essen, D.C., Woolrich, M.W., 2017. The heritability of multi-modal connectivity in human brain activity. eLife 6, e20178. https://doi.org/10.7554/eLife.20178.
Cole, D.M., Smith, S.M., Beckmann, C.F., 2010. Advances and pitfalls in the analysis and interpretation of resting-state FMRI data. Front. Syst. Neurosci. 4https://doi.org/10.3389/fnsys.2010.00008. 8-8.
D'Angelo, G.M., Lazar, N.A., Zhou, G., Eddy, W.F., Morris, J.C., Sheline, Y.I., 2012. Bootstrapping GEE models for fMRI regional connectivity. NeuroImage 63, 1890–1900. https://doi.org/10.1016/j.neuroimage.2012.08.036.
Damoiseaux, J.S., 2017. Effects of aging on functional and structural brain connectivity. NeuroImage 160, 32–40. https://doi.org/10.1016/j.neuroimage.2017.01.077.
Damoiseaux, J.S., Seeley, W.W., Zhou, J., Shirer, W.R., Coppola, G., Karydas, A., Rosen, H.J., Miller, B.L., Kramer, J.H., Greicius, M.D., 2012. Gender modulates the APOE epsilon4 effect in healthy older adults: convergent evidence from functional brain connectivity and spinal fluid tau levels. J. Neurosci. 32, 8254–8262. https://doi.org/10.1523/jneurosci.0305-12.2012.
Dennis, E.L., Thompson, P.M., 2014. Functional brain connectivity using fMRI in aging and Alzheimer's disease. Neuropsychol. Rev. 24, 49–62. https://doi.org/10.1007/s11065-014-9249-6.
Dennis, E.L., Jahanshad, N., McMahon, K.L., de Zubicaray, G.I., Martin, N.G., Hickie, I.B., Toga, A.W., Wright, M.J., Thompson, P.M., 2013. Development of brain structural connectivity between ages 12 and 30: a 4-Tesla diffusion imaging study in 439 adolescents and adults. NeuroImage 64, 671–684. https://doi.org/10.1016/j.neuroimage.2012.09.004.
Dennis, E.L., Thompson, P.M., Jahanshad, N., 2019. Genetics of brain networks and connectivity. Chapter 8 In: Munsell, B.C., Wu, G., Bonilha, L., Laurienti, P.J. (Eds.), Connectomics. Academic Press, pp. 155–179.
DiBattista, A.M., Dumanis, S.B., Newman, J., Rebeck, G.W., 2016. Identification and modification of amyloid-independent phenotypes of APOE4 mice. Exp Neurol. 280, 97–105. https://doi.org/10.1016/j.expneurol.2016.04.014. In press.
Dowell, N.G., Evans, S.L., Tofts, P.S., King, S.L., Tabet, N., Rusted, J.M., 2016. Structural and resting-state MRI detects regional brain differences in young and mid-age healthy APOE-e4 carriers compared with non-APOE-e4 carriers. NMR Biomed. 29, 614–624. https://doi.org/10.1002/nbm.3502.
Elliott, L.T., Sharp, K., Alfaro-Almagro, F., Shi, S., Miller, K.L., Douaud, G., Marchini, J., Smith, S.M., 2018. Genome-wide association studies of brain imaging phenotypes in UK Biobank. Nature 562, 210–216. https://doi.org/10.1038/s41586-018-0571-7.
Elliott, M.L., Knodt, A.R., Cooke, M., Kim, M.J., Melzer, T.R., Keenan, R., Ireland, D., Ramrakha, S., Poulton, R., Caspi, A., Moffitt, T.E., Hariri, A.R., 2019. General Functional Connectivity: shared features of resting-state and task fMRI drive reliable and heritable individual differences in functional brain networks. bioRxiv 330530. https://doi.org/10.1101/330530.
Farrer, L.A., Cupples, L.A., Haines, J.L., Hyman, B., Kukull, W.A., Mayeux, R., Myers, R.H., Pericak-Vance, M.A., Risch, N., van Duijn, C.M., 1997. Effects of age, sex, and ethnicity on the association between apolipoprotein E genotype and Alzheimer disease. A meta-analysis. APOE and Alzheimer Disease Meta Analysis Consortium. Jama 278, 1349–1356.
Filippini, N., MacIntosh, B.J., Hough, M.G., Goodwin, G.M., Frisoni, G.B., Smith, S.M., Matthews, P.M., Beckmann, C.F., Mackay, C.E., 2009. Distinct patterns of brain activity in young carriers of the APOE-epsilon4 allele. Proc. Natl. Acad. Sci. U.S.A. 106, 7209–7214. https://doi.org/10.1073/pnas.0811879106.
Fornito, A., Zalesky, A., Bassett, D.S., Meunier, D., Ellison-Wright, I., Yucel, M., Wood, S.J., Shaw, K., O'Connor, J., Nertney, D., Mowry, B.J., Pantelis, C., Bullmore, E.T., 2011. Genetic influences on cost-efficient organization of human cortical functional networks. J. Neurosci. 31, 3261–3270. https://doi.org/10.1523/jneurosci.4858-10.2011.
Gallarda, B.W., Bonanomi, D., Müller, D., Brown, A., Alaynick, W.A., Andrews, S.E., Lemke, G., Pfaff, S.L., Marguardt, T., 2008. Segregation of axial motor and sensory pathways via heterotypic trans-axonal signaling. Science 320, 233–236. https://doi.org/10.1126/science.1153758.
Gatz, M., Reynolds, C.A., Fratiglioni, L., Johansson, B., Mortimer, J.A., Berg, S., Fiske, A., Pedersen, N.L., 2006. Role of genes and environments for explaining Alzheimer disease. Arch. Gen. Psychiatry 63, 168–174. https://doi.org/10.1001/archpsyc.63.2.168.
Ge, T., Holmes, A.J., Buckner, R.L., Smoller, J.W., Sabuncu, M.R., 2017. Heritability analysis with repeat measurements and its application to resting-state functional connectivity. Proc. Natl. Acad. Sci. U.S.A. 114, 5521–5526. https://doi.org/10.1073/pnas.1700765114.
Geerligs, L., Renken, R.J., Saliasi, E., Maurits, N.M., Lorist, M.M., 2015. A brain-wide study of age-related changes in functional connectivity. Cereb. Cortex 25, 1987–1999. https://doi.org/10.1093/cercor/bhu012.
Glahn, D.C., Winkler, A.M., Kochunov, P., Almasy, L., Duggirala, R., Carless, M.A., Curran, J.C., Olvera, R.L., Laird, A.R., Smith, S.M., Beckmann, C.F., Fox, P.T., Blangero, J., 2010. Genetic control over the resting brain. Proc. Natl. Acad. Sci. 107, 1223. https://doi.org/10.1073/pnas.0909969107.
Gong, G., Rosa-Neto, P., Carbonell, F., Chen, Z.J., He, Y., Evans, A.C., 2009. Age- and gender-related differences in the cortical anatomical network. J. Neurosci. 29, 15684. https://doi.org/10.1523/JNEUROSCI.2308-09.2009.
Goveas, J.S., Xie, C., Chen, G., Li, W., Ward, B.D., Franczak, M.B., Jones, J.L., Antuono, P.G., Li, S.J., 2013. Functional network endophenotypes unravel the effects of apolipoprotein E epsilon 4 in middle-aged adults. PLoS One 8, e55902. https://doi.org/10.1371/journal.pone.0055902.
Grayson, D.S., Fair, D.A., 2017. Development of large-scale functional networks from birth to adulthood: a guide to the neuroimaging literature. NeuroImage 160, 15–31. https://doi.org/10.1016/j.neuroimage.2017.01.079.
Hagmann, P., Cammoun, L., Gigandet, X., Meuli, R., Honey, C.J., Wedeen, V.J., Sporns, O., 2008. Mapping the structural core of human cerebral cortex. PLoS Biol. 6, e159. https://doi.org/10.1371/journal.pbio.0060159.
Hayasaka, S., Laurienti, P.J., 2010. Comparison of characteristics between region-and voxel-based network analyses in resting-state fMRI data. Neuroimage 1, 499–508. https://doi.org/10.1016/j.neuroimage.2009.12.051.
Heise, V., Filippini, N., Trachtenberg, A.J., Suri, S., Ebmeier, K.P., Mackay, C.E., 2014. Apolipoprotein E genotype, gender and age modulate connectivity of the hippocampus in healthy adults. NeuroImage 98, 23–30. https://doi.org/10.1016/j.neuroimage.2014.04.081.
Huang, Y., Mahley, R.W., 2014. Apolipoprotein E: structure and function in lipid metabolism, neurobiology, and Alzheimer's diseases. Neurobiol. Dis. 72 (Pt A), 3–12. https://doi.org/10.1016/j.nbd.2014.08.025.
Huang, C.C., Hsieh, W.J., Lee, P.L., Peng, L.N., Liu, L.K., Lee, W.J., Huang, J.K., Chen, L.K., Lin, C.P., 2015. Age-related changes in resting-state networks of a large sample size of healthy elderly. CNS Neurosci. Ther. 21, 817–825. https://doi.org/10.1111/cns.12396.
Huttenlocher, P.R., 1979. Synaptic density in human frontal cortex - developmental changes and effects of aging. Brain Res. 163, 195–205.
Hwang, J.Y., Aromolaran, K.A., Zukin, R.S., 2017. The emerging field of epigenetics in neurodegeneration and neuroprotection. Nature reviews. Neuroscience 18, 347–361. https://doi.org/10.1038/nrn.2017.46.
Ismaylova, E., Di Sante, J., Szyf, M., Nemoda, Z., Yu, W.J., Pomares, F.B., Turecki, G., Gobbi, G., Vitaro, F., Tremblay, R.E., Booij, L., 2017. Serotonin transporter gene promoter methylation in peripheral cells in healthy adults: neural correlates and tissue specificity. Eur. Neuropsychopharmacol. 27, 1032–1041. https://doi.org/10.1016/j.euroneuro.2017.07.005.
Jiang, P., Vuontela, V., Tokariev, M., Lin, H., Aronen, E.T., Ma, Y.Y., Carlson, S., 2018. Functional connectivity of intrinsic cognitive networks during resting state and task performance in preadolescent children. PLoS One 13, e0205690. https://doi.org/10.1371/journal.pone.0205690.
Kanchibhotla, S.C., Mather, K.A., Wen, W., Schofield, P.R., Kwok, J.B., Sachdev, P.S., 2013. Genetics of ageing-related changes in brain white matter integrity - a review. Ageing Res. Rev. 12, 391–401. https://doi.org/10.1016/j.arr.2012.10.003.
Karch, C.M., Goate, A.M., 2015. Alzheimer's disease risk genes and mechanisms of disease pathogenesis. Biol. Psychiatry 77, 43–51. https://doi.org/10.1016/j.biopsych.2014.05.006.
Korgaonkar, M.S., Ram, K., Williams, L.M., Gatt, J.M., Grieve, S.M., 2014. Establishing the resting state default mode network derived from functional magnetic resonance imaging tasks as an endophenotype: a twins study. Hum. Brain Mapp. 35, 3893–3902. https://doi.org/10.1002/hbm.22446.
Korthauer, L.E., Zhan, L., Ajilore, O., Leow, A., Driscoll, I., 2018. Disrupted topology of the resting state structural connectome in middle-aged APOE epsilon4 carriers. NeuroImage 178, 295–305. https://doi.org/10.1016/j.neuroimage.2018.05.052.
Lam, D., Ancelin, M.L., Ritchie, K., Freak-Poli, R., Saffery, R., Ryan, J., 2018. Genotype-dependent associations between serotonin transporter gene (SLC6A4) DNA methylation and late-life depression. BMC Psychiatry 18, 282–291. https://doi.org/10.1186/s12888-018-1850-4.
Lee, M.H., Smyser, C.D., Shimony, J.S., 2013. Resting-state fMRI: a review of methods and clinical applications. AJNR Am. J. Neuroradiol. 34, 1866–1872. https://doi.org/10.3174/ajnr.A3263.
Li, W., Antuono, P.G., Xie, C., Chen, G., Jones, J.L., Ward, B.D., Singh, S.P., Franczak, M.B., Goveas, J.S., Li, S.J., 2014. Aberrant functional connectivity in Papez circuit correlates with memory performance in cognitively intact middle-aged APOE4 carriers. Cortex 57, 167–176. https://doi.org/10.1016/j.cortex.2014.04.006.
Liang, Y., Li, Z., Wei, J., Li, C., Zhang, X., Neuroimaging Initiative, A.D., 2017. Frequency specific effects of ApoE epsilon4 allele on resting-state networks in nondemented elders. Biomed Res. Int. 2017, 9823501. https://doi.org/10.1155/2017/9823501.
Liu, Z., Dai, X., Zhang, J., Li, X., Chen, Y., Ma, C., Chen, K., Peng, D., Zhang, Z., 2018. The interactive effects of age and PICALM rs541458 polymorphism on cognitive performance, brain structure, and function in non-demented elderly. Mol. Neurobiol. 55, 1271–1283. https://doi.org/10.1007/s12035-016-0358-5.
Lu, H., Ma, S.L., Wong, S.W., Tam, C.W., Cheng, S.T., Chan, S.S., Lam, L.C., 2017. Aberrant interhemispheric functional connectivity within default mode network and

its relationships with neurocognitive features in cognitively normal APOE epsilon 4 elderly carriers. Int. Psychogeriatr. 29, 805–814. https://doi.org/10.1017/s1041610216002477.
Luo, X., Qiu, T., Xu, X., Huang, P., Gu, Q., Shen, Z., Yu, X., Jia, Y., Guan, X., Song, R., Zhang, M., 2016. Decreased inter-hemispheric functional connectivity in cognitively intact elderly APOE varepsilon4 carriers: a preliminary study. J. Alzheimers Dis. 50, 1137–1148. https://doi.org/10.3233/jad-150989.
Luo, X., Qiu, T., Jia, Y., Huang, P., Xu, X., Yu, X., Shen, Z., Jiaerken, Y., Guan, X., Zhou, J., Zhang, M., 2017. Intrinsic functional connectivity alterations in cognitively intact elderly APOE epsilon4 carriers measured by eigenvector centrality mapping are related to cognition and CSF biomarkers: a preliminary study. Brain Imaging Behav. 11, 1290–1301. https://doi.org/10.1007/s11682-016-9600-z.
Lv, H., Wang, Z., Tong, E., Williams, L.M., Zaharchuk, G., Zeineh, M., Goldstein-Piekarski, A.N., Ball, T.M., Liao, C., Wintermark, M., 2018. Resting-state functional MRI: everything that nonexperts have always wanted to know. AJNR Am. J. Neuroradiol. 39, 1390–1399. https://doi.org/10.3174/ajnr.A5527.
Ma, C., Zhang, Y., Li, X., Chen, Y., Zhang, J., Liu, Z., Chen, K., Zhang, Z., 2016. The TT allele of rs405509 synergizes with APOE epsilon4 in the impairment of cognition and its underlying default mode network in non-demented elderly. Curr. Alzheimer Res. 13, 708–717.
Machulda, M.M., Jones, D.T., Vemuri, P., McDade, E., Avula, R., Przybelski, S., Boeve, B.F., Knopman, D.S., Petersen, R.C., Jack Jr., C.R., 2011. Effect of APOE epsilon4 status on intrinsic network connectivity in cognitively normal elderly subjects. Arch. Neurol. 68, 1131–1136. https://doi.org/10.1001/archneurol.2011.108.
Markov, N.T., Ercsey-Ravasz, M., Lamy, C., Gomes, A.R., Magrou, L., Misery, P., Giroud, P., Barone, P., Dehay, C., Toroczkai, Z., Knoblauch, K., Van Essen, D.C., Kenndey, H., 2013. The role of long-range connections on specificity of the macque interareal cortial network. Proc. Natl. Acad. Sci. U.S.A. 110, 5187–5192. https://doi.org/10.1073/pnas.1218972110.
Matura, S., Prvulovic, D., Butz, M., Hartmann, D., Sepanski, B., Linnemann, K., Oertel-Knochel, V., Karakaya, T., Fusser, F., Pantel, J., van de Ven, V., 2014. Recognition memory is associated with altered resting-state functional connectivity in people at genetic risk for Alzheimer's disease. Eur. J. Neurosci. 40, 3128–3135. https://doi.org/10.1111/ejn.12659.
Mauch, D.H., Nagler, K., Schumacher, S., Goritz, C., Muller, E.C., Otto, A., Pfrieger, F.W., 2001. CNS synaptogenesis promoted by glia-derived cholesterol. Science 294, 1354–1357. https://doi.org/10.1126/science.294.5545.1354.
Mayhew, A.J., Meyre, D., 2017. Assessing the heritability of complex traits in humans: methodological challenges and opportunities. Curr. Genomics 18, 332–340. https://doi.org/10.2174/1389202918666170307161450.
McKenna, F., Koo, B.B., Killiany, R., 2016. Comparison of ApoE-related brain connectivity differences in early MCI and normal aging populations: an fMRI study. Brain Imaging Behav. 10, 970–983. https://doi.org/10.1007/s11682-015-9451-z.
Meunier, D., Achard, S., Morcom, A., Bullmore, E., 2009. Age-related changes in modular organization of human brain functional networks. NeuroImage 44, 715–723. https://doi.org/10.1016/j.neuroimage.2008.09.062.
Mevel, K., Chételat, G., Eustache, F., Desgranges, B., 2011. The default mode network in healthy aging and Alzheimer's disease. Int. J. Alzheimers Dis. 2011.
Miranda-Dominguez, O., Feczko, E., Grayson, D.S., Walum, H., Nigg, J.T., Fair, D.A., 2017. Heritability of the human connectome: a connectotyping study. Netw. Neurosci. 2, 175–199. https://doi.org/10.1162/netn_a_00029.
Montembeault, M., Joubert, S., Doyon, J., Carrier, J., Gagnon, J.F., Monchi, O., Lungu, O., Belleville, S., Brambati, S.M., 2012. The impact of aging on gray matter structural covariance networks. NeuroImage 63, 754–759. https://doi.org/10.1016/j.neuroimage.2012.06.052.
Muehlhan, M., Kirschbaum, C., Wittchen, H.U., Alexander, N., 2015. Epigenetic variation in the serotonin transporter gene predicts resting state functional connectivity strength within the salience-network. Hum. Brain Mapp. 36, 4361–4371. https://doi.org/10.1002/hbm.22923.
Ng, K.K., Qiu, Y., Lo, J.C., Koay, E.S., Koh, W.P., Chee, M.W., Zhou, J., 2018. Functional segregation loss over time is moderated by APOE genotype in healthy elderly. Hum. Brain Mapp. 39, 2742–2752. https://doi.org/10.1002/hbm.24036.
O'Rawe, J.F., Ide, J.S., Leung, H.C., 2019. Model testing for distinctive functional connectivity gradients with resting-state fMRI data. NeuroImage 185, 102–110. https://doi.org/10.1016/j.neuroimage.2018.10.022.
Onoda, K., Ishihara, M., Yamaguchi, S., 2012. Decreased functional connectivity by aging is associated with cognitive decline. J. Cogn. Neurosci. 24, 2186–2198. https://doi.org/10.1162/jocn_a_00269.
Otte, W.M., van Diessen, E., Paul, S., Ramaswamy, R., Subramanyam Rallabandi, V.P., Stam, C.J., Roy, P.K., 2015. Aging alterations in whole-brain networks during adulthood mapped with the minimum spanning tree indices: the interplay of density, connectivity cost and life-time trajectory. NeuroImage 109, 171–189. https://doi.org/10.1016/j.neuroimage.2015.01.011.
Papenberg, G., Lindenberger, U., Backman, L., 2015. Aging-related magnification of genetic effects on cognitive and brain integrity. Trends Cogn. Sci. 19, 506–514. https://doi.org/10.1016/j.tics.2015.06.008.
Patel, K.T., Stevens, M.C., Pearlson, G.D., Winkler, A.M., Hawkins, K.A., Skudlarski, P., Bauer, L.O., 2013. Default mode network activity and white matter integrity in healthy middle-aged ApoE4 carriers. Brain Imaging Behav. 7, 60–67. https://doi.org/10.1007/s11682-012-9187-y.
Patnala, R., Clements, J., Batra, J., 2013. Candidate gene association studies: a comprehensive guide to useful in silico tools. BMC Genet. 14, 39. https://doi.org/10.1186/1471-2156-14-39.
Perry, A., Wen, W., Lord, A., Thalamuthu, A., Roberts, G., Mitchell, P.B., Sachdev, P.S., Breakspear, M., 2015. The organisation of the elderly connectome. NeuroImage 114, 414–426. https://doi.org/10.1016/j.neuroimage.2015.04.009.
Power, J.D., Fair, D.A., Schlaggar, B.L., Petersen, S.E., 2010. The development of human functional brain networks. Neuron 67, 735–748. https://doi.org/10.1016/j.neuron.2010.08.017.
Quevenco, F.C., Preti, M.G., van Bergen, J.M., Hua, J., Wyss, M., Li, X., Schreiner, S.J., Steininger, S.C., Meyer, R., Meier, I.B., Brickman, A.M., Leh, S.E., Gietl, A.F., Buck, A., Nitsch, R.M., Pruessmann, K.P., van Zijl, P.C., Hock, C., Van De Ville, D., Unschuld, P.G., 2017. Memory performance-related dynamic brain connectivity indicates pathological burden and genetic risk for Alzheimer's disease. Alzheimers Res. Ther. 9, 24. https://doi.org/10.1186/s13195-017-0249-7.
Reineberg, A.E., Hatoum, A.S., Hewitt, J.K., Banich, M.T., Friedman, N.P., 2018. Genetic and environmental influence on the human functional connectome. bioRxiv 277996. https://doi.org/10.1101/277996.
Rosazza, C., Minati, L., 2011. Resting-state brain networks: literature review and clinical applications. Neurol. Sci. 32, 773–785. https://doi.org/10.1007/s10072-011-0636-y.
Rubinov, M., Sporns, O., 2010. Complex network measures of brain connectivity: uses and interpretations. NeuroImage 52, 1059–1069. https://doi.org/10.1016/j.neuroimage.2009.10.003.
Sheline, Y.I., Morris, J.C., Snyder, A.Z., Price, J.L., Yan, Z., D'Angelo, G., Liu, C., Dixit, S., Benzinger, T., Fagan, A., Goate, A., Mintun, M.A., 2010. APOE4 allele disrupts resting state fMRI connectivity in the absence of amyloid plaques or decreased CSF Abeta42. J. Neurosci. 30, 17035–17040. https://doi.org/10.1523/jneurosci.3987-10.2010.
Shen, J., Zhang, P., Liu, H., Xu, L., Xu, J., Qin, W., Liu, B., Jiang, T., Yu, C., 2016. Modulation effect of the SORL1 gene on functional connectivity density in healthy young adults. Brain Struct. Funct. 221, 4103–4110. https://doi.org/10.1007/s00429-015-1149-x.
Shen, J., Qin, W., Xu, Q., Xu, L., Xu, J., Zhang, P., Liu, H., Liu, B., Jiang, T., Yu, C., 2017. Modulation of APOE and SORL1 genes on hippocampal functional connectivity in healthy young adults. Brain Struct. Funct. 222, 2877–2889. https://doi.org/10.1007/s00429-017-1377-3.
Shi, G.F., Yue, G., Zhou, R.P., 2010. EphA3 functions are regulated by collaborating phosphotyrosine residues. Cell Res. 20, 1263–1275. https://doi.org/10.1038/cr.2010.11.
Shu, H., Shi, Y., Chen, G., Wang, Z., Liu, D., Yue, C., Ward, B.D., Li, W., Xu, Z., Chen, G., Guo, Q., Xu, J., Li, S.-J., Zhang, Z., 2016. Opposite neural trajectories of apolipoprotein e ε4 and ε2 alleles with aging associated with different risks of alzheimer's disease. Cereb. Cortex 26, 1421–1429. https://doi.org/10.1093/cercor/bhu237.
Sierra, M.I., Fernandez, A.F., Fraga, M.F., 2015. Epigenetics of aging. Curr. Genomics 16, 435–440. https://doi.org/10.2174/1389202916666150817203459.
Sinclair, B., Hansell, N.K., Blokland, G.A., Martin, N.G., Thompson, P.M., Breakspear, M., de Zubicaray, G.I., Wright, M.J., McMahon, K.L., 2015. Heritability of the network architecture of intrinsic brain functional connectivity. NeuroImage 121, 243–252. https://doi.org/10.1016/j.neuroimage.2015.07.048.
Song, H., Long, H., Zuo, X., Yu, C., Liu, B., Wang, Z., Wang, Q., Wang, F., Han, Y., Jia, J., 2015. APOE effects on default mode network in chinese cognitive normal elderly: relationship with clinical cognitive performance. PLoS One 10, e0133179. https://doi.org/10.1371/journal.pone.0133179.
Speed, D., Cai, N., The, U.C, Johnson, M.R., Nejentsev, S., Balding, D.J., 2017. Reevaluation of SNP heritability in complex human traits. Nat. Genet. 49, 986. https://doi.org/10.1038/ng.3865.
Spreng, R.N., Schacter, D.L., 2012. Default network modulation and large-scale network interactivity in healthy young and old adults. Cereb. Cortex 22, 2610–2621. https://doi.org/10.1093/cercor/bhr339.
Staffaroni, A.M., Brown, J.A., Casaletto, K.B., Elahi, F.M., Deng, J., Neuhaus, J., Cobigo, Y., Mumford, P.S., Walters, S., Saloner, R., Karydas, A., Coppola, G., Rosen, H.J., Miller, B.L., Seeley, W.W., Kramer, J.H., 2018. The longitudinal trajectory of default mode network connectivity in healthy older adults varies As a function of age and is associated with changes in episodic memory and processing speed. J. Neurosci. 38, 2809–2817. https://doi.org/10.1523/jneurosci.3067-17.2018.
Stern, Y., 2002. What is cognitive reserve? Theory and research application of the reserve concept. J. Int. Neuropsychol. Soc. 8, 448–460.
Su, Y.Y., Liang, X., Schoepf, U.J., Varga-Szemes, A., West, H.C., Qi, R., Kong, X., Chen, H.J., Lu, G.M., Zhang, L.J., 2015. APOE polymorphism affects brain default mode network in healthy young adults: a STROBE article. Medicine 94, e1734. https://doi.org/10.1097/md.0000000000001734.
Su, Y.Y., Zhang, X.D., Schoepf, U.J., Varga-Szemes, A., Stubenrauch, A., Liang, X., Zheng, L.J., Zheng, G., Kong, X., Xu, Q., Wang, S.J., Qi, R.F., Lu, G.M., Zhang, L.J., 2017. Lower functional connectivity of default mode network in cognitively normal young adults with mutation of APP, presenilins and APOE epsilon4. Brain Imaging Behav. 11, 818–828. https://doi.org/10.1007/s11682-016-9556-z.
Thompson, P.M., Ge, T., Glahn, D.C., Jahanshad, N., Nichols, T.E., 2013. Genetics of the connectome. NeuroImage 80, 475–488. https://doi.org/10.1016/j.neuroimage.2013.05.013.
Trachtenberg, A.J., Filippini, N., Ebmeier, K.P., Smith, S.M., Karpe, F., Mackay, C.E., 2012. The effects of APOE on the functional architecture of the resting brain. NeuroImage 59, 565–572. https://doi.org/10.1016/j.neuroimage.2011.07.059.
Tuminello, E.R., Han, S.D., 2011. The apolipoprotein E antagonistic pleitropy hypothesis: review and recommendations. Int. J. Alzheimers Dis. 726197, 1–12. https://doi.org/10.4061/2011/726197.
van den Heuvel, M.P., Hulshoff Pol, H.E., 2010. Exploring the brain network: a review on resting-state fMRI functional connectivity. Eur. Neuropsychopharmacol. 20, 519–534. https://doi.org/10.1016/j.euroneuro.2010.03.008.
van der Lee, S.J., Knol, M.J., Chauhan, G., Satizabal, C.L., Smith, A.V., Hofer, E., Bis, J.C., Hibar, D.P., Hilal, S., van den Akker, E.B., Arfanakis, K., Bernard, M., Yanek, L.R., Amin, N., Crivello, F., Cheung, J.W., Harris, T.B., Saba, Y., Lopez, O.L., Li, S., van der Grond, J., Yu, L., Paus, T., Roshchupkin, G.V., Amouyel, P., Jahanshad, N., Taylor, K.D., Yang, Q., Mathias, R.A., Boehringer, S., Mazoyer, B., Rice, K., Cheng, C.Y.,

Maillard, P., van Heemst, D., Wong, T.Y., Niessen, W.J., Beiser, A.S., Beekman, M., Zhao, W., Nyquist, P.A., Chen, C., Launer, L.J., Psaty, B.M., Ikram, M.K., Vernooij, M.W., Schmidt, H., Pausova, Z., Becker, D.M., De Jager, P.L., Thompson, P.M., van Duijn, C.M., Bennett, D.A., Slagboom, P.E., Schmidt, R., Longstreth, W.T., Ikram, M.A., Seshadri, S., Debette, S., Gudnason, V., Adams, H.H.H., DeCarli, C., 2019. A genome-wide association study identifies genetic loci associated with specific lobar brain volumes. Commun. Biol. 2, 285. https://doi.org/10.1038/s42003-019-0537-9.

Vantansever, D., Menon, D.K., Stamatakis, E.A., 2017. Default mode contributions to automated information processing. Proc. Natl. Acad. Sci. U.S.A. 114, 12821–12826. https://doi.org/10.1073/pnas.1710521114.

Visscher, P.M., Hill, W.G., Wray, N.R., 2008. Heritability in the genomics era — concepts and misconceptions. Nat. Rev. Genet. 9, 255. https://doi.org/10.1038/nrg2322.

Wang, L., Roe, C.M., Snyder, A.Z., Brier, M.R., Thomas, J.B., Xiong, C., Benzinger, T.L., Morris, J.C., Ances, B.M., 2012. Alzheimer disease family history impacts resting state functional connectivity. Ann. Neurol. 72, 571–577. https://doi.org/10.1002/ana.23643.

Wang, D., Liu, B., Qin, W., Wang, J., Zhang, Y., Jiang, T., Yu, C., 2013. KIBRA gene variants are associated with synchronization within the default-mode and executive control networks. NeuroImage 69, 213–222. https://doi.org/10.1016/j.neuroimage.2012.12.022.

Westlye, E.T., Lundervold, A., Rootwelt, H., Lundervold, A.J., Westlye, L.T., 2011. Increased hippocampal default mode synchronization during rest in middle-aged and elderly APOE epsilon4 carriers: relationships with memory performance. J. Neurosci. 31, 7775–7783. https://doi.org/10.1523/jneurosci.1230-11.2011.

Wink, A.M., Tijms, B.M., Ten Kate, M., Raspor, E., de Munck, J.C., Altena, E., Ecay-Torres, M., Clerigue, M., Estanga, A., Garcia-Sebastian, M., Izagirre, A., Martinez-Lage Alvarez, P., Villanua, J., Barkhof, F., Sanz-Arigita, E., 2018. Functional brain network centrality is related to APOE genotype in cognitively normal elderly. Brain Behav. 8, e01080. https://doi.org/10.1002/brb3.1080.

Witte, A.V., Kobe, T., Kerti, L., Rujescu, D., Floel, A., 2016. Impact of KIBRA polymorphism on memory function and the Hippocampus in older adults. Neuropsychopharmacology 41, 781–790. https://doi.org/10.1038/npp.2015.203.

Wu, K., Taki, Y., Sato, K., Kinomura, S., Goto, R., Okada, K., Kawashima, R., He, Y., Evans, A.C., Fukuda, H., 2012. Age-related changes in topological organization of structural brain networks in healthy individuals. Hum. Brain Mapp. 33, 552–568. https://doi.org/10.1002/hbm.21232.

Wu, X., Li, Q., Yu, X., Chen, K., Fleisher, A.S., Guo, X., Zhang, J., Reiman, E.M., Yao, L., Li, R., 2016. A triple network connectivity study of large-scale brain systems in cognitively normal APOE4 carriers. Front. Aging Neurosci. 8. https://doi.org/10.3389/fnagi.2016.00231.

Yan, F.-X., Wu, C.W., Chao, Y.-P., Chen, C.-J., Tseng, Y.-C., 2015. APOE-ε4 allele altered the rest-stimulus interactions in healthy middle-aged adults. PLoS One 10, e0128442. https://doi.org/10.1371/journal.pone.0128442.

Yang, A.C., Huang, C.-C., Liu, M.-E., Liou, Y.-J., Hong, C.-J., Lo, M.-T., Huang, N.E., Peng, C.-K., Lin, C.-P., Tsai, S.-J., 2014. The APOE ε4 allele affects complexity and functional connectivity of resting brain activity in healthy adults. Hum. Brain Mapp. 35, 3238–3248. https://doi.org/10.1002/hbm.22398.

Yang, Z., Zuo, X.N., McMahon, K.L., Craddock, R.C., Kelly, C., de Zubicaray, G.I., Hickie, I., Bandettini, P.A., Castellanos, F.X., Milham, M.P., Wright, M.J., 2016. Genetic and environmental contributions to functional connectivity architecture of the human brain. Cereb. Cortex 26, 2341–2352. https://doi.org/10.1093/cercor/bhw027.

Ye, Q., Su, F., Shu, H., Gong, L., Xie, C., Zhang, Z., Bai, F., 2017. The apolipoprotein E gene affects the three-year trajectories of compensatory neural processes in the left-lateralized hippocampal network. Brain Imaging Behav. 11, 1446–1458. https://doi.org/10.1007/s11682-016-9623-5.

Zhang, P., Qin, W., Wang, D., Liu, B., Zhang, Y., Jiang, T., Yu, C., 2015a. Impacts of PICALM and CLU variants associated with Alzheimer's disease on the functional connectivity of the hippocampus in healthy young adults. Brain Struct. Funct. 220, 1463–1475. https://doi.org/10.1007/s00429-014-0738-4.

Zhang, X., Yu, J.T., Li, J., Wang, C., Tan, L., Liu, B., Jiang, T., 2015b. Bridging integrator 1 (BIN1) genotype effects on working memory, hippocampal volume, and functional connectivity in young healthy individuals. Neuropsychopharmacology 40, 1794–1803. https://doi.org/10.1038/npp.2015.30.

Zhang, N., Liu, H., Qin, W., Liu, B., Jiang, T., Yu, C., 2017. APOE and KIBRA interactions on brain functional connectivity in healthy young adults. Cereb. Cortex 27, 4797–4805. https://doi.org/10.1093/cercor/bhw276.

Zhao, H., Han, Z., Ji, X., Luo, Y., 2016. Epigenetic regulation of oxidative stress in ischemic stroke. Aging Dis. 7, 295–306. https://doi.org/10.14336/ad.2015.1009.

Zhu, W., Wen, W., He, Y., Xia, A., Anstey, K.J., Sachdev, P., 2012. Changing topological patterns in normal aging using large-scale structural networks. Neurobiol. Aging 33, 899–913. https://doi.org/10.1016/j.neurobiolaging.2010.06.022.

REVIEW

The many ages of man: diverse approaches to assessing ageing-related biological and psychological measures and their relationship to chronological age

Heidi Foo[a], Karen A. Mather[a], Anbupalam Thalamuthu[a], and Perminder S. Sachdev[a,b]

Purpose of review
Chronological age is a crude measure and may not be the best indicator of the ageing process. Establishing valid and reliable biomarkers to understand the true effect of ageing is of great interest. We provide an overview of biological and psychological characteristics that change with age and can potentially serve as markers of the ageing process, and discuss if an integration of these characteristics may more accurately measure the true age of a person. We also describe the clinicopathological continuum of these ageing-related changes.

Recent findings
Ageing-related changes in the biological and psychological systems of the body have been studied to varying degrees and with differing emphases. Despite the development of ageing indices, there is no single indicator that can holistically estimate the ageing process. Differential ageing of bodily systems remains poorly understood, and valid methods have not been developed for composite markers of biological and psychological processes.

Summary
The ageing process is complex and heterogeneous. Incorporating biological and psychological measures may improve accuracy in reflecting an individual's 'true age,' and elucidate why some people age successfully, whereas others show ageing-related decline and disease.

Keywords
ageing process, biological age, biomarker, psychological age

INTRODUCTION

According to a 2017 United Nations report on the global ageing population, the number of persons aged 60 and above is projected to more than double to 2.1 billion by 2050 [1]. Unfortunately, ageing is associated with decline in many bodily organs and functions. Such declines at molecular, cellular, and physiological levels are a major risk factor for ageing-related diseases such as neurodegenerative disorders, cancer, and cardiovascular diseases [2].

Ageing is typically defined in terms of the chronological age, which is an index of the length of life in years since birth [3]. Although there is evidence that chronological age is associated with functional impairments, chronic diseases, and mortality, there is heterogeneity in the health outcomes of older individuals as the impact of ageing differs markedly across individuals and for various organs in the same individual [4]. The chronological age is, therefore, but a crude measure of the ageing process, and ageing-related changes in multiple tissues and functions should arguably be examined separately to form a comprehensive picture of ageing of the organism [5]. This is understandable, as ageing involves complex and multifactorial processes that

[a]Centre for Healthy Brain Ageing, CHeBA, School of Psychiatry, UNSW Medicine, UNSW Sydney and [b]Neuropsychiatric Institute, Euroa Centre, Prince of Wales Hospital, Randwick, New South Wales, Australia

Correspondence to Heidi Foo, Jing Ling, Centre for Healthy Brain Ageing (CHeBA), School of Psychiatry, UNSW Medicine, NSW 2052, Australia. Tel: +61 2 93823763; e-mail: heidi.foo@student.unsw.edu.au

Curr Opin Psychiatry 2018, 32:000–000
DOI:10.1097/YCO.0000000000000473

KEY POINTS

- Chronological age is not an adequate measure of the ageing process.
- A composite measure of biological ages of different systems as well as psychological ages may be more accurate measures of the ageing process.
- The integration of both biological and psychological aspects of ageing may provide new insights into the pathophysiology of ageing.

are influenced by genetic, environmental, and stochastic factors [6••,7].

Gerontology researchers have argued that measurements of biological and psychological age may predict ageing process and its relationship to ageing-related diseases and lifespan more accurately than chronological age. Biological age, which purportedly identifies ageing-related changes in body function of an individual in reference to one's chronologically aged peers, may be able to account for the interindividual differences in health outcomes [8–9,10•]. The aim of investigating biological ageing is to inform diagnostics and interventions, as well as to improve and/or maintain overall health [11]. However, biological ageing models often determine the rate of ageing in different populations and subgroups instead of informing clinical outcomes [11–14]. Moreover, despite the presence of many biological age calculators online, which compare measurements for a range of health risk factors to the average population, there is variability in their estimation because of the distinct risk factors modelled and the oversimplification of the concept of biological age. Furthermore, biological mechanisms in ageing are often confounded by a plethora of ageing-related diseases, making it challenging to discriminate between disease-related and ageing-related alterations [15]. In fact, many processes that underlie biological ageing, such as oxidative stress and inflammation, are also the basis for disease, and clear separation of 'normal' ageing from pathological ageing is not possible [11]. Some have suggested that ageing should be regarded as a disease for which therapeutic interventions should be explored [11]. In contrast, psychological age refers to an individual's psychological development in cognitive functioning and emotional responsiveness [3]. Previous studies have demonstrated that the psychological aspects of an individual were associated with successful ageing and that mental health 'balance' contributed toward health and optimal functionality [16]. Hence, the integration of both biological and psychological ages may quantify one's true age more effectively, and better serve both research and clinical practice in addressing the deleterious effects of ageing [11].

A review integrating various biological measurements from the brain and the rest of the body to build a comprehensive model of the biological ageing process was recently published [17••]. In contrast, this article aims to provide an overview of several approaches to measuring biological age in different organs of multiple systems as well as the psychological aspects of ageing, and how these can together present a more comprehensive overview of ageing (Fig. 1). We also comment on the clinicopathological continuum between healthy ageing and ageing-related disease.

APPROACHES TO ESTIMATING BIOLOGICAL AGE

Four guiding principles have been suggested for the qualification of a biological ageing biomarker: to predict rate of ageing; to monitor biological mechanisms in the ageing process independent of disease processes; to repeat testing without causing harm; and for translational work from animals to humans [17••].

Common molecular features of ageing, including decreased telomere length and changes in DNA methylation (DNAm), have been identified [8,17••,18]. Other physiological measures of ageing including blood pressure, heart rate, grip strength, and walking speed have shown relatively moderate correlations with chronological age [17••]. Moreover, multiple system-related ages – such as brain, cardiovascular, renal, endocrine, and musculoskeletal – have also demonstrated their usefulness in predicting the rate of ageing. Taken together, these measures are beneficial in predicting disease and mortality. However, examining each feature in isolation fails to comprehensively explain and capture the variability of the ageing process. Therefore, integrating several measures of biological age may allow us to better study the complexity of different ageing trajectories. In this section, we review the various biological ageing-related alterations.

Epigenetic age

Epigenetics refer to changes in gene expression because of other mechanisms and modifications independent of the DNA sequence [19]. One epigenetic modification, DNAm, has been investigated as a biomarker of ageing in human samples [20,21]. Epigenetic age is a putative biomarker of ageing based on the methylation status of cytosine-

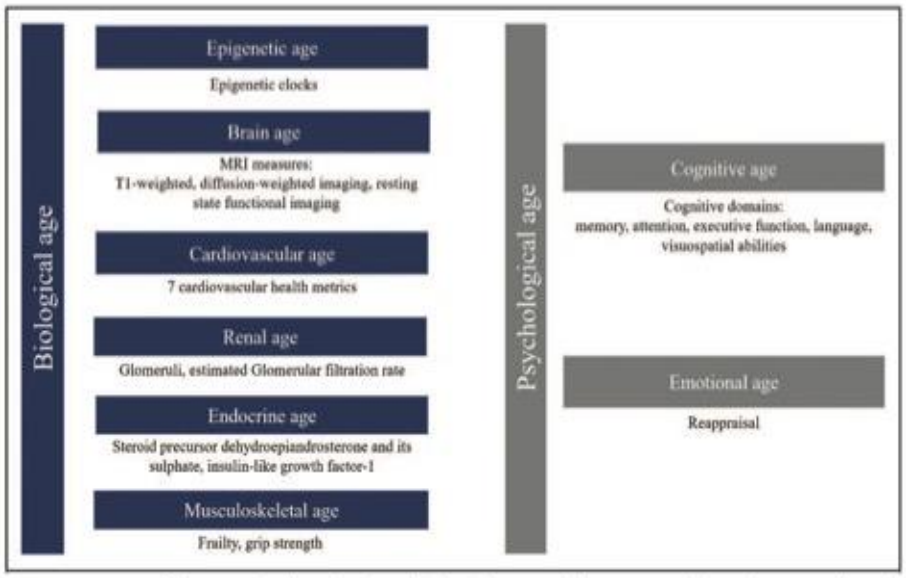

FIGURE 1. Summary of the various biological and psychological ages and their associated key indicators. Biological age includes epigenetic age, brain age, cardiovascular age, renal age, endocrine age, and musculoskeletal age. Psychological age includes cognitive age and emotional age.

phosphate-guanine (CpG) sites that are highly correlated with chronological age [20,21]. The two most commonly used measures of epigenetic age are the blood-based algorithm of Hannum *et al.* [20] and the multitissue algorithm by Horvath *et al.* [21]. Epigenetic age may be influenced by genetic and environmental factors [6••], and can be applied to multiple tissues and to the whole age spectrum [6••,7,22,23].

Across the adult lifespan, accelerated epigenetic age has been associated with indicators of physical and mental health [22–25]. In addition to all-cause mortality, accelerated epigenetic ageing is associated with 20% greater cardiovascular disease mortality and higher cancer risk in a population-based cohort of older adults [25]. Studies of exceptional longevity showed that long-lived individuals of above 95 years had a younger epigenetic age compared with their chronological age [7,26] and that younger epigenetic age at the chronological age between 55 and 80 years might contribute to preserved episodic memory functioning, potentially resulting in reduced risk of dementia [5]. Although epigenetic age shows great promise as a general biomarker of healthy ageing and for identifying regulatory mechanisms for disease development and ageing-related decline in biological functioning [22,24–25], future work should examine the efficacy of using blood tissue to study the DNAm of the whole organism compared with multiple tissues.

Brain age

Ageing of the brain is accompanied by the loss of volume and a progressive decline in some cognitive functions [27]. Rates of annual brain volume loss accelerate with increasing age; brain volume loss is only 0.2% per annum at the age of 35 years and increases to 0.52% per annum by the age of 75 years [28]. Previous studies have shown ageing-related changes in brain structural morphology [29–32] and networks [33–36], and associations of amyloid positivity and cognitive dysfunction [37,38]. Despite the apparent physiological ageing process of the brain, questions remain about what constitutes neurophysiological or neuropathological brain ageing as per these MRI parameters; and what the underlying reasons are as to why some older adults do not develop overt symptoms despite changes in the brain morphology. Good measures of brain age may help address these questions.

Three notable studies have developed brain-based measures using various MRI parameters as potential biomarkers of ageing [10•,39,40•]. Cole *et al.* [10•] used cortical volume data derived from T1-weighted MRI scans and found that brain ageing

index was associated with poorer physical and cognitive health, such as weaker grip strength, poorer lung function, slower walking speed, lower fluid general intelligence, and greater allostatic load, and higher mortality risk. Using T1-weighted scans, Aycheh *et al.* [39] demonstrated that cortical thinning might be a better brain-age measure compared with chronological age. Additionally, multimodal neuroimaging data incorporating T1-weighted and resting-state functional MRI scans increased prediction performance when brain age was evaluated against chronological age, and also found that brain ageing was accelerated in participants with cognitive impairment [40•]. As structural changes may not always accompany robust functional changes [41•], the combination of both structural and functional scans may result in a more accurate measure of the brain age. Thus, using such an index of brain age as a proxy measure may inform the ageing process related to neurophysiological processes in adults.

Cardiovascular age

Pathophysiological changes of the cardiovascular system at the structural, cellular, molecular, and functional levels accompanying ageing can contribute to an increased risk of developing cardiovascular diseases (CVD), other related diseases, and mortality [42,43•]. The odds of developing cardiovascular ageing-related diseases sharply increase after age 40 years, where the odds of developing disease are 50% for chronic CVD, 85% for hypertension, and 20% for chronic heart disease [42]. Key vascular modifications associated with ageing include generalized endothelial dysfunction and central arterial stiffness, which predispose older adults to CVD and stroke [43•,44]. Although these cardiovascular features have been observed in atherosclerosis-free individuals, they are also present in atherosclerotic vessels, where the difference lies in the eventual development of focal lesions, vessel stenosis, and plaque rupture in the latter individuals compared with the former [15]. Importantly, these 'normal' cardiovascular ageing individuals may eventually manifest CVD at later stages, possibly dependent upon lifestyle influences – such as exercise and diet [45] – and health factors including physical function [46]. This suggests that ageing in the cardiovascular system is not a homogenous process and that changes with age do not necessarily occur at the same rate [45]. In addition, cardiovascular health plays an important role in brain health. Using seven cardiovascular health metrics from the American Heart Association, one longitudinal study established strong associations between cardiovascular health status at baseline and incidence of dementia at later stages in community-dwelling older adults [47]. Another study demonstrated that cardiovascular health factors were associated with variations in the brain vascular structure and function even in young adulthood [48]. Despite the risk of cardiovascular ageing and its consequences on other biological systems, its pathophysiological implications remain under-studied as their manifestations cannot be readily detected [42]. Moreover, variations in definition and measurements of heart age make it challenging to study how heart age can effectively measure cardiovascular risks [49]. Hence, examining cardiovascular ageing and its associated factors may allow us to better understand its effect on the biological system.

Renal age

Alterations in kidney's morphology and dysfunction, which can be accelerated by diseases, such as diabetes mellitus and hypertension [50], may result in chronic kidney disease (CKD) and mortality in older adults [51]. The prevalence of CKD in older adults over 65 years of age is approximately 44% [51]. Evidence from histological studies of the kidney's microanatomy showed that nephrosclerosis, including glomerulosclerosis, arteriosclerosis, tubular atrophy, and interstitial fibrosis increased progressively with age, from 28% for 40–49-year olds to 73% for 70–77-year olds [52]. Morphological kidney changes, such as an increase in the proportion of small sclerosed glomeruli and the size of functional glomeruli may occur with age [53]. Functionally, ageing-related declines have been observed in glomerular filtration rate (GFR), the ability to conserve and secrete sodium, and urine concentrating and diluting abilities [54]. One study on community-dwelling older adults found that diminished estimated glomerular filtration rate (eGFR) was related to orthostatic hypotension, which predicted cardiovascular outcomes [55]. Poor renal function across all stages of CKD was also associated with cognitive impairment, especially in executive function, and vascular subtype dementia [56,57]. Another large population-based cohort of older men with stage 3 CKD (eGFR of 30.0–59.9 ml/min per 173 m^2) showed greater risk of any fracture than those without CKD [58]. Collectively, these studies show that renal ageing may influence other body systems to result in observable ageing-related changes.

Endocrine age

Endocrine functions are pertinent for maintaining homeostasis and regulation. Ageing-related changes

include declines in circulating levels and responses of pituitary growth hormones, gonadal steroid hormones, the steroid precursor dehydroepiandrosterone (DHEA) and its sulphate (DHEAS), and insulin-like growth factor-1 [59,60]. High-to-normal range of free cortisol concentrations have been associated with increased risk of Alzheimer's disease and mortality, and decrease of DHEA and DHEAS have been associated with increased cardiovascular-related mortality in older adults [61•]. However, not all ageing-related changes in the endocrine system are detrimental. The ageing process modulates the concentration of thyroid hormones, which, despite its variability among individuals, shows an overall decline with age [61•]. This is reflected by an increase in thyroid-stimulating hormones and decrease in free tri-iodothyronine concentrations [61•], which are associated with decreased risk of stroke [62] and increased longevity [63]. Moreover, endocrine hormones may interact and affect phenotypic variations seen in older adults. One study has demonstrated that in men with mean age of 56.3 years, testosterone levels were inversely related to hippocampal volume and memory performance when cortisol levels were low [64]. This evidence suggests that further research into ageing and the endocrine system to better understand the molecular processes may be useful to promote healthy ageing.

Musculoskeletal age

Ageing is associated with deterioration in multiple aspects of the musculoskeletal system, such as the bone, skeletal muscles, and fat, which may result in osteoporosis, osteoarthritis, physical frailty, and eventual mortality [65,66]. Muscle mass decreases by 30–50% between the ages of 40 and 80 years, with reported losses in functional capacity of about 3% each year beyond 60 years [67]. Frailty, measured by weakness (assessed by grip strength), slowness (assessed by gait speed), low levels of physical activity, low energy levels, and unintentional weight loss, includes many ageing-related musculoskeletal changes and is a common feature of ageing [68]. Importantly, evidence has demonstrated that mild frailty was associated with a 5-year risk of death odds ratio of 4.82, increasing to 7.34 in those with severe frailty [69]. Similarly, grip strength has also been associated with mortality and cardiovascular diseases in community-dwelling population [70]. The cellular and extracellular components of the musculoskeletal system do not decline in a uniform fashion, resulting in inter-individual differences in ageing-related phenotypic alterations [65,71,72]. For instance, loss of bone mineral density may be mediated by oestrogen, an important factor for musculoskeletal ageing in women [71], whereas muscle mass may be influenced more so by lifestyle factors including exercise and diet [72]. Thus, understanding the heterogeneity of the ageing-related musculoskeletal changes may inform the study of the ageing process, and musculoskeletal age is a useful measure of the status of the individual.

APPROACHES TO ESTIMATING THE PSYCHOLOGICAL AGE

The psychology of ageing has primarily focused on cognition, the self, and personality [3]. Cognition is not a single entity; it consists of distinct components including but not limited to memory, attention, executive function, language, and visuospatial abilities [73,74]. These abilities have unique development trajectories between individuals and across the adult lifespan. Self and personality encompass a multifaceted description of individuals including their thoughts, beliefs, and emotions, which are influenced by personal experiences and alter as individuals age [75]. In this section, we briefly review how cognition and emotional function change with increasing age.

Cognitive age

Ageing-related changes in cognition not only affect memory but also processing speed and decision-making; and they are highly variable among individuals as they are influenced by a multitude of factors, such as health status, lifestyle, education, emotions, socioeconomic status, and genetics [76]. However, older age is not invariably associated with decline, and some aspects of cognition, such as crystallized intelligence, remain stable at older ages [76]. This observed heterogeneity may be, in part, because of the complex cascade of ageing processes that interact to affect cognitive function [77]. This heterogeneous pattern in cognitive ageing across individuals was also observed in a longitudinal study in an East Asian cohort wherein attention, executive function, verbal, and visual spatial memory were relatively preserved in older adults despite a decline in processing speed [78]. Larger corpus callosum volumes at baseline, lower levels of inflammation and insulin, and physical activity have shown to predict stability in processing speed in older adults above 60 years over a follow-up period of 2.5 years [77]. Similarly, genetic factors have been observed to contribute to the stability of general cognitive abilities whereas change reflected non-shared environmental influences in a longitudinal twin study from young adulthood to late midlife [79]. Another longitudinal study investigated the

relationship between beta-amyloid (Aß) deposition, white matter hyperintensities, cortical thickness, and cognition in successful agers with superior episodic memory compared with their peers [80]. They observed that despite having superior memory like those between 18 and 32-year olds, successful agers still experienced typical-for-age Aß deposition and longitudinal ageing-related brain atrophy [80]. This calls to question why specific individuals have superior memory despite typical neurodegeneration. Future studies should examine how cognition can inform the trajectory of ageing of an individual.

Emotional age

Emotional function, that is emotional motivation and competence [81], shows less decline in normal ageing than many other processes. In some cases, older adults are either comparable or more effective at emotional regulation than younger adults [82▪]. Two prominent theories, namely the socioemotional selectivity theory and the dynamic integration theory, have been proposed to explain emotional ageing with the emphasis on ageing-related shift in the overall ratio of positive-to-negative memories [83]. Given the interindividual differences in emotional function, attempts have been made to link emotional ageing with emotional-regulation processes and neurophysiological mechanisms. One study found that older adults were less likely to fixate on negative visual stimuli but reacted with greater negative emotions such as sadness than younger adults, and this relationship was associated with the frequency of positive reappraisal [84]. This was corroborated by another study, which found that older people tended to reappraise less as reappraisal constituted a more cognitively demanding task [85]. This implies that cognitive reappraisal may be a key process in accounting for the positivity shift in the emotional-regulation process in older adults. Furthermore, there is evidence that the preservation of brain regions pivotal for emotional processing (i.e. amygdala and the ventromedial prefrontal cortex) and ageing-related declines in the dopaminergic and noradrenergic neurotransmitter systems may partly account for the positivity effect [82▪]. Taken together, shifts in emotional regulation and the relative efficacy of various brain systems may contribute to the strategies older adults use to cope with emotions, and may result in net slowing down of emotional ageing than the chronological age would imply.

CONCLUSION

Although there are several published indices of biological ageing, there is no single indicator that can comprehensively estimate the ageing process [86]. A multidimensional approach to estimating the true age of an individual is necessary to understand why some individuals develop disease, and in turn why disease does not always lead to disability. Differentiating whether ageing-related alterations are because of the physiological ageing process or are related to accumulating diseases is difficult. Composite measures integrating various biological and psychological ages of individuals may allow us to accurately measure their true age and comprehensively study the ageing process across all the bodily systems, eventually informing longevity therapeutics.

Acknowledgements

Many thanks to the UNSW Scientia Scholarship for their support.

Financial support and sponsorship

None.

Conflicts of interest

There are no conflicts of interests.

REFERENCES AND RECOMMENDED READING

Papers of particular interest, published within the annual period of review, have been highlighted as:
▪ of special interest
▪▪ of outstanding interest

1. United Nations Department of Economic and Social Affairs, Population Division. World Population Prospects: the 2017 Revision, Key Findings and Advance Tables; 2017.
2. López-Otín C, Blasco MA, Partridge L, *et al.* The hallmarks of aging. Cell 2013; 153:1194–1217.
3. Uotinen V. I'm as old as I feel: subjective age in Finnish adults. Korhonen T, Olsbo P, editors. Jyväskylä, Finland: University of Jyväskylä; 2005.
4. Lowsky DJ, Olshansky SJ, Bhattacharya J, *et al.* Heterogeneity in healthy aging. J Gerontol A Biol Sci Med Sci 2014; 69:640–649.
5. Degerman S, Josefsson M, Adolfsson AN, *et al.* Maintained memory in aging is associated with young epigenetic age. Neurobiol Aging 2017; 55:161–171.
6. ▪▪ Horvath S, Raj K. DNA methylation-based biomarkers and the epigenetic clock theory of ageing. Nature Rev Genet 2018; 19:371–384.
A high quality and up-to-date review of how epigenetic biomarkers are useful in accurately measuring age estimates for any tissue across the entire life course and potentially explain why humans age.
7. Armstrong NJ, Mather KA, Thalamuthu A, *et al.* Aging, exceptional longevity and comparisons of the Hannum and Horvath epigenetic clocks. Epigenomics 2017; 9:689–700.
8. Jylhävä J, Pedersen NL, Hägg S. Biological age predictors. EBioMedicine 2017; 21:29–36.
9. Karasik D, Demissie S, Cupples LA, Kiel DP. Disentangling the genetic determinants of human aging: biological age as an alternative to the use of survival measures. J Gerontol A Biol Sci Med Sci 2005; 60:574–587.
10. ▪ Cole JH, Ritchie SJ, Bastin ME, *et al.* Brain age predicts mortality. Mol Psychiatry 2018; 23:1385–1392.
Novel method used to predict the brain age.
11. Tuttle CSL, Maier AB. Towards a biological geriatric assessment. Exp Gerontol 2018; 107:102–107.
12. Putin E, Mamoshina P, Aliper A, *et al.* Deep biomarkers of human aging: application of deep neural networks to biomarker development. Aging 2016; 8:1021–1030.
13. Jee HM, Park JH. Selection of an optimal set of biomarkers and comparative analyses of biological age estimation models in Korean females. Arch Gerontol Geriatr 2017; 70:84–91.

14. Bürkle A, Moreno-Villanueva M, Bernhard J, et al. MARK-AGE biomarkers of ageing. Mech Ageing Dev 2015; 151:2–12.
15. Ferrari AU, Radaelli A, Cantola M. Invited review: aging and the cardiovascular system. J Appl Physiol 2003; 95:2591–2597.
16. Paúl C, Teixeira L, Ribeiro O. Active aging in very old age and the relevance of psychological aspects. Front Med(Lausanne) 2017; 4:181.
17. Cole HA, Marioni RE, Harris SE, et al. Brain age and other bodily 'ages': ▪▪ implications for neuropsychiatry. Mol Psychiatry 2018. [Epub ahead of print]
A well illustrated review of the different types of biological measurements that could be used to build a comprehensive model of biological aging process and how these measurements may be useful in predicting brain and body health in aging and disease.
18. Kanherkar RR, Bhatia-Dey N, Csoka AB. Epigenetics across the human lifespan. Front Cell Dev Biol 2014; 2:49.
19. Johnson KC, Christensen BC. Genome-wide DNA methylation changes during aging. In: Fraga MF, Fernández AF, editors. Epigenomics in health disease, 1st ed. Cambridge, Massachusetts, USA: Academic Press; 2015. pp. 127–144.
20. Hannum G, Guinney J, Zhao L, et al. Genome-wide methylation profiles reveal quantitative views of human aging rates. Mol Cell 2013; 49:359–367.
21. Horvath S, Mah V, Lu AT, et al. The cerebellum ages slowly according to the epigenetic clock. Aging 2015; 7:294–305.
22. Marioni RE, Shah S, McRae AF, et al. DNA methylation age of blood predicts all-cause mortality in later life. Genome Biol 2015; 16:25.
23. Chen BH, Marioni RE, Colicino E, et al. DNA methylation-based measures of biological age: meta-analysis predicting time to death. Ageing 2016; 8:1844–1859.
24. Christiansen L, Lenart A, Tan QH, et al. DNA methylation age is associated with mortality in a longitudinal Danish twin study. Aging Cell 2016; 15:149–154.
25. Perna L, Zhang Y, Mons U, et al. Epigenetic age acceleration predicts cancer, cardiovascular, and all-cause mortality in a German case cohort. Clin Epigenetics 2016; 8:64.
26. Horvath S, Pirazzini C, Bacalini MG, et al. Decreased epigenetic age of PBMCs from Italian semi-supercentenarians and their offspring. Aging 2015; 7:1159–1170.
27. Barrick TR, Charlton RA, Clark CA, et al. White matter structural decline in normal ageing: a prospective longitudinal study using tract-based spatial statistics. Neuroimage 2010; 51:565–577.
28. Schippling S, Ostwaldt AC, Suppa P, et al. Global and regional annual brain volume loss rates in physiological aging. J Neurol 2017; 264:520–528.
29. DeCarli C, Massaro J, Harvey D, et al. Measures of brain morphology and infarction in the Framingham heart study: Establishing what is normal. Neurobiol Aging 2005; 26:491–510.
30. Yang ZX, Wen W, Jiang J, et al. Age-associated differences on structural brain MRI in nondemented individuals from 71 to 103 years. Neurobiol Aging 2016; 40:86–97.
31. Fjell AM, Westlye LT, Grydeland H, et al. Critical ages in the life-course of the adult brain: nonlinear subcortical aging. Neurobiol Aging 2014; 34:2239–2247.
32. Madden DJ, Parks EL, Tallman CW, et al. Sources of disconnection in neurocognitive aging: cerebral white-matter integrity, resting-state functional connectivity, and white-matter hyperintensity volume. Neurobiol Aging 2017; 54:199–213.
33. Chan MY, Park DC, Savalia NK, et al. Decreased segregation of brain systems across the healthy adult lifespan. Proc Natl Acad Sci U S A 2014; 11:E4997–E5006.
34. Geerligs L, Renken RJ, Saliasi E, et al. Age-related changes in functional connectivity. Cerebral Cortex 2015; 25:1987–1999.
35. Mårtensson J, Lätt J, Åhs F, et al. Diffusion tensor imaging and tractography of the white matter in normal aging: the rate-of-change differs between segments within tracts. J Magn Reson Imaging 2018; 45:113–119.
36. Bennett IJ, Greenia DE, Maillard P, et al. Age-related white matter integrity differences in oldest-old without dementia. Neurobiol Aging 2017; 56:108–114.
37. Jansen WJ, Ossenkoppele R, Knol DL, et al. Prevalence of cerebral amyloid pathology in persons without dementia: a meta-analysis. JAMA 2015; 313:1924–1938.
38. Kawas CH, Greenia DE, Bullain SS, et al. Amyloid imaging and cognitive decline in nondemented oldest-old: the 90+ study. Alzheimers Dement 2013; 9:199–203.
39. Aycheh HM, Seong JK, Shin JH, et al. Biological brain age prediction using cortical thickness data: a large scale cohort study. Frontiers Aging Res 2018; 10:252.
40. Liem F, Varoquaux G, Kynast J, et al. Predicting brain-age from multimodal ▪ imaging data captures cognitive impairment. Neuroimage 2017; 148: 179–188.
Novel approach that uses multimodal neuroimaging to predict the brain age of individuals.
41. Liu H, Yang YY, Xia YG, et al. Aging of cerebral white matter. Aging Res Rev ▪ 2017; 34:64–76.
Comprehensive review on the aging of cerebral white matter and how changes influence the progression of various brain disorders.
42. Lakatta EG. So! What's aging? Is cardiovascular aging a disease? J Mol Cell Cardiol 2015; 83:1–13.
43. Paneni F, Cañestro CD, Libby P, et al. The aging cardiovascular system. ▪ Understanding it at the cellular and clinical levels. J Am Coll Cardiol 2017; 69:1952–1967.
A helpful review on the mechanisms underlying age-related changes of the cardiovascular system.
44. De Almeida AJPO, Ribeiro TP, de Medeiros IA. Aging: molecular pathways and implications on the cardiovascular system. Oxi Med Cell Longev 2017; 2017:7941563.
45. Nakou ES, Parthenakis FI, Kallergis EM, et al. Healthy aging and myocardium: a complicated process with various effects in cardiac structure and physiology. Int J Cardiol 2016; 209:167–175.
46. Jin Y, Tanaka T, Ma Y, et al. Cardiovascular health is associated with physical function among older community dwelling men and women. J Gerontol Med Sci 2017; 72:1710–1716.
47. Samieri C, Perier MC, Gaye B, et al. Association of cardiovascular health level in older age with cognitive decline and incident dementia. JAMA 2018; 320:657–664.
48. Williamson W, Lewandowski AJ, Forkert ND, et al. Associations of cardiovascular risk factors with MRI indices of cerebrovascular structure and function and white matter hyperintensities in young adults. JAMA 2018; 320:665–673.
49. Greenewegen KA, den Ruijter HM, Pasterkamp G, et al. Vascular age to determine cardiovascular disease risk: a systematic review of its concepts, definitions, and clinical applications. Eur J Prev Cardiol 2016; 23:264–274.
50. Zhou XJ, Rakheja D, Yu XQ, et al. The aging kidney. Kidney Int 2008; 74:710–720.
51. Garimella PS, Biggs ML, Katz R, et al. Urinary uromodulin, kidney function, and cardiovascular disease in older adults. Kidney Int 2015; 88:1126–1134.
52. Rule AD, Amer H, Cornell LD, et al. The association between age and nephrosclerosis on renal biopsy among healthy adults. Ann Intern Med 2010; 152:561–567.
53. Glassrock RJ, Rule AD. The implications of anatomical and functional changes of the aging kidney: with an emphasis on the glomeruli. Kidney Int 2012; 82:270–277.
54. Sturmlechner I, Durik M, Sieben CJ, et al. Cellular senescence in renal ageing and disease. Nat Rev Nephrol 2017; 13:77–89.
55. Canney M, O'Connell MDL, Sexton DJ, et al. Graded association between kidney function and impaired orthostatic blood pressure stabilization in older adults. J Am Heart Assoc 2017; 6:; pii: e005661.
56. Darsie B, Shlipak MG, Sarnak MJ, et al. Kidney function and cognitive health in older adults: the Cardiovascular Health Study. Am J Epidemiol 2014; 180:68–75.
57. Zammit AR, Katz MJ, Bitzer M, et al. Cognitive impairment and dementia in older adults with chronic kidney disease: a review. Alzheimer Dis Assoc Disord 2016; 30:357–366.
58. Hall RK, Sloane R, Pieper C, et al. Competing risks of fracture and death in older adults with chronic kidney disease. J Am Geriatr Soc 2018; 66:532–538.
59. Chahal HS, Drake WM. The endocrine system and ageing. J Pathol 2007; 2:173–180.
60. Jones CM, Boelaert K. The endocrinology of ageing: a mini-review. Gerontology 2015; 61:291–300.
61. Van den Beld AW, Kaufman JM, Zillikens MC, et al. The physiology ▪ of endocrine systems with ageing. Lancet Diabetes Endocrinol 2018; 6:647–658.
A comprehensive and up-to-date review of the effects of age on the different hypothalamic–pituitary hormonal organ axes, as well as age-related changes in calcium and bone metabolism and glucose homeostasis.
62. Chaker L, Baumgartner C, den Elzen WP, et al., Thyroid Studies Collaboration. Thyroid function within the reference range and the risk of stroke: an individual participant data analysis. J Clin Endocrinol Metab 2016; 101:4270–4282.
63. Bowers J, Terrien J, Clerget-Froidevaux MS, et al. Thyroid hormone signaling and homeostasis during aging. Endocr Rev 2013; 34:556–589.
64. Panizzon MS, Hauger RL, Xian H, et al. Interactive effects of testosterone and cortisol on hippocampal volume and episodic memory in middle-aged men. Psychoneuroendocrinology 2018; 91:115–122.
65. Boros K, Freemont T. Physiology of ageing of the musculoskeletal system. Best Pract Res Clin Rheumatol 2017; 31:203–217.
66. Roberts S, Colombier P, Sowman A, et al. Ageing in the musculoskeletal systems: cellular function and dysfunction throughout life. Acta Orthopaedica 2016; 87:15–25.
67. Nolan M, Nitz J, Choy N, et al. Age-related changes in musculoskeletal function, balance and mobility measures in men aged 30-80 years. Aging Male 2010; 13:194–201.
68. Dawson A, Dennison E. Measuring the musculoskeletal aging phenotype. Maturitas 2016; 93:13–17.
69. Rockwood K, Howlett SE, Macknight C, et al. Prevalence, attributes, and outcomes of fitness and frailty in community-dwelling older adults: report from the Canadian study of health and aging. J Gerontol A Biol Sci Med Sci 2004; 59:1310–1317.

70. Wu YL, Wang WJ, Liu TW, *et al.* Association of grip strength with risk of all-cause mortality, cardiovascular diseases, and cancer in community-dwelling populations: a meta-analysis of prospective cohort studies. J Am Med Dir Assoc 2017; 18:; 551.e17–551.e35.
71. Patel HP, Syddall HE, Jameson K, *et al.* Prevalence of sarcopenia in community-dwelling older people in the UK using the European Working Group on Sarcopenia in Older People (EWGSOP) definition: findings from the Hertfordshire Cohort Study (HCS). Age Ageing 2013; 42:378–384.
72. Denison HJ, Cooper C, Sayer AA, *et al.* Prevention and optimal management of sarcopenia: a review of combined exercise and nutrition interventions to improve muscle outcomes in older people. Clin Interv Aging 2015; 10:859–869.
73. Fisher GG, Chaffee DS, Tetrick LE, *et al.* Cognitive functioning, aging, and work: a review and recommendations for research and practice. J Occup Health Psychol 2017; 22:314–336.
74. Murman D. The impact of age on cognition. Semin Hear 2015; 36:111–121.
75. Franks MM. Psychological perspectives on aging. In: Morgan LA, Kunkel S, editors. Aging: the social context, 2nd ed. California, USA: Pine Forge Press; 2001. pp. 143–154.
76. Blazer DG, Yaffe K, Liverman CT. Cognitive aging: progress in understanding and opportunities for action. Edited by Committee on the Public Health Dimensions of Cognitive Aging, Board on Health Sciences Policy, Institute of Medicine (Editors). Washington, DC, USA: The National Academies Press; 2015.
77. Bott NT, Bettcher BM, Yokoyama JS, *et al.* Youthful processing speed in older adults: genetic, biological, and behavioural predictors of cognitive processing speed trajectories in aging. Front Aging Neurosci 2017; 9:1–9.
78. Leong RLF, Lo JC, Sim SKY, *et al.* Longitudinal brain structure and cognitive changes over 8 years in an East Asian cohort. Neuroimage 2017; 147:852–860.
79. Lyons MJ, Panizzon MS, Liu W, *et al.* A longitudinal twin study of general cognitive ability over 40 decades. Dev Psychol 2017; 53:1170–1177.
80. Harrison TM, Maass A, Baker SL, *et al.* Brain morphology, cognition, and β-amyloid in older adults with superior memory performance. Neurobiol Ageing 2018; 67:162–170.
81. Scheibe S, Cartensen LL. Emotional aging: recent findings and future trends. J Gerontol 2010; 65B:135–144.
82. Mather M. The affective neuroscience of aging. Annu Rev Psychol 2016; ▪ 67:213–238.
An easy-to-read review examining how age-related brain changes influence emotional processes.
83. Kunzmann U, Isaacowitz D. Emotional aging: taking the immediate context seriously. Res Human Dev 2017; 14:182–199.
84. Wirth M, Isaacowitz DM, Kunzmann U. Visual attention and emotional reactions to negative stimuli: the role of age and cognitive reappraisal. Psychol Aging 2017; 32:543–556.
85. Scheibe S, Sheppes G, Staudinger UM. Distract or reappraise? Age-related differences in emotion-regulation choice. Emotion 2015; 15:677–681.
86. Jia LP, Zhang WG, Chen XM. Common methods of biological age estimation. Clin Interv Aging 2017; 12:759–772.

Appendix B. Publication for Chapter 3

www.nature.com/scientificreports

scientific reports

Check for updates

OPEN

Novel genetic variants associated with brain functional networks in 18,445 adults from the UK Biobank

Heidi Foo[1], Anbupalam Thalamuthu[1], Jiyang Jiang[1], Forrest C. Koch[1], Karen A. Mather[1,2], Wei Wen[1] & Perminder S. Sachdev[1,3]

Here, we investigated the genetics of weighted functional brain network graph theory measures from 18,445 participants of the UK Biobank (44–80 years). The eighteen measures studied showed low heritability (mean h^2_{SNP} = 0.12) and were highly genetically correlated. One genome-wide significant locus was associated with strength of somatomotor and limbic networks. These intergenic variants were located near the *PAX8* gene on chromosome 2. Gene-based analyses identified five significantly associated genes for five of the network measures, which have been implicated in sleep duration, neuronal differentiation/development, cancer, and susceptibility to neurodegenerative diseases. Further analysis found that somatomotor network strength was phenotypically associated with sleep duration and insomnia. Single nucleotide polymorphism (SNP) and gene level associations with functional network measures were identified, which may help uncover novel biological pathways relevant to human brain functional network integrity and related disorders that affect it.

During aging, the human brain undergoes functional changes which affect the integration of information within and between functional brain networks, and these have been shown to be associated with behavioral changes[1]. By modelling large-scale brain networks using graph theory, defined by a collection of nodes (brain regions) and edges (magnitude of temporal correlation in functional magnetic resonance imaging (fMRI) activity between two brain regions)[2,3], it is possible to investigate aging-related topological changes. Previous functional graph theory studies have mainly considered edge presence or absence represented as a binary variable[4–6], which precludes information about variations in connectivity weights between networks. Given that connection weights exhibit high heterogeneity over several orders of magnitude[7], studying weighted brain networks may provide greater insights into their underlying hierarchy and organizational principles.

Genetics may play an important role in influencing changes in the functional topology of the aging brain. Graph theoretical brain functional measures are reported to be heritable[8,9]. While a previous study[10] has looked at genetics of functional connectivity from resting-state fMRI images, to date, there has not been any population-based study investigating the genetic contribution to functional connectivity using graph theory measures. Studying the genetic architecture of graph theory brain functional measures has important implications[11]—firstly, it can identify genes associated with network topology; and secondly, it may provide insights into the underlying biological mechanisms of macroscopic network topology in aging and how it alters during disease states.

Here, we address the question of how genetics is associated with the integrity of functional connectivity as measured by graph theory measures in resting-state fMRI (rs-fMRI) data. We assessed graph theory measures, including global efficiency, characteristic path length, Louvain modularity, transitivity, local efficiency and strength of default, dorsal attention, frontoparietal, limbic, salience, somatomotor, and visual networks, which are typically examined and found to change in aging[6] as well as multiple neuropathological processes[12–14]. A UK Biobank sample comprising 18,445 participants of British ancestry was used in this study. We first estimated single nucleotide polymorphism (SNP) heritability (h^2). Subsequently, genome-wide association studies (GWAS) were performed to identify genetic variants associated with each graph theory measure. Gene-based association

[1]Centre for Healthy Brain Aging, CHeBA, School of Psychiatry, University of New South Wales Medicine, Kensington, Sydney, NSW 2052, Australia. [2]Neuroscience Research Australia, Randwick, Sydney, NSW 2031, Australia. [3]Neuropsychiatric Institute, Euroa Centre, Prince of Wales Hospital, Randwick, Sydney, NSW 2031, Australia. [✉]email: heidi.foo@student.unsw.edu.au

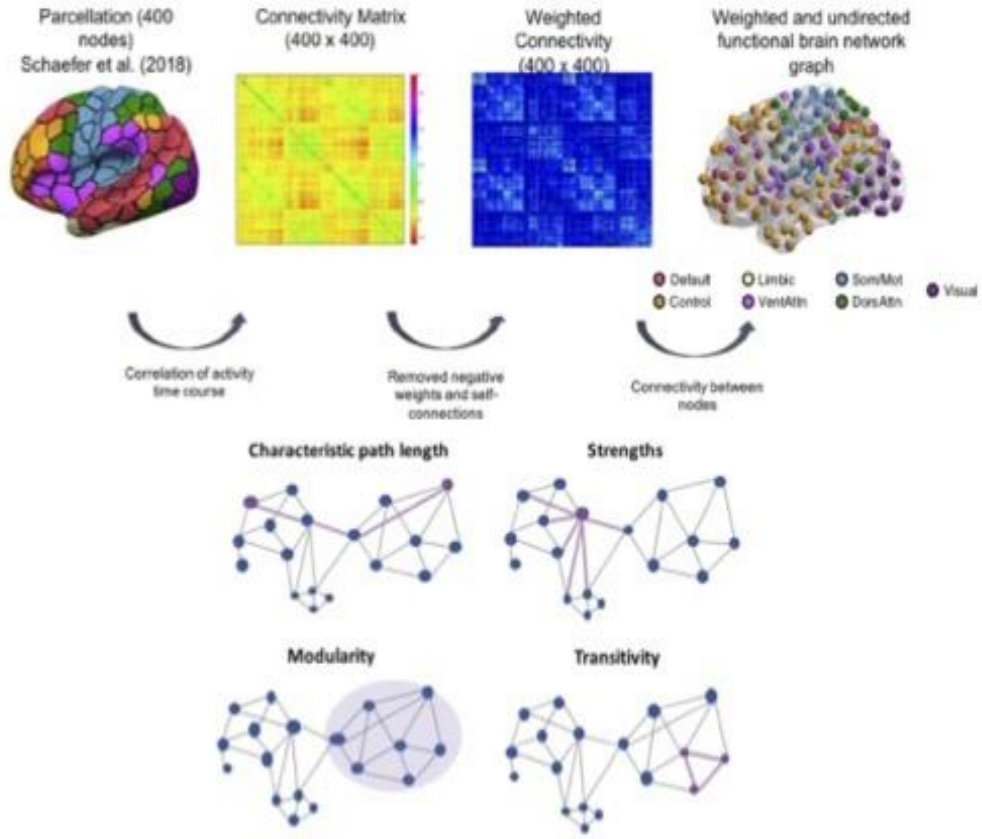

Figure 1. Schematic representation of brain network construction using graph theory analysis. After pre-processing, the brain was divided into different parcels using the Schaefer et al. (2018) parcellation scheme. Subsequently, activity time course was extracted from each region to create the correlation matrix. We used the correlation matrix and removed all the self-connected and negative weights to derive a corresponding weighted undirected brain network matrix and functional brain network graph. Lastly, we used the network matrix to calculate the sets of topological graph theory measures.

analysis was carried out to uncover gene-level associations, and the functional consequences of the significant genetic variants were explored.

Results

Demographics and graph theory measures. After imaging and genetic pre-processing and quality control, 2153 UK Biobank participants were excluded resulting in a final sample of 18,445 participants of British ancestry. There were 9773 females and 8672 males with a mean age (sd) of 62.47 (7.47). Eighteen weighted graph theory measures were derived by parcellating the rs-fMRI data using the Schaefer atlas into 400 regions[15], which is a fine-grained parcellation scheme based on Yeo-7 network. These 18 measures include: global efficiency and characteristic path length (network integration); modularity, transitivity, and local efficiency of 7 networks (network segregation); and strength of 7 networks. Supplementary Table 1 defines each of the measures and provides evidence of their association with aging and neuropathological diseases. Supplementary Table 2 shows the mean and standard deviation of the demographics and graph theory measures. Figure 1 shows the brain network reconstruction using rs-fMRI data.

Phenotypic correlations between the measures were examined (Supplementary Fig. 1). High correlations were observed between the following measures: characteristic path length and modularity were negatively correlated with all other graph theory measures ($r = -0.661$ to -0.989); global efficiency and transitivity were positively correlated with local efficiency and strength of all the networks ($r = 0.753$ to 0.952); local efficiencies of networks were positively correlated with each other ($r = 0.784$ to 0.902); and strengths of networks were positively correlated with each other ($r = 0.772$ to 0.927).

SNP heritability estimates and genetic correlations. SNP heritability, h^2_{SNP}, was estimated using the proportion of variance in each graph theory measure that is explained by GWAS SNPs. All graph theory meas-

ures, except for strength of the visual network, were significantly heritable ($p < 0.05$), ranging from $h^2_{SNP} = 0.07$ for local efficiency of visual network to $h^2_{SNP} = 0.17$ for the strength of limbic network, with a mean h^2_{SNP} of 0.12 (Supplementary Table 3; Fig. 2A). Notably, higher h^2_{SNP} estimates (0.11–0.17) were observed for global efficiency, characteristic path length, transitivity, and strength of limbic, somatomotor, default, salience, and frontoparietal networks compared to the other measures. In addition, genetic and environmental correlations were examined. Strong genetic correlations between the network measures were observed. All measures were positively associated with each other with the exception of Louvain modularity and characteristic path length being negatively correlated with all other measures (Supplementary Table 4; Fig. 2B).

Genome-wide association study. GWAS of the rs-fMRI data for each individual graph theory measure (n = 18) were carried out using an additive genetic model adjusted for age, age^2, sex, age × sex, age^2 × sex, head motion from resting-state fMRI, head position, volumetric scaling factor needed to normalize for head size, genotyping array and 10 genetic principal components.

At the genome-wide significance level of $p < 5 \times 10^{-8}$ (unadjusted for the number of measures assessed), there were 31 SNPs significantly associated with nine of the 18 graph theory measures namely, global efficiency, characteristic path length, Louvain modularity, local efficiency of default and somatomotor networks, strength of default, limbic, salience, and somatomotor networks (Supplementary Table 5). Supplementary Fig. 2 shows the Manhattan and quantile–quantile plots of all the 18 graph theory measures. However, after adjusting for the number of independent tests using this method by Nyholt and colleagues [16] (n = 6 tests for this study; p-threshold = $5 \times 10^{-8}/6 = 8.33 \times 10^{-9}$), only fourteen variants from a single locus remained significant with strength of the somatomotor network (lead SNP: rs12616641), and one of which also was significant for strength of the limbic network (rs62158161) (Table 1; Fig. 3A,B). All SNPs were located in an intergenic region near *PAX8* (Paired box gene 8) on chromosome 2 (BP 114065390—114092549) (Fig. 3C).

The conditional and joint association (COJO) analysis using the GWAS summary data of the network measures did not identify any additional SNPs apart from the top associated within each locus (Supplementary Table 5). There is high linkage disequilibrium in the genomic region (114065390–114110568) on chromosome 2 (Supplementary Fig. 3).

Multivariate association test. Since all network measures were highly correlated, to increase power a multivariate analysis using GWAS summary statistics from multiple network measures was performed. Based on their network properties, pooled summary statistics as implemented in metaUSAT[17] were obtained for (i) global efficiency and characteristic path length; (ii) modularity and transitivity; (iii) local efficiency of all networks; and (iv) strength across all networks. Multivariate analysis of the combined strength network measures yielded 31 significant associations at $p < 1.25 \times 10^{-8}$ (adjusted for four tests). Out of this, 23 were found in GWAS of somatomotor strength measure reported in supplementary table 5 and the remaining 8 SNPs were found for combined strength measure (Table 2). No additional hits were found in the multivariate analysis of the other three grouped measures.

Gene-based association analysis. Gene-based association analysis was performed using the software MAGMA[18] (Table 3). Our results showed that five genes – *SLC25A33* (Solute Carrier Family 25 Member 33), *TMEM201* (Transmembrane Protein 201), *ZEB1* (Zinc Finger E-Box Binding Homeobox 1), *SH2B3* (SH2B Adaptor Protein 3), and *ATXN2* (Ataxin 2) – were associated with global efficiency, characteristic path length, and strength of default, dorsal attention, and somatomotor networks after adjusting for the number of independent tests (n = 6) and number of genes (n = 18,319) i.e. p-threshold $< 0.05/(6 \times 18{,}319) = 4.56 \times 10^{-7}$. Supplementary Table 6 describes the genes associated with the graph theory measures.

Functional annotations. We assessed the potential functions of the 39 significant SNPs from the GWAS (n = 31) and multivariate association tests (n = 8) in SNPnexus[19]. The results showed that many of the network associated variants were associated with other phenotypes including sleep patterns, psychiatric disorders, coronary artery disease, cholesterol, and blood pressure (Supplementary Tables 7 and 8). None of the variants were found to be eQTLs.

Gene expression enrichment analysis of the list of significant genes in our results was subsequently performed using the Functional Mapping and Annotation (FUMA) platform[20]. They were expressed in the brain but also across other tissue types (Supplementary Fig. 4). Moreover, there was no enrichment in brain tissue types (Supplementary Table 9).

Genetic correlations with other traits. Given that the most robust GWAS result was observed for the strength of somatomotor network, we examined its genetic correlations with other traits via linkage disequilibrium (LD) score regression (LDSC)[21] (Supplementary Table 10). Results showed that strength of somatomotor network was genetically correlated with other traits, such as nervous feelings, sleep traits, neuroticism, depressive symptoms, blood pressure, education (unadjusted $p \leq 0.05$). However, none of them passed multiple comparisons correction.

Correlations with other associated traits. As the SNPs in our study have been associated with sleep and insomnia in previous GWAS studies (Supplementary Table 7), we explored the phenotypic correlations between the graph theory and sleep-related measures in the UK Biobank data (Supplementary Tables 11 and 12). Self-reported sleep duration and insomnia were significantly associated with the graph theory measures.

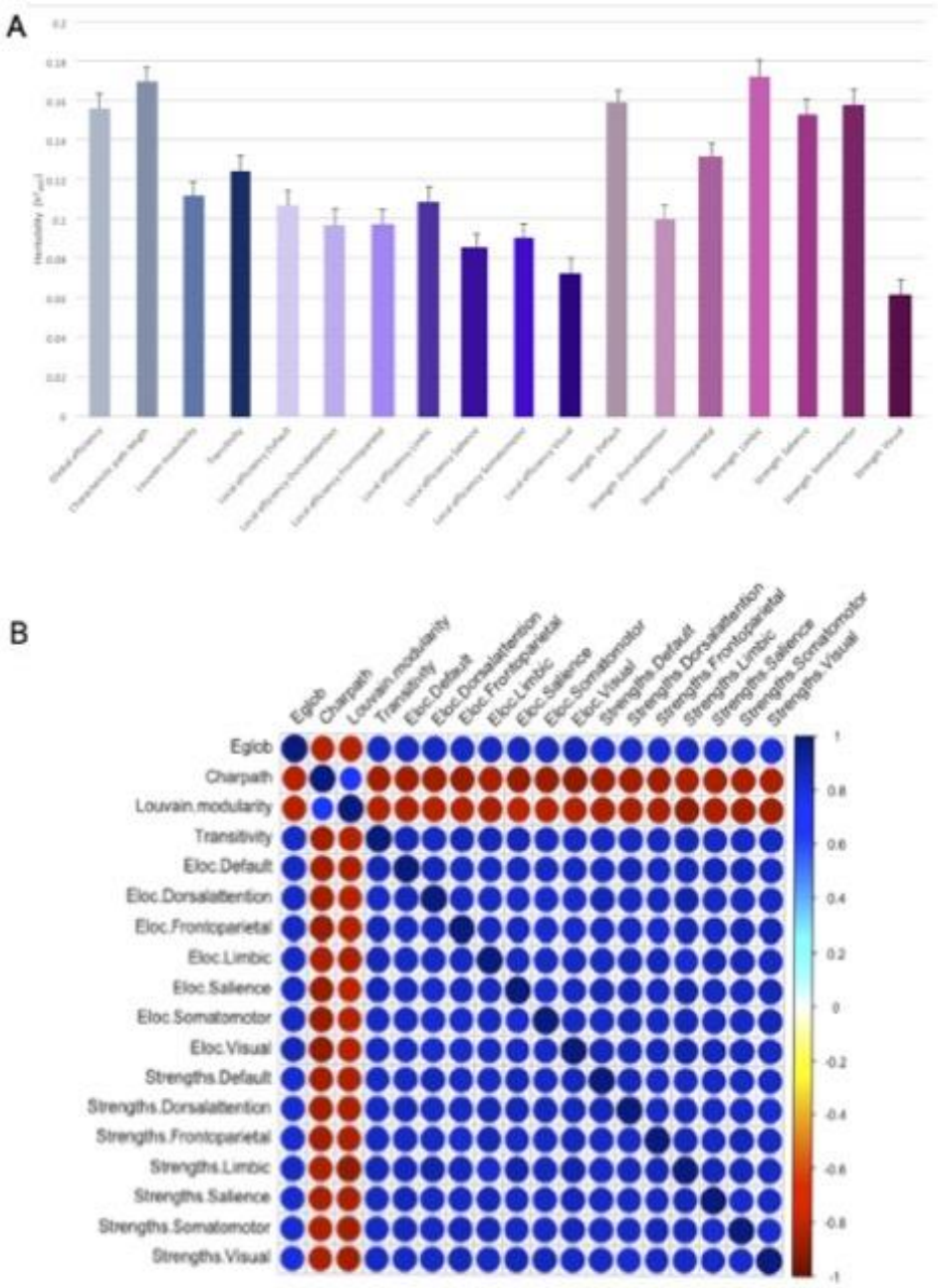

Figure 2. Genetic and environmental correlations between the 18 weighted graph theory measures. (**A**) represents the heritability estimates for each of the graph theory measures. Gray represents the network integration as characterized by global efficiency and characteristic path length; blue represents network segregation as characterized by Louvain modularity and transitivity; purple represents networks of local efficiency; and pink represents strength of the networks. (**B**) Genetic correlations were estimated using LDSC (https://github.com/bulik/ldsc). Strong genetic and environmental correlations between the network measures were observed (see Supplementary Table 4 for more details). Abbreviations: Eglob, global efficiency; Charpath, characteristic path length; Eloc, local efficiency.

SNP and measures	Chr	Position	Function	Nearest gene	A1/A2	EAF	β	SE	p
Strength Limbic									
rs62158161	2	114065572	Intergenic	*PAX8*	C/T	0.749	0.069	0.012	4.70E−09
Strength Somatomotor									
rs62158160	2	114065390	Intergenic	*PAX8*	C/T	0.742	0.066	0.011	6.90E−09
rs62158161	2	114065572	Intergenic	*PAX8*	C/T	0.749	0.069	0.012	2.40E−09
rs62158166	2	114077218	Intergenic	*PAX8*	G/C	0.773	0.073	0.012	1.20E−09
rs62158168	2	114078381	Intergenic	*PAX8*	C/G	0.773	0.073	0.012	1.20E−09
rs12616641*	2	114079248	Intergenic	*PAX8*	C/A	0.774	0.073	0.012	9.90E−10
rs62158169	2	114081827	Intergenic	*PAX8*	C/T	0.784	0.072	0.012	3.50E−09
rs62158170	2	114082175	Intergenic	*PAX8*	A/G	0.784	0.073	0.012	2.60E−09
rs199993536	2	114082628	Intergenic	*PAX8*	T/A	0.783	0.072	0.012	3.10E−09
rs6737318	2	114083120	Intergenic	*PAX8*	A/G	0.779	0.070	0.012	6.20E−09
rs62158206	2	114084596	Intergenic	*PAX8*	T/C	0.779	0.071	0.012	4.10E−09
rs7556815	2	114085785	Intergenic	*PAX8*	G/A	0.780	0.071	0.012	4.70E−09
rs2863957	2	114089551	Intergenic	*PAX8*	C/A	0.779	0.071	0.012	4.10E−09
rs1823125	2	114090412	Intergenic	*PAX8*	A/G	0.779	0.071	0.012	3.30E−09
rs60873293	2	114092549	Intergenic	*PAX8*	G/T	0.779	0.070	0.012	5.70E−09

Table 1. GWAS genome-wide significant results for brain functional network measures. Linear regression models were adjusted for age, age^2, sex, age × sex, age^2 × sex, head motion from resting-state fMRI, head position, volumetric scaling factor needed to normalize for head size, and 10 genetic principal components. *P* values are two-tailed. Only results that survived Bonferroni correction ($p < 5 \times 10^{-8}/6$) were reported here. *rs12616641 was the lead SNP. Abbreviations: SNP, single nucleotide polymorphism; Chr, chromosome; A1, coded allele; A2, non-coded allele; EAF, effect allele frequency; β, beta; SE, standard error.

Strength of somatomotor network showed the most significant association with sleep duration ($p = 8.33 \times 10^{-11}$) and insomnia ($p = 0.0019$).

Discussion

Functional graph theory measures reflect the underlying functional topography of the brain. To date, this is the first study investigating the genetics of weighted functional graph theory measures. We present h^2_{SNP} estimates and results from GWAS of graph theory measures using resting-state fMRI data from 18,445 UK Biobank participants. We identified significant SNPs and gene associations that survived multiple correction testing with six of the 18 graph theory measures including global efficiency, characteristic path length, and strength of default, dorsal attention, limbic, and somatomotor networks. The novel contributions of this paper are the identification of new genetic associations at the variant, locus, and gene levels, providing insights into the genetic architecture of graph theory metrics using resting-state fMRI data.

Similar to the study by Elliot and colleagues[18] who showed that resting-state fMRI connectivity edges had the lowest levels of h^2_{SNP}, we found low h^2_{SNP} across all the graph theory measures. This is in contrast to previous classical twin study design studies that have shown moderate to high heritability of 0.52 to 0.64 for global efficiency, 0.47 to 0.61 for mean clustering coefficient, and 0.38 to 0.59 for modularity[8]. One of the plausible explanations is that h^2_{SNP} typically provides smaller heritability estimates due to uncaptured rare genetic variants compared to those provided by the classic twin study design[10]. High genetic correlations observed between graph theory measures may be due to the high phenotypic correlations between the measures.

The GWAS results found that strength of limbic and somatomotor networks were associated with SNPs located in an intergenic region near *PAX8* (Paired box gene 8) on chromosome 2, which is the closest gene to the top SNP. The *PAX* gene family encodes transcription factors which are essential during development and tissue homeostasis[22]. Specifically, *PAX8* protein is considered as a master regulator for key cellular processes in DNA repair, replication, and metabolism[23]. It has also been shown to regulate several genes involved in the production of thyroid hormone[24], essential for brain development and function such as neuronal differentiation, synaptogenesis, and dendritic proliferation[25,26]. A previous study has also linked reductions in intrinsic functional connectivity in the somatomotor network to participants with subclinical hypothyroidism compared to controls[27]. Interestingly, studies have also found subclinical thyroid dysfunction to be associated with sleep quality[28,29]. Other genes located in this intergenic region near *PAX8* include *CBWD2* and *CHCHD5*, which have also been associated with sleep duration in prior studies[30,31]. Considering that we also observed phenotypic correlations between sleep duration, insomnia and graph theory measures, it is possible that variants in or near *PAX8* and other genes in this region may play a role in the regulation of genes associated with functional brain network properties and sleep.

Results from multivariate SNP-based analyses from combined network strength measures found associations with SNPs on chromosome 2, which were associated with inflammation and oncogenesis. The majority of these SNPs were located in intergenic regions close to non-coding RNA genes. *LINC01826* (long intergenic non-protein coding RNA 1826) has been associated with inflammatory responses of the vascular endothelial cells, which

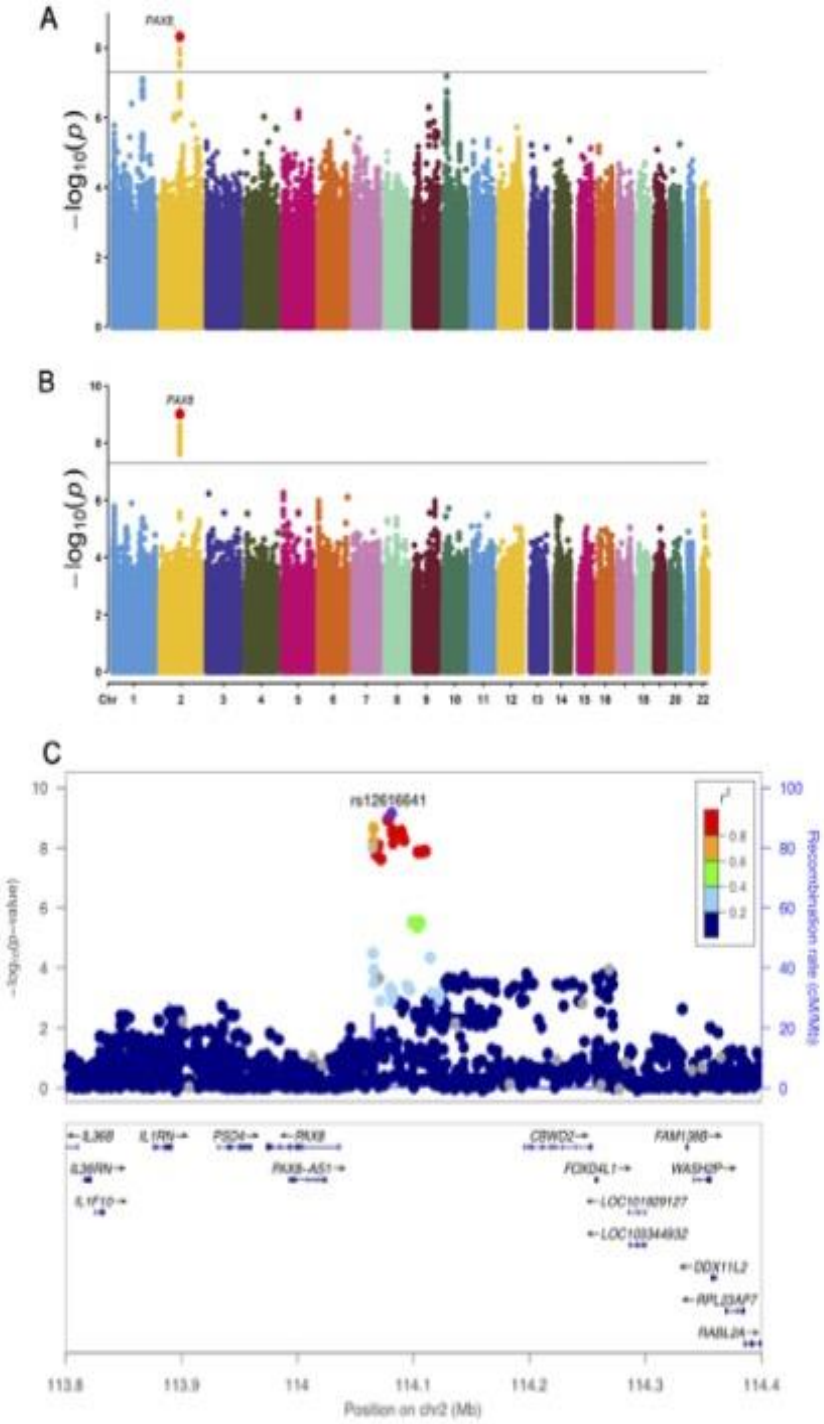

Figure 3. GWAS Manhattan Plots for strength of limbic and somatomotor networks and the locus zoom plot for the identified chromosome 2 region. (**A**) represents the Manhattan plot for strength of limbic network; (**B**) represents the Manhattan plot for strength of somatomotor network. For each of the Manhattan plots, each point represents a single genetic variant plotted according to its genomic position (x-axis) and its association with the relevant graph theory measure is shown by the corresponding $-\log_{10}(P)$ values on the y-axis. Linear regression models were adjusted for age, age^2, sex, age × sex, age^2 × sex, head motion from resting-state fMRI, head position, volumetric scaling factor needed to normalize for head size, genotyping array and 10 genetic principal components. The black solid line represents the classical GWAS significance threshold of $p < 5 \times 10^{-8}$. (**C**) The Locus zoom plot showing the chromosome 2 locus significantly associated with both the strength of somatomotor and limbic networks. Rs12616641 is the lead SNP.

Measure	SNP	Chr	Position	Function	Nearest gene	p
Combined network strength	rs145868127	2	144721440	ncRNA_exonic	*LOC101928386*	3.92E−18
	rs2680724	2	134822146	Intergenic	*MIR3679*	4.04E−18
	rs62165320	2	131541110	Intergenic	*AMER3*	5.08E−18
	rs2661030	2	123837766	Intergenic	*LINC01826*	5.33E−11
	rs2661035	2	123839945	Intergenic	*LINC01826*	5.45E−11
	rs1880544	2	121222694	ncRNA_exonic	*LINC01101*	1.35E−10
	rs2089478	2	123837764	Intergenic	*LINC01826*	1.56E−10
	rs12474078	2	211330092	ncRNA_intronic	*LANCL1-AS1*	2.50E−09

Table 2. Multivariate SNP-based analyses for combined network strength measure. Only results that survived Bonferroni correction ($p < 5 \times 10^{-8}/4 = 1.25 \times 10^{-8}$) are reported. Abbreviations: SNP, single nucleotide polymorphism; Chr, chromosome; ncRNA, non-coding RNA; *LOC101928386*, Uncharacterized LOC101928386; *MIR3679*, MicroRNA 3679; *AMER3*, APC Membrane Recruitment Protein 3; *LINC01826*, Long Intergenic Non-Protein Coding RNA 1826; *LINC01101*, Long Intergenic Non-Protein Coding RNA 1101; *LANCL1-AS1*, LANCL1 Antisense RNA 1.

Gene	Graph theory measures	Chr	Position	NSNPs	P
SLC25A33	Global efficiency	1	9599528	69	5.64E−08
	Characteristic path length	1	9599528	69	5.23E−08
TMEM201	Global efficiency	1	9648932	43	1.83E−08
	Characteristic path length	1	9648932	43	1.48E−08
	Strength dorsal attention	1	9648932	43	1.36E−07
	Strength somatomotor	1	9648932	43	2.09E−07
ZEB1	Global efficiency	10	31607825	323	3.27E−07
	Characteristic path length	10	31607825	323	2.29E−07
SH2B3	Strength default	12	111843720	50	2.95E−07
ATXN2	Strength default	12	111890018	149	2.48E−07

Table 3. Gene-based association analysis identified five significant gene-level associations for brain functional network measures. Gene-based association analysis was performed via MAGMA[18], which uses 1000G reference panel for calculation of LD between the SNPs and gene coordinates based on NCBI build 37. Only genes that passed the Bonferroni correction ($p < 4.56 \times 10^{-7}$) are reported here. Abbreviations: Chr, chromosome; NSNP, number of single nucleotide polymorphisms. *SLC25A33*, Solute Carrier Family 25 Member 33; *TMEM201*, Transmembrane Protein 201; *ZEB1*, Zinc Finger E-Box Binding Homeobox 1; *SH2B3*, SH2B Adaptor Protein 3; *ATXN2*, Ataxin 2.

are important in the development of cardio-cerebrovascular diseases[32]. *MIR3679* (microRNA 3679) is a short non-coding RNA involved in post-transcriptional regulation of gene expression, which has been postulated to function as a tumor suppressor due to lower levels observed in patients with diffuse glioma than controls[33]. *LINC01101* (long intergenic non-protein coding RNA 1101), on the other hand, has been down-regulated in cervical cancer[34]. The identified genes may contribute to understanding the relationship between strength of brain networks and disease.

Gene-based association analysis showed associations with genes involved in neuronal differentiation/development, cancer, and susceptibility to neurodegenerative diseases. *ZEB1* has been implicated in neuronal glioblastoma[35] whereas *SLC25A33* has been associated with insulin/insulin-like growth factor 1 (IGF-1) necessary for metabolism, cell growth, and survival[36] and showed higher expression in transformed fibroblasts and cancer cell lines compared to non-transformed cells[36,37]. *TMEM201* mice, which undergo accelerated senescence, exhibited an early onset age-related decline in antibody response and have a higher rate of mortality[38]. *ATXN2* belongs to a class of genes associated with microsatellite-expansion diseases, where an interrupted CAG repeat expansion has been associated with brain-related diseases including spinocerebellar ataxia type 2 (SCA2), frontotemporal lobar degeneration (FTLD), and amyotrophic lateral sclerosis (ALS)[39,40]. A neighbouring gene *SH2B3* to *ATXN2* has also been implicated in increased ALS risk[40]. Consistent with previous studies that identified functional graph theory measures that were associated with the most common FTLD (behavioral variant of frontotemporal dementia)[41,42], we observed similar graph theory measures to be associated with the *ATXN2* gene. This implies that *ATXN2* may be involved in the relationship between the disruption of brain networks and neurological/neuromuscular disorders.

In addition, we also observed that brain functional networks are associated with self-reported sleep traits. Consistent with a previous study showing that individuals with chronic insomnia also showed disrupted global and local properties of the brain involving networks such as default mode, dorsal attention, and sensory-motor[43], we found that insomnia was most significantly associated with decreased strength of somatomotor network.

Therefore, it seems that changes in sleep quality may have a profound impact on the brain functional networks. Given that we observed genes associated with these networks, it is possible that altered networks may be driving the sleep abnormality. The reverse is also possible, with sleep disturbance influencing the activity in the networks. The directionality of the relationship between brain networks and sleep traits may be determined using longitudinal data in future studies.

The strengths of this study include the well characterized sample and its large sample size, and uniform MRI methods. The results, however, should be interpreted with caution. While using weighted undirected matrix circumvents issues surrounding filtering/thresholding the connectivity matrix to maintain significant edge weights represented in a binary matrix, there are inherent difficulties associated with the interpretation of the results. As brain signals recorded from resting-state fMRI are typically noisy, it is possible that edge weights may be affected by non-neural contributions[44]. Despite this, with careful denoising of the resting-state fMRI data[45,46] and covarying for motion, it is possible to minimize the noise in the data. In addition, previous studies have suggested that stronger edge weights make greater contributions in the computation of graph metrics than lower weight connections[47,48]. This implies that when evaluating weighted graphs, false positive connections based on lower correlations may have a less disruptive impact on the network topology[49]. Given that the brain is a complex system with hierarchical network structure, studying weighted networks, as was done in this study, may provide a more holistic representation of the brain functional network. Future studies may benefit from investigating the genetic effects between binarized and weighted graph theory metrics. Moreover, given the high correlations between the graph theory measures suggest that these measures may account for the same phenotype, or at least almost account for the same variability in the population, performing GWAS on each of these measures may not be necessary. However, these measures have shown to affect different disease states in older age. Moreover, this is an exploratory study and the findings presented are purely correlative. Despite so, the findings from the paper provide a new preliminary support for combining resting-state fMRI, graph theory methods, and GWAS to identify genetic variants associated with the various graph theory measures. It may also shed light to direct future studies in determining what graph theory imaging phenotypes should be included. In order to further understand the mechanisms about brain function at a more basic level, it may be useful for future studies to use developmental and adult human brain gene expression data to associate the expression of a single gene or genes with specific graph theory measures and phenotypes. Furthermore, given that the UK Biobank has recently released additional data, replication may be possible in the future.

In summary, this is the first study to investigate the genetics of weighted functional graph theory measures in a large and well characterized cohort. We observed multiple SNPs and genes associated with weighted graph theory measures, which have been observed to be implicated in sleep duration, neuronal differentiation/development, cancer, and susceptibility to neurodegenerative diseases. Our findings may help in the identification of novel biological pathways relevant to human brain functional network integrity and disease.

Methods

Study population. Our study was approved by the UK Biobank in December 2018 (Application number: 45262). rs-fMRI data for 20,598 participants with British ancestry was downloaded in March 2019[50]. The imaging assessment took place at three different assessment centres with the majority assessed in Manchester, more recently scans were undertaken at Newcastle and Reading, UK. The UK Biobank study was conducted under approval from the NHS National Research Ethics Service (approval letter dated 17th June 2011, ref. 11/NW/0382), project 10279. All data and materials are available via UK Biobank (http://www.ukbiobank.ac.uk). Only individuals with both genetics and rs-fMRI data were included in this study.

Image processing. Briefly, the UK Biobank structural T1-weighted MRI scans were acquired on three 3 T Siemens Skyra MRI scanners (software platform VD13) at three sites (Reading, Newcastle, and Manchester) using a 32-channel receiving head coil and a 3D MPRAGE protocol (1.0 × 1.0 × 1.0 mm resolution, matrix 208 × 256 × 256, inversion time (TI)/repetition time (TR) = 880/2,000 ms, in-plane acceleration 2). An extensive overview of the data acquisition protocols and image processing carried out on behalf of the UK Biobank can be found elsewhere[51]. Rs-fMRI data previously pre-processed by the UK Biobank [51] were used. Briefly, motion correction, intensity normalization, highpass temporal filtering, echo-planar imaging (EPI) unwarping, and gradient distortion correction were performed. Subsequently, structured artefacts were removed by ICA + FIX processing (Independent component analysis followed by FMRIB's ICA-based X-noiseifier)[52–54]. We removed participants with motion of > 2 mm/degrees of translation/rotation. After image quality control and removal of participants with head motion outliers, we excluded 1,626 participants and 18,972 participants remained.

Graph theory analyses. The Schaefer atlas[15] was used as it met the following requirements: (1) it integrated both local gradient and global similarity approaches (i.e. Markov Random Field model) for parcellation, which showed greater homogeneity than four other previously published parcellations implying that it will not overestimate local connectivity of the regions; (2) it revealed neurobiologically meaningful features of the brain organization; and (3) it was based of the Yeo 7-parcels atlas[55] and provided a more fine-grained parcellation, which allowed us to look at an average of the parcels across the 7 networks for local efficiency and nodal strength. 3dNetCorr command from Analysis of Functional Neuroimages (AFNI)[56] was used to produce network adjacency matrix for each participant. The mean time-series for each region was correlated with the mean time-series for all other regions and extracted for each participant. Partial correlation, r, between all pairs of signals was computed to form a 400-by-400 (Schaefer atlas) connectivity matrix, which was then Fisher z-transformed. Self-connections and negative correlations were set to zero. The main network analysis was performed on positive weighted networks. Given that connection weights in brain networks can vary across magnitude, undirected

weighted connectivity matrices were used instead of binary connectivity matrices. The higher the weight, the stronger the functional connectivity is between the brain regions[44].

All graph theory measures were quantified by using the brain connectivity toolbox (BCT)[2]. Global-level measure included global efficiency, characteristic path length, transitivity, and Louvain modularity. A single value is derived for each of these four measures and quantitatively represent the whole brain network. Network level measures, such as local efficiency and strength, were estimated for each node and averaged across the all parcels within each network. Subsequently, we averaged the left-right hemisphere to derive a value for each node and averaged within each network to derive a value for each of the 7 networks.

To assess integration of information, we calculated global efficiency and characteristic path length[2,57]. Global efficiency represents how effectively the information is transmitted at a global level and is the average inverse shortest path length while the latter measures the integrity of the network and how fast and easily information can flow within the network. To assess network segregation, which characterizes the specialized processing of the brain at a local level, we calculated the Louvain modularity, transitivity, and local efficiency indices[2,57]. Louvain modularity is a community detection method, which iteratively transforms the network into a set of communities, each consisting of a group of nodes. Higher modularity values indicate denser within-modular connections but sparer connections between nodes that are in different modules. Transitivity refers to the sum of all the clustering coefficients around each node in the network and is normalized collectively. Local efficiency is a node-specific measure and is defined relative to the sub-graph comprising of the immediate neighbours of a node. Finally, strength (weighted degree) is described as the sum of all neighbouring edge weights[2]. High connectivity strength indicates stronger connectivity between the regions, which provides an estimation of functional importance of each network.

Genotype data in UK Biobank. Genetic data for approximately 500,000 were available and full details on the genetics data used were described previously[58]. The samples were collected from stored blood samples in the UK Biobank and genotyped either using the UK Bileve or the UK biobank axiom array. Genotyping was performed on 33 batches of ~4700 samples by Affymetrix (High Wycombe, UK). Further details on the UK Biobank sample pre-processing are available here http://biobank.ctsu.ox.ac.uk/crystal/refer.cgi?id=155583.

An imputed data set was made available where the UK Biobank interim release was imputed to a reference set that consisted of > 92 million autosomal variants imputed from the Haplotype Reference Consortium (HRC)[59] and UK10K + 1000 Genomes resources reference panels.. After SNP QC filters (MAF > 0.1% and imputation information score > 0.3), 9926107 SNPs were used in the GWAS analysis.

Further quality control measures were performed. Due to the confounds associated with population structure[60], only samples reported to have recent British ancestry were used in the GWAS analysis. Outliers, including those with high missingness, relatedness, quality control failure, and sex mismatch, were removed. The final UK Biobank sample, after genotyping quality control and including those with rs-fMRI data, was n = 18,445 participants.

Sleep behavioral data in UK Biobank. Self-reported sleep data, namely sleep duration and frequency of insomnia, were used. Sleep duration was recorded as the number of reported hours of sleep in every 24 h and frequency of insomnia was recorded as never/rarely, sometimes, or usually. More details can be found on http://biobank.ndph.ox.ac.uk/showcase/field.cgi?id=1160 and http://biobank.ndph.ox.ac.uk/showcase/field.cgi?id=1200.

Potential confounds. In accordance with previous GWAS of brain imaging phenotypes in the UK Biobank[10], we controlled for similar confounding variables in this study. In addition to age at scanning and sex (i.e. age, age^2, age × sex, age^2 × sex), covariates relating to imaging parameters and genetic ancestry were also included. These included: head motion from resting-state fMRI, head position, volumetric scaling factor needed to normalize for head size, and the 10 genetic principal components.

SNP heritability. Heritability analysis, which is defined as the proportion of observed phenotypic variance explained by additive genetic factors of all common autosomal variants[61], estimates the relative contribution of genes and the environment on a phenotype. Using BOLT-REML[62] implemented in BOLT-LMM v2.3[63], we estimated the heritability accounted by autosomal SNPs among the graph theory measures. BOLT-REML uses multiple component modelling to partition SNP heritability and applies Monte Carlo algorithm for variance component analysis.

Genome-wide association analysis. BOLT-LMM v2.3[63] was used to conduct GWAS for the graph theory measures in the UK Biobank sample and adjusted for potential confounds. To correct for multiple hypothesis testing, we estimated the number of independent tests used based on Nyholt et al. method[16] and derived n = 6 independent tests for this study. The genome-wide significant threshold was set at $p < (5 \times 10^{-8}/6) = 8.33 \times 10^{-9}$. Findings with unadjusted threshold of $p < 5 \times 10^{-8}$ were also reported in Supplementary Table 5. Quantile and Manhattan plots were also presented for each of the graph theory measure in Supplementary Fig. 2. Manhattan and QQ plots were made using the R-package[64]. Locus Zoom[65] was used for the visualization of the nearest genes within a ± 500-kilobase genomic region for the strength of somatomotor and limbic networks based on the hg19 UCSC Genome Browser assembly (Fig. 3).

Linkage disequilibrium and independent SNPs. The linkage disequilibrium plot of the associated genomic region was made using the LD plot function in the R package "gaston"[66]. To identify independent SNPs associated with each of the network measures a stepwise model selection method as implemented in the COJO[67] (cojo-slct) procedure of GCTA[68] package with default parameters was used.

Multivariate association analysis. Multivariate association analysis was conducted using metaUSAT[17]. The method uses summary statistics from individual studies and is suitable for correlated traits. MetaUSAT derives strength from two methods of multivariate association tests (score test and multivariate analysis variance test) as it uses convex linear combination of two test statistics. Data-driven minimum p-value corresponding to the best-linear combination is obtained. The significant threshold was set as $p < (5 \times 10^{-8}/4) = 1.25 \times 10^{-8}$.

Gene-based association analysis and functional mapping. Gene-based association analysis was performed via MAGMA[18] (v1.07, https://ctg.cncr.nl/software/magma/). MAGMA uses 1000G reference panel for calculation of LD between the SNPs and gene coordinates based on NCBI build 37. SNPs were mapped to a gene if they were within ± 5 kb of the gene co-ordinates. Gene-based association test statistic was derived using the default option, which is the sum of −log(SNP p-value). The Bonferroni correction was used for significance of the gene-based association tests (p-value of the gene-based tests / (number of independent tests × number of genes tested)). In other words, significant threshold was set as $p < 0.05/(6 \times 18{,}319) = 4.56 \times 10^{-7}$.

Functional annotation. We performed lookups for variants that passed the suggestive GWAS threshold of $p < 5 \times 10^{-8}$ to investigate the previously reported associations with the other traits. NHGRI-EBI GWAS Catalogue[69] included previous GWAS publications (Supplementary Table 7) and SNPnexus[19] included all other publications (Supplementary Table 8).

FUMA[20] gene2func online platform (version 1.3.4, http://fuma.ctglab.nl/) was used to explore the functional consequences of significant genes. All the genes in the GWAS analysis and the gene-based analysis after nominal significance were used as input (a total of 18 genes). Using the FUMA platform, the GTEx v7 30 general tissue types data set was used for tissue specificity analyses. Differentially expressed gene (DEG) sets were pre-calculated by performing two-tailed t-test for any one of the tissue type against all others. Expression values were normalized (zero-mean) following a $\log_2$ transformation of expression values. Using the genes as background gene set, 2 × 2 enrichment sets were performed. Genes with p-value ≤ 0.05 were after Bonferroni correction were defined as differentially expressed and colored in red in Supplementary Fig. 3.

Genetic correlation estimation with LDSC. LD Hub (v1.9.1, http://ldsc.broadinstitute.org/ldhub/) was used to estimate the genetic correlation between graph theory measures and corresponding traits. Summary statistics were uploaded to LD hub where it calculates the genetic correlations using the LDSC software (v1.0.0, https:// github.com/bulik/ldsc).

Test of associations with graph theory measures. The graph theory measures were normalized using ranked transformed using the rntransform() function in R from GeneABEL package[70] and age were z-transformed for regression analysis. Regression model similar to GWAS analysis was used to test the association of self-reported sleep duration and frequency of insomnia variables with the graph theory measures. Only results with a two-tailed $p < 0.05/18$ (number of graph theory measures) were considered significant. Data management, derivation of summary statistics and other statistical analyses, and correlation plots were performed using R (V 4.0.0) software[64].

Received: 2 March 2021; Accepted: 7 July 2021
Published online: 16 July 2021

References

1. Chan, M. Y., Park, D. C., Savalia, N. K., Petersen, S. E. & Wig, G. S. Decreased segregation of brain systems across the healthy adult lifespan. *Proc. Natl. Acad. Sci.* **111**, E4997. https://doi.org/10.1073/pnas.1415122111 (2014).
2. Rubinov, M. & Sporns, O. Complex network measures of brain connectivity: Uses and interpretations. *Neuroimage* **52**, 1059–1069. https://doi.org/10.1016/j.neuroimage.2009.10.003 (2010).
3. Bertolero, M. A., Yeo, B. T. T., Bassett, D. S. & D'Esposito, M. A mechanistic model of connector hubs, modularity and cognition. *Nat. Hum. Behav.* **2**, 765–777. https://doi.org/10.1038/s41562-018-0420-6 (2018).
4. Geerligs, L., Renken, R. J., Saliasi, E., Maurits, N. M. & Lorist, M. M. A Brain-wide study of age-related changes in functional connectivity. *Cerebral Cortex (New York, N.Y.: 1991)* **25**, 1987–1999, https://doi.org/10.1093/cercor/bhu012 (2015).
5. Cohen, J. R. & D'Esposito, M. The segregation and integration of distinct brain networks and their relationship to cognition. *J. Neurosci.: Off. J. Soc. Neurosci.* **36**, 12083–12094. https://doi.org/10.1523/jneurosci.2965-15.2016 (2016).
6. Song, J. *et al.* Age-related reorganizational changes in modularity and functional connectivity of human brain networks. *Brain Connect.* **4**, 662–676. https://doi.org/10.1089/brain.2014.0286 (2014).
7. Markov, N. T. *et al.* The role of long-range connections on the specificity of the macaque interareal cortical network. *Proc. Natl. Acad. Sci.* **110**, 5187. https://doi.org/10.1073/pnas.1218972110 (2013).
8. Sinclair, B. *et al.* Heritability of the network architecture of intrinsic brain functional connectivity. *Neuroimage* **121**, 243–252. https://doi.org/10.1016/j.neuroimage.2015.07.048 (2015).
9. Fornito, A. *et al.* Genetic influences on cost-efficient organization of human cortical functional networks. *J. Neurosci.: Off. J. Soc. Neurosci.* **31**, 3261–3270. https://doi.org/10.1523/jneurosci.4858-10.2011 (2011).

10. Elliott, L. T. *et al.* Genome-wide association studies of brain imaging phenotypes in UK Biobank. *Nature* **562**, 210–216. https://doi.org/10.1038/s41586-018-0571-7 (2018).
11. Thompson, P. M., Ge, T., Glahn, D. C., Jahanshad, N. & Nichols, T. E. Genetics of the connectome. *Neuroimage* **80**, 475–488. https://doi.org/10.1016/j.neuroimage.2013.05.013 (2013).
12. Munilla, J. *et al.* Construction and analysis of weighted brain networks from SICE for the Study of Alzheimer's Disease. *Front. Neuroinform.* https://doi.org/10.3389/fninf.2017.00019 (2017).
13. Khazaee, A., Ebrahimzadeh, A. & Babajani-Feremi, A. Identifying patients with Alzheimer's disease using resting-state fMRI and graph theory. *Clin. Neurophysiol.: Off. J. Int. Federat. Clin. Neurophysiol.* **126**, 2132–2141. https://doi.org/10.1016/j.clinph.2015.02.060 (2015).
14. Lebedev, A. *et al.* Large-scale resting state network correlates of cognitive impairment in Parkinson's disease and related dopaminergic deficits. *Front. Syst. Neurosci.* https://doi.org/10.3389/fnsys.2014.00045 (2014).
15. Schaefer, A. *et al.* Local-Global Parcellation of the Human Cerebral Cortex from Intrinsic Functional Connectivity MRI. *Cerebral cortex (New York, N.Y. : 1991)* **28**, 3095–3114, https://doi.org/10.1093/cercor/bhx179 (2018).
16. Nyholt, D. R. A simple correction for multiple testing for single-nucleotide polymorphisms in linkage disequilibrium with each other. *Am. J. Hum. Genet.* **74**, 765–769. https://doi.org/10.1086/383251 (2004).
17. Ray, D. & Boehnke, M. Methods for meta-analysis of multiple traits using GWAS summary statistics. *Genet. Epidemiol.* **42**, 134–145. https://doi.org/10.1002/gepi.22105 (2018).
18. de Leeuw, C. A., Mooij, J. M., Heskes, T. & Posthuma, D. MAGMA: generalized gene-set analysis of GWAS data. *PLoS Comput. Biol.* **11**, e1004219. https://doi.org/10.1371/journal.pcbi.1004219 (2015).
19. Dayem Ullah, A. Z. *et al.* SNPnexus: assessing the functional relevance of genetic variation to facilitate the promise of precision medicine. *Nucleic Acids Res.* **46**, W109–W113. https://doi.org/10.1093/nar/gky399 (2018).
20. Watanabe, K., Taskesen, E., van Bochoven, A. & Posthuma, D. Functional mapping and annotation of genetic associations with FUMA. *Nat. Commun.* **8**, 1826. https://doi.org/10.1038/s41467-017-01261-5 (2017).
21. Bulik-Sullivan, B. *et al.* An atlas of genetic correlations across human diseases and traits. *Nat. Genet.* **47**, 1236–1241. https://doi.org/10.1038/ng.3406 (2015).
22. Blake, J. A. & Ziman, M. R. Pax genes: regulators of lineage specification and progenitor cell maintenance. *Development* **141**, 737. https://doi.org/10.1242/dev.091785 (2014).
23. Ruiz-Llorente, S. *et al.* Genome-wide analysis of Pax8 binding provides new insights into thyroid functions. *BMC Genomics* **13**, 147–147. https://doi.org/10.1186/1471-2164-13-147 (2012).
24. Pasca di Magliano, M., Di Lauro, R. & Zannini, M. Pax8 has a key role in thyroid cell differentiation. *Proc. Natl. Acad. Sci. USA* **97**, 13144–13149. https://doi.org/10.1073/pnas.240336397 (2000).
25. Williams, G. R. Neurodevelopmental and neurophysiological actions of thyroid hormone. *J. Neuroendocrinol.* **20**, 784–794. https://doi.org/10.1111/j.1365-2826.2008.01733.x (2008).
26. Bernal, J. Thyroid hormone receptors in brain development and function. *Nat. Clin. Pract. Endocrinol. Metab.* **3**, 249–259. https://doi.org/10.1038/ncpendmet0424 (2007).
27. Kumar, M. *et al.* Alteration in intrinsic and extrinsic functional connectivity of resting state networks associated with subclinical hypothyroid. *J. Neuroendocrinol.* https://doi.org/10.1111/jne.12587 (2018).
28. Kim, W. *et al.* Association between sleep duration and subclinical thyroid dysfunction based on nationally representative data. *J. Clin. Med.* https://doi.org/10.3390/jcm8112010 (2019).
29. Song, L. *et al.* The Association Between Subclinical Hypothyroidism and Sleep Quality: A population-based study. *Risk Manag. Healthc. Policy* **12**, 369–374. https://doi.org/10.2147/RMHP.S234552 (2019).
30. Veatch, O. J., Keenan, B. T., Gehrman, P. R., Malow, B. A. & Pack, A. I. Pleiotropic genetic effects influencing sleep and neurological disorders. *Lancet Neurol.* **16**, 158–170. https://doi.org/10.1016/S1474-4422(16)30339-8 (2017).
31. Doherty, A. *et al.* GWAS identifies 14 loci for device-measured physical activity and sleep duration. *Nat. Commun.* **9**, 5257. https://doi.org/10.1038/s41467-018-07743-4 (2018).
32. Lin, Z. *et al.* Let-7e modulates the inflammatory response in vascular endothelial cells through ceRNA crosstalk. *Sci. Rep.* **7**, 42498. https://doi.org/10.1038/srep42498 (2017).
33. Ohno, M. *et al.* Assessment of the diagnostic utility of serum MicroRNA classification in patients with diffuse glioma. *JAMA Netw. Open* **2**, e1916953–e1916953. https://doi.org/10.1001/jamanetworkopen.2019.16953 (2019).
34. Iancu, I. V. *et al.* LINC01101 and LINC00277 expression levels as novel factors in HPV-induced cervical neoplasia. *J. Cell Mol. Med.* **21**, 3787–3794. https://doi.org/10.1111/jcmm.13288 (2017).
35. Yu, W., Liang, S. & Zhang, C. Aberrant miRNAs regulate the biological hallmarks of glioblastoma. *NeuroMol. Med.* **20**, 452–474. https://doi.org/10.1007/s12017-018-8507-9 (2018).
36. Favre, C., Zhdanov, A., Leahy, M., Papkovsky, D. & O'Connor, R. Mitochondrial pyrimidine nucleotide carrier (PNC1) regulates mitochondrial biogenesis and the invasive phenotype of cancer cells. *Oncogene* **29**, 3964–3976. https://doi.org/10.1038/onc.2010.146 (2010).
37. Floyd, S. *et al.* The insulin-like growth factor-I-mTOR signaling pathway induces the mitochondrial pyrimidine nucleotide carrier to promote cell growth. *Mol. Biol. Cell* **18**, 3545–3555. https://doi.org/10.1091/mbc.e06-12-1109 (2007).
38. Shimada, A. & Hasegawa-Ishii, S. Senescence-accelerated Mice (SAMs) as a model for brain aging and immunosenescence. *Aging Dis.* **2**, 414–435 (2011).
39. Fournier, C. *et al.* Interrupted CAG expansions in ATXN2 gene expand the genetic spectrum of frontotemporal dementias. *Acta Neuropathol. Commun.* **6**, 41. https://doi.org/10.1186/s40478-018-0547-8 (2018).
40. Lahut, S. *et al.* ATXN2 and its neighbouring gene SH2B3 are associated with increased ALS risk in the Turkish population. *PLoS ONE* **7**, e42956–e42956. https://doi.org/10.1371/journal.pone.0042956 (2012).
41. Reyes, P. *et al.* Functional connectivity changes in behavioral, semantic, and nonfluent variants of frontotemporal dementia. *Behav. Neurol.* **9684129–9684129**, 2018. https://doi.org/10.1155/2018/9684129 (2018).
42. Agosta, F. *et al.* Brain network connectivity assessed using graph theory in frontotemporal dementia. *Neurology* **81**, 134–143. https://doi.org/10.1212/WNL.0b013e31829a33f8 (2013).
43. Li, Z. *et al.* Disrupted brain network topology in chronic insomnia disorder: A resting-state fMRI study. *NeuroImage: Clin.* **18**, 178–185. https://doi.org/10.1016/j.nicl.2018.01.012 (2018).
44. Fallani, F. D. V., Richiardi, J., Chavez, M. & Achard, S. Graph analysis of functional brain networks: practical issues in translational neuroscience. *Philos. Trans. R. Soc. B: Biolo. Sci.* **369**, 20130521. https://doi.org/10.1098/rstb.2013.0521 (2014).
45. Parkes, L., Fulcher, B., Yucel, M. & Fornito, A. An evaluation of the efficacy, reliability, and sensitivity of motion correction strategies for resting-state functional MRI. *Neuroimage* **171**, 415–436. https://doi.org/10.1016/j.neuroimage.2017.12.073 (2018).
46. Power, J. D., Plitt, M., Laumann, T. O. & Martin, A. Sources and implications of whole-brain fMRI signals in humans. *Neuroimage* **146**, 609–625. https://doi.org/10.1016/j.neuroimage.2016.09.038 (2017).
47. Drakesmith, M. *et al.* Overcoming the effects of false positives and threshold bias in graph theoretical analyses of neuroimaging data. *Neuroimage* **118**, 313–333. https://doi.org/10.1016/j.neuroimage.2015.05.011 (2015).
48. Ginestet, C. E., Fournel, A. P. & Simmons, A. Statistical network analysis for functional MRI: summary networks and group comparisons. *Front. Comput. Neurosci.* **8**, 51. https://doi.org/10.3389/fncom.2014.00051 (2014).

49. van den Heuvel, M. P. *et al.* Proportional thresholding in resting-state fMRI functional connectivity networks and consequences for patient-control connectome studies: Issues and recommendations. *Neuroimage* **152**, 437–449. https://doi.org/10.1016/j.neuroimage.2017.02.005 (2017).
50. Sudlow, C. *et al.* UK biobank: an open access resource for identifying the causes of a wide range of complex diseases of middle and old age. *PLoS Med.* **12**, e1001779. https://doi.org/10.1371/journal.pmed.1001779 (2015).
51. Alfaro-Almagro, F. *et al.* Image processing and Quality Control for the first 10,000 brain imaging datasets from UK Biobank. *Neuroimage* **166**, 400–424. https://doi.org/10.1016/j.neuroimage.2017.10.034 (2018).
52. Beckmann, C. F. & Smith, S. M. Probabilistic independent component analysis for functional magnetic resonance imaging. *IEEE Trans. Med. Imaging* **23**, 137–152. https://doi.org/10.1109/tmi.2003.822821 (2004).
53. Griffanti, L. *et al.* ICA-based artefact removal and accelerated fMRI acquisition for improved resting state network imaging. *Neuroimage* **95**, 232–247. https://doi.org/10.1016/j.neuroimage.2014.03.034 (2014).
54. Salimi-Khorshidi, G. *et al.* Automatic denoising of functional MRI data: combining independent component analysis and hierarchical fusion of classifiers. *Neuroimage* **90**, 449–468. https://doi.org/10.1016/j.neuroimage.2013.11.046 (2014).
55. Yeo, B. T. *et al.* The organization of the human cerebral cortex estimated by intrinsic functional connectivity. *J. Neurophysiol.* **106**, 1125–1165. https://doi.org/10.1152/jn.00338.2011 (2011).
56. Cox, R. W. AFNI: software for analysis and visualization of functional magnetic resonance neuroimages. *Comput. Biomed. Res. Int. J.* **29**, 162–173 (1996).
57. Deco, G., Tononi, G., Boly, M. & Kringelbach, M. L. Rethinking segregation and integration: contributions of whole-brain modelling. *Nat. Rev. Neurosci.* **16**, 430–439. https://doi.org/10.1038/nrn3963 (2015).
58. Bycroft, C. *et al.* The UK Biobank resource with deep. phenotyping and genomic data. *Nature* **562**, 203–209. https://doi.org/10.1038/s41586-018-0579-z (2018).
59. McCarthy, S. *et al.* A reference panel of 64,976 haplotypes for genotype imputation. *Nat. Genet.* **48**, 1279–1283. https://doi.org/10.1038/ng.3643 (2016).
60. Marchini, J., Cardon, L. R., Phillips, M. S. & Donnelly, P. The effects of human population structure on large genetic association studies. *Nat. Genet.* **36**, 512–517. https://doi.org/10.1038/ng1337 (2004).
61. Yang, J., Zeng, J., Goddard, M. E., Wray, N. R. & Visscher, P. M. Concepts, estimation and interpretation of SNP-based heritability. *Nat. Genet.* **49**, 1304. https://doi.org/10.1038/ng.3941 (2017).
62. Loh, P.-R. *et al.* Contrasting genetic architectures of schizophrenia and other complex diseases using fast variance-components analysis. *Nat. Genet.* **47**, 1385–1392. https://doi.org/10.1038/ng.3431 (2015).
63. Loh, P.-R., Kichaev, G., Gazal, S., Schoech, A. P. & Price, A. L. Mixed-model association for biobank-scale datasets. *Nat. Genet.* **50**, 906–908. https://doi.org/10.1038/s41588-018-0144-6 (2018).
64. Team, R. C. R: A language and environment for statistical computing. R Foundation for Statistical Computing, Vienna, Austria (2020).
65. Pruim, R. J. *et al.* LocusZoom: regional visualization of genome-wide association scan results. *Bioinformatics* **26**, 2336–2337. https://doi.org/10.1093/bioinformatics/btq419 (2010).
66. Hervé Perdry, C. D.-R., Deepak Bandyopadhyay, Lutz Kettner. Gaston: Genetic Data Handling (QC, GRM, LD, PCA) & Linear Mixed Models. (2020).
67. Yang, J. *et al.* Conditional and joint multiple-SNP analysis of GWAS summary statistics identifies additional variants influencing complex traits. *Nat. Genet.* **44**, 369–375. https://doi.org/10.1038/ng.2213 (2012).
68. Yang, J., Lee, S. H., Goddard, M. E. & Visscher, P. M. GCTA: A tool for genome-wide complex trait analysis. *Am J Hum Genet* **88**, 76–82. https://doi.org/10.1016/j.ajhg.2010.11.011 (2011).
69. Buniello, A. *et al.* The NHGRI-EBI GWAS Catalog of published genome-wide association studies, targeted arrays and summary statistics 2019. *Nucleic Acids Res* **47**, D1005–d1012. https://doi.org/10.1093/nar/gky1120 (2019).
70. Karssen, L. C., van Duijn, C. M. & Aulchenko, Y. S. The GenABEL Project for statistical genomics. *F1000Res* **5**, 914–914, https://doi.org/10.12688/f1000research.8733.1 (2016).

Author contributions

H.F. devised the study; H.F., and A.T. jointly designed the analyses, analyzed the data, interpreted and wrote the paper with technical support and guidance with data interpretation from K.M., W.W., and P.S.; H.F., A.T., J.Y.J., and F.C.K. contributed to the statistical concepts; and P.S. supervised the work. All authors commented on the manuscript.

Competing interests

The authors declare no competing interests.

Additional information

Supplementary Information The online version contains supplementary material available at https://doi.org/10.1038/s41598-021-94182-9.

Correspondence and requests for materials should be addressed to H.F.